

Optimal Output Modification and Robust Control Using Minimum Gain and the Large Gain Theorem

by

Ryan James Caverly

A dissertation submitted in partial fulfillment
of the requirements for the degree of
Doctor of Philosophy
(Aerospace Engineering)
in The University of Michigan
2018

Doctoral Committee:

Assistant Professor James R. Forbes, Chair
Professor Dennis S. Bernstein
Professor Ilya V. Kolmanovsky
Associate Professor Jeffrey T. Scruggs

Ryan James Caverly
caverly@umich.edu
ORCID iD: 0000-0001-7315-7322

© Ryan James Caverly 2018

All Rights Reserved

To my family for always believing in me.

Acknowledgements

First and foremost, I would like to thank my family. My Mom and Dad gave me every opportunity possible to succeed and have always been there for me, even to help me with a number of interstate and international moves. Mehrsa Zahiremami continuously supported me and gave me the motivation to pursue my dreams. My brother Dylan was always willing to listen to me when I was excited to share something new I learned or discovered. I can never thank you all enough for your endless support.

Thank you to my supervisor and mentor, Prof. James Richard Forbes, who has had the single greatest impact on my academic career. From the time I started working with him as an undergraduate student and throughout my Ph.D., Prof. Forbes has gone above and beyond what I could have ever have expected from a research supervisor. I am profoundly grateful for his encouragement and support.

I would also like to thank the members of my dissertation committee, Prof. Dennis Bernstein, Prof. Ilya Kolmanovsky, and Prof. Jeffrey Scruggs, for taking the time to review my work and provide insightful comments and suggestions.

I greatly appreciate the financial support of the Natural Sciences and Engineering Research Council (NSERC) of Canada, the Fonds de recherche du Québec - Nature et technologies (FRQNT), Office of Naval Research (ONR) grant number N00014-13-0383, NASA Armstrong Research Center contract number NNX15CD24P, National Science Foundation (NSF) award number 1550103, and the University of Michigan Aerospace Engineering Department, which made this dissertation possible.

Finally, I would like to thank my fellow Ph.D. students Dr. Leila J. Bridgeman, Dr. Alex Walsh, David E. Zlotnik, as well as all my friends and colleagues at the University of Michigan, McGill University, and Mitsubishi Electric Research Laboratories for their help, guidance, and interesting discussions over these last four years. In particular, this dissertation would not have been possible if not for Dr. Bridgeman's guidance early on in my doctoral studies. Her original insight into minimum gain and the Large Gain Theorem provided the inspiration for this dissertation.

Preface

The novel contributions of this dissertation are listed in this preface. Modified versions of most of this dissertation have appeared as archival journal or conference publications or are currently under review for publication. Any contribution that has appeared in a publication is referenced accordingly in this preface. **The contributions related to minimum gain and optimal output modification in Part II are as follows.**

- Chapter 3
 - A proof that nonminimum phase single-input single-output (SISO) linear time-invariant (LTI) systems have zero minimum gain (Lemma 3.4, p. 26) [1, 2].
 - A proof that multi-input multi-output (MIMO) LTI systems with transmission zeros in the open right-half plane (ORHP) have zero minimum gain (Lemma 3.5, p. 27) [2].
 - The relationship between minimum gain and the minimum singular value of a minimum phase LTI system (Lemma 3.7, p. 28) [3].
 - A proof that a cascaded system has a minimum gain that is the product of minimum gains of the systems within the cascade (Lemma 3.8, p. 29) [4].
 - A sufficient LMI condition for a discrete-time LTI system to have minimum gain (Lemma 3.10, p. 30).
- Chapter 4
 - A direct method to synthesize \mathcal{H}_∞ -optimal static (Section 4.3.1, p. 38) and weighted \mathcal{H}_∞ -optimal dynamic (Section 4.4.1, p. 42) parallel feedforward controllers that lead to a minimum phase augmented system using a non-zero minimum gain constraint [5].
 - An indirect method to synthesize \mathcal{H}_∞ -optimal static (Section 4.3.2, p. 39) and weighted \mathcal{H}_∞ -optimal dynamic (Section 4.4.2, p. 45) parallel feedforward controllers that lead to a minimum phase augmented system using

the inverse of an asymptotically stabilizing feedback controller [5].

- Demonstration of \mathcal{H}_∞ -optimal static and weighted \mathcal{H}_∞ -optimal dynamic parallel feedforward controller synthesis methods on a numerical example with comparison to an analytically-derived \mathcal{H}_∞ -optimal static parallel feedforward controller (Section 5.4, p. 56) [5].

- Chapter 5

- A method to linearly combine a set of system measurements in such a manner that the new system obtained is strictly positive real (SPR) while minimizing the difference in an \mathcal{H}_2 - or \mathcal{H}_∞ - sense between the new system and a given desired system (Section 5.3, p. 54) [6].
- Demonstration of the \mathcal{H}_2 - and \mathcal{H}_∞ -optimal sensor interpolation techniques on numerical simulations of a single degree-of-freedom (DOF) mass-spring system (Section 5.4.1, p. 56) and a 2 DOF flexible-joint robotic manipulator (Section 5.4.2, p. 61) [6].

The contributions related to the Large Gain Theorem in Part III are as follows.

- Chapter 7

- Nyquist stability criterion interpretations of the Large Gain Theorem for SISO (Theorem 7.3, p. 76) and MIMO (Theorem 7.4, p. 77) LTI systems [3, 4].
- Three additional Large Gain Theorem-based stability results for LTI systems using the Nyquist stability criterion (Section 7.3.2, p. 76) [3].

- Chapter 8

- The equivalence of Large Gain Theorem-based robust control and Small Gain Theorem-based robust control for robust stabilization and nominal performance (Section 8.2.2, p. 95 and Section 8.3.2, p. 102).
- A framework to perform robust performance with the Large Gain Theorem that guarantees the closed-loop performance transfer matrix has nonzero minimum gain and is minimum phase (Section 8.4.2, p. 105).
- Definition of a structured minimum singular value (Definition 8.5, p. 98) for the robust stability analysis of systems whose uncertainty is structured and has nonzero minimum gain (Theorem 8.6, p. 98).

- Chapter 9
 - Full-state feedback controller synthesis methods using the Large Gain Theorem for robust stabilization, robust stabilizaiton and nominal performance, and robust performance (Section 9.3, p. 114) [1].
 - Dynamic feedback controller synthesis methods using the Large Gain Theorem for robust stabilization, a special case of robust stabilization and nominal performance, and robust performance (Section 9.4, p. 119).
 - Robust controllers synthesized with the Large Gain Theorem for robust stabilization and robust performance were tested on a numerical benchmark problem and compared to robust controllers synthesized with the Small Gain Theorem (Section 9.5, p. 125).

All proofs, plots, illustrations, text, and numerical results in this dissertation were produced by Ryan J. Caverly. Prof. James R. Forbes provided guidance and suggested edits throughout the dissertation. The sole exceptions are Theorem 7.8 in Chapter 7, which was derived in collaboration with Dr. Richard Pates, and the insight to explore the equivalence of robust control with the Large Gain Theorem and the Small Gain Thoeorem, which was provided by Prof. Jeffrey Scruggs.

Table of Contents

Dedication	ii
Acknowledgements	iii
Preface	iv
List of Figures	xi
List of Tables	xvi
List of Abbreviations	xvii
List of Symbols	xviii
Abstract	xx
Part I Introduction	1
Chapter	
1. Introduction	2
1.1 Motivation and Objectives	3
1.1.1 Minimum Gain and Optimal Output Modification	3
1.1.2 The Large Gain Theorem	4
1.2 Outline and Contributions	5
2. Preliminaries	7
2.1 Signals and Input-Output Theory	7
2.1.1 Vector Spaces and Norms	7
2.1.2 Inner Product Spaces	8
2.1.3 Input-Output Theory	9
2.2 Optimization and LMIs	9

2.2.1	Convex Sets	10
2.2.2	Linear Matrix Inequalities	10
2.3	Linear Systems Theory	13
2.3.1	Stability of Linear Systems	13
2.3.2	\mathcal{H}_∞ and \mathcal{H}_2 Norms of LTI Systems	14
2.3.3	Zeros of Linear Systems	15
2.3.4	The Generalized LTI Plant	17

Part II Minimum Gain and Optimal Output Modification 23

3.	Preliminaries and Introduction to Minimum Gain	24
3.1	Introduction	24
3.2	Minimum Gain	25
3.2.1	Properties of Minimum Gain	26
3.2.2	Numerical Examples of Minimum Gain	32
4.	\mathcal{H}_∞-Optimal Parallel Feedforward Control using Minimum Gain	35
4.1	Introduction	35
4.2	Preliminaries	36
4.2.1	Problem Statement	36
4.2.2	High-Gain Parallel Feedforward Control	37
4.3	Static Parallel Feedforward Controller	38
4.3.1	Direct Method using Minimum Gain	38
4.3.2	Indirect Method using Inversion and Minimum Gain	39
4.3.3	Discussion	41
4.4	Dynamic Parallel Feedforward Controller	41
4.4.1	Direct Method using Minimum Gain	42
4.4.2	Indirect Method using Inversion and Minimum Gain	45
4.4.3	Discussion	47
4.5	Numerical Example	47
4.6	Closing Remarks	50
5.	Linearly Combining Sensor Measurements Optimally to Enforce an SPR Transfer Matrix	51
5.1	Introduction	51
5.2	Preliminaries	52
5.2.1	Problem Statement	53
5.3	Optimal Sensor Interpolation	54
5.3.1	\mathcal{H}_2 -Optimal Sensor Interpolation	55
5.3.2	\mathcal{H}_∞ -Optimal Sensor Interpolation	55

5.3.3	Discussion	55
5.4	Numerical Examples	56
5.4.1	Single DOF Mass-Spring System	56
5.4.2	2 DOF Flexible-Joint Serial Manipulator	61
5.5	Closing Remarks	66
 Part III The Large Gain Theorem		68
 6. Introduction to the Large Gain Theorem		69
6.1	Introduction	69
6.2	The Large Gain Theorem	70
 7. Nyquist Interpretation of the Large Gain Theorem		74
7.1	Introduction	74
7.2	Preliminaries	75
7.3	Main Results	76
7.3.1	Motivation	76
7.3.2	Large Gain Theorem Nyquist Interpretations	76
7.3.3	Comparison of Large Gain Theorem and Small Gain Theorem Nyquist Interpretations	82
7.4	Numerical Examples	83
7.4.1	Large Gain Theorem with LTI MIMO Systems	84
7.4.2	Robust Stabilization Example	86
7.5	Closing Remarks	88
 8. Robust Control with the Large Gain Theorem		90
8.1	Introduction	90
8.2	Robust Stabilization	92
8.2.1	Robust Stabilization with the Small Gain Theorem and the Structured Singular Value	94
8.2.2	Robust Stabilization with the Large Gain Theorem and the Structured Minimum Singular Value	95
8.3	Nominal Performance	100
8.3.1	Nominal Performance with the Small Gain Theorem	102
8.3.2	Nominal Performance with the Large Gain Theorem	102
8.4	Robust Performance	104
8.4.1	Robust Performance with the Small Gain Theorem and the Structured Singular Value	105
8.4.2	Robust Performance with the Large Gain Theorem and the Structured Minimum Singular Value	105

8.4.3	Robust Performance with a Mixed Structured Singular Value	109
8.5	Closing Remarks	109
9.	Robust Controller Synthesis using the Large Gain Theorem	111
9.1	Introduction	111
9.2	Problem Statement	113
9.3	Full-State Feedback Controller Synthesis	114
9.3.1	Robust Stabilization	115
9.3.2	Robust Stabilization and Nominal Performance	116
9.3.3	Robust Performance	118
9.4	Dynamic Feedback Controller Synthesis	119
9.4.1	Robust Stabilization	119
9.4.2	Robust Stabilization and Nominal Performance	122
9.4.3	Robust Performance	123
9.5	Numerical Example	125
9.5.1	Robust Stabilization with Full-State Feedback	129
9.5.2	Robust Stabilization with Dynamic Output Feedback	130
9.5.3	Robust Performance with Full-State Feedback	132
9.5.4	Robust Performance with Dynamic Output Feedback	134
9.5.5	Discussion	137
9.6	Closing Remarks	138
Part IV	Conclusion	145
10.	Closing Remarks and Future Work	146
Appendix	149
Bibliography	157

List of Figures

Figure

2.1	Block diagram of the generalized plant \mathbf{G} with the controller \mathcal{G}_c . . .	17
2.2	Block diagram of the basic servo loop with plant $\mathbf{G}_p(s)$, controller $\mathbf{G}_c(s)$, and weighting transfer matrices $\mathbf{W}_r(s)$, $\mathbf{W}_d(s)$, and $\mathbf{W}_n(s)$. .	18
2.3	Block diagram of the generalized plant \mathbf{G} with the uncertainty Δ and the controller \mathcal{G}_c	20
2.4	Block diagram of the basic servo loop with plant $\mathbf{G}_p(s)$, uncertainty $\Delta(s)$, weighting transfer matrix $\mathbf{W}_\Delta(s)$, and controller $\mathbf{G}_c(s)$	21
3.1	Bode magnitude plot of $G_1(s)$ and $G_2(s)$ with $k = 1$ in Example 3.12. Black dashed lines represent $\nu^* = \inf_{\omega \in \mathbb{R}_{\geq 0}} G(j\omega) $ of each system. .	33
3.2	Plots of the minimum singular value of $\mathbf{G}_1(s)$, $\mathbf{G}_2(s)$, and $\mathbf{G}_4(s)$ versus frequency with $k = 1$ in Examples 3.13 and 3.14. Black dashed lines represent $\nu^* = \inf_{\omega \in \mathbb{R}_{\geq 0}} \underline{\sigma}\{\mathbf{G}(j\omega)\}$ of each system.	33
4.1	Block diagrams of (a) the plant and (b) the plant augmented with a parallel feedforward controller.	36
4.2	Bode plots of $G(s)$, $\bar{G}(s) = G(s) + k_{\text{ff}}$, $\bar{G}(s) = G(s) + G_{\text{ff},1}(s)$, and $\bar{G}(s) = G(s) + G_{\text{ff},2}(s)$. The magnitudes of $\bar{G}(s) = G(s) + G_{\text{ff},1}(s)$ and $\bar{G}(s) = G(s) + G_{\text{ff},2}(s)$ more closely match the magnitude of $G(s)$ at low frequencies compared to $\bar{G}(s) = G(s) + k_{\text{ff}}$, as a result of the chosen weighting functions $W_1(s) = 4 \times 10^{-8}(s + 500)^2/(s + 1)^2$ and $W_2(s) = (s + 1)^2/(s + 500)^2$	48
4.3	Bode plots of k_{ff} , $G_{\text{ff},1}(s)$, and $G_{\text{ff},2}(s)$. The gain of $G_{\text{ff},1}(s)$ is the lowest of the three parallel feedforward controllers for all frequencies.	49
5.1	Block diagrams of (a) the plant with interpolated sensor measurements, and (b) the error between the plant with interpolated sensor measurements and the desired plant.	54
5.2	Schematic of the mass-spring system from the numerical example of Section 5.4.1.	57
5.3	Bode plots of $G_d(s)$, $\bar{G}_{\mathcal{H}_2}(s)$, and $\bar{G}_{\mathcal{H}_\infty}(s)$ in the numerical example of Section 5.4.1. The gains of $\bar{G}_{\mathcal{H}_2}(s)$ and $\bar{G}_{\mathcal{H}_\infty}(s)$ closely match the gain of $G_d(s)$ at low frequencies. The Bode phase plot shows that $G_d(s)$ is not positive real, while $\bar{G}_{\mathcal{H}_2}(s)$ and $\bar{G}_{\mathcal{H}_\infty}(s)$ are.	58

5.4	Bode plots of the transfer matrices $\tilde{G}_{\mathcal{H}_2}(s) = \bar{G}_{\mathcal{H}_2}(s) - G_d(s)$ and $\tilde{G}_{\mathcal{H}_\infty}(s) = \bar{G}_{\mathcal{H}_\infty}(s) - G_d(s)$ in the numerical example of Section 5.4.1.	58
5.5	Block diagram of the system $\bar{\mathbf{G}}(s)$ in a negative feedback interconnection with a controller $\mathbf{G}_c(s)$, where $\mathbf{r}(s)$ is the reference signal that $\bar{\mathbf{y}}(s)$ should track and $\mathbf{n}(s)$ is measurement noise.	59
5.6	Closed-loop responses of $y_d(t)$ and the tracking error $y_d(t) - r(t)$ for both the \mathcal{H}_2 - and \mathcal{H}_∞ -optimal sensor interpolations in the numerical example of Section 5.4.1. The tracking error is less with the \mathcal{H}_∞ -optimal sensor interpolation during the nonzero portion of the reference trajectory, as the gain of $\tilde{G}_{\mathcal{H}_\infty}(s)$ is less than the gain of $\tilde{G}_{\mathcal{H}_2}(s)$ at lower frequencies.	60
5.7	Closed-loop responses of $\bar{y}(t)$ and the tracking error $\bar{y}(t) - r(t)$ for both the \mathcal{H}_2 - and \mathcal{H}_∞ -optimal sensor interpolations in the numerical example of Section 5.4.1.	61
5.8	Plots of the maximum singular values and minimum Hermitian parts of $\mathbf{G}_d(s)$, $\bar{\mathbf{G}}_{\mathcal{H}_2}(s)$, and $\bar{\mathbf{G}}_{\mathcal{H}_\infty}(s)$ in the numerical example of Section 5.4.2. The gain of $\bar{\mathbf{G}}_{\mathcal{H}_\infty}(s)$ closely matches the gain of $\mathbf{G}_d(s)$ at low frequencies, whereas the gain of $\bar{\mathbf{G}}_{\mathcal{H}_2}(s)$ is deviates less from the gain of $\mathbf{G}_d(s)$ compared to $\bar{\mathbf{G}}_{\mathcal{H}_\infty}(s)$ over all frequencies. The minimum Hermitian part plot shows that $\mathbf{G}_d(s)$ is not positive real, while $\bar{\mathbf{G}}_{\mathcal{H}_2}(s)$ and $\bar{\mathbf{G}}_{\mathcal{H}_\infty}(s)$ are.	62
5.9	Plots of the maximum singular values and minimum Hermitian parts of $\tilde{\mathbf{G}}_{\mathcal{H}_2}(s) = \bar{\mathbf{G}}_{\mathcal{H}_2}(s) - \mathbf{G}_d(s)$ and $\tilde{\mathbf{G}}_{\mathcal{H}_\infty}(s) = \bar{\mathbf{G}}_{\mathcal{H}_\infty}(s) - \mathbf{G}_d(s)$	63
5.10	Closed-loop responses of (a) $y_{d1}(t)$ and $y_{d2}(t)$, and (b) the tracking errors $y_{d1}(t) - r_1(t)$ and $y_{d2}(t) - r_2(t)$ for both the \mathcal{H}_2 - and \mathcal{H}_∞ -optimal sensor interpolations in the numerical example of Section 5.4.2. The tracking error is less with the \mathcal{H}_∞ -optimal sensor interpolation during the nonzero portion of the reference trajectory, as the maximum singular value of $\tilde{\mathbf{G}}_{\mathcal{H}_\infty}(s)$ more closely matches that of $\mathbf{G}_d(s)$ at lower frequencies than the maximum singular value of $\tilde{\mathbf{G}}_{\mathcal{H}_2}(s)$ does.	65
5.11	Closed-loop responses of (a) $\bar{y}_1(t)$ and $\bar{y}_2(t)$, and (b) the tracking errors $\bar{y}_1(t) - r_1(t)$ and $\bar{y}_2(t) - r_2(t)$ for both the \mathcal{H}_2 - and \mathcal{H}_∞ -optimal sensor interpolations in the numerical example of Section 5.4.2.	66
6.1	A negative feedback interconnection involving \mathcal{G}_1 and \mathcal{G}_2	70
7.1	Plots of the regions (shaded pink) that the Nyquist plot of $-1 + \det(\mathbf{1} + \mathbf{L}(s))$ cannot lie based on the conditions set forth in the (a) Small Gain Theorem and (b) Large Gain Theorem. Example Nyquist plots of $-1 + \det(\mathbf{1} + \mathbf{L}(s))$ that satisfy these theorems are illustrated in blue. Note that the Nyquist plot of $-1 + \det(\mathbf{1} + \mathbf{L}(s))$ in (b) could also lie to the right or the left of the unit disk, and does not necessarily encircle the point $(-1, 0)$	83

7.2	(a) Plots of the minimum singular value of $\mathbf{G}_1(s)$ and $\mathbf{G}_2(s)$ versus frequency with $k = 1$ in Example 7.12. Black dashed lines represent $\nu^* = \inf_{\omega \in \mathbb{R}^+} \underline{\sigma}\{\mathbf{G}(j\omega)\}$ of each system. (b) Nyquist plots of $-1 + \det(\mathbf{1} + \mathbf{L}(s))$ for Example 7.12 with $k = 1$. The Nyquist plots are generated on a logarithmic scale, where the gridlines are red, except for the 0 dB gridline, which is a black dashed line. The point $(-1, 0)$ is labeled by a black circular marker.	84
7.3	(a) Plots of the minimum singular value of $\mathbf{G}_1(s)$ and $\mathbf{G}_2(s)$ versus frequency with $k = 0.45$ in Example 7.13. Black dashed lines represent $\nu^* = \inf_{\omega \in \mathbb{R}^+} \underline{\sigma}\{\mathbf{G}(j\omega)\}$ of each system. (b) Nyquist plots of $-1 + \det(\mathbf{1} + \mathbf{L}(s))$ for Example 7.13 with $k = 0.45$. The Nyquist plots are generated on a logarithmic scale, where the gridlines are red, except for the 0 dB gridline, which is a black dashed line. The point $(-1, 0)$ is labeled by a black circular marker.	85
7.4	Block diagram of the system considered in the robust control Example 7.15.	87
7.5	Block diagrams used in Example 7.15 of (a) the nominal closed-loop system in a feedback interconnection with the uncertainty $\Delta(s)$ and (b) the nominal closed-loop system in a feedback interconnection with the uncertainty $\Delta(s)$, where the contents of the transfer matrix $\mathbf{G}_{CL}(s)$ have been expanded.	88
7.6	Nyquist plot of the transfer function $L(s) = G_{CLqp}(s)\Delta(s)$ in Example 7.15, where $k_p = 2$, $\delta = 1.1$ and $b = 5$ rad/s. Notice that the Nyquist plot encircles the point $(-1, 0)$ once in the CCW direction, which corresponds to the number of CRHP poles of $L(s)$. The Nyquist plots are generated on a logarithmic scale, where the gridlines are red, except for the 0 dB gridline, which is a black dashed line. The point $(-1, 0)$ is labeled by a black circular marker.	89
8.1	Feedback interconnection involving the nominal plant \mathcal{G} , the controller \mathcal{G}_c , and the uncertainty Δ	92
8.2	Feedback interconnection involving the nominal closed-loop system \mathcal{G}_{CLqp} and the uncertainty Δ	93
8.3	Feedback interconnection involving the inverted nominal closed-loop system $\bar{\mathbf{G}}_{CLpq} = \mathbf{G}_{CLqp}^{-1}$ and the uncertainty $\bar{\Delta} = \Delta^{-1}$	96
8.4	Feedback interconnection involving the nominal closed-loop system $\hat{\mathbf{G}}_{CLqp}$ and the uncertainty $\hat{\Delta}$, where a loop transformation with $\hat{\mathbf{D}}_{33}$ has been performed.	98
8.5	Feedback interconnection involving the nominal plant \mathcal{G} , the controller \mathcal{G}_c , and the uncertainty Δ , with the exogenous input signal \mathbf{w} and the performance output signal \mathbf{z}	100
8.6	Feedback interconnection involving the nominal closed-loop system \mathcal{G}_{CL} and the uncertainty Δ , with the exogenous input signal \mathbf{w} and the performance output signal \mathbf{z}	101

8.7	Feedback interconnection involving the LTI nominal closed-loop system \mathbf{G}_{CL} and the uncertainty Δ , with the exogenous input signal \mathbf{w} and the performance output signal \mathbf{z}	102
8.8	Feedback interconnection involving the LTI nominal closed-loop system \mathbf{G}_{CL} and the uncertainty Δ , which when combined yield the uncertain closed-loop system $\mathbf{G}_{\text{CL}\Delta zw}$	104
8.9	Equivalent feedback interconnections of $\tilde{\mathbf{G}}_{\text{CL}}$ and $\tilde{\Delta}$ used for robust performance, where the contents of $\tilde{\mathbf{G}}_{\text{CL}}$ and $\tilde{\Delta}$ are expanded in (a) and written compactly in (b).	106
8.10	Equivalent feedback interconnections of (a) $\mathbf{G}_{\text{CL}\Delta zw}$ and Δ_P and (b) $\tilde{\mathbf{G}}_{\text{CL}}$, Δ , and Δ_P used for the proof of Theorem 8.11.	107
9.1	Feedback interconnection involving the nominal plant \mathbf{G} , the controller \mathbf{G}_c , and the uncertainty Δ	113
9.2	Schematic of the mass-spring system from the numerical example of Section 9.5	125
9.3	Block diagram of the generalized plant \mathbf{G} and uncertainty Δk in the numerical example of Section 9.5.	127
9.4	Block diagram of the generalized plant $\hat{\mathbf{G}}$ and uncertainty $\Delta \hat{k} = \Delta k / (1 + \Delta k D_{33})$ following a loop transformation in the numerical example of Section 9.5.	128
9.5	Block diagram of the inverted generalized plant $\bar{\mathbf{G}}$ and uncertainty $\Delta \bar{k} = \Delta \hat{k}^{-1}$ in the numerical example of Section 9.5.	129
9.6	Closed-loop response of $x_2(t)$ and the control inputs $u_1(t)$ and $u_2(t)$ for $0.5 \leq k \leq 2$ with full-state feedback controllers designed using the (a) Small Gain Theorem and (b) the Large Gain Theorem for robust performance.	140
9.7	Closed-loop response of $x_2(t)$ and the control inputs $u_1(t)$ and $u_2(t)$ for $-1.81 \leq k \leq 12.5$ with a full-state feedback controller designed using the Small Gain Theorem for robust performance.	141
9.8	Closed-loop response of $x_2(t)$ and the control inputs $u_1(t)$ and $u_2(t)$ for $-1071 \leq k \leq 12.5$ with a full-state feedback controller designed using the Large Gain Theorem for robust performance.	141
9.9	Closed-loop response of $x_2(t)$ and the control inputs $u_1(t)$ and $u_2(t)$ for $0.5 \leq k \leq 2$ with dynamic output feedback controllers designed using the (a) Small Gain Theorem and (b) the Large Gain Theorem for robust performance.	142
9.10	Closed-loop response of $x_2(t)$ and the control inputs $u_1(t)$ and $u_2(t)$ for $0.023 \leq k \leq 2.946$ with a dynamic output feedback controller designed using the Small Gain Theorem for robust performance. . .	143
9.11	Closed-loop response of $x_2(t)$ and the control inputs $u_1(t)$ and $u_2(t)$ for $0.001 \leq k \leq 12.21$ with a dynamic output feedback controller designed using the Large Gain Theorem for robust performance. . .	143

9.12 Closed-loop response of $x_2(t)$ and the control inputs $u_1(t)$ and $u_2(t)$ for $0.5 \leq k \leq 2$ and measurement noise of $n(t) = 0.001 \sin(200\pi t)$ with dynamic output feedback controllers designed using the (a) Small Gain Theorem and (b) the Large Gain Theorem for robust performance. 144

List of Tables

Table

9.1	Robustness properties of the closed-loop system with full-state feedback designed for robust stabilization in Section 9.5.1, including the gain margin for robust stability using either the Small Gain Theorem or Large Gain Theorem and the range of k for which the closed-loop system is asymptotically stable.	130
9.2	Robustness properties of the closed-loop system with dynamic output feedback designed for robust stabilization in Section 9.5.2, including the gain margin for robust stability using either the Small Gain Theorem or Large Gain Theorem and the range of k for which the closed-loop system is asymptotically stable.	131
9.3	Robustness properties of the closed-loop system with full-state feedback designed for robust performance in Section 9.5.3, including the gain margin (GM) for robust performance using either the Small Gain Theorem or Large Gain Theorem, the range of k for which the closed-loop system is asymptotically stable (AS), the range of k for which $\ \mathbf{G}_{\text{CL}\Delta zw}\ _{\infty} < 0.5$, and the range of k for which $\mathbf{G}_{\text{CL}\Delta zw}(s)$ is minimum phase.	133
9.4	Robustness properties of the closed-loop system with dynamic output feedback designed for robust performance in Section 9.5.4, including the gain margin (GM) for robust performance using either the Small Gain Theorem or Large Gain Theorem, the range of k for which the closed-loop system is asymptotically stable (AS), the range of k for which $\ \mathbf{G}_{\text{CL}\Delta zw}\ _{\infty} < 0.5$, and the range of k for which $\mathbf{G}_{\text{CL}\Delta zw}(s)$ is minimum phase.	135

List of Abbreviations

AS	asymptotically stable
ASPR	almost strictly positive real
BMI	bilinear matrix inequality
CCW	counter-clockwise
CRHP	closed right-half plane
CW	clockwise
DOF	degree-of-freedom
GM	gain margin
KYP	Kalman-Yakubovich-Popov
LFT	linear fractional transformation
LMI	linear matrix inequality
LTI	linear time-invariant
MIMO	multiple-input multiple-output
OLHP	open left-half plane
ORHP	open right-half plane
PR	positive real
SISO	single-input single-output
SPR	strictly positive real

List of Symbols

\mathcal{X}	a normed inner-product space
\mathcal{X}_e	an extended normed inner-product space
$\langle \cdot, \cdot \rangle$	a generic inner product
$\ \cdot\ $	a generic norm
\mathcal{L}_2	the Lebesgue space
\mathcal{L}_{2e}	the extended Lebesgue space
\mathbb{R}	the set of real numbers
\mathbb{C}	the set of complex numbers
$\mathbb{R}_{>0}, \mathbb{R}_{\geq 0}, \dots$	real numbers in the interval $(0, \infty), [0, \infty), \dots$
$\text{tr}(\cdot)$	trace
$\det(\cdot)$	determinant
$(\cdot)^T$	transpose
$(\cdot)^H$	complex conjugate transpose
$\mathcal{G} : (\cdot) \rightarrow (\cdot)$	operator
$\mathbf{G} : (\cdot) \rightarrow (\cdot)$	linear operator
$G(s)$	transfer function
$\mathbf{G}(s)$	transfer matrix
$\mathbf{0}$	matrix filled with zeros

$\mathbf{1}$	identity matrix
$\text{diag}\{\mathbf{M}_1, \dots, \mathbf{M}_n\}$	matrix with block diagonals $\mathbf{M}_1, \dots, \mathbf{M}_n$, and zeros elsewhere
$\mathbf{M} = \mathbf{M}^T > 0$	matrix \mathbf{M} is positive definite. Positive semidefinite, negative definite, and negative semidefinite are denoted similarly
*	symmetric portion of a matrix
$\lambda_i(\cdot)$	eigenvalue of a matrix
$\sigma_i(\cdot)$	singular value of a matrix
$\bar{\sigma}(\cdot), \underline{\sigma}(\cdot)$	maximum and minimum singular values
$\text{wno}\{G(s)\}$	number of counter-clockwise (CCW) encirclements of the origin made by the Nyquist plot of the transfer function $G(s)$, also known as the winding number about the origin
$\bar{\eta}(\mathbf{G}(s))$	number of closed right-half plane (CRHP) poles of the transfer matrix $\mathbf{G}(s)$ counted according to the Smith-McMillan degree [7, p. 154]
$\text{Re}\{\cdot\}$	real part of a complex number
$\text{Im}\{\cdot\}$	imaginary part of a complex number
$\mathcal{X} \rightarrow \mathcal{Y}$	a mapping from \mathcal{X} to \mathcal{Y}
$x \rightarrow y$	x approaches y
\iff	if and only if
\implies	implies
\forall	for all
$ \cdot $	absolute value
$\mathcal{L}(\cdot)$	Laplace transform
$\mathcal{F}_u(\cdot, \cdot)$	upper linear fractional transformation (LFT)

Abstract

When confronted with a control problem, the input-output properties of the system to be controlled play an important role in determining strategies that can or should be applied, as well as the achievable closed-loop performance. Optimal output modification is a process in which the system output is modified in such a manner that the modified system has a desired input-output property and the modified output is as similar as possible to a specified desired output. The first part of this dissertation develops linear matrix inequality (LMI)-based optimal output modification techniques to render a linear time-invariant (LTI) system minimum phase using parallel feedforward control or strictly positive real by linearly interpolating sensor measurements. \mathcal{H}_∞ -optimal parallel feedforward controller synthesis methods that rely on the input-output system property of minimum gain are derived and tested on a numerical example. The \mathcal{H}_2 - and \mathcal{H}_∞ -optimal sensor interpolation techniques are implemented in numerical simulations of noncollocated elastic mechanical systems.

All mathematical models of physical systems are, to some degree, uncertain. Robust control can provide a guarantee of closed-loop stability and/or performance of a system subject to uncertainty, and is often performed using the well-known Small Gain Theorem. The second part of this dissertation introduces the lesser-known Large Gain Theorem and establishes its use for robust control. A proof of the Large Gain Theorem for LTI systems using the familiar Nyquist stability criterion is derived, with the goal of drawing parallels to the Small Gain Theorem and increasing the understanding and appreciation of this theorem within the control systems community. LMI-based robust controller synthesis methods using the Large Gain Theorem are presented and tested numerically on a robust control benchmark problem with a comparison to \mathcal{H}_∞ robust control. The numerical results demonstrate the practicality of performing robust control with the Large Gain Theorem, including its ability to guarantee an uncertain closed-loop system is minimum phase, which is a robust performance problem that previous robust control techniques could not solve.

Part I

Introduction

Chapter 1

Introduction

A certainty in science and engineering is that all mathematical models of physical systems are, to some degree, wrong. Every model contains a degree of uncertainty and is therefore only an approximation of the actual system. Control systems engineers often rely on uncertain models to design controllers that shape a system's behavior, making it imperative that the properties and limitations of the model are fully understood when the controller is designed and eventually implemented in practice. For example, a mathematical aircraft model will never contain exact information of the aircraft's mass, aerodynamic properties, structural dynamics, and mechanical degradation, but will still be used to predict its behavior and design a flight controller. One possible approach to deal with an uncertain model is to determine system properties that are invariant to the possible model uncertainty, such as input-output properties of the system. If it can be shown that the uncertain system maintains useful properties, such as being minimum phase, passive, finite gain, interior conic, or exterior conic, then an appropriate control technique and stability result can be used to determine robust stability properties of the uncertain closed-loop system. When a system does not exactly meet the desired input-output properties, it is sometimes possible to use a slight modification of the system output to correct this, which is known as output modification. Another approach to the control of uncertain systems, is to determine a set of uncertainty that contains all possible inaccuracies and design a controller that provides stability and/or performance guarantees for the entire uncertainty set. This is the approach used in many robust control techniques, including the \mathcal{H}_∞ control framework, which relies on the well-known input-output stability result of the Small Gain Theorem.

1.1 Motivation and Objectives

This dissertation is presented into two parts. The first part focuses on the relatively new concept of minimum gain and optimal output modification, which is a technique to perform output modification in such a manner that the modified output is as similar as possible to a desired system output. The second part introduces the Large Gain Theorem, a little known input-output stability theorem, and presents the framework for it be used for robust control, much like the Small Gain Theorem is used for \mathcal{H}_∞ robust control.

1.1.1 Minimum Gain and Optimal Output Modification

Minimum gain is a system property related to a lower bound on the gain of the system. Despite being a relatively simple concept, it was only formally defined for systems with quiescent initial conditions by Zahedzadeh et al. in 2008 [8] and more generally for systems with nonzero initial conditions by Bridgeman and Forbes in 2015 [9]. Minimum gain is a property that is relevant to both linear systems and nonlinear system, however the calculation of minimum gain for linear time-invariant (LTI) systems is much more established and can be accomplished using a linear matrix inequality (LMI) approach [9]. As minimum gain was only recently defined, the literature on this topic and its uses is quite limited [8–12]. The Large Gain Theorem [8], which is an input-output stability theorem discussed in the second part of this dissertation, is the primary application of minimum gain. Minimum gain has been used within this context to demonstrate the robust stabilization of certain classes of system in [9, 11, 12]. One of the objectives of this dissertation is to provide insight into some of the properties of minimum gain in an effort to determine more useful applications of minimum gain.

Output modification is a well-known concept that is found in the literature under many different names, including parallel feedforward control [13], positivity embedding [14–17], sensor selection [18–21], zero assignment [22], zero shaping [23, 24], squaring up [25–27], and μ -tip control [28, 29]. At their core, these techniques are all based on the notion of adjusting a system’s output (and/or input) to enforce some desired input-output properties on the modified system. This dissertation focuses on output modification for LTI systems that is capable on rendering a modified system minimum phase using parallel feedforward control or strictly positive real (SPR) using sensor interpolation, which is similar to positivity embedding. The main objective of the proposed output modification techniques is that they are performed in

an optimal manner. When modifying the output of a system, the modified system output may be substantially different from the original output in order to meet the desired specifications. This is undesirable, as a well-behaved output in this case does not necessarily correspond to a well-behaved original output. For example, consider a situation where output modification is performed on an aircraft whose original output is pitch rate and a desired pitch rate is to be tracked. In this example, if the modified output is capable of tracking the desired pitch rate, but is considerably different than the original output, then it is unknown whether the true pitch rate tracking error performance is acceptable. In order to avoid situations like this, it is necessary to perform output modification optimally. The parallel feedforward controller synthesis methods in this dissertation focus on minimizing the difference between the original system and the modified system in an \mathcal{H}_∞ - or a frequency-dependent weighted \mathcal{H}_∞ -sense. The enforcement of an SPR transfer matrix by sensor interpolation is tasked with minimizing the difference between a system with a desired output and the modified system in an \mathcal{H}_2 - or \mathcal{H}_∞ -sense.

1.1.2 The Large Gain Theorem

Input-output stability theory, pioneered in the 1960's by Zames [30] and Sandberg [31], is widely used in many areas of control systems engineering, including robust, nonlinear, and optimal control. Input-output stability theorems are capable of determining the input-output stability of a negative feedback interconnection, which is of fundamental importance in of control systems engineering. Most notably, the Small Gain Theorem [30] and the Passivity Theorem [30] are input-output stability results that are regularly used in robust control. It was recently shown in [32] that every input-output stability result that makes use of information about norms and inner products of inputs and outputs, including gain [30], passivity [30, 33], conic sectors [30], passivity indices [34], γ -passivity [35], β -bounds [36], and minimum gain [8, 9], are all special cases of the Extended Conic Sector Theorem [37].

The Large Gain Theorem, whose concept was introduced in [38] and formalized in [8, 9], is one special case of the Extended Conic Sector Theorem that makes use of the property of minimum gain. The Large Gain Theorem is similar to the Small Gain Theorem, in that it only considers information on the gain of two systems within a negative feedback without regard for the phase of the systems. The difference between the Large Gain Theorem and the Small Gain Theorem is that the Large Gain Theorem involves lower bounds on the gains of the systems within a negative feedback interconnection, while the Small Gain Theorem involves upper bounds on

the gains of these systems. This can be thought of as a duality between the two input-output stability results, which is discussed throughout this dissertation. Although the Small Gain Theorem is a widely-used result, thus far, the Large Gain Theorem has few applications [9, 11, 12]. The work of [9] includes a numerical example where the Large Gain Theorem is used to guarantee robust input-output stability of a simple single-input single-output (SISO) linear system. Feedforward controllers are designed in [11, 12] using the Large Gain Theorem to stabilize a class of nonlinear systems in Lur'e form [11] and a class of SISO Takagi-Sugeno fuzzy systems [12].

The Large Gain Theorem is a much less intuitive input-output stability result than the Small Gain Theorem, which is potentially why its applications are limited. Existing proofs of the Large Gain Theorem in the literature use input-output stability theory [8, 9], which provide mathematically rigorous explanations of the theorem, but little intuition. This dissertation aims to improve intuition of the Large Gain Theorem by developing an alternate proof for LTI systems using the well-known Nyquist stability criterion. The second aim of this part of the dissertation is to provide a means for the Large Gain Theorem to be used for robust control, in a similar manner to the Small Gain Theorem, including effective robust controller synthesis methods. Due to the differences between the Large Gain Theorem and the Small Gain Theorem, this will ultimately allow for new types of robust control problems to be posed and solved.

1.2 Outline and Contributions

General concepts and theory used throughout this dissertation are reviewed in Chapter 2, including signals and input-output theory, optimization and LMIs, and linear systems theory. Part II is dedicated to the concepts of minimum gain and optimal output modification. Part II begins with Chapter 3, which introduces the definition, important properties, and numerical examples of minimum gain. Chapters 4 and 5 are devoted to optimal output modification strategies. In particular, Chapter 4 presents the synthesis of \mathcal{H}_∞ -optimal parallel feedforward controllers that are capable of rendering an LTI system minimum phase and make use of the properties of minimum gain. Chapter 5 addresses a different output modification problem, namely the task of selecting a linear combination of available sensor measurements to render an LTI system SPR in an \mathcal{H}_2 - or \mathcal{H}_∞ -optimal manner.

Part III of this dissertation focuses on the Large Gain Theorem. Chapter 6 introduces the Large Gain Theorem and compares its significance and relevance to

other input-output stability results, including the well-known Small Gain Theorem. Chapter 7 proves the Large Gain Theorem for LTI systems using the Nyquist stability criterion and presents additional stability results for feedback interconnections of LTI systems based on the Large Gain Theorem. Chapters 8 and 9 cover the notion of using the Large Gain Theorem for robust control in a very similar manner to how the Small Gain Theorem is often used in robust control. Specifically, Chapter 8 includes the framework in which the Large Gain Theorem can be used to solve robust stabilization, nominal performance, and robust performance problems, as well as the definition of a new structured minimum singular value. Chapter 9 presents full-state feedback and dynamic output feedback controller synthesis methods to solve the robust control problems discussed in Chapter 8 and demonstrates the controllers' abilities on a numerical benchmark problem. Chapter 10 in Part IV summarizes the importance of the contributions in this dissertation and suggests future research directions. A detailed list of the novel contributions presented in this dissertation and the publications in which they appear is found in the Preface.

Chapter 2

Preliminaries

The work of this dissertation relies heavily on input-output theory, optimization, and linear systems theory. As such, a brief review of each of these topics is provided in this chapter. In particular, Section 2.1 focuses on the properties of signals and input-output theory, Section 2.2 is concerned with convex optimization and LMIs, and Section 2.3 reviews relevant linear systems theory.

2.1 Signals and Input-Output Theory

The inputs and outputs of a system are signals, whose properties determine the system's input-output characteristics.

2.1.1 Vector Spaces and Norms

Definition 2.1 (Vector Space [39]). Consider the space \mathcal{V} and field \mathbb{F} . The operations of vector addition and scalar multiplication are defined as

1. for every pair $\mathbf{u}, \mathbf{v} \in \mathcal{V}$, a unique element $\mathbf{z} = \mathbf{u} + \mathbf{v} \in \mathcal{V}$ is assigned and called their sum, and
2. for all $a \in \mathbb{F}$ and $\mathbf{u} \in \mathcal{V}$, there is a unique element $\mathbf{v} = a\mathbf{u} \in \mathcal{V}$ called their product.

The space \mathcal{V} is a vector space if the following properties hold for all $\mathbf{u}, \mathbf{v}, \mathbf{w} \in \mathcal{V}$ and for all $a, b \in \mathbb{F}$, for addition

1. there exists an additive identity, denoted $\mathbf{0} \in \mathcal{V}$, such that $\mathbf{u} + \mathbf{0} = \mathbf{u}$,
2. there exists an inverse, denoted $-\mathbf{u} \in \mathcal{V}$, such that $\mathbf{u} + (-\mathbf{u}) = \mathbf{0}$,

3. the commutativity relationship $\mathbf{u} + \mathbf{v} = \mathbf{v} + \mathbf{u}$ holds,
4. the associativity property $\mathbf{u} + (\mathbf{v} + \mathbf{w}) = (\mathbf{u} + \mathbf{v}) + \mathbf{w}$ holds,

and for multiplication

1. there exists a multiplicative identity, denoted $1 \in \mathbb{F}$, such that $1\mathbf{u} = \mathbf{u}$,
2. the associativity property $a(b\mathbf{u}) = (ab)\mathbf{u}$ holds,
3. the vector distributivity property $a(\mathbf{u} + \mathbf{v}) = a\mathbf{u} + b\mathbf{v}$ holds, and
4. the scalar distributivity property $(a + b)\mathbf{u} = a\mathbf{u} + b\mathbf{u}$.

Definition 2.2 (Vector Norm [39]). A norm $\|\cdot\|$ on a vector space \mathcal{V} is a function that maps $\mathcal{V} \rightarrow \mathbb{R}_{\geq 0}$, for all $\mathbf{u} \in \mathcal{V}$ that satisfies

1. $\|\mathbf{u}\| = 0$ if and only if $\mathbf{u} = \mathbf{0}$,
2. $\|a\mathbf{u}\| = |a| \|\mathbf{u}\|$ for all $a \in \mathbb{F}$, and
3. the triangle inequality $\|\mathbf{u} + \mathbf{v}\| \leq \|\mathbf{u}\| + \|\mathbf{v}\|$, for all $\mathbf{v} \in \mathcal{V}$.

2.1.2 Inner Product Spaces

Definition 2.3 (Inner Product [39]). An inner product $\langle \cdot, \cdot \rangle$ on a vector space \mathcal{V} is a function mapping $\mathcal{V} \times \mathcal{V} \rightarrow \mathbb{F}$ such that

1. for all $\mathbf{u} \in \mathcal{V}$, $\langle \mathbf{u}, \mathbf{u} \rangle \geq 0$,
2. for all $\mathbf{u} \in \mathcal{V}$, $\langle \mathbf{u}, \mathbf{v} \rangle = 0$ if and only if $\mathbf{v} = \mathbf{0}$,
3. for all $\mathbf{u}, \mathbf{v}, \mathbf{w} \in \mathcal{V}$ and $a, b \in \mathbb{F}$, $\langle \mathbf{u}, a\mathbf{v} + b\mathbf{w} \rangle = a \langle \mathbf{u}, \mathbf{v} \rangle + b \langle \mathbf{u}, \mathbf{w} \rangle$. This condition implies that the mapping $\mathbf{u} \mapsto \langle \mathbf{v}, \mathbf{u} \rangle$ is linear on \mathcal{V} .

Definition 2.4 (Inner Product Space [40]). Given an inner product $\langle \cdot, \cdot \rangle : \mathbb{R}^n \times \mathbb{R}^n \rightarrow \mathbb{R}$, an inner product space, \mathcal{X} , is defined by

$$\mathcal{X} = \left\{ \mathbf{x} : \mathbb{R}_{\geq 0} \rightarrow \mathbb{R}^n \mid \|\mathbf{x}\|^2 = \int_0^{\infty} \langle \mathbf{x}(t), \mathbf{x}(t) \rangle dt < \infty \right\}.$$

The extended inner product space, \mathcal{X}_e , is given by

$$\mathcal{X}_e = \left\{ \mathbf{x} : \mathbb{R}_{\geq 0} \rightarrow \mathbb{R}^n \mid \|\mathbf{x}\|_T^2 = \int_0^T \langle \mathbf{x}(t), \mathbf{x}(t) \rangle dt < \infty, \forall T \in \mathbb{R}_{\geq 0} \right\}.$$

Definition 2.5 (Lebesgue Space [40]). The Lebesgue space, \mathcal{L}_2 , is an inner product space, and is given by all square integral functions defined by

$$\mathcal{L}_2 = \left\{ \mathbf{x} : \mathbb{R}_{\geq 0} \rightarrow \mathbb{R}^n \mid \|\mathbf{x}\|_2^2 = \int_0^\infty \mathbf{x}^\top(t)\mathbf{x}(t)dt < \infty \right\}.$$

The extended Lebesgue space, \mathcal{L}_{2e} , is given by

$$\mathcal{L}_{2e} = \left\{ \mathbf{x} : \mathbb{R}_{\geq 0} \rightarrow \mathbb{R}^n \mid \|\mathbf{x}\|_{2T}^2 = \int_0^T \mathbf{x}^\top(t)\mathbf{x}(t)dt < \infty, \forall T \in \mathbb{R}_{\geq 0} \right\}.$$

Definition 2.6 (\mathcal{L}_∞ Space [40]). A function $\mathbf{u} \in \mathcal{L}_\infty$ if

$$\|\mathbf{u}\|_\infty = \sup_{t \in \mathbb{R}_{\geq 0}} \left[\max_{i=1, \dots, n} |u_i(t)| \right] < \infty,$$

where $\mathbf{u}^\top(t) = [u_1(t) \ \cdots \ u_n(t)]$.

2.1.3 Input-Output Theory

Definition 2.7 (Input-Output Stable [41]). The system $\mathbf{y} = \mathcal{G}\mathbf{u}$, with the operator $\mathcal{G} : \mathcal{X}_e \rightarrow \mathcal{X}_e$, is input-output stable if $\mathcal{G}\mathbf{u} \in \mathcal{X}$ for all $\mathbf{u} \in \mathcal{X}$.

Definition 2.8 (\mathcal{L}_2 Stable [41]). The system $\mathbf{y} = \mathcal{G}\mathbf{u}$, with the operator $\mathcal{G} : \mathcal{L}_{2e} \rightarrow \mathcal{L}_{2e}$, is \mathcal{L}_2 stable if $\mathcal{G}\mathbf{u} \in \mathcal{L}_2$ for all $\mathbf{u} \in \mathcal{L}_2$.

Definition 2.9 (Finite \mathcal{L}_2 Gain [41]). The system $\mathbf{y} = \mathcal{G}\mathbf{u}$, with operator $\mathcal{G} : \mathcal{L}_{2e} \rightarrow \mathcal{L}_{2e}$, has finite \mathcal{L}_2 gain if there exists a constant $\gamma \in \mathbb{R}_{>0}$ and a function β such that

$$\|\mathcal{G}\mathbf{u}\|_{2T} \leq \gamma \|\mathbf{u}\|_{2T} + \beta, \quad \forall \mathbf{u} \in \mathcal{L}_{2e}, \quad \forall T \in \mathbb{R}_{\geq 0}. \quad (2.1)$$

A system that has finite \mathcal{L}_2 gain is \mathcal{L}_2 stable. The \mathcal{L}_2 gain of \mathcal{G} is the infimum of the set of γ values satisfying (2.1) [42].

2.2 Optimization and LMIs

Optimization is a central theme of this dissertation, particularly convex optimization with LMI constraints. Convex optimization is used in Part II of this dissertation

for the synthesis of \mathcal{H}_∞ -optimal parallel feedforward controllers and the optimal linear combination of sensor measurements, and in Part III for the synthesis of robust controllers.

2.2.1 Convex Sets

Definition 2.10 (Convexity [43]). A set, \mathcal{S} , in a real inner product space is convex if for all $\mathbf{x}, \mathbf{y} \in \mathcal{S}$ and $\alpha \in [0, 1]$, $\alpha\mathbf{x} + (1 - \alpha)\mathbf{y} \in \mathcal{S}$. A function, $f : \mathcal{S} \rightarrow \mathbb{R}$, is strictly convex if for all $\mathbf{x}, \mathbf{y} \in \mathcal{S}$, $\alpha \in (0, 1)$, and $\mathbf{x} \neq \mathbf{y}$, $f(\alpha\mathbf{x} + (1 - \alpha)\mathbf{y}) < \alpha f(\mathbf{x}) + (1 - \alpha)f(\mathbf{y})$.

Proposition 2.11 (Uniqueness of a Convex Function Minimizer [43]). *Suppose that $f : \mathcal{S} \rightarrow \mathbb{R}$ is strictly convex and continuous. If $\mathcal{S} \subset \mathbb{R}^n$ is closed, bounded, and convex, then a unique minimizer of f exists in \mathcal{S} .*

2.2.2 Linear Matrix Inequalities

Definition 2.12 (Definiteness of a Matrix [40]). Consider the symmetric matrix $\mathbf{A} = \mathbf{A}^\top \in \mathbb{R}^{n \times n}$. The matrix \mathbf{A} is positive definite if $\mathbf{x}^\top \mathbf{A} \mathbf{x} > 0$, $\forall \mathbf{x} \neq \mathbf{0} \in \mathbb{R}^n$ and positive semi-definite if $\mathbf{x}^\top \mathbf{A} \mathbf{x} \geq 0$, $\forall \mathbf{x} \in \mathbb{R}^n$. Conversely, the matrix \mathbf{A} is negative definite if $\mathbf{x}^\top \mathbf{A} \mathbf{x} < 0$, $\forall \mathbf{x} \neq \mathbf{0} \in \mathbb{R}^n$ and negative semi-definite if $\mathbf{x}^\top \mathbf{A} \mathbf{x} \leq 0$, $\forall \mathbf{x} \in \mathbb{R}^n$. The matrix \mathbf{A} is indefinite if $\mathbf{x}^\top \mathbf{A} \mathbf{x}$ is neither positive nor negative.

Definition 2.13 (Matrix Inequality). A matrix inequality, $\mathcal{G} : \mathbb{R}^m \rightarrow \mathbb{R}^{n \times n}$, in the variable $\mathbf{x} \in \mathbb{R}^m$ is an expression of the form

$$\mathcal{G}(\mathbf{x}) = \mathbf{G}_0 + \sum_{i=1}^p f_i(\mathbf{x}) \mathbf{G}_i \leq 0,$$

where $\mathbf{x}^\top = [x_1 \cdots x_m]$, $\mathbf{G}_i = \mathbf{G}_i^\top \in \mathbb{R}^{n \times n}$, $i = 0, \dots, p$.

Definition 2.14 (Bilinear Matrix Inequality). A bilinear matrix inequality (BMI), $\mathcal{H} : \mathbb{R}^m \rightarrow \mathbb{R}^{n \times n}$, in the variable $\mathbf{x} \in \mathbb{R}^m$ is an expression of the form

$$\mathcal{H}(\mathbf{x}) = \mathbf{H}_0 + \sum_{i=1}^m \sum_{j=1}^m x_i x_j \mathbf{H}_{i,j} \leq 0,$$

where $\mathbf{x}^\top = [x_1 \cdots x_m]$, $\mathbf{H}_0 = \mathbf{H}_0^\top \in \mathbb{R}^{n \times n}$, $\mathbf{H}_{i,j} = \mathbf{H}_{i,j}^\top \in \mathbb{R}^{n \times n}$, $i = 1, \dots, m$, $j = 1, \dots, m$.

Definition 2.15 (Linear Matrix Inequality). [44, 45] A linear matrix inequality (LMI), $\mathbf{F} : \mathbb{R}^m \rightarrow \mathbb{R}^{n \times n}$, in the variable $\mathbf{x} \in \mathbb{R}^m$ is an expression of the form

$$\mathbf{F}(\mathbf{x}) = \mathbf{F}_0 + \sum_{i=1}^m x_i \mathbf{F}_i \leq 0, \quad (2.2)$$

where $\mathbf{x}^\top = [x_1 \cdots x_m]$, $\mathbf{F}_i = \mathbf{F}_i^\top \in \mathbb{R}^{n \times n}$, $i = 0, \dots, m$.

Example 2.16. [44] Consider the matrices $\mathbf{A} \in \mathbb{R}^{n \times n}$ and $\mathbf{Q} \in \mathbb{R}^{n \times n}$, where $\mathbf{Q} = \mathbf{Q}^\top > 0$. It is desired to find a symmetric matrix $\mathbf{P} \in \mathbb{R}^{n \times n}$ satisfying the inequality

$$\mathbf{P}\mathbf{A} + \mathbf{A}^\top\mathbf{P} + \mathbf{Q} < 0, \quad (2.3)$$

where $\mathbf{P} = \mathbf{P}^\top > 0$. The elements of \mathbf{P} are the design variables in this problem, and although (2.3) is an LMI in the matrix variable \mathbf{P} , it does not resemble the LMI in (2.2). For simplicity, consider the case of $n = 2$ so that each matrix is of dimension 2×2 , and $\mathbf{x} = [p_1 \ p_2 \ p_3]^\top$. Writing the matrix \mathbf{P} in terms of a basis $\mathbf{E}_i \in \mathbb{R}^{2 \times 2}$, $i = 1, 2, 3$, yields

$$\mathbf{P} = \begin{bmatrix} p_1 & p_2 \\ p_2 & p_3 \end{bmatrix} = p_1 \underbrace{\begin{bmatrix} 1 & 0 \\ 0 & 0 \end{bmatrix}}_{\mathbf{E}_1} + p_2 \underbrace{\begin{bmatrix} 0 & 1 \\ 1 & 0 \end{bmatrix}}_{\mathbf{E}_2} + p_3 \underbrace{\begin{bmatrix} 0 & 0 \\ 0 & 1 \end{bmatrix}}_{\mathbf{E}_3}.$$

Note that the matrices \mathbf{E}_i are linearly independent and symmetric, thus forming a basis for the symmetric matrix \mathbf{P} . The matrix inequality in (2.3) can be written as

$$p_1 (\mathbf{E}_1\mathbf{A} + \mathbf{A}^\top\mathbf{E}_1) + p_2 (\mathbf{E}_2\mathbf{A} + \mathbf{A}^\top\mathbf{E}_2) + p_3 (\mathbf{E}_3\mathbf{A} + \mathbf{A}^\top\mathbf{E}_3).$$

Defining $\mathbf{F}_0 = \mathbf{Q}$ and $\mathbf{F}_i = \mathbf{F}_i^\top = \mathbf{E}_i\mathbf{A} + \mathbf{A}^\top\mathbf{E}_i$, $i = 1, 2, 3$, yields

$$\mathbf{F}_0 + \sum_{i=1}^3 p_i \mathbf{F}_i < 0,$$

which now resembles the definition of an LMI in (2.2). Throughout this dissertation, LMIs are typically written in the matrix form of (2.3), rather than the scalar form of (2.2).

Since LMIs are often written as a function of symmetric matrices, repeated blocks within symmetric matrices are replaced by $*$ in this dissertation for brevity and clarity.

For example,

$$\mathbf{A} = \mathbf{A}^\top = \begin{bmatrix} \mathbf{B} & \mathbf{C} \\ \mathbf{C}^\top & \mathbf{D} \end{bmatrix} = \begin{bmatrix} \mathbf{B} & \mathbf{C} \\ * & \mathbf{D} \end{bmatrix}.$$

Proposition 2.17 (Convexity of LMIs [44]). *An LMI, $\mathbf{F} : \mathbb{R}^m \rightarrow \mathbb{R}^{n \times n}$, is convex.*

Proof. Consider $\mathbf{x}, \mathbf{y} \in \mathbb{R}^m$ and $\alpha \in [0, 1]$, and suppose that \mathbf{x} and \mathbf{y} satisfy (2.2). The LMI $\mathbf{F} : \mathbb{R}^m \rightarrow \mathbb{R}^{n \times n}$ is convex, since

$$\begin{aligned} \mathbf{F}(\alpha\mathbf{x} + (1 - \alpha)\mathbf{y}) &= \mathbf{F}_0 + \sum_{i=1}^m (\alpha x_i + (1 - \alpha)y_i) \mathbf{F}_i \\ &= \mathbf{F}_0 - \alpha\mathbf{F}_0 + \alpha\mathbf{F}_0 + \alpha \sum_{i=1}^m x_i \mathbf{F}_i + (1 - \alpha) \sum_{i=1}^m y_i \mathbf{F}_i \\ &= \alpha\mathbf{F}_0 + \alpha \sum_{i=1}^m x_i \mathbf{F}_i + (1 - \alpha)\mathbf{F}_0 + (1 - \alpha) \sum_{i=1}^m y_i \mathbf{F}_i \\ &= \alpha\mathbf{F}(\mathbf{x}) + (1 - \alpha)\mathbf{F}(\mathbf{y}). \end{aligned}$$

□

LMIs are useful in optimization because they are convex, as shown in Proposition 2.17. An optimization problem with a convex objective function and whose constraints are linear and/or LMIs will have a unique minimizer, as stated in Proposition 2.11. Due to their attractive properties, LMIs are used throughout this dissertation as constraints in a number of controller synthesis methods.

The following LMI properties and tools are useful in transforming a BMI, or more generally a matrix inequality, into an LMI.

Lemma 2.18 (Strict Schur complement [7, 44]). *Consider the matrices $\mathbf{A} = \mathbf{A}^\top \in \mathbb{R}^{n \times n}$, $\mathbf{C} = \mathbf{C}^\top \in \mathbb{R}^{m \times m}$, and $\mathbf{B} \in \mathbb{R}^{m \times n}$. The following conditions are equivalent.*

1. $\begin{bmatrix} \mathbf{A} & \mathbf{B} \\ \mathbf{B}^\top & \mathbf{C} \end{bmatrix} < 0$.
2. $\mathbf{A} - \mathbf{B}\mathbf{C}^{-1}\mathbf{B}^\top < 0$, $\mathbf{C} < 0$.
3. $\mathbf{C} - \mathbf{B}^\top\mathbf{A}^{-1}\mathbf{B} < 0$, $\mathbf{A} < 0$.

Lemma 2.19 (Nonstrict Schur complement [44]). *Consider the matrices $\mathbf{A} = \mathbf{A}^\top \in \mathbb{R}^{n \times n}$, $\mathbf{C} = \mathbf{C}^\top \in \mathbb{R}^{m \times m}$, and $\mathbf{B} \in \mathbb{R}^{m \times n}$. The following conditions are equivalent.*

1. $\begin{bmatrix} \mathbf{A} & \mathbf{B} \\ \mathbf{B}^\top & \mathbf{C} \end{bmatrix} \leq 0$.

2. $\mathbf{A} - \mathbf{B}\mathbf{C}^+\mathbf{B}^\top < 0$, $\mathbf{C} \leq 0$, $\mathbf{B}(\mathbf{1} - \mathbf{C}\mathbf{C}^+) = \mathbf{0}$, where \mathbf{C}^+ is the Moore-Penrose inverse of \mathbf{C} .

3. $\mathbf{C} - \mathbf{B}^\top\mathbf{A}^+\mathbf{B} < 0$, $\mathbf{A} \leq 0$, $\mathbf{B}^\top(\mathbf{1} - \mathbf{A}\mathbf{A}^+) = \mathbf{0}$, where \mathbf{A}^+ is the Moore-Penrose inverse of \mathbf{A} .

Lemma 2.20 (Young's Relation [46, 47]). Consider the matrices $\mathbf{X} \in \mathbb{R}^{n \times m}$, $\mathbf{Y} \in \mathbb{R}^{n \times p}$, and $\mathbf{S} \in \mathbb{R}^{n \times n}$, where $\mathbf{S} = \mathbf{S}^\top > 0$. The matrix inequality

$$\mathbf{X}^\top\mathbf{Y} + \mathbf{Y}^\top\mathbf{X} \leq \mathbf{X}^\top\mathbf{S}^{-1}\mathbf{X} + \mathbf{Y}^\top\mathbf{S}\mathbf{Y}$$

is known as Young's relation.

Lemma 2.21 (Congruence Transformation [7]). Suppose $\mathbf{Q} = \mathbf{Q}^\top \in \mathbb{R}^{n \times n}$ and $\mathbf{W} \in \mathbb{R}^{n \times n}$ with $\text{rank}(\mathbf{W}) = n$. The LMI $\mathbf{Q} < 0$ is satisfied if and only if $\mathbf{W}\mathbf{Q}\mathbf{W}^\top < 0$.

2.3 Linear Systems Theory

The majority of the controller synthesis methods presented in this dissertation involve LTI transfer matrices and state-space representations of LTI transfer matrices. A review of linear systems theory is provided in this section, in particular the stability of LTI systems, the \mathcal{H}_2 and \mathcal{H}_∞ norms of LTI systems, the zeros of LTI transfer matrices, and the concept of the generalized LTI plant.

2.3.1 Stability of Linear Systems

Lemma 2.22 (Nonstrict Lyapunov Inequality [48]). Let $\mathbf{A} \in \mathbb{R}^{n \times n}$ and assume there exists $\mathbf{P} \in \mathbb{R}^{n \times n}$, where $\mathbf{P} = \mathbf{P}^\top > 0$, satisfying

$$\mathbf{A}^\top\mathbf{P} + \mathbf{P}\mathbf{A} \leq 0.$$

Then $\text{Re}\{\lambda_i(\mathbf{A})\} \leq 0$, $i = 1, \dots, n$, and the equilibrium point $\mathbf{x} = \mathbf{0}$ of the system $\dot{\mathbf{x}}(t) = \mathbf{A}\mathbf{x}(t)$ is Lyapunov stable.

Lemma 2.23 (Strict Lyapunov Inequality [48]). Let $\mathbf{A} \in \mathbb{R}^{n \times n}$ and assume there exists $\mathbf{P} \in \mathbb{R}^{n \times n}$, where $\mathbf{P} = \mathbf{P}^\top > 0$, satisfying

$$\mathbf{A}^\top\mathbf{P} + \mathbf{P}\mathbf{A} < 0.$$

Then $\text{Re}\{\lambda_i(\mathbf{A})\} < 0$, $i = 1, \dots, n$, the matrix \mathbf{A} is Hurwitz, and the equilibrium point $\mathbf{x} = \mathbf{0}$ of the system $\dot{\mathbf{x}}(t) = \mathbf{A}\mathbf{x}(t)$ is asymptotically stable.

2.3.2 \mathcal{H}_∞ and \mathcal{H}_2 Norms of LTI Systems

Definition 2.24 (\mathcal{H}_∞ Norm of a Linear System [7, 41]). The \mathcal{H}_∞ norm of the asymptotically stable linear system $\mathbf{G} : \mathcal{L}_{2e} \rightarrow \mathcal{L}_{2e}$, denoted as $\|\mathbf{G}\|_\infty$, is given by

$$\|\mathbf{G}\|_\infty = \sup_{\mathbf{u} \in \mathcal{L}_2 \setminus \{\mathbf{0}\}} \frac{\|\mathbf{G}\mathbf{u}\|_2}{\|\mathbf{u}\|_2},$$

or equivalently

$$\|\mathbf{G}\|_\infty = \sup_{\omega \in \mathbb{R}} \bar{\sigma}\{\mathbf{G}(j\omega)\}.$$

Lemma 2.25 (Bounded Real Lemma [49]). *Consider an LTI system, $\mathbf{G} : \mathcal{L}_{2e} \rightarrow \mathcal{L}_{2e}$, with state-space realization $(\mathbf{A}, \mathbf{B}, \mathbf{C}, \mathbf{D})$ and transfer matrix $\mathbf{G}(s) = \mathbf{C}(s\mathbf{1} - \mathbf{A})^{-1}\mathbf{B} + \mathbf{D} \in \mathbb{C}^{n_y \times n_u}$. The inequality $\|\mathbf{G}\|_\infty < \gamma$ holds if and only if there exists $\mathbf{P} = \mathbf{P}^\top > 0$ and $0 < \gamma < \infty$ such that*

$$\begin{bmatrix} \mathbf{P}\mathbf{A} + \mathbf{A}^\top\mathbf{P} & \mathbf{P}\mathbf{B} & \mathbf{C}^\top \\ * & -\gamma\mathbf{1} & \mathbf{D}^\top \\ * & * & -\gamma\mathbf{1} \end{bmatrix} < 0. \quad (2.4)$$

The \mathcal{H}_∞ norm of \mathbf{G} is the minimum value of $0 < \gamma < \infty$ that satisfies (2.4) with $\mathbf{P} = \mathbf{P}^\top > 0$.

Definition 2.26 (\mathcal{H}_2 Norm of a Linear System [48]). The \mathcal{H}_2 norm of the asymptotically stable linear system $\mathbf{G} : \mathcal{L}_{2e} \rightarrow \mathcal{L}_{2e}$, denoted as $\|\mathbf{G}\|_2$, is given by

$$\|\mathbf{G}\|_2 = \sqrt{\int_0^\infty \text{tr}(\mathbf{G}^\top(t)\mathbf{G}(t)) dt},$$

where $\mathbf{G}(t)$ is the impulse response of the transfer matrix $\mathbf{G}(s)$. Equivalently,

$$\|\mathbf{G}\|_2 = \sqrt{\frac{1}{2\pi} \int_{-\infty}^\infty \text{tr}(\mathbf{G}^\mathbf{H}(j\omega)\mathbf{G}(j\omega)) d\omega}.$$

Lemma 2.27 (\mathcal{H}_2 Norm of a Linear System with LMIs [44, 50]). *Consider an LTI system, $\mathbf{G} : \mathcal{L}_{2e} \rightarrow \mathcal{L}_{2e}$, with state-space realization $(\mathbf{A}, \mathbf{B}, \mathbf{C}, \mathbf{0})$ and transfer matrix $\mathbf{G}(s) = \mathbf{C}(s\mathbf{1} - \mathbf{A})^{-1}\mathbf{B} \in \mathbb{C}^{n_y \times n_u}$. The inequality $\|\mathbf{G}\|_2 < \mu$ holds if and only if there*

exists $\mathbf{Q} = \mathbf{Q}^\top > 0$, $\mathbf{Z} = \mathbf{Z}^\top > 0$, and $0 < \mu < \infty$ such that

$$\mathbf{Q}\mathbf{A} + \mathbf{A}^\top\mathbf{Q} + \mathbf{Q}\mathbf{B}\mathbf{B}^\top\mathbf{Q} < 0, \quad (2.5)$$

$$\begin{bmatrix} \mathbf{Q} & \mathbf{C}^\top \\ * & \mathbf{Z} \end{bmatrix} > 0, \quad (2.6)$$

$$\text{tr}\mathbf{Z} < \mu^2. \quad (2.7)$$

The \mathcal{H}_2 norm of \mathbf{G} is the minimum value of $0 < \mu < \infty$ that satisfies (2.5), (2.6), and (2.7) with $\mathbf{Q} = \mathbf{Q}^\top > 0$ and $\mathbf{Z} = \mathbf{Z}^\top > 0$.

2.3.3 Zeros of Linear Systems

Definition 2.28 (Blocking Zero [51]). A causal LTI system represented by the transfer matrix $\mathbf{G}(s) \in \mathbb{C}^{n_y \times n_u}$ has a blocking zero at $z \in \mathbb{C}$ if $\mathbf{G}(z) = \mathbf{0}$.

Example 2.29. The transfer matrix $\mathbf{G}(s) \in \mathbb{C}^{2 \times 2}$ has a blocking zero at $z = 3$, where

$$\mathbf{G}(s) = \begin{bmatrix} \frac{s-3}{s+1} & \frac{s-3}{(s+3)(s+5)} \\ \frac{s-3}{s+5} & \frac{s-3}{s+1} \end{bmatrix}.$$

In this case $\mathbf{G}(z) = \mathbf{0}$ when $z = 3$.

Definition 2.30 (Normal Rank of a Transfer Matrix [48]). The normal column rank and the normal row rank of the transfer matrix $\mathbf{G}(s) \in \mathbb{C}^{n_y \times n_u}$ are the maximum column rank and row rank of $\mathbf{G}(s)$, respectively, over all $s \in \mathbb{C}$ that are not poles of $\mathbf{G}(s)$. The normal rank of $\mathbf{G}(s)$ is the minimum of the normal column rank and normal row rank of $\mathbf{G}(s)$.

Definition 2.31 (Transmission Zero [52, 53]). A causal LTI system represented by the transfer matrix $\mathbf{G}(s) \in \mathbb{C}^{n_y \times n_u}$ with full normal column rank (i.e., the normal column rank of $\mathbf{G}(s)$ is n_u) has a transmission zero at $z \in \mathbb{C}$ if $\lim_{s \rightarrow z} (\mathbf{G}(s)\mathbf{u}(s)) = \mathbf{0}$ for some finite and non-zero $\mathbf{u}(z) \in \mathbb{C}^{n_u}$. Additionally, if z is not a pole of $\mathbf{G}(s)$, z is a transmission zero of $\mathbf{G}(s)$ if $\mathbf{G}(z)$ does not have full column rank (i.e., $\mathbf{G}(z)\mathbf{u}_0 = \mathbf{0}$ for $\mathbf{u}_0 \in \mathbb{R}^{n_u}$, $\mathbf{u}_0 \neq \mathbf{0}$).

Remark 2.32. A transfer matrix blocking zero is a special case of a transfer matrix transmission zero. In the special case of $n_y = n_u = 1$, the blocking zeros of the transfer function $G(s) \in \mathbb{C}$ are simply zeros.

Remark 2.33. A more general definition of transmission zeros when the transfer matrix does not have full normal column rank is found in [48, 54], which is omitted in this dissertation, as only transfer matrices with full normal column rank are considered.

Example 2.34. The transfer matrix $\mathbf{G}(s) \in \mathbb{C}^{2 \times 2}$ has a transmission zero at $z = 2$, where

$$\mathbf{G}(s) = \begin{bmatrix} 1 & \frac{s-2}{s+3} \\ 1 & 0 \end{bmatrix}.$$

The normal column rank of $\mathbf{G}(s)$ is 2. Evaluating $\mathbf{G}(z)$ with $z = 2$ yields a matrix with rank 1 and choosing the input $\mathbf{u}_0 = \begin{bmatrix} 0 & 1 \end{bmatrix}^T$ gives $\mathbf{G}(z)\mathbf{u}_0 = \mathbf{0}$, where $\mathbf{u}_0 \neq \mathbf{0}$.

Example 2.35. The transfer matrix $\mathbf{G}(s) \in \mathbb{C}^{2 \times 2}$ has a pole and a transmission zero at $z = 1$, where

$$\mathbf{G}(s) = \begin{bmatrix} 1 & \frac{1}{s-1} \\ 0 & 1 \end{bmatrix}.$$

The normal column rank of $\mathbf{G}(s)$ is 2. Choosing the input $\mathbf{u}(s) = \begin{bmatrix} -1 & s-1 \end{bmatrix}^T$ gives $\lim_{s \rightarrow z} (\mathbf{G}(s)\mathbf{u}(s)) = \mathbf{0}$, where $\mathbf{u}(z) = \begin{bmatrix} -1 & 0 \end{bmatrix}^T$ is finite and nonzero.

Definition 2.36 (Minimum Phase Transmission Zeros [55, 56]). A transmission zero of $\mathbf{G}(s) \in \mathbb{C}^{n_y \times n_u}$ at $z \in \mathbb{C}$ is minimum phase if $\text{Re}(z) < 0$. Conversely, a transmission zero of $\mathbf{G}(s) \in \mathbb{C}^{n_y \times n_u}$ at $z \in \mathbb{C}$ is nonminimum phase if $\text{Re}(z) \geq 0$.

Definition 2.37 (Minimum Phase Transfer Matrix [56]). A transfer matrix $\mathbf{G}(s) \in \mathbb{C}^{n_y \times n_u}$ is minimum phase if all of its transmission zeros are minimum phase. Conversely, a transfer matrix $\mathbf{G}(s) \in \mathbb{C}^{n_y \times n_u}$ is nonminimum phase if it has at least one nonminimum phase transmission zero.

Lemma 2.38 (Inverse of a Square System [22]). *Consider a square causal LTI system, $\mathbf{G} : \mathcal{L}_{2e} \rightarrow \mathcal{L}_{2e}$, with minimal state-space realization given by*

$$\dot{\mathbf{x}}(t) = \mathbf{A}\mathbf{x}(t) + \mathbf{B}\mathbf{u}(t), \quad (2.8)$$

$$\mathbf{y}(t) = \mathbf{C}\mathbf{x}(t) + \mathbf{D}\mathbf{u}(t), \quad (2.9)$$

where $\mathbf{x}(t) \in \mathbb{R}^{n_x}$, $\mathbf{u}(t) \in \mathbb{R}^{n_u}$, $\mathbf{y}(t) \in \mathbb{R}^{n_y}$, $n_u = n_y$, and it is assumed that \mathbf{D} is invertible. A minimal state-space realization of the inverse of \mathbf{G} is given by

$$\dot{\mathbf{x}}(t) = (\mathbf{A} - \mathbf{B}\mathbf{D}^{-1}\mathbf{C})\mathbf{x}(t) + \mathbf{B}\mathbf{D}^{-1}\mathbf{y}(t), \quad (2.10)$$

$$\mathbf{u}(t) = -\mathbf{D}^{-1}\mathbf{C}\mathbf{x}(t) + \mathbf{D}^{-1}\mathbf{y}(t). \quad (2.11)$$

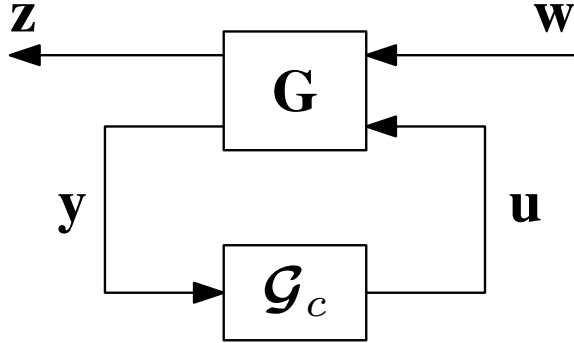


Figure 2.1: Block diagram of the generalized plant \mathbf{G} with the controller \mathcal{G}_c .

Lemma 2.39 (Poles of an Inverse Square System [22, 57]). *The transmission zeros of a square causal LTI transfer matrix, $\mathbf{G}(s) \in \mathbb{C}^{m \times m}$, with minimal state-space realization given in (2.8) and (2.9), where \mathbf{D} is invertible, are the poles of the inverse system defined in (2.10) and (2.11).*

2.3.4 The Generalized LTI Plant

Definition 2.40 (Generalized LTI Plant [48]). Consider the generalized LTI plant $\mathbf{G} : \mathcal{L}_{2e} \rightarrow \mathcal{L}_{2e}$, shown in Figure 2.1, with a minimal state-space realization

$$\begin{aligned}\dot{\mathbf{x}}(t) &= \mathbf{A}\mathbf{x}(t) + \mathbf{B}_1\mathbf{w}(t) + \mathbf{B}_2\mathbf{u}(t), \\ \mathbf{z}(t) &= \mathbf{C}_1\mathbf{x}(t) + \mathbf{D}_{11}\mathbf{w}(t) + \mathbf{D}_{12}\mathbf{u}(t), \\ \mathbf{y}(t) &= \mathbf{C}_2\mathbf{x}(t) + \mathbf{D}_{21}\mathbf{w}(t) + \mathbf{D}_{22}\mathbf{u}(t),\end{aligned}$$

where $\mathbf{x}(t) \in \mathbb{R}^{n_x}$ is the system state, $\mathbf{z}(t) \in \mathbb{R}^{n_z}$ is the performance signal, $\mathbf{y}(t) \in \mathbb{R}^{n_y}$ is the measurement signal, $\mathbf{w}(t) \in \mathbb{R}^{n_w}$ is the exogenous signal, $\mathbf{u}(t) \in \mathbb{R}^{n_u}$ is the control input signal, and the state-space matrices have appropriate dimensions. The generalized LTI plant can also be written in transfer matrix form as

$$\begin{bmatrix} \mathbf{z}(s) \\ \mathbf{y}(s) \end{bmatrix} = \mathbf{G}(s) \begin{bmatrix} \mathbf{w}(s) \\ \mathbf{u}(s) \end{bmatrix},$$

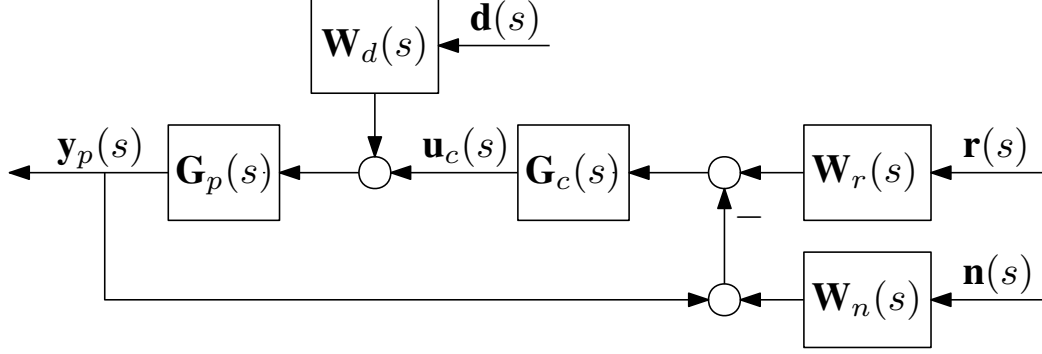


Figure 2.2: Block diagram of the basic servo loop with plant $\mathbf{G}_p(s)$, controller $\mathbf{G}_c(s)$, and weighting transfer matrices $\mathbf{W}_r(s)$, $\mathbf{W}_d(s)$, and $\mathbf{W}_n(s)$.

where the transfer matrix $\mathbf{G}(s) \in \mathbb{C}^{(n_z+n_y) \times (n_w+n_u)}$ is partitioned as

$$\mathbf{G}(s) = \begin{bmatrix} \mathbf{G}_{zw}(s) & \mathbf{G}_{zu}(s) \\ \mathbf{G}_{yw}(s) & \mathbf{G}_{yu}(s) \end{bmatrix} = \begin{bmatrix} \mathbf{C}_1 (s\mathbf{I} - \mathbf{A})^{-1} \mathbf{B}_1 + \mathbf{D}_{11} & \mathbf{C}_1 (s\mathbf{I} - \mathbf{A})^{-1} \mathbf{B}_2 + \mathbf{D}_{12} \\ \mathbf{C}_2 (s\mathbf{I} - \mathbf{A})^{-1} \mathbf{B}_1 + \mathbf{D}_{21} & \mathbf{C}_2 (s\mathbf{I} - \mathbf{A})^{-1} \mathbf{B}_2 + \mathbf{D}_{22} \end{bmatrix}.$$

The generalized plant, also known as the standard control problem in [48], is useful, as it is possible to represent a number of LTI systems in this form, as shown in the following example.

Example 2.41 (Basic Servo Loop Tracking). Consider the basic servo loop shown in Figure 2.2 involving the LTI controller $\mathbf{G}_c(s) \in \mathbb{C}^{n_{yc} \times n_{uc}}$ and the plant $\mathbf{G}_p(s) \in \mathbb{C}^{n_{yp} \times n_{up}}$, where the weighting transfer matrices are simply chosen as $\mathbf{W}_r(s) = \mathbf{1}$, $\mathbf{W}_d(s) = \mathbf{1}$, and $\mathbf{W}_n(s) = \mathbf{1}$. The plant has a minimal state-space realization $(\mathbf{A}_p, \mathbf{B}_p, \mathbf{C}_p, \mathbf{D}_p)$ and the state $\mathbf{x}_p(t)$. The performance variables are the true tracking error $\mathbf{z}_1(t) = \mathbf{e}(t) = \mathbf{r}(t) - \mathbf{y}_p(t)$ and the control effort $\mathbf{z}_2(t) = \mathbf{u}_c(t)$, where $\mathbf{z}^\top(t) = \begin{bmatrix} \mathbf{z}_1^\top(t) & \mathbf{z}_2^\top(t) \end{bmatrix}$. The generalized plant can be formulated with minimal state-space representation

$$\begin{aligned} \dot{\mathbf{x}}(t) &= \mathbf{A}_p \mathbf{x}(t) + \begin{bmatrix} \mathbf{0} & \mathbf{B}_p & \mathbf{0} \end{bmatrix} \mathbf{w}(t) + \mathbf{B}_p \mathbf{u}(t), \\ \mathbf{z}(t) &= \begin{bmatrix} -\mathbf{C}_p \\ \mathbf{0} \end{bmatrix} \mathbf{x}(t) + \begin{bmatrix} \mathbf{1} & -\mathbf{D}_p & \mathbf{0} \\ \mathbf{0} & \mathbf{0} & \mathbf{0} \end{bmatrix} \mathbf{w}(t) + \begin{bmatrix} -\mathbf{D}_p \\ \mathbf{1} \end{bmatrix} \mathbf{u}(t), \\ \mathbf{y}(t) &= -\mathbf{C}_p \mathbf{x}(t) + \begin{bmatrix} \mathbf{1} & -\mathbf{D}_p & -\mathbf{1} \end{bmatrix} \mathbf{w}(t) - \mathbf{D}_p \mathbf{u}(t), \end{aligned}$$

where $\mathbf{x}(t) = \mathbf{x}_p(t)$, $\mathbf{u}(t) = \mathbf{u}_c(t)$, $\mathbf{w}^\top(t) = \begin{bmatrix} \mathbf{r}^\top(t) & \mathbf{d}^\top(t) & \mathbf{n}^\top(t) \end{bmatrix}$, and $\mathbf{y}(t) = \mathbf{r}(t) - \mathbf{y}_p(t) - \mathbf{n}(t)$.

Example 2.42 (Basic Servo Loop Tracking with Weights). Consider the same basic servo loop shown in Figure 2.2 involving the LTI controller $\mathbf{G}_c(s) \in \mathbb{C}^{n_{yc} \times n_{uc}}$, the plant $\mathbf{G}_p(s) \in \mathbb{C}^{n_{yp} \times n_{up}}$, and the weighting transfer matrices $\mathbf{W}_r(s) \in \mathbb{C}^{n_r \times n_r}$, $\mathbf{W}_d(s) \in \mathbb{C}^{n_d \times n_d}$, and $\mathbf{W}_n(s) \in \mathbb{C}^{n_n \times n_n}$. The plant has a minimal state-space realization $(\mathbf{A}_p, \mathbf{B}_p, \mathbf{C}_p, \mathbf{D}_p)$ and the weighting transfer matrices $\mathbf{W}_r(s)$, $\mathbf{W}_d(s)$, and $\mathbf{W}_n(s)$ have minimal state-space realizations $(\mathbf{A}_r, \mathbf{B}_r, \mathbf{C}_r, \mathbf{D}_r)$, $(\mathbf{A}_d, \mathbf{B}_d, \mathbf{C}_d, \mathbf{D}_d)$, and $(\mathbf{A}_n, \mathbf{B}_n, \mathbf{C}_n, \mathbf{D}_n)$, respectively. The performance variable is defined as the weighted true tracking error $\mathbf{z}_1(s) = \mathbf{W}_e(s)\mathbf{e}(s) = \mathbf{W}_e(s)(\mathbf{W}_r(s)\mathbf{r}(s) - \mathbf{y}_p(s))$ and the weighted control effort $\mathbf{z}_2(s) = \mathbf{W}_u(s)\mathbf{u}_c(s)$, where $\mathbf{z}^\top(s) = \begin{bmatrix} \mathbf{z}_1^\top(s) & \mathbf{z}_2^\top(s) \end{bmatrix}$ and $\mathbf{W}_e(s) \in \mathbb{C}^{n_e \times n_e}$, $\mathbf{W}_u(s) \in \mathbb{C}^{n_u \times n_u}$ are weighting transfer matrices with minimal state-space realizations $(\mathbf{A}_e, \mathbf{B}_e, \mathbf{C}_e, \mathbf{D}_e)$ and $(\mathbf{A}_u, \mathbf{B}_u, \mathbf{C}_u, \mathbf{D}_u)$, respectively. The generalized plant can be formulated with minimal state-space representation

$$\begin{aligned} \dot{\mathbf{x}}(t) &= \begin{bmatrix} \mathbf{A}_p & \mathbf{0} & \mathbf{B}_p\mathbf{C}_d & \mathbf{0} & \mathbf{0} & \mathbf{0} \\ \mathbf{0} & \mathbf{A}_r & \mathbf{0} & \mathbf{0} & \mathbf{0} & \mathbf{0} \\ \mathbf{0} & \mathbf{0} & \mathbf{A}_d & \mathbf{0} & \mathbf{0} & \mathbf{0} \\ \mathbf{0} & \mathbf{0} & \mathbf{0} & \mathbf{A}_n & \mathbf{0} & \mathbf{0} \\ -\mathbf{B}_e\mathbf{C}_p & \mathbf{B}_e\mathbf{C}_r & -\mathbf{B}_e\mathbf{C}_d & \mathbf{0} & \mathbf{A}_e & \mathbf{0} \\ \mathbf{0} & \mathbf{0} & \mathbf{0} & \mathbf{0} & \mathbf{0} & \mathbf{A}_u \end{bmatrix} \mathbf{x}(t) \\ &\quad + \begin{bmatrix} \mathbf{0} & \mathbf{B}_p\mathbf{D}_d & \mathbf{0} \\ \mathbf{B}_r & \mathbf{0} & \mathbf{0} \\ \mathbf{0} & \mathbf{B}_d & \mathbf{0} \\ \mathbf{0} & \mathbf{0} & \mathbf{B}_n \\ \mathbf{B}_e\mathbf{D}_r & -\mathbf{B}_e\mathbf{D}_p\mathbf{D}_d & \mathbf{0} \\ \mathbf{0} & \mathbf{0} & \mathbf{0} \end{bmatrix} \mathbf{w}(t) + \begin{bmatrix} \mathbf{B}_p \\ \mathbf{0} \\ \mathbf{0} \\ \mathbf{0} \\ -\mathbf{B}_e\mathbf{D}_p \\ \mathbf{B}_u \end{bmatrix} \mathbf{u}(t), \\ \mathbf{z}(t) &= \begin{bmatrix} -\mathbf{D}_e\mathbf{C}_p & \mathbf{D}_e\mathbf{C}_r & -\mathbf{D}_e\mathbf{D}_p\mathbf{C}_d & \mathbf{0} & \mathbf{C}_e & \mathbf{0} \\ \mathbf{0} & \mathbf{0} & \mathbf{0} & \mathbf{0} & \mathbf{0} & \mathbf{C}_u \end{bmatrix} \mathbf{x}(t) \\ &\quad + \begin{bmatrix} \mathbf{D}_e\mathbf{D}_r & -\mathbf{D}_e\mathbf{D}_p\mathbf{D}_d & \mathbf{0} \\ \mathbf{0} & \mathbf{0} & \mathbf{0} \end{bmatrix} \mathbf{w}(t) + \begin{bmatrix} -\mathbf{B}_e\mathbf{D}_p \\ \mathbf{D}_u \end{bmatrix} \mathbf{u}(t), \\ \mathbf{y}(t) &= \begin{bmatrix} -\mathbf{C}_p & \mathbf{C}_r & -\mathbf{D}_p\mathbf{C}_d & -\mathbf{C}_n & \mathbf{0} & \mathbf{0} \end{bmatrix} \mathbf{x}(t) + \begin{bmatrix} \mathbf{D}_r & -\mathbf{D}_p\mathbf{D}_d & -\mathbf{D}_n \end{bmatrix} \mathbf{w}(t) - \mathbf{D}_p\mathbf{u}(t), \end{aligned}$$

where $\mathbf{x}^\top(t) = \begin{bmatrix} \mathbf{x}_p^\top(t) & \mathbf{x}_r^\top(t) & \mathbf{x}_d^\top(t) & \mathbf{x}_n^\top(t) & \mathbf{x}_e^\top(t) & \mathbf{x}_u^\top(t) \end{bmatrix}$, $\mathbf{u}(t) = \mathbf{u}_c(t)$, $\mathbf{w}^\top(t) = \begin{bmatrix} \mathbf{r}^\top(t) & \mathbf{d}^\top(t) & \mathbf{n}^\top(t) \end{bmatrix}$, $\mathbf{y}(s) = \mathbf{W}_r(s)\mathbf{r}(s) - \mathbf{y}_p(s) - \mathbf{W}_n(s)\mathbf{n}(s)$, and $\mathbf{x}_r(t)$, $\mathbf{x}_d(t)$, $\mathbf{x}_n(t)$, $\mathbf{x}_e(t)$, and $\mathbf{x}_u(t)$ are the states associated with the state-space realizations of the weighting transfer matrices $\mathbf{W}_r(s)$, $\mathbf{W}_d(s)$, $\mathbf{W}_n(s)$, $\mathbf{W}_e(s)$, and $\mathbf{W}_u(s)$, respectively.

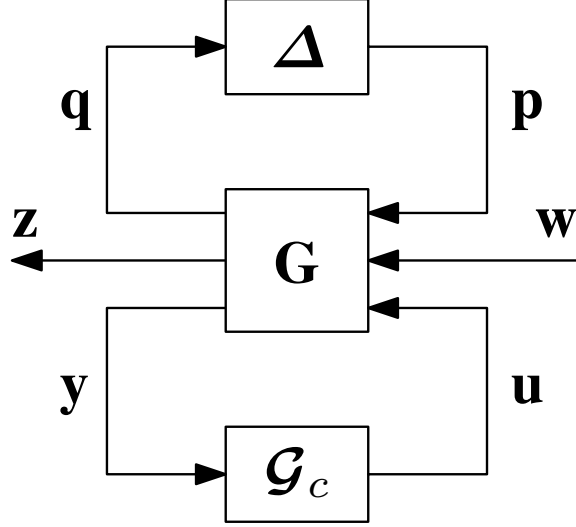


Figure 2.3: Block diagram of the generalized plant \mathbf{G} with the uncertainty Δ and the controller \mathcal{G}_c .

Definition 2.43 (Generalized LTI Plant with Uncertainty). When the generalized LTI plant is subject to uncertainty, as shown in Figure 2.3, it is defined as $\mathbf{G} : \mathcal{L}_{2e} \rightarrow \mathcal{L}_{2e}$ with minimal state-space realization given by

$$\begin{aligned}
 \dot{\mathbf{x}}(t) &= \mathbf{A}\mathbf{x}(t) + \mathbf{B}_1\mathbf{w}(t) + \mathbf{B}_2\mathbf{u}(t) + \mathbf{B}_3\mathbf{p}(t) \\
 \mathbf{z}(t) &= \mathbf{C}_1\mathbf{x}(t) + \mathbf{D}_{11}\mathbf{w}(t) + \mathbf{D}_{12}\mathbf{u}(t) + \mathbf{D}_{13}\mathbf{p}(t), \\
 \mathbf{y}(t) &= \mathbf{C}_2\mathbf{x}(t) + \mathbf{D}_{21}\mathbf{w}(t) + \mathbf{D}_{22}\mathbf{u}(t) + \mathbf{D}_{23}\mathbf{p}(t), \\
 \mathbf{q}(t) &= \mathbf{C}_3\mathbf{x}(t) + \mathbf{D}_{31}\mathbf{w}(t) + \mathbf{D}_{32}\mathbf{u}(t) + \mathbf{D}_{33}\mathbf{p}(t),
 \end{aligned}$$

where $\mathbf{q}(t) \in \mathbb{R}^{n_q}$ is the robustness output signal, $\mathbf{p}(t) \in \mathbb{R}^{n_p}$ is the robustness input signal, the signals common to the generalized plant without uncertainty are defined the same, and the state-space matrices have appropriate dimensions. The generalized LTI plant with uncertainty can also be written in transfer matrix form as

$$\begin{bmatrix} \mathbf{z}(s) \\ \mathbf{y}(s) \\ \mathbf{q}(s) \end{bmatrix} = \mathbf{G}(s) \begin{bmatrix} \mathbf{w}(s) \\ \mathbf{u}(s) \\ \mathbf{p}(s) \end{bmatrix},$$

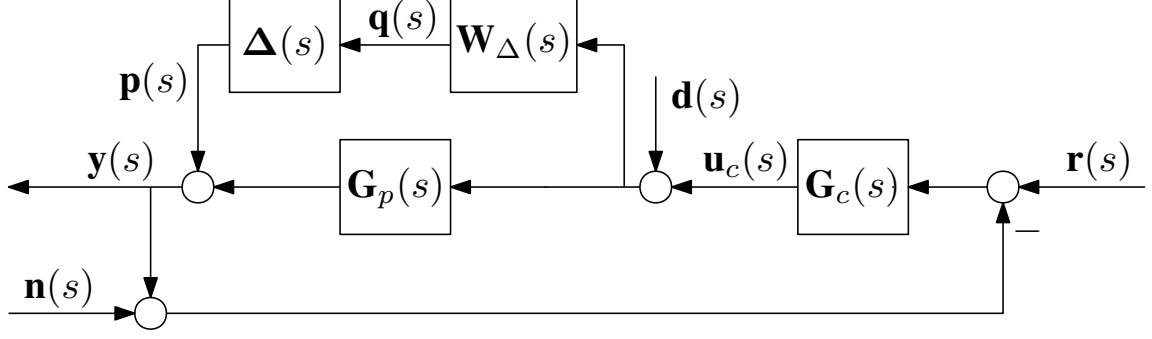


Figure 2.4: Block diagram of the basic servo loop with plant $\mathbf{G}_p(s)$, uncertainty $\Delta(s)$, weighting transfer matrix $\mathbf{W}_\Delta(s)$, and controller $\mathbf{G}_c(s)$.

where the transfer matrix $\mathbf{G}(s) \in \mathbb{C}^{(n_z+n_y+n_q) \times (n_w+n_u+n_p)}$ is partitioned as

$$\mathbf{G}(s) = \begin{bmatrix} \mathbf{G}_{zw}(s) & \mathbf{G}_{zu}(s) & \mathbf{G}_{zp}(s) \\ \mathbf{G}_{yw}(s) & \mathbf{G}_{yu}(s) & \mathbf{G}_{yp}(s) \\ \mathbf{G}_{qw}(s) & \mathbf{G}_{qu}(s) & \mathbf{G}_{qp}(s) \end{bmatrix} = \begin{bmatrix} \mathbf{C}_1 (s\mathbf{1} - \mathbf{A})^{-1} \mathbf{B}_1 + \mathbf{D}_{11} & \mathbf{C}_1 (s\mathbf{1} - \mathbf{A})^{-1} \mathbf{B}_2 + \mathbf{D}_{12} & \mathbf{C}_1 (s\mathbf{1} - \mathbf{A})^{-1} \mathbf{B}_3 + \mathbf{D}_{13} \\ \mathbf{C}_2 (s\mathbf{1} - \mathbf{A})^{-1} \mathbf{B}_1 + \mathbf{D}_{21} & \mathbf{C}_2 (s\mathbf{1} - \mathbf{A})^{-1} \mathbf{B}_2 + \mathbf{D}_{22} & \mathbf{C}_2 (s\mathbf{1} - \mathbf{A})^{-1} \mathbf{B}_3 + \mathbf{D}_{23} \\ \mathbf{C}_3 (s\mathbf{1} - \mathbf{A})^{-1} \mathbf{B}_1 + \mathbf{D}_{31} & \mathbf{C}_3 (s\mathbf{1} - \mathbf{A})^{-1} \mathbf{B}_2 + \mathbf{D}_{32} & \mathbf{C}_3 (s\mathbf{1} - \mathbf{A})^{-1} \mathbf{B}_3 + \mathbf{D}_{33} \end{bmatrix}.$$

Example 2.44 (Servo Loop Tracking with Uncertainty). Consider the same basic servo loop from Example 2.41 with $\mathbf{W}_r(s) = \mathbf{1}$, $\mathbf{W}_d(s) = \mathbf{1}$, and $\mathbf{W}_n(s) = \mathbf{1}$, but now with additive plant uncertainty, as shown in Figure 2.4. Once again, the plant has a minimal state-space realization $(\mathbf{A}_p, \mathbf{B}_p, \mathbf{C}_p, \mathbf{D}_p)$ and the performance variable is the true tracking error $\mathbf{e}(t) = \mathbf{r}(t) - \mathbf{y}(t)$. When the weighting transfer matrix is simply $\mathbf{W}_\Delta(s) = \mathbf{1}$, the generalized plant can be formulated with a minimal state-space representation

$$\begin{aligned} \dot{\mathbf{x}}(t) &= \mathbf{A}_p \mathbf{x}(t) + \begin{bmatrix} \mathbf{0} & \mathbf{B}_p & \mathbf{0} \end{bmatrix} \mathbf{w}(t) + \mathbf{B}_p \mathbf{u}(t), \\ \mathbf{z}(t) &= -\mathbf{C}_p \mathbf{x}(t) + \begin{bmatrix} \mathbf{1} & -\mathbf{D}_p & \mathbf{0} \end{bmatrix} \mathbf{w}(t) - \mathbf{D}_p \mathbf{u}(t) - \mathbf{p}(t), \\ \mathbf{y}(t) &= -\mathbf{C}_p \mathbf{x}(t) + \begin{bmatrix} \mathbf{1} & -\mathbf{D}_p & -\mathbf{1} \end{bmatrix} \mathbf{w}(t) - \mathbf{D}_p \mathbf{u}(t) - \mathbf{p}(t), \\ \mathbf{q}(t) &= \begin{bmatrix} \mathbf{0} & \mathbf{1} & \mathbf{0} \end{bmatrix} \mathbf{w}(t) + \mathbf{u}(t), \end{aligned}$$

where $\mathbf{x}(t)$, $\mathbf{u}(t)$, $\mathbf{w}(t)$, and $\mathbf{y}(t)$ are defined in Example 2.41.

When the weighting transfer matrix $\mathbf{W}_\Delta(s) \in \mathbb{C}^{n_q \times n_q}$ has a minimal state-space realization $(\mathbf{A}_w, \mathbf{B}_w, \mathbf{C}_w, \mathbf{D}_w)$, the generalized plant is described with a minimal state-

space realization

$$\begin{aligned}
\dot{\mathbf{x}}(t) &= \begin{bmatrix} \mathbf{A}_p & \mathbf{0} \\ \mathbf{0} & \mathbf{A}_w \end{bmatrix} \mathbf{x}(t) + \begin{bmatrix} \mathbf{0} & \mathbf{B}_p & \mathbf{0} \\ \mathbf{0} & \mathbf{B}_w & \mathbf{0} \end{bmatrix} \mathbf{w}(t) + \begin{bmatrix} \mathbf{B}_p \\ \mathbf{B}_w \end{bmatrix} \mathbf{u}(t), \\
\mathbf{z}(t) &= \begin{bmatrix} -\mathbf{C}_p & \mathbf{0} \end{bmatrix} \mathbf{x}(t) + \begin{bmatrix} \mathbf{1} & -\mathbf{D}_p & \mathbf{0} \end{bmatrix} \mathbf{w}(t) - \mathbf{D}_p \mathbf{u}(t) - \mathbf{p}(t), \\
\mathbf{y}(t) &= \begin{bmatrix} -\mathbf{C}_p & \mathbf{0} \end{bmatrix} \mathbf{x}(t) + \begin{bmatrix} \mathbf{1} & -\mathbf{D}_p & -\mathbf{1} \end{bmatrix} \mathbf{w}(t) - \mathbf{D}_p \mathbf{u}(t) - \mathbf{p}(t), \\
\mathbf{q}(t) &= \begin{bmatrix} \mathbf{0} & \mathbf{C}_w \end{bmatrix} \mathbf{x}(t) + \begin{bmatrix} \mathbf{0} & \mathbf{D}_w & \mathbf{0} \end{bmatrix} \mathbf{w}(t) + \mathbf{D}_w \mathbf{u}(t),
\end{aligned}$$

where $\mathbf{x}^\top(t) = \begin{bmatrix} \mathbf{x}_p^\top(t) & \mathbf{x}_w^\top(t) \end{bmatrix}$ and $\mathbf{x}_w(t)$ is the state of the weighting transfer matrix $\mathbf{W}_\Delta(s)$.

The generalized LTI plant with uncertainty can be formulated with weights on the reference, disturbance, noise, and performance signals, as done in Example 2.42. An example of this is omitted from this dissertation, as Example 2.42 and Example 2.44 can simply be combined to illustrate this possibility.

The generalized plant with uncertainty is used extensively in Chapter 8 and Chapter 9 when discussing robust control using the Large Gain Theorem.

Part II

Minimum Gain and Optimal Output Modification

Chapter 3

Preliminaries and Introduction to Minimum Gain

3.1 Introduction

The input-output system property of minimum gain [8, 9] is a relatively new concept that, despite its limited use, has intriguing characteristics. In order to elaborate on the useful applications of minimum gain, it is essential to gain a better understanding of its properties. Minimum gain is formally defined in this chapter, followed by a number of its useful properties and their proofs, including its relation to the \mathcal{H}_∞ norm and the minimum singular value of a minimum phase transfer matrix, the minimum gain of a nonminimum phase system, the minimum gain of a cascaded system, and LMI-based methods to calculate minimum gain of LTI systems. The properties of minimum gain derived in this chapter provide the foundation for practical applications of minimum gain, including the synthesis of optimal parallel feedforward controllers in Chapter 4 and the use of the Large Gain Theorem for robust control in Chapter 8 and Chapter 9.

When designing a feedback controller for a system, the input-output properties of the open-loop system greatly affect the suitable choices of controllers and the achievable closed-loop performance. For example, a system with open-loop nonminimum phase zeros will not be suitable for certain adaptive control schemes and its achievable closed-loop performance will be limited. The concept of output modification is concerned with modifying the output of the open-loop system in such a manner that the modified open-loop system has properties that are beneficial for the design of a feedback controller and/or improve the achievable closed-loop performance. In the

case of an open-loop nonminimum phase system, if the system output can be modified to make the modified open-loop system minimum phase, then a wider range of control strategies are available to the control systems engineer and improved closed-loop performance may be possible. A concern when performing output modification is that the new system output may be substantially different from the original system output. If the original system output represents a performance signal, say an output that is to be regulated to zero, then a difference between the modified and original system outputs may lead to poor performance in the original performance signal. For this reason, it is essential to perform output modification in an optimal manner, such that the modified system output is as close as possible to the original system output, which is the topic of Chapters 4 and 5.

The optimal output modification considered in Chapter 4 concerns the synthesis of \mathcal{H}_∞ -optimal parallel feedforward controllers that modify the system output such that the new system is minimum phase. The frequency-dependent weighted \mathcal{H}_∞ norm of the parallel feedforward controller is minimized so that the modified system is as close to the original system within a specified frequency band, in an \mathcal{H}_∞ -sense. Minimum gain plays an important role in the the synthesis of \mathcal{H}_∞ -optimal parallel feedforward controllers in this chapter.

Optimal output modification is also performed in Chapter 5, where the available sensor measurements of an LTI system are linearly combined in such a manner that the modified system is SPR and the system output is as close as possible to a specified desired system output in an \mathcal{H}_2 - or \mathcal{H}_∞ -sense. By rendering the modified system SPR, the choice of an asymptotically stabilizing negative feedback controller is simple, as any positive real (PR) controller will accomplish this.

The remainder of this chapter introduces the concept of minimum gain and presents its useful properties along with numerical examples involving minimum gain.

3.2 Minimum Gain

Definition 3.1 (Minimum Gain [8, 9]). A causal system, $\mathcal{G} : \mathcal{L}_{2e} \rightarrow \mathcal{L}_{2e}$, has a minimum gain $0 \leq \nu < \infty$ if there exists $\beta \in \mathbb{R}$ such that

$$\|\mathcal{G}\mathbf{u}\|_{2T} - \nu \|\mathbf{u}\|_{2T} \geq \beta, \quad \forall \mathbf{u} \in \mathcal{L}_{2e}, \quad \forall T \in \mathbb{R}_{\geq 0}. \quad (3.1)$$

Definition 3.2 (Least Conservative Minimum Gain). The least conservative minimum gain of a causal system, $\mathcal{G} : \mathcal{L}_{2e} \rightarrow \mathcal{L}_{2e}$, denoted as ν^* , is the supremum of

$0 \leq \nu < \infty$ satisfying (3.1) with $\beta \in \mathbb{R}$.

3.2.1 Properties of Minimum Gain

Lemma 3.3 (Least Conservative Minimum Gain and the \mathcal{L}_2 Gain [8]). *The \mathcal{L}_2 gain of a causal invertible system, $\mathcal{G} : \mathcal{L}_{2e} \rightarrow \mathcal{L}_{2e}$, is the inverse of the least conservative minimum gain of the inverse system. That is, $\gamma(\mathcal{G}) = (\nu^*(\mathcal{G}^{-1}))^{-1}$, where $\gamma(\mathcal{G})$ is the \mathcal{L}_2 of \mathcal{G} and $\nu^*(\mathcal{G}^{-1})$ is the least conservative minimum gain of \mathcal{G}^{-1} . If $\mathbf{G} : \mathcal{L}_{2e} \rightarrow \mathcal{L}_{2e}$ is a causal linear invertible system, then $\gamma(\mathbf{G})$ is the \mathcal{H}_∞ norm of \mathbf{G} .*

Lemma 3.4 (Minimum Gain of a Nonminimum Phase Transfer Function). *A non-minimum phase causal LTI SISO system has minimum gain $\nu = 0$.*

Proof. A proof of $\nu = 0$ is found in [8] for asymptotically stable nonminimum phase LTI SISO systems without consideration of initial conditions. The proof using the definition of minimum gain from [9] is presented here.

Consider a causal LTI SISO system represented by the biproper transfer function $G(s) \in \mathbb{C}$ and the minimal state-space realization $(\mathbf{A}, \mathbf{B}, \mathbf{C}, D)$. Assume that the numerator and denominator of $G(s)$ have no common roots, which implies that the pair (\mathbf{A}, \mathbf{B}) is controllable and the pair (\mathbf{A}, \mathbf{C}) is observable. Also, assume that the system has a pair of complex conjugate nonminimum phase zeros at $s = \sigma_0 \pm j\omega_0$, where $\sigma_0 \in \mathbb{R}_{\geq 0}$ and $\omega_0 \in \mathbb{R}$. Since (\mathbf{A}, \mathbf{C}) is observable, the system can be written in the observable canonical form $(\mathbf{A}_{\text{oc}}, \mathbf{B}_{\text{oc}}, \mathbf{C}_{\text{oc}}, D_{\text{oc}})$. The expression for $y(s) = \mathcal{L}\{y(t)\}$ is $y(s) = \mathbf{C}_{\text{oc}}(s\mathbf{1} - \mathbf{A}_{\text{oc}})^{-1}\mathbf{x}_0 + G(s)u(s)$. The definition of minimum gain can be rewritten for the system as

$$\|y\|_{2T} - \nu \|u\|_{2T} \geq \beta. \quad (3.2)$$

The inequality in (3.2) must hold for all $u \in \mathcal{L}_{2e}$ for the system to have minimum gain $0 \leq \nu < \infty$. The input is chosen as $u(t) = w\hat{u}(t) = we^{\sigma_0 t}$ if $\omega_0 = 0$, or $u(t) = w\hat{u}(t) = we^{\sigma_0 t} \sin(\omega_0 t)$ if $\omega_0 \neq 0$, where $w \in \mathbb{R}$. Substituting either expression into $y(s)$ yields

$$y(s) = \mathbf{C}_{\text{oc}}(s\mathbf{1} - \mathbf{A}_{\text{oc}})^{-1}\mathbf{x}_0 + \mathbf{C}_{\text{oc}}(s\mathbf{1} - \mathbf{A}_{\text{oc}})^{-1}\tilde{\mathbf{B}}_{\text{oc}}w, \quad (3.3)$$

where $\tilde{\mathbf{B}}_{\text{oc}}$ is the “ \mathbf{B}_{oc} ” matrix associated with the transfer function $G(s)\hat{u}(s)$ in observable canonical form. The transfer function $G(s)\hat{u}(s)$ has the same poles as $G(s)$, but one less zero (or two less zeros if $\omega_0 \neq 0$). The order of the numerator of

$G(s)\hat{u}(s)$ is one (or two) less than that of $G(s)$, which makes it strictly proper and explains why the matrix D_{oc} is no longer present in (3.3).

The inequality of (3.2) must hold for all initial conditions, so the initial condition $\mathbf{x}_0 = -\tilde{\mathbf{B}}_{oc}\mathbf{w}$ is chosen, which leads to $y(s) = 0$ and $y(t) = 0$. For the chosen input, $\|u\|_{2T} \rightarrow \infty$ as $T \rightarrow \infty$. By increasing T , the value of ν in (3.2) becomes arbitrarily small, and therefore the minimum gain must be $\nu = 0$ for $\beta \in \mathbb{R}$. \square

Lemma 3.5 (Minimum Gain of a Nonminimum Phase Transfer Matrix). *A causal LTI system $\mathbf{G}(s) \in \mathbb{C}^{n_y \times n_u}$ with full normal column rank and a nonminimum phase transmission zero at $z \in \mathbb{C}$ has minimum gain $\nu = 0$.*

Proof. Consider a causal LTI system represented by the transfer matrix $\mathbf{G}(s) \in \mathbb{C}^{n_y \times n_u}$ with a minimal state-space realization $(\mathbf{A}, \mathbf{B}, \mathbf{C}, \mathbf{D})$. Note that the pair (\mathbf{A}, \mathbf{C}) is observable. The proof for a nonminimum phase blocking zero is first presented which is very similar to the proof of Lemma 3.4, followed by the proof of a nonminimum phase transmission zero.

The case of a blocking zero at z with $0 < \text{Re}(z)$ is first considered, which bears many similarities to the proof of Lemma 3.4. By the definition of a blocking zero, $\mathbf{G}(z) = \mathbf{0}$, which is equivalent to every transfer function composing the entries of $\mathbf{G}(s)$ having a zero at z .

Since (\mathbf{A}, \mathbf{C}) is observable, the system can be written in observable canonical form $(\mathbf{A}_{oc}, \mathbf{B}_{oc}, \mathbf{C}_{oc}, \mathbf{D}_{oc})$. The expression for $\mathbf{y}(s) = \mathcal{L}\{\mathbf{y}(t)\}$ is

$$\mathbf{y}(s) = \mathbf{C}_{oc}(s\mathbf{1} - \mathbf{A}_{oc})^{-1}\mathbf{x}_0 + \mathbf{G}(s)\mathbf{u}(s). \quad (3.4)$$

The inequality in (3.1) must hold for all $\mathbf{u} \in \mathcal{L}_{2e}$ for $0 \leq \nu < \infty$ to be a minimum gain of the system. Consider $z \in \mathbb{C}$. If $\text{Im}(z) = 0$ so that z is a real number, the input $\mathbf{u}(t) = \mathbf{w}\hat{u}(t) = \mathbf{w}e^{\sigma_0 t}$ is chosen, whereas the input is chosen as $\mathbf{u}(t) = \mathbf{w}\hat{u}(t) = \mathbf{w}e^{\sigma_0 t} \sin(\omega_0 t)$ otherwise, where $\sigma_0 = \text{Re}(z)$, $\omega_0 = \text{Im}(z)$, and $\mathbf{w} \in \mathbb{R}^{n_u}$, $\mathbf{w} \neq \mathbf{0}$. Note that if $\text{Im}(z) \neq 0$ so that z is not a real number, then it is assumed that the complex conjugate pair (z, \bar{z}) are both zeros. Substituting either expression into (3.4) yields

$$\mathbf{y}(s) = \mathbf{C}_{oc}(s\mathbf{1} - \mathbf{A}_{oc})^{-1}\mathbf{x}_0 + \mathbf{C}_{oc}(s\mathbf{1} - \mathbf{A}_{oc})^{-1}\tilde{\mathbf{B}}_{oc}\mathbf{w},$$

where $\tilde{\mathbf{B}}_{oc}$ is the “ \mathbf{B}_{oc} ” matrix associated with the transfer matrix $\mathbf{G}(s)\hat{u}(s)$ in observable canonical form. The transfer matrix $\mathbf{G}(s)\hat{u}(s)$ has the same poles as $\mathbf{G}(s)$, but one less zero (or two less zeros if $\omega_0 \neq 0$).

The inequality of (3.1) must hold for all initial conditions, so the initial condition $\mathbf{x}_0 = -\tilde{\mathbf{B}}_{oc}\mathbf{w}$ is chosen, which leads to $\mathbf{y}(s) = \mathbf{0}$ and $\mathbf{y}(t) = \mathbf{0}$. Since $0 < \text{Re}(z)$, for the chosen input $\mathbf{u}(t) \rightarrow \infty$ as $t \rightarrow \infty$ we have $\|\mathbf{u}\|_{2T} \rightarrow \infty$ as $T \rightarrow \infty$. By increasing T , the value of ν in (3.1) becomes arbitrarily small, and therefore the minimum gain must be $\nu = 0$ for β to be finite.

The case of a transmission zero at z with $0 < \text{Re}(z)$, where z is not a pole of $\mathbf{G}(s)$ is considered. By the definition of a transmission zero for $\mathbf{G}(s)$ with full normal column rank, $\text{rank}(\mathbf{G}(z)) < n_u$ or $\mathbf{G}(z)\mathbf{u}_0 = \mathbf{0}$ for $\mathbf{u}_0 \in \mathbb{R}^{n_u}$, $\mathbf{u}_0 \neq \mathbf{0}$. Let $\tilde{\mathbf{G}}(s) = \mathbf{G}(s)\mathbf{u}_0$, where $\tilde{\mathbf{G}}(z) = \mathbf{0}$. The newly defined transfer matrix $\tilde{\mathbf{G}}(s)$ has a blocking zero at z , which was shown to have a minimum gain of $\nu = 0$. Since $\mathbf{u}_0 \neq \mathbf{0}$ and $\tilde{\mathbf{G}}(s) = \mathbf{G}(s)\mathbf{u}_0$ has a minimum gain of $\nu = 0$, it follows that $\mathbf{G}(s)$ has a minimum gain of $\nu = 0$.

The case of a transmission zero at z with $0 < \text{Re}(z)$, where z may be a pole of $\mathbf{G}(s)$. By the definition of a transmission zero for $\mathbf{G}(s)$ with full normal column rank, $\lim_{s \rightarrow z} (\mathbf{G}(s)\mathbf{u}(s)) = \mathbf{0}$ for some finite and non-zero $\mathbf{u}(z)$. Let $\hat{\mathbf{G}}(s) = \mathbf{G}(s)\mathbf{u}(s)$, where $\hat{\mathbf{G}}(z) = \mathbf{0}$. Similar to the previous part of the proof, $\mathbf{u}(z) \neq \mathbf{0}$ and $\hat{\mathbf{G}}(s)$ has a blocking zero at z , so it follows that $\mathbf{G}(s)$ has a minimum gain of $\nu = 0$. \square

Remark 3.6. A transfer matrix $\mathbf{G}(s) \in \mathbb{C}^{n_y \times n_u}$, where $n_y < n_u$, will not have full normal column rank and will have a minimum gain of $\nu = 0$. Since $\mathbf{G}(s)$ does not have full normal column rank, a nonzero input $\mathbf{u}(s) \in \mathbb{C}^{n_u}$ can be found such that $\mathbf{y}(s) = \mathbf{G}(s)\mathbf{u}(s) = \mathbf{0}$ regardless of the presence or location of transmission zeros. Following similar arguments to the proof of Lemma 3.5, it can be shown that such a transfer matrix has a minimum gain of zero.

Lemma 3.7. (*Minimum Gain of a Transfer Matrix*) *A causal LTI system represented by the minimum phase transfer matrix $\mathbf{G}(s) \in \mathbb{C}^{n_y \times n_u}$ has a minimum gain $0 \leq \nu < \infty$ if and only if*

$$0 \leq \nu \leq \inf_{\omega \in \mathbb{R}_{\geq 0}} \sigma\{\mathbf{G}(j\omega)\}. \quad (3.5)$$

Proof. Assume (3.1) holds and $\beta = 0$. Since Lemma 3.7 only concerns transfer matrices, the assumption $\beta = 0$ is made without loss of generality. Rearranging (3.1) and squaring both sides of the inequality yields $\|\mathbf{G}\mathbf{u}\|_{2T}^2 \geq \nu^2 \|\mathbf{u}\|_{2T}^2$. Using Parseval's Theorem [58, p. 15] and rearranging gives

$$\int_{-\infty}^{\infty} \mathbf{u}_T^H(j\omega) (\mathbf{G}^H(j\omega)\mathbf{G}(j\omega) - \nu^2\mathbf{1}) \mathbf{u}_T(j\omega) d\omega \geq 0. \quad (3.6)$$

Equation (3.6) must be satisfied for any choice of $\mathbf{u}(j\omega) \in \mathcal{L}_{2e}$, which requires that

$\mathbf{G}^H(j\omega)\mathbf{G}(j\omega) - \nu^2\mathbf{1} \geq 0, \forall \omega \in \mathbb{R}_{\geq 0}$. This implies that $\inf_{\omega \in \mathbb{R}_{\geq 0}} \lambda\{\mathbf{G}^H(j\omega)\mathbf{G}(j\omega) - \nu^2\mathbf{1}\} \geq 0$, which is equivalent to the inequality $\inf_{\omega \in \mathbb{R}_{\geq 0}} \lambda\{\mathbf{G}^H(j\omega)\mathbf{G}(j\omega)\} \geq \nu^2$ or $\inf_{\omega \in \mathbb{R}_{\geq 0}} \underline{\sigma}\{\mathbf{G}(j\omega)\} \geq \nu$. Taking the square root of both sides of this inequality yields $\inf_{\omega \in \mathbb{R}_{\geq 0}} \underline{\sigma}\{\mathbf{G}(j\omega)\} \geq \nu$, which is (3.5) and proves that (3.1) \implies (3.5).

The proof of (3.5) \implies (3.1) is done in the contrapositive by showing $\neg(3.1) \implies \neg(3.5)$. Assume that $\beta = 0$ and \mathcal{G} is an LTI system with transfer matrix $\mathbf{G}(s)$ satisfying $\mathbf{y}(s) = \mathbf{G}(s)\mathbf{u}(s)$. The negation of (3.1) is that $\forall \nu \in \mathbb{R}_{>0}, \exists \mathbf{u} \in \mathcal{L}_{2e}, \exists T \in \mathbb{R}_{\geq 0}$, such that

$$\|\mathbf{y}\|_{2T} < \nu \|\mathbf{u}\|_{2T}. \quad (3.7)$$

The case of $\nu = 0$ is not considered, since $\nu = 0$ always satisfies (3.1). Nonminimum phase systems have minimum gain of $\nu = 0$, which makes this proof only valid for minimum phase systems. Squaring both sides of (3.7) and using Parseval's Theorem yields

$$\int_{-\infty}^{\infty} \mathbf{u}_T^H(j\omega) (\mathbf{G}^H(j\omega)\mathbf{G}(j\omega) - \nu^2\mathbf{1}) \mathbf{u}_T(j\omega) d\omega < 0.$$

Following the same procedure as the first part of this proof, it can be shown that $\inf_{\omega \in \mathbb{R}_{\geq 0}} \underline{\sigma}\{\mathbf{G}(j\omega)\} < \nu$.

To summarize, $\neg(3.1) \implies \inf_{\omega \in \mathbb{R}_{\geq 0}} \underline{\sigma}\{\mathbf{G}(j\omega)\} < \nu$. This is the negation of (3.5), which states that $\nu \leq \inf_{\omega \in \mathbb{R}_{\geq 0}} \underline{\sigma}\{\mathbf{G}(j\omega)\}$. This proves that (3.5) \implies (3.1).

Knowing that (3.1) \implies (3.5) and (3.5) \implies (3.1), it can be concluded that (3.1) and (3.5) are equivalent. \square

Lemma 3.8 (Minimum Gain of Cascaded Systems). *A cascaded system, $\mathcal{G}_3 : \mathcal{L}_{2e} \rightarrow \mathcal{L}_{2e}$, has minimum gain $\nu_3 = \nu_1\nu_2$, where $\mathbf{y}_2 = \mathcal{G}_3\mathbf{u}_1$, $\mathbf{y}_1 = \mathbf{u}_2 = \mathcal{G}_1\mathbf{u}_1$, $\mathbf{y}_2 = \mathcal{G}_2\mathbf{u}_2$, and ν_1 and ν_2 are minimum gains of \mathcal{G}_1 and \mathcal{G}_2 , respectively.*

Proof. Consider the cascaded systems $\mathcal{G}_1 : \mathcal{L}_{2e} \rightarrow \mathcal{L}_{2e}$ and $\mathcal{G}_2 : \mathcal{L}_{2e} \rightarrow \mathcal{L}_{2e}$ with minimum gains ν_1 and ν_2 , respectively, that satisfy

$$\|\mathcal{G}_1\mathbf{u}_1\|_{2T} - \nu_1 \|\mathbf{u}_1\|_{2T} \geq \beta_1, \quad (3.8)$$

$$\|\mathcal{G}_2\mathbf{u}_2\|_{2T} - \nu_2 \|\mathbf{u}_2\|_{2T} \geq \beta_2, \quad (3.9)$$

where \mathbf{u}_1 is the input to \mathcal{G}_1 and $\mathbf{u}_2 = \mathbf{y}_1 = \mathcal{G}_1\mathbf{u}_1$ is the input to \mathcal{G}_2 . Substituting $\mathbf{u}_2 = \mathbf{y}_1 = \mathcal{G}_1\mathbf{u}_1$ and (3.8) into (3.9) gives

$$\|\mathcal{G}_2\mathbf{y}_1\|_{2T} - \nu_1\nu_2 \|\mathbf{u}_1\|_{2T} \geq \nu_2\beta_1 + \beta_2,$$

which can be rewritten as $\|\mathcal{G}_3 \mathbf{u}_1\|_{2T} - \nu_3 \|\mathbf{u}_1\|_{2T} \geq \beta_3$, where $\mathcal{G}_2 \mathbf{y}_1 = \mathcal{G}_3 \mathbf{u}_1$, $\nu_3 = \nu_1 \nu_2$, and $\beta_3 = \nu_2 \beta_1 + \beta_2$. Therefore, \mathcal{G}_3 has minimum gain $\nu_3 = \nu_1 \nu_2$. \square

Lemma 3.9 (Minimum Gain Lemma [9]). *Consider an LTI system, $\mathbf{G} : \mathcal{L}_{2e} \rightarrow \mathcal{L}_{2e}$, with state-space realization $(\mathbf{A}, \mathbf{B}, \mathbf{C}, \mathbf{D})$. A sufficient condition for \mathbf{G} to have minimum gain $0 \leq \nu < \infty$ is that there exists a matrix $\mathbf{P} = \mathbf{P}^\top \geq 0$ such that*

$$\begin{bmatrix} \mathbf{P}\mathbf{A} + \mathbf{A}^\top \mathbf{P} - \mathbf{C}^\top \mathbf{C} & \mathbf{P}\mathbf{B} - \mathbf{C}^\top \mathbf{D} \\ * & \nu^2 \mathbf{1} - \mathbf{D}^\top \mathbf{D} \end{bmatrix} \leq 0. \quad (3.10)$$

If \mathbf{G} is a square system or $\text{span}(\mathbf{C}) \subseteq \text{span}(\mathbf{D})$, then the preceding condition is necessary and sufficient for \mathbf{G} to have minimum gain $0 \leq \nu < \infty$.

The Minimum Gain Lemma is a special case of the Exterior Conic Sector Lemma found in [59], with a cone whose bounds are symmetric.

Lemma 3.10 (The Discrete-Time Minimum Gain Lemma). *Consider an LTI system, $\mathbf{G} : \mathcal{L}_{2e} \rightarrow \mathcal{L}_{2e}$, with discrete-time state-space realization $(\mathbf{A}_d, \mathbf{B}_d, \mathbf{C}_d, \mathbf{D}_d)$. The system \mathbf{G} has minimum gain $0 \leq \nu < \infty$ if there exists a matrix $\mathbf{P} = \mathbf{P}^\top \geq 0$ such that*

$$\begin{bmatrix} \mathbf{A}_d^\top \mathbf{P} \mathbf{A}_d - \mathbf{P} - \mathbf{C}_d^\top \mathbf{C}_d & \mathbf{A}_d^\top \mathbf{P} \mathbf{B}_d - \mathbf{C}_d^\top \mathbf{D}_d \\ * & \mathbf{B}_d^\top \mathbf{P} \mathbf{B}_d + \nu^2 \mathbf{1} - \mathbf{D}_d^\top \mathbf{D}_d \end{bmatrix} \leq 0. \quad (3.11)$$

Proof. Consider the non-negative function $V(\mathbf{x}_k) = \mathbf{x}_k^\top \mathbf{P} \mathbf{x}_k$. Evaluating $V(\mathbf{x}_{k+1})$ yields

$$\begin{aligned} V(\mathbf{x}_{k+1}) &= \mathbf{x}_{k+1}^\top \mathbf{P} \mathbf{x}_{k+1} \\ &= (\mathbf{A}_d \mathbf{x}_k + \mathbf{B}_d \mathbf{u}_k)^\top \mathbf{P} (\mathbf{A}_d \mathbf{x}_k + \mathbf{B}_d \mathbf{u}_k) \\ &= \mathbf{x}_k^\top \mathbf{A}_d \mathbf{P} \mathbf{A}_d \mathbf{x}_k + \mathbf{x}_k^\top \mathbf{A}_d \mathbf{P} \mathbf{B}_d \mathbf{u}_k + \mathbf{u}_k^\top \mathbf{B}_d^\top \mathbf{P} \mathbf{A}_d \mathbf{x}_k + \mathbf{u}_k^\top \mathbf{B}_d^\top \mathbf{P} \mathbf{B}_d \mathbf{u}_k \\ &\quad + \mathbf{y}_k^\top \mathbf{y}_k - \mathbf{y}_k^\top \mathbf{y}_k + \nu^2 \mathbf{u}_k^\top \mathbf{u}_k - \nu^2 \mathbf{u}_k^\top \mathbf{u}_k \\ &= \mathbf{y}_k^\top \mathbf{y}_k - \nu^2 \mathbf{u}_k^\top \mathbf{u}_k + \mathbf{x}_k^\top (\mathbf{A}_d \mathbf{P} \mathbf{A}_d - \mathbf{C}_d^\top \mathbf{C}_d) \mathbf{x}_k + \mathbf{x}_k^\top (\mathbf{A}_d \mathbf{P} \mathbf{B}_d - \mathbf{C}_d^\top \mathbf{D}_d) \mathbf{u}_k \\ &\quad + \mathbf{u}_k^\top (\mathbf{B}_d^\top \mathbf{P} \mathbf{A}_d - \mathbf{D}_d^\top \mathbf{C}_d^\top) \mathbf{x}_k + \mathbf{u}_k^\top (\mathbf{B}_d^\top \mathbf{P} \mathbf{B}_d + \nu^2 \mathbf{1} - \mathbf{D}_d^\top \mathbf{D}_d) \mathbf{u}_k. \end{aligned}$$

Subtracting $V(\mathbf{x}_k)$ from $V(\mathbf{x}_{k+1})$ and rearranging in matrix form gives

$$\begin{aligned}
V(\mathbf{x}_{k+1}) - V(\mathbf{x}_k) &= \mathbf{x}_k^\top (\mathbf{A}_d \mathbf{P} \mathbf{A}_d - \mathbf{P} - \mathbf{C}_d^\top \mathbf{C}_d) \mathbf{x}_k + \mathbf{x}_k^\top (\mathbf{A}_d \mathbf{P} \mathbf{B}_d - \mathbf{C}_d^\top \mathbf{D}_d) \mathbf{u}_k \\
&\quad + \mathbf{u}_k^\top (\mathbf{B}_d^\top \mathbf{P} \mathbf{A}_d - \mathbf{D}_d^\top \mathbf{C}_d^\top) \mathbf{x}_k + \mathbf{u}_k^\top (\mathbf{B}_d^\top \mathbf{P} \mathbf{B}_d + \nu^2 \mathbf{1} - \mathbf{D}_d^\top \mathbf{D}_d) \mathbf{u}_k \\
&\quad + \mathbf{y}_k^\top \mathbf{y}_k - \nu^2 \mathbf{u}_k^\top \mathbf{u}_k \\
&= \begin{bmatrix} \mathbf{x}_k \\ \mathbf{u}_k \end{bmatrix}^\top \begin{bmatrix} \mathbf{A}_d^\top \mathbf{P} \mathbf{A}_d - \mathbf{P} - \mathbf{C}_d^\top \mathbf{C}_d & \mathbf{A}_d^\top \mathbf{P} \mathbf{B}_d - \mathbf{C}_d^\top \mathbf{D}_d \\ * & \mathbf{B}_d^\top \mathbf{P} \mathbf{B}_d + \nu^2 \mathbf{1} - \mathbf{D}_d^\top \mathbf{D}_d \end{bmatrix} \begin{bmatrix} \mathbf{x}_k \\ \mathbf{u}_k \end{bmatrix} \\
&\quad + \mathbf{y}_k^\top \mathbf{y}_k - \nu^2 \mathbf{u}_k^\top \mathbf{u}_k. \tag{3.12}
\end{aligned}$$

Assuming (3.11) holds, it follows from (3.12) that

$$V(\mathbf{x}_{k+1}) - V(\mathbf{x}_k) \leq \mathbf{y}_k^\top \mathbf{y}_k - \nu^2 \mathbf{u}_k^\top \mathbf{u}_k.$$

Using induction it can be shown that

$$V(\mathbf{x}_N) - V(\mathbf{x}_0) \leq \sum_{i=0}^N \mathbf{y}_i^\top \mathbf{y}_i - \nu^2 \sum_{i=0}^N \mathbf{u}_i^\top \mathbf{u}_i.$$

Since $V(\mathbf{x}_N) \geq 0$, it is also follows that

$$\sum_{i=0}^N \mathbf{y}_i^\top \mathbf{y}_i - \nu^2 \sum_{i=0}^N \mathbf{u}_i^\top \mathbf{u}_i \geq -V(\mathbf{x}_0). \tag{3.13}$$

Making the substitution $N = T/\Delta T$, where $0 < T < \infty$ and ΔT is the discretization time step, (3.13) becomes

$$\|\mathbf{y}\|_{2T}^2 - \nu^2 \|\mathbf{u}\|_{2T}^2 \geq -V(\mathbf{x}_0).$$

Therefore, the discrete-time LTI system, $\mathbf{G} : \mathcal{L}_{2e} \rightarrow \mathcal{L}_{2e}$, with state-space realization $(\mathbf{A}_d, \mathbf{B}_d, \mathbf{C}_d, \mathbf{D}_d)$ has minimum gain $0 \leq \nu < \infty$. \square

Lemma 3.11 (Modified Minimum Gain Lemma). *Consider an LTI system, $\mathbf{G} : \mathcal{L}_{2e} \rightarrow \mathcal{L}_{2e}$, with state-space realization $(\mathbf{A}, \mathbf{B}, \mathbf{C}, \mathbf{D})$. A sufficient condition for \mathbf{G} to have minimum gain $0 \leq \nu < \infty$ is that there exists a matrix $\mathbf{P} = \mathbf{P}^\top \geq 0$ such that*

$$\bar{\mathbf{M}}(\mathbf{P}, \nu) = \begin{bmatrix} \mathbf{P} \mathbf{A} + \mathbf{A}^\top \mathbf{P} & \mathbf{P} \mathbf{B} - \mathbf{C}^\top \mathbf{D} \\ * & \nu^2 \mathbf{1} - \mathbf{D}^\top \mathbf{D} \end{bmatrix} \leq 0.$$

Proof. Assuming $\bar{\mathbf{M}} \leq 0$, it is shown that

$$\begin{aligned}
\|\mathcal{G}\mathbf{u}\|_{2T}^2 - \nu^2 \|\mathbf{u}\|_{2T}^2 &= \int_0^T \left(|\mathbf{C}\mathbf{x} + \mathbf{D}\mathbf{u}|^2 - \nu^2 |\mathbf{u}|^2 + \frac{d}{dt} (\mathbf{x}^\top \mathbf{P}\mathbf{x}) \right. \\
&\quad \left. - 2\mathbf{x}^\top \mathbf{P}(\mathbf{A}\mathbf{x} + \mathbf{B}\mathbf{u}) - \mathbf{x}^\top \mathbf{C}^\top \mathbf{C}\mathbf{x} + \mathbf{x}^\top \mathbf{C}^\top \mathbf{C}\mathbf{x} \right) dt, \\
&= \int_0^T \left(- \begin{bmatrix} \mathbf{x}^\top & \mathbf{u}^\top \end{bmatrix} \begin{bmatrix} \mathbf{P}\mathbf{A} + \mathbf{A}^\top \mathbf{P} & \mathbf{P}\mathbf{B} - \mathbf{C}^\top \mathbf{D} \\ * & \nu^2 \mathbf{1} - \mathbf{D}^\top \mathbf{D} \end{bmatrix} \begin{bmatrix} \mathbf{x} \\ \mathbf{u} \end{bmatrix} \right. \\
&\quad \left. + \frac{d}{dt} (\mathbf{x}^\top \mathbf{P}\mathbf{x}) + \mathbf{x}^\top \mathbf{C}^\top \mathbf{C}\mathbf{x} \right) dt, \\
&= \int_0^T \left(- \begin{bmatrix} \mathbf{x}^\top & \mathbf{u}^\top \end{bmatrix} \bar{\mathbf{M}} \begin{bmatrix} \mathbf{x} \\ \mathbf{u} \end{bmatrix} + \frac{d}{dt} (\mathbf{x}^\top \mathbf{P}\mathbf{x}) + \mathbf{x}^\top \mathbf{C}^\top \mathbf{C}\mathbf{x} \right) dt \\
&\geq -\mathbf{x}_0^\top \mathbf{P}\mathbf{x}_0 = \tilde{\beta},
\end{aligned}$$

which proves that \mathbf{G} has minimum gain $0 \leq \nu < \infty$. □

3.2.2 Numerical Examples of Minimum Gain

Example 3.12 (Minimum Gain of a SISO Transfer Function). Consider the LTI SISO systems given by the minimum phase transfer functions

$$G_1(s) = \frac{10s + 2}{s + 3k}, \quad G_2(s) = \frac{2s^2 + 30s + 4}{s^2 + ks + 2}, \quad G_3(s) = \frac{6s^2 + 0.9s + 1}{2s^2 + ks + 1}, \quad k = \pm 1. \tag{3.14}$$

Bode magnitude plots of $G_1(s)$, $G_2(s)$, and $G_3(s)$ with $k = 1$ are shown in Figure 3.1. From Figure 3.1 it can be gleaned that for $k = 1$, $G_1(s)$ has an \mathcal{H}_∞ norm of $\gamma_1 = 10$ and a least conservative minimum gain of $\nu_1^* = 2/3$, $G_2(s)$ has an \mathcal{H}_∞ norm of $\gamma_2 = 30$ and a least conservative minimum gain of $\nu_2^* = 2$, and $G_3(s)$ has an \mathcal{H}_∞ norm of $\gamma_3 = 3.61$ and a least conservative minimum gain of $\nu_3^* = 0.45$. Note that the least conservative minimum gains of $G_1(s)$, $G_2(s)$, and $G_3(s)$ remain unchanged for $k = -1$.

Example 3.13 (Minimum Gain of a Square Multi-Input Multi-Output (MIMO))

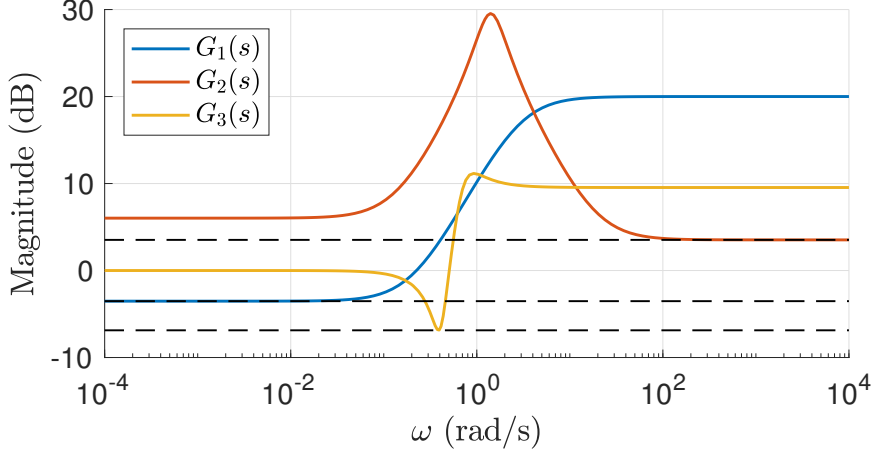


Figure 3.1: Bode magnitude plot of $G_1(s)$ and $G_2(s)$ with $k = 1$ in Example 3.12. Black dashed lines represent $\nu^* = \inf_{\omega \in \mathbb{R}_{\geq 0}} |G(j\omega)|$ of each system.

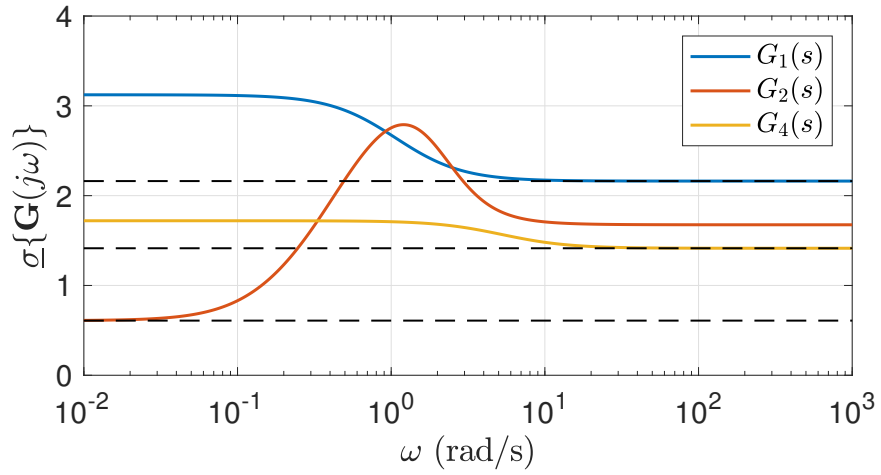


Figure 3.2: Plots of the minimum singular value of $\mathbf{G}_1(s)$, $\mathbf{G}_2(s)$, and $\mathbf{G}_4(s)$ versus frequency with $k = 1$ in Examples 3.13 and 3.14. Black dashed lines represent $\nu^* = \inf_{\omega \in \mathbb{R}_{\geq 0}} \underline{\sigma}\{\mathbf{G}(j\omega)\}$ of each system.

Transfer Matrix). Consider the MIMO transfer matrices

$$\mathbf{G}_1(s) = \begin{bmatrix} \frac{2s+5}{s-1} & 1 \\ -1 & \frac{4s+3}{s-1} \end{bmatrix},$$

$$\mathbf{G}_2(s) = \begin{bmatrix} \frac{2s^2+15s+4}{s^2+2s+2} & -\frac{s+1}{s+2} \\ \frac{7s-3}{s+1} & \frac{3s^2+10s+2}{s^2+3s+1} \end{bmatrix}.$$

Plots of the minimum singular values of $\mathbf{G}_1(s)$ and $\mathbf{G}_2(s)$ are shown in Figure 3.2. It can be seen in Figure 3.2 that $\mathbf{G}_1(s)$ has a least conservative minimum gain of $\nu_1^* = 2.16$, while $\mathbf{G}_2(s)$ has a least conservative minimum gain of $\nu_2^* = 0.61$.

Example 3.14 (Minimum Gain of a Nonsquare MIMO Transfer Matrix). Consider the MIMO transfer matrices

$$\mathbf{G}_3(s) = \begin{bmatrix} \frac{s-1}{s+5} & 1 \end{bmatrix}, \quad \mathbf{G}_4(s) = \begin{bmatrix} 1 \\ \frac{s+7}{s+5} \end{bmatrix}.$$

The minimum gain of $\mathbf{G}_3(s)$ is $\nu_3 = 0$, and the least conservative minimum gain of $\mathbf{G}_4(s)$ is $\nu_4^* = 1.41$. A plot of the minimum singular values of $\mathbf{G}_4(s)$ is given in Figure 3.2. The minimum singular value of $\mathbf{G}_3(s)$ is zero for all frequencies, and therefore is not plotted.

Chapter 4

\mathcal{H}_∞ -Optimal Parallel Feedforward Control using Minimum Gain

4.1 Introduction

There are well-established feedback controller synthesis methods that are capable of enforcing closed-loop system properties, including the location of closed-loop poles. However, in general feedback control is not capable of placing the transmission zeros of the closed-loop system. Parallel feedforward control, introduced in [13, 22, 25], is capable of placing closed-loop zeros by creating an augmented system with a new output. Parallel feedforward control has been used in the literature to render systems minimum phase for adaptive control schemes that have a minimum phase requirement [13, 60–62].

Despite having intriguing properties, including a duality with feedback control [63], the literature on parallel feedforward control is limited. A challenge in synthesizing a useful parallel feedforward controller stems from the fact that it is difficult to minimize the difference between the original system output and the augmented system output. For example, when synthesizing a feedback controller that is inverted to obtain a parallel feedforward controller, minimizing the \mathcal{H}_∞ norm of the parallel feedforward controller requires maximizing the least conservative minimum gain of the feedback controller. Minimum gain has previously been used for the purposes of rendering a system minimum phase using feedback control on plants with a specific structure [2, 24]. The work of [2, 24] is based on the notion that a system with nonzero minimum gain is minimum phase (Lemma 3.5).

In this chapter, \mathcal{H}_∞ -optimal static and dynamic parallel feedforward controller

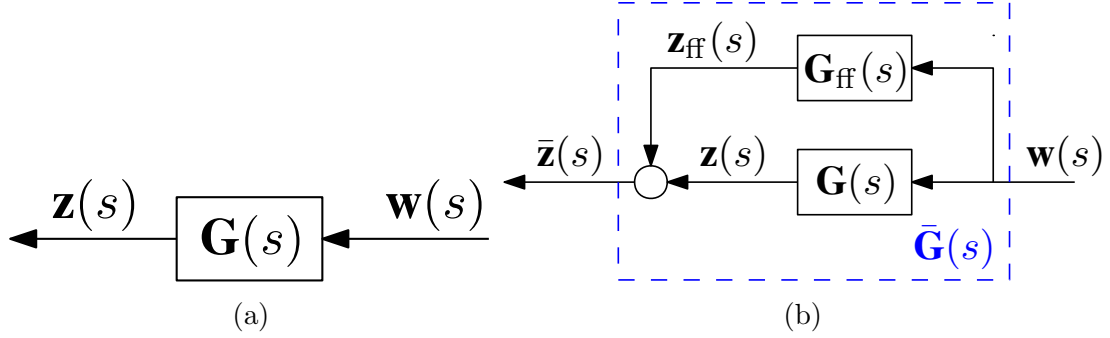


Figure 4.1: Block diagrams of (a) the plant and (b) the plant augmented with a parallel feedforward controller.

synthesis methods are presented that render the augmented system minimum phase. An indirect method is presented that is based on the parallel feedforward control method of [13], where a minimum gain of the feedback controller is maximized, which yields an \mathcal{H}_∞ -optimal parallel feedforward controller when inverted. This is done using an LMI condition for minimum gain from [9]. A direct method is also proposed that directly synthesizes the parallel feedforward controller by imposing a nonzero minimum gain condition on the augmented system, which ensures that it is minimum phase. The direct and indirect dynamic parallel feedforward controller synthesis methods are designed with their \mathcal{H}_∞ norm minimized within a frequency band specified by a weighting transfer matrix. The novel contributions of this chapter include two systematic LMI-based methods to synthesize \mathcal{H}_∞ -optimal parallel feedforward controllers: an indirect method based on [13] and a direct method that both make use of the properties of minimum gain.

The remaining sections of this chapter proceed as follows. Section 4.2 introduces the notation used throughout the paper, the problem statement, as well as important definitions and theorems. The proposed static and dynamic parallel feedforward controller synthesis methods are presented in Sections 4.3 and 4.4, respectively. Numerical results with the parallel feedforward controllers are included in Section 4.5. Concluding remarks are given in Section 4.6.

4.2 Preliminaries

4.2.1 Problem Statement

Consider the square LTI plant $\mathbf{G}(s) \in \mathbb{C}^{n_z \times n_w}$, shown in Figure 4.1a, with input signal $\mathbf{w}(s)$ and output signal $\mathbf{z}(s)$, where $n_z = n_w$. The goal is to design a parallel feedforward controller $\mathbf{G}_{\text{ff}}(s) \in \mathbb{C}^{n_z \times n_w}$ such that the augmented system $\bar{\mathbf{G}}(s) =$

$\mathbf{G}(s) + \mathbf{G}_{\text{ff}}(s)$, shown in Figure 4.1b, only features minimum phase transmission zeros, and the \mathcal{H}_∞ norm of $\mathbf{G}_{\text{ff}}(s) = \bar{\mathbf{G}}(s) - \mathbf{G}(s)$ or $\mathbf{W}(s)\mathbf{G}_{\text{ff}}(s) = \mathbf{W}(s)(\bar{\mathbf{G}}(s) - \mathbf{G}(s))$ is minimized, where $\mathbf{W}(s)$ is a weighting transfer matrix. It may be important to ensure the difference between $\bar{\mathbf{G}}(s)$ and $\mathbf{G}(s)$ is close to zero in specific frequency bands, while in others it may not matter. The weighting transfer matrix allows the designer to encode this information into the synthesis problem. The plant $\mathbf{G}(s)$ can be described by the minimal state-space realization

$$\begin{aligned}\dot{\mathbf{x}}(t) &= \mathbf{A}\mathbf{x}(t) + \mathbf{B}\mathbf{w}(t), \\ \mathbf{z}(t) &= \mathbf{C}\mathbf{x}(t) + \mathbf{D}\mathbf{w}(t).\end{aligned}$$

If the system is not square, then a squaring-up procedure is performed prior to parallel feedforward controller synthesis [25–27]. It is also assumed that $\mathbf{G}(s)$ has poles in the open left-half plane (OLHP), which simplifies the choice of an initial controller in the synthesis methods presented in Sections 4.3 and 4.4. If this is not the case, then an asymptotically stabilizing feedback controller is designed prior to the synthesis of the parallel feedforward controller.

4.2.2 High-Gain Parallel Feedforward Control

Consider the SISO plant $G(s) = n(s)/d(s)$ and the SISO parallel feedforward controller $G_{\text{ff}}(s) = kn_{\text{ff}}(s)/d_{\text{ff}}(s)$, where $0 \leq k < \infty$. The augmented plant with parallel feedforward control is

$$\bar{G}(s) = G(s) + G_{\text{ff}}(s) = \frac{n(s)d_{\text{ff}}(s) + kn_{\text{ff}}(s)d(s)}{d(s)d_{\text{ff}}(s)}.$$

The zeros of $\bar{G}(s)$ are the roots of $n(s)d_{\text{ff}}(s) + kn_{\text{ff}}(s)d(s) = 0$. Notice that as $k \rightarrow \infty$, the zeros of $\bar{G}(s)$ approach the roots of $n_{\text{ff}}(s)d(s) = 0$. Therefore, assuming $G(s)$ has only OLHP poles, $G_{\text{ff}}(s)$ is minimum phase, and k is sufficiently large, then $\bar{G}(s)$ is minimum phase. This property extends to MIMO plants and parallel feedforward controllers. Although it is not practical to design parallel feedforward controllers with high gain, this property is exploited in the controller synthesis methods of Sections 4.3 and 4.4 to find an initial feasible controller.

4.3 Static Parallel Feedforward Controller

A static parallel feedforward controller of the form $\mathbf{z}_{\text{ff}}(s) = \mathbf{K}_{\text{ff}}\mathbf{w}(s)$ is considered, where $\mathbf{K}_{\text{ff}} \in \mathbb{R}^{n_z \times n_w}$. The augmented system has state-space representation

$$\begin{aligned}\dot{\mathbf{x}}(t) &= \mathbf{A}\mathbf{x}(t) + \mathbf{B}\mathbf{w}(t), \\ \bar{\mathbf{z}}(t) &= \mathbf{C}\mathbf{x}(t) + (\mathbf{D} + \mathbf{K}_{\text{ff}})\mathbf{w}(t),\end{aligned}$$

where

$$\bar{\mathbf{z}}(s) = \mathbf{z}(s) + \mathbf{z}_{\text{ff}}(s) = (\mathbf{G}(s) + \mathbf{K}_{\text{ff}})\mathbf{w}(s) = \bar{\mathbf{G}}(s)\mathbf{w}(s).$$

In this case, minimizing the \mathcal{H}_∞ norm of $\bar{\mathbf{G}}(s) - \mathbf{G}(s)$ is equivalent to minimizing $\bar{\sigma}(\mathbf{K}_{\text{ff}})$.

4.3.1 Direct Method using Minimum Gain

The direct method solves for \mathbf{K}_{ff} directly by ensuring that $\bar{\mathbf{G}}(s)$ has non-zero minimum gain, and therefore only has minimum phase transmission zeros.

A minimum gain of the augmented system can be found using the Minimum Gain Lemma (Lemma 3.9) and expanding the terms, which gives

$$\begin{bmatrix} \mathbf{P}\mathbf{A} + \mathbf{A}^\top\mathbf{P} - \mathbf{C}^\top\mathbf{C} & \mathbf{P}\mathbf{B} - \mathbf{C}^\top\mathbf{D} & \mathbf{0} \\ * & -\mathbf{D}^\top\mathbf{D} - \mathbf{D}^\top\mathbf{K}_{\text{ff}} - \mathbf{K}_{\text{ff}}^\top\mathbf{D} - \mathbf{K}_{\text{ff}}^\top\mathbf{K}_{\text{ff}} & \bar{\nu}\mathbf{1} \\ * & * & -\mathbf{1} \end{bmatrix} \leq 0. \quad (4.1)$$

Lemma 4.1. *The matrix inequality of (4.1) is implied by the matrix inequality in the variables \mathbf{K}_{ff} , \mathbf{Y} , $\mathbf{P} = \mathbf{P}^\top \geq 0$, and $0 \leq \bar{\nu} < \infty$, given by*

$$\begin{bmatrix} \mathbf{P}\mathbf{A} + \mathbf{A}^\top\mathbf{P} - \mathbf{C}^\top\mathbf{C} & \mathbf{P}\mathbf{B} - \mathbf{C}^\top\mathbf{D} & \mathbf{0} & \mathbf{0} \\ * & -\mathbf{D}^\top\mathbf{D} - \mathbf{D}^\top\mathbf{K}_{\text{ff}} - \mathbf{K}_{\text{ff}}^\top\mathbf{D} - \mathbf{Y}^\top\mathbf{K}_{\text{ff}} - \mathbf{K}_{\text{ff}}^\top\mathbf{Y} & \bar{\nu}\mathbf{1} & \mathbf{Y}^\top \\ * & * & -\mathbf{1} & \mathbf{0} \\ * & * & * & -\mathbf{1} \end{bmatrix} \leq 0. \quad (4.2)$$

Proof. Consider a special case of Young's relation in Lemma 2.20 with $\mathbf{S} = \mathbf{1}$ and $\mathbf{X} = \mathbf{K}_{\text{ff}}$. With some rearranging this yields the matrix inequality

$$-\mathbf{K}_{\text{ff}}^\top\mathbf{K}_{\text{ff}} \leq -(\mathbf{Y}^\top\mathbf{K}_{\text{ff}} + \mathbf{K}_{\text{ff}}^\top\mathbf{Y}) + \mathbf{Y}^\top\mathbf{Y}. \quad (4.3)$$

Substituting (4.3) into (4.1) and using the Schur Complement on the term $\mathbf{Y}^\top\mathbf{Y}$, it is

shown that (4.2) \implies (4.1). □

Lemma 4.2. [44] Consider the square matrix $\mathbf{K}_{\text{ff}} \in \mathbb{R}^{n \times n}$. The inequality $0 < \bar{\sigma}(\mathbf{K}_{\text{ff}}) < \gamma$ is satisfied for $0 < \gamma < \infty$ if and only if \mathbf{K}_{ff} satisfies the LMI

$$\begin{bmatrix} \gamma \mathbf{1} & \mathbf{K}_{\text{ff}} \\ * & \gamma \mathbf{1} \end{bmatrix} > 0. \quad (4.4)$$

Synthesis Method 1. The controller synthesis method is performed with the following iterative steps.

1. Set $\mathbf{K}_{\text{ff},0}$ to some large value and set $k = 0$.
2. Fix $\mathbf{K}_{\text{ff},k}$ and solve for $\mathbf{Y}_k, \mathbf{P} = \mathbf{P}^\top > 0$, and $0 < \nu < \infty$, that satisfy (4.2). If $k = 0$ and this step is infeasible, then return to Step 1) and set $\mathbf{K}_{\text{ff},0}$ to a larger value.
3. Fix \mathbf{Y}_k and solve for $\mathbf{K}_{\text{ff},k+1}, \mathbf{P} = \mathbf{P}^\top > 0$, $0 < \nu < \infty$, and $0 < \gamma < \infty$ that minimize $\mathcal{J}(\gamma) = \gamma$ subject to (4.2) and (4.4).
4. If a specified stopping criteria is satisfied (e.g., the difference between γ is successive iterations is less than a specified tolerance), exit and set $\mathbf{K}_{\text{ff}} = \mathbf{K}_{\text{ff},k+1}$. Otherwise, set $k = k + 1$ and repeat Steps 2) and 3).

4.3.2 Indirect Method using Inversion and Minimum Gain

The indirect method solves for the static output feedback gain $\mathbf{K} = \mathbf{K}_{\text{ff}}^{-1}$ that asymptotically stabilizes the closed-loop system, which ensures that $\bar{\mathbf{G}}(s)$ only features minimum phase transmission zeros. This method requires the assumption that $(\mathbf{A}, \mathbf{B}, \mathbf{C})$ is static output feedback stabilizable. A static feedback controller of the form $\mathbf{u} = -\mathbf{K}\mathbf{y}$ asymptotically stabilizes $\mathbf{G}(s)$ if and only if there exists $\mathbf{P} = \mathbf{P}^\top > 0$ such that

$$\mathbf{P}(\mathbf{A} - \mathbf{B}\bar{\mathbf{K}}\mathbf{C}) + (\mathbf{A} - \mathbf{B}\bar{\mathbf{K}}\mathbf{C})\mathbf{P} < 0, \quad (4.5)$$

where $\bar{\mathbf{K}} = (\mathbf{1} + \mathbf{K}\mathbf{D})^{-1}\mathbf{K}$ is the result of simplifying an algebraic loop. The algebraic loop is simplified by knowing that

$$\mathbf{u}(t) = -\mathbf{K}\mathbf{y}(t) = -\mathbf{K}(\mathbf{C}\mathbf{x}(t) + \mathbf{D}\mathbf{u}(t)),$$

which is rearranged to yield $(\mathbf{1} + \mathbf{KD}) \mathbf{u}(t) = -\mathbf{KCx}(t)$ and

$$\mathbf{u}(t) = -(\mathbf{1} + \mathbf{KD})^{-1} \mathbf{KCx}(t) = -\bar{\mathbf{K}}\mathbf{Cx}(t).$$

The indirect method maximizes $\underline{\sigma}(\mathbf{K})$, which is equivalent to minimizing $\bar{\sigma}(\mathbf{K}_{\text{ff}})$.

Lemma 4.3. *Consider the square matrix $\mathbf{K} = (\mathbf{1} - \mathbf{D}\bar{\mathbf{K}})^{-1} \bar{\mathbf{K}} \in \mathbb{R}^{n \times n}$. The inequality $\nu < \underline{\sigma}(\mathbf{K}) < \infty$ is satisfied for $0 < \nu < \infty$ if \mathbf{K} satisfies the matrix inequality*

$$\begin{bmatrix} -\mathbf{Z}^{\top} \bar{\mathbf{K}} - \bar{\mathbf{K}}^{\top} \mathbf{Z} & \mathbf{Z}^{\top} (\mathbf{1} - \mathbf{D}\bar{\mathbf{K}}) & \nu \mathbf{1} \\ * & -\mathbf{1} & \mathbf{0} \\ * & * & -\mathbf{1} \end{bmatrix} < 0. \quad (4.6)$$

Proof. The inequality $\nu < \underline{\sigma}(\mathbf{K}) < \infty$ is satisfied if and only if

$$\begin{bmatrix} -\mathbf{K}^{\top} \mathbf{K} & \nu \mathbf{1} \\ * & -\mathbf{1} \end{bmatrix} < 0. \quad (4.7)$$

Using Young's Relation with $\mathbf{X} = \mathbf{K}$, $\mathbf{Y} = (\mathbf{1} - \mathbf{D}\bar{\mathbf{K}})^{\top} \mathbf{Z}$, and $\mathbf{S} = \mathbf{1}$, it can be shown that

$$-\mathbf{K}^{\top} \mathbf{K} \leq -\bar{\mathbf{K}}^{\top} \mathbf{Z} - \mathbf{Z}^{\top} \bar{\mathbf{K}} + \mathbf{Z}^{\top} (\mathbf{1} - \mathbf{D}\bar{\mathbf{K}}) (\mathbf{1} - \mathbf{D}\bar{\mathbf{K}})^{\top} \mathbf{Z}. \quad (4.8)$$

From (4.8), it is known that (4.7) is implied by

$$\begin{bmatrix} -\bar{\mathbf{K}}^{\top} \mathbf{Z} - \mathbf{Z}^{\top} \bar{\mathbf{K}} + \mathbf{Z}^{\top} (\mathbf{1} - \mathbf{D}\bar{\mathbf{K}}) (\mathbf{1} - \mathbf{D}\bar{\mathbf{K}})^{\top} \mathbf{Z} & \nu \mathbf{1} \\ * & -\mathbf{1} \end{bmatrix} < 0. \quad (4.9)$$

Using the Schur complement on (4.9) yields (4.6). \square

Synthesis Method 2. *The controller synthesis method is performed iteratively in the following four steps.*

1. Find a controller gain $\bar{\mathbf{K}}_0 = (\mathbf{1} + \mathbf{K}_0 \mathbf{D})^{-1} \mathbf{K}_0$ that asymptotically stabilizes the closed-loop system, and set $k = 0$.
2. Fix $\bar{\mathbf{K}}_k$ and solve for \mathbf{P}_k , \mathbf{Z}_k , and $0 < \nu < \infty$ that maximize $\mathcal{J}(\nu) = \nu$ subject to the LMIs in (4.5) and (4.6).
3. Fix \mathbf{P}_k and \mathbf{Z}_k and solve for $\bar{\mathbf{K}}_{k+1}$ and $0 < \nu < \infty$ that maximize $\mathcal{J}(\nu) = \nu$ subject to the LMIs in (4.5) and (4.6).

4. If a specified stopping criteria is satisfied, exit. Otherwise, set $k = k + 1$ and repeat Steps 2) and 3).

The controller gain is recovered as $\mathbf{K} = (\mathbf{1} - \mathbf{D}\bar{\mathbf{K}}_{k+1})^{-1} \bar{\mathbf{K}}_{k+1}$, and the static parallel feedforward controller is given by $\mathbf{K}_{\text{ff}} = \mathbf{K}^{-1}$.

4.3.3 Discussion

Both direct and indirect static parallel feedforward controller synthesis methods are iterative and require the selection of an initial feasible controller gain. Due to the non-convexity of the synthesis methods, the solution will only converge to a controller gain that represents a local minimizer. As such, the selection of the initial controller gain greatly affects sub-optimal solution obtained. It is observed through numerical examples where the global minimizer is known analytically, including the one in Section 5.4, that initializing the direct synthesis methods with a sufficiently large positive or negative gain can yield the global minimizer. Analogously, the indirect method should be initialized with either a sufficiently small positive or negative gain.

4.4 Dynamic Parallel Feedforward Controller

A dynamic parallel feedforward controller is considered with state-space representation given by

$$\dot{\mathbf{x}}_{\text{ff}}(t) = \mathbf{A}_{\text{ff}}\mathbf{x}_{\text{ff}}(t) + \mathbf{B}_{\text{ff}}\mathbf{w}(t),$$

$$\mathbf{z}_{\text{ff}}(t) = \mathbf{C}_{\text{ff}}\mathbf{x}_{\text{ff}}(t) + \mathbf{D}_{\text{ff}}\mathbf{w}(t).$$

The augmented system $\bar{\mathbf{z}}(s) = \mathbf{z}(s) + \mathbf{z}_{\text{ff}}(s) = \bar{\mathbf{G}}(s)\mathbf{w}$ has a state-space realization

$$\dot{\bar{\mathbf{x}}}(t) = \bar{\mathbf{A}}\bar{\mathbf{x}}(t) + \bar{\mathbf{B}}\mathbf{w}(t), \quad (4.10)$$

$$\bar{\mathbf{z}}(t) = \bar{\mathbf{C}}\bar{\mathbf{x}}(t) + \bar{\mathbf{D}}\mathbf{w}(t), \quad (4.11)$$

where $\bar{\mathbf{x}}^{\text{T}} = \begin{bmatrix} \mathbf{x}^{\text{T}} & \mathbf{x}_{\text{ff}}^{\text{T}} \end{bmatrix}$,

$$\bar{\mathbf{A}} = \begin{bmatrix} \mathbf{A} & \mathbf{0} \\ \mathbf{0} & \mathbf{A}_{\text{ff}} \end{bmatrix}, \quad \bar{\mathbf{B}} = \begin{bmatrix} \mathbf{B} \\ \mathbf{B}_{\text{ff}} \end{bmatrix}, \quad \bar{\mathbf{C}} = \begin{bmatrix} \mathbf{C} & \mathbf{C}_{\text{ff}} \end{bmatrix}, \quad \bar{\mathbf{D}} = \mathbf{D} + \mathbf{D}_{\text{ff}}.$$

The \mathcal{H}_∞ norm of $\mathbf{W}(s)\mathbf{G}_{\text{ff}}(s) = \tilde{\mathbf{C}}_{\text{ff}}(s\mathbf{1} - \tilde{\mathbf{A}}_{\text{ff}})^{-1}\tilde{\mathbf{B}}_{\text{ff}} + \tilde{\mathbf{D}}_{\text{ff}}$ is the minimum value of $0 < \gamma < \infty$ that satisfies the Bounded Real Lemma (Lemma 2.25), given by

$$\begin{bmatrix} \tilde{\mathbf{P}}\tilde{\mathbf{A}}_{\text{ff}} + \tilde{\mathbf{A}}_{\text{ff}}^T\tilde{\mathbf{P}} & \tilde{\mathbf{P}}\tilde{\mathbf{B}}_{\text{ff}} & \tilde{\mathbf{C}}_{\text{ff}}^T \\ * & -\gamma\mathbf{1} & \tilde{\mathbf{D}}_{\text{ff}}^T \\ * & * & -\gamma\mathbf{1} \end{bmatrix} < 0, \quad (4.12)$$

where $\tilde{\mathbf{P}} = \tilde{\mathbf{P}}^T > 0$,

$$\tilde{\mathbf{A}} = \begin{bmatrix} \mathbf{A}_{\text{ff}} & \mathbf{0} \\ \mathbf{B}_w\mathbf{C}_{\text{ff}} & \mathbf{A}_w \end{bmatrix}, \quad \tilde{\mathbf{B}} = \begin{bmatrix} \mathbf{B}_{\text{ff}} \\ \mathbf{B}_w\mathbf{D}_{\text{ff}} \end{bmatrix}, \quad \tilde{\mathbf{C}} = \begin{bmatrix} \mathbf{D}_w\mathbf{C}_{\text{ff}} & \mathbf{C}_w \end{bmatrix},$$

$\tilde{\mathbf{D}} = \mathbf{D}_w\mathbf{D}_{\text{ff}}$, and $\mathbf{W}(s)$ is a transfer matrix with a minimal state-space realization $(\mathbf{A}_w, \mathbf{B}_w, \mathbf{C}_w, \mathbf{D}_w)$.

4.4.1 Direct Method using Minimum Gain

The direct method solves for $\mathbf{G}_{\text{ff}}(s)$ directly by ensuring that $\bar{\mathbf{G}}(s)$ has non-zero minimum gain, and therefore only has minimum phase transmission zeros.

A minimum gain of the augmented system described by (4.10) and (4.11) is any value of $0 \leq \bar{\nu} < \infty$ satisfying the Minimum Gain Lemma, given by

$$\begin{bmatrix} \bar{\mathbf{P}}\bar{\mathbf{A}} + \bar{\mathbf{A}}^T\bar{\mathbf{P}} - \bar{\mathbf{C}}^T\bar{\mathbf{C}} & \bar{\mathbf{P}}\bar{\mathbf{B}} - \bar{\mathbf{C}}^T\bar{\mathbf{D}} & \mathbf{0} \\ * & -\bar{\mathbf{D}}^T\bar{\mathbf{D}} & \bar{\nu}\mathbf{1} \\ * & * & -\mathbf{1} \end{bmatrix} \leq 0, \quad (4.13)$$

where $\bar{\mathbf{P}} = \bar{\mathbf{P}}^T \geq 0$.

Lemma 4.4. *The matrix inequality of (4.13) is implied by the matrix inequality in $\hat{\mathbf{A}}_{\text{ff}} = \mathbf{P}_2\mathbf{A}_{\text{ff}}$, $\hat{\mathbf{B}}_{\text{ff}} = \mathbf{P}_2\mathbf{B}_{\text{ff}}$, \mathbf{C}_{ff} , \mathbf{D}_{ff} , \mathbf{Y}_1 , \mathbf{Y}_2 , $\bar{\mathbf{P}} = \bar{\mathbf{P}}^T \geq 0$, $\mathbf{P}_2 = \mathbf{P}_2^T > 0$, and $0 \leq \bar{\nu} < \infty$, given by*

$$\begin{bmatrix} \mathbf{N}_{11} & \hat{\mathbf{A}}_{\text{ff}} + \mathbf{A}^T\mathbf{P}_2 - \mathbf{C}^T\mathbf{C}_{\text{ff}} & \mathbf{N}_{13} & \mathbf{0} & \mathbf{0} \\ * & \hat{\mathbf{A}}_{\text{ff}} + \hat{\mathbf{A}}_{\text{ff}}^T - \mathbf{C}_{\text{ff}}^T\mathbf{Y}_1 - \mathbf{Y}_1^T\mathbf{C}_{\text{ff}} & \mathbf{N}_{23} & \mathbf{Y}_1^T & \mathbf{0} \\ * & * & \mathbf{N}_{33} & \mathbf{Y}_2^T & \bar{\nu}\mathbf{1} \\ * & * & * & -\mathbf{1} & \mathbf{0} \\ * & * & * & * & -\mathbf{1} \end{bmatrix} \leq 0, \quad (4.14)$$

where

$$\begin{aligned}
\mathbf{N}_{11} &= \mathbf{P}_1 \mathbf{A} + \mathbf{A} \mathbf{P}_1 - \mathbf{C}^\top \mathbf{C}, \\
\mathbf{N}_{13} &= \mathbf{P}_1 \mathbf{B} + \hat{\mathbf{B}}_{\text{ff}} - \mathbf{C}^\top (\mathbf{D} + \mathbf{D}_{\text{ff}}), \\
\mathbf{N}_{23} &= \mathbf{P}_2 \mathbf{B} + \hat{\mathbf{B}}_{\text{ff}} - \mathbf{C}_{\text{ff}}^\top (\mathbf{D} + \mathbf{Y}_2) - \mathbf{Y}_1^\top \mathbf{D}_{\text{ff}}, \\
\mathbf{N}_{33} &= -\mathbf{D}^\top \mathbf{D} - (\mathbf{D} + \mathbf{Y}_2)^\top \mathbf{D}_{\text{ff}} - \mathbf{D}_{\text{ff}}^\top (\mathbf{D} + \mathbf{Y}_2), \\
\bar{\mathbf{P}} &= \begin{bmatrix} \mathbf{P}_1 & \mathbf{P}_2 \\ \mathbf{P}_2 & \mathbf{P}_2 \end{bmatrix}.
\end{aligned}$$

Proof. Substituting the expressions for $\bar{\mathbf{A}}$, $\bar{\mathbf{B}}$, $\bar{\mathbf{C}}$, $\bar{\mathbf{D}}$, and $\bar{\mathbf{P}}$ into (4.13) and performing the change of variables $\hat{\mathbf{A}}_{\text{ff}} = \mathbf{P}_2 \mathbf{A}_{\text{ff}}$ and $\hat{\mathbf{B}}_{\text{ff}} = \mathbf{P}_2 \mathbf{B}_{\text{ff}}$ yields

$$\begin{bmatrix} \mathbf{N}_{11} & \hat{\mathbf{A}}_{\text{ff}} + \mathbf{A}^\top \mathbf{P}_2 - \mathbf{C}^\top \mathbf{C}_{\text{ff}} & \bar{\mathbf{N}}_{13} & \mathbf{0} \\ * & \hat{\mathbf{A}}_{\text{ff}} + \hat{\mathbf{A}}_{\text{ff}}^\top - \mathbf{C}_{\text{ff}}^\top \mathbf{C}_{\text{ff}} & \bar{\mathbf{N}}_{23} & \mathbf{0} \\ * & * & \bar{\mathbf{N}}_{33} & \bar{\nu} \mathbf{1} \\ * & * & * & -\mathbf{1} \end{bmatrix} \leq 0, \quad (4.15)$$

where

$$\begin{aligned}
\bar{\mathbf{N}}_{13} &= \mathbf{P}_1 \mathbf{B} + \hat{\mathbf{B}}_{\text{ff}} - \mathbf{C}^\top (\mathbf{D} + \mathbf{D}_{\text{ff}}), \\
\bar{\mathbf{N}}_{23} &= \mathbf{P}_2 \mathbf{B} + \hat{\mathbf{B}}_{\text{ff}} - \mathbf{C}_{\text{ff}}^\top (\mathbf{D} + \mathbf{D}_{\text{ff}}), \\
\bar{\mathbf{N}}_{33} &= -(\mathbf{D} + \mathbf{D}_{\text{ff}})^\top (\mathbf{D} + \mathbf{D}_{\text{ff}}).
\end{aligned}$$

The form of $\bar{\mathbf{P}}$ and the restriction $\mathbf{P}_2 = \mathbf{P}_2^\top > 0$ are deliberately chosen to allow for the change of variables. Applying a special case of Young's Relation, where $\mathbf{S} = \mathbf{1}$, yields the inequality

$$-\begin{bmatrix} \mathbf{C}_{\text{ff}}^\top \\ \mathbf{D}_{\text{ff}}^\top \end{bmatrix} \begin{bmatrix} \mathbf{C}_{\text{ff}} & \mathbf{D}_{\text{ff}} \end{bmatrix} \leq \begin{bmatrix} \mathbf{Y}_1^\top \\ \mathbf{Y}_2^\top \end{bmatrix} \begin{bmatrix} \mathbf{Y}_1 & \mathbf{Y}_2 \end{bmatrix} - \begin{bmatrix} \mathbf{C}_{\text{ff}}^\top \\ \mathbf{D}_{\text{ff}}^\top \end{bmatrix} \begin{bmatrix} \mathbf{Y}_1 & \mathbf{Y}_2 \end{bmatrix} - \begin{bmatrix} \mathbf{Y}_1^\top \\ \mathbf{Y}_2^\top \end{bmatrix} \begin{bmatrix} \mathbf{C}_{\text{ff}} & \mathbf{D}_{\text{ff}} \end{bmatrix}. \quad (4.16)$$

Substituting (4.16) into (4.15) and rearranging, it is shown that that (4.15) is implied by

$$\begin{bmatrix} \mathbf{N}_{11} & \hat{\mathbf{A}}_{\text{ff}} + \mathbf{A}^\top \mathbf{P}_2 - \mathbf{C}^\top \mathbf{C}_{\text{ff}} & \mathbf{N}_{13} & \mathbf{0} \\ * & \hat{\mathbf{A}}_{\text{ff}} + \hat{\mathbf{A}}_{\text{ff}}^\top - \mathbf{C}_{\text{ff}}^\top \mathbf{Y}_1 - \mathbf{Y}_1^\top \mathbf{C}_{\text{ff}} & \mathbf{N}_{23} & \mathbf{0} \\ * & * & \mathbf{N}_{33} & \bar{\nu} \mathbf{1} \\ * & * & * & -\mathbf{1} \end{bmatrix} - \begin{bmatrix} \mathbf{Y}_1^\top \\ \mathbf{Y}_2^\top \end{bmatrix} (-\mathbf{1})^{-1} \begin{bmatrix} \mathbf{Y}_1 & \mathbf{Y}_2 \end{bmatrix} \leq 0. \quad (4.17)$$

Applying the nonstrict Schur Complement Lemma (Lemma 2.19) to (4.17) gives the matrix inequality of (4.14). \square

Lemma 4.5. *The matrix inequality of (4.12) is implied by the matrix inequality in $\hat{\mathbf{A}}_{\text{ff}} = \mathbf{P}_2 \mathbf{A}_{\text{ff}}$, $\hat{\mathbf{B}}_{\text{ff}} = \mathbf{P}_2 \mathbf{B}_{\text{ff}}$, \mathbf{C}_{ff} , \mathbf{D}_{ff} , $\tilde{\mathbf{P}} = \tilde{\mathbf{P}}^{\text{T}} \geq 0$, $\mathbf{P}_2 = \mathbf{P}_2^{\text{T}} > 0$, and $0 < \gamma < \infty$, given by*

$$\begin{bmatrix} \tilde{\mathbf{N}}_{11} & \tilde{\mathbf{N}}_{12} & \hat{\mathbf{B}}_{\text{ff}} + \mathbf{P}_2 \mathbf{B}_w \mathbf{D}_{\text{ff}} & \mathbf{C}_{\text{ff}}^{\text{T}} \mathbf{D}_w^{\text{T}} \\ * & \mathbf{P}_3 \mathbf{A}_w + \mathbf{A}_w^{\text{T}} \mathbf{P}_3 & \hat{\mathbf{B}}_{\text{ff}} + \mathbf{P}_3 \mathbf{B}_w \mathbf{D}_{\text{ff}} & \mathbf{C}_w^{\text{T}} \\ * & * & -\gamma \mathbf{1} & \mathbf{D}_{\text{ff}}^{\text{T}} \mathbf{D}_w^{\text{T}} \\ * & * & * & -\gamma \mathbf{1} \end{bmatrix} < 0, \quad (4.18)$$

where

$$\begin{aligned} \tilde{\mathbf{N}}_{11} &= \hat{\mathbf{A}}_{\text{ff}} + \hat{\mathbf{A}}_{\text{ff}}^{\text{T}} + \mathbf{P}_2 \mathbf{B}_w \mathbf{C}_{\text{ff}} + \mathbf{C}_{\text{ff}}^{\text{T}} \mathbf{B}_w^{\text{T}} \mathbf{P}_2, \\ \tilde{\mathbf{N}}_{12} &= \mathbf{P}_2 \mathbf{A}_w + \hat{\mathbf{A}}_{\text{ff}}^{\text{T}} + \mathbf{C}_{\text{ff}}^{\text{T}} \mathbf{B}_w^{\text{T}} \mathbf{P}_3, \\ \tilde{\mathbf{P}} &= \begin{bmatrix} \mathbf{P}_2 & \mathbf{P}_2 \\ \mathbf{P}_2 & \mathbf{P}_3 \end{bmatrix}. \end{aligned}$$

Proof. Substituting the expressions for $\tilde{\mathbf{A}}$, $\tilde{\mathbf{B}}$, $\tilde{\mathbf{C}}$, and $\tilde{\mathbf{D}}$, and $\tilde{\mathbf{P}}$ into (4.12) and performing the change of variables $\hat{\mathbf{A}}_{\text{ff}} = \mathbf{P}_2 \mathbf{A}_{\text{ff}}$ and $\hat{\mathbf{B}}_{\text{ff}} = \mathbf{P}_2 \mathbf{B}_{\text{ff}}$ yields (4.18). \square

Synthesis Method 3. *The controller synthesis method is performed iteratively in the following four steps.*

1. Find a controller $(\mathbf{A}_{\text{ff},0}, \mathbf{B}_{\text{ff},0}, \mathbf{C}_{\text{ff},0}, \mathbf{D}_{\text{ff},0})$ that renders the transfer matrix from $\mathbf{w}(s)$ to $\bar{\mathbf{z}}(s)$ minimum phase, and set $k = 0$. This can typically be done by choosing a parallel feedforward controller with sufficiently large gain.
2. Fix $\mathbf{C}_{\text{ff},k}$, $\mathbf{D}_{\text{ff},k}$, and solve for $\hat{\mathbf{A}}_{\text{ff}}$, $\hat{\mathbf{B}}_{\text{ff}}$, $\mathbf{P}_1 = \mathbf{P}_1^{\text{T}} \geq 0$, $\mathbf{P}_3 = \mathbf{P}_3^{\text{T}} \geq 0$, $\mathbf{P}_2 = \mathbf{P}_2^{\text{T}} > 0$, $\mathbf{Y}_{1,k}$, $\mathbf{Y}_{2,k}$, $0 < \nu < \infty$, and $0 < \gamma < \infty$ that minimize $\mathcal{J}(\gamma) = \gamma$ subject to $\tilde{\mathbf{P}} \geq 0$, $\bar{\mathbf{P}} \geq 0$, and the LMIs in (4.14) and (4.18).
3. Fix $\mathbf{Y}_{1,k}$, $\mathbf{Y}_{2,k}$, \mathbf{P}_2 , and \mathbf{P}_3 , and solve for $\hat{\mathbf{A}}_{\text{ff}}$, $\hat{\mathbf{B}}_{\text{ff}}$, $\mathbf{C}_{\text{ff},k+1}$, $\mathbf{D}_{\text{ff},k+1}$, $\mathbf{P}_1 = \mathbf{P}_1^{\text{T}} \geq 0$, $0 < \nu < \infty$, and $0 < \gamma < \infty$ that minimize $\mathcal{J}(\gamma) = \gamma$ subject to $\bar{\mathbf{P}} \geq 0$, and the LMIs in (4.14) and (4.18).
4. If a specified stopping criteria is satisfied, exit and set $\mathbf{A}_{\text{ff}} = \mathbf{P}_2^{-1} \hat{\mathbf{A}}_{\text{ff}}$, $\mathbf{B}_{\text{ff}} = \mathbf{P}_2^{-1} \hat{\mathbf{B}}_{\text{ff}}$, $\mathbf{C}_{\text{ff}} = \mathbf{C}_{\text{ff},k+1}$, and $\mathbf{D}_{\text{ff}} = \mathbf{D}_{\text{ff},k+1}$. Otherwise, set $k = k + 1$ and repeat Steps 2) and 3).

4.4.2 Indirect Method using Inversion and Minimum Gain

The indirect method solves for the dynamic output feedback controller $\mathbf{G}_c(s) = \mathbf{G}_{\text{ff}}^{-1}(s)$ that asymptotically stabilizes the closed-loop system, which ensures that $\bar{\mathbf{G}}(s)$ only features minimum phase transmission zeros. This method requires the assumption that (\mathbf{A}, \mathbf{B}) is stabilizable and (\mathbf{A}, \mathbf{C}) is detectable. The indirect method presented in this section requires a weighting transfer matrix that is biproper and invertible, as the \mathcal{H}_∞ norm of $\mathbf{W}(s)\mathbf{G}_{\text{ff}}(s)$ is minimized by maximizing a minimum gain of $\mathbf{G}_c(s)\hat{\mathbf{W}}(s)$, where $\hat{\mathbf{W}}(s) = \mathbf{W}^{-1}(s)$.

The dynamic output feedback controller $\mathbf{G}_c(s)$ is chosen to be an observer-based compensator of the form

$$\begin{aligned}\dot{\mathbf{x}}_c(t) &= \mathbf{A}_c \mathbf{x}_c(t) + \mathbf{B}_c \mathbf{y}(t), \\ \mathbf{y}_c(t) &= \mathbf{C}_c \mathbf{x}_c(t) + \mathbf{D}_c \mathbf{y}(t),\end{aligned}$$

where

$$\begin{aligned}\mathbf{A}_c &= \mathbf{A} - \mathbf{B}\hat{\mathbf{D}}_c\mathbf{C} - \hat{\mathbf{B}}\mathbf{C}_c - \mathbf{B}_c(\hat{\mathbf{C}} - \hat{\mathbf{D}}_c\mathbf{C}_c), \\ \hat{\mathbf{B}} &= \mathbf{B}(\mathbf{1} + \mathbf{D}_c\mathbf{D})^{-1}, \\ \hat{\mathbf{C}} &= (\mathbf{1} - \mathbf{D}\hat{\mathbf{D}}_c)\mathbf{C}, \\ \hat{\mathbf{D}} &= \mathbf{D}(\mathbf{1} + \mathbf{D}_c\mathbf{D})^{-1}, \\ \hat{\mathbf{D}}_c &= (\mathbf{1} + \mathbf{D}_c\mathbf{D})^{-1}\mathbf{D}_c.\end{aligned}$$

Defining $\mathbf{e}(t) = \mathbf{x}(t) - \mathbf{x}_c(t)$, the closed-loop feedback interconnection is written as

$$\begin{bmatrix} \dot{\mathbf{x}}(t) \\ \dot{\mathbf{e}}(t) \end{bmatrix} = \begin{bmatrix} \hat{\mathbf{A}} - \hat{\mathbf{B}}\mathbf{C}_c & \hat{\mathbf{B}}\mathbf{C}_c \\ \mathbf{0} & \hat{\mathbf{A}} - \mathbf{B}_c\hat{\mathbf{C}} \end{bmatrix} \begin{bmatrix} \mathbf{x}(t) \\ \mathbf{e}(t) \end{bmatrix}, \quad (4.19)$$

where $\hat{\mathbf{A}} = \mathbf{A} - \mathbf{B}\hat{\mathbf{D}}_c\mathbf{C}$. Based on the upper-triangular nature of the closed-loop dynamics matrix in (4.19), the closed-loop feedback interconnection is asymptotically stable if and only if there exists $\mathbf{P}_1 = \mathbf{P}_1^\top > 0$ and $\mathbf{Q} = \mathbf{Q}^\top > 0$ such that

$$\left(\hat{\mathbf{A}} - \hat{\mathbf{B}}\mathbf{C}_c\right)\mathbf{Q} + \mathbf{Q}\left(\hat{\mathbf{A}} - \hat{\mathbf{B}}\mathbf{C}_c\right)^\top < 0, \quad (4.20)$$

$$\mathbf{P}_1\left(\hat{\mathbf{A}} - \mathbf{B}_c\hat{\mathbf{C}}\right) + \left(\hat{\mathbf{A}} - \mathbf{B}_c\hat{\mathbf{C}}\right)^\top\mathbf{P}_1 < 0. \quad (4.21)$$

Theorem 4.6. *The controller $\mathbf{G}_c(s)$ asymptotically stabilizes the closed-loop feedback*

interconnection and $\mathbf{G}_c(s)\hat{\mathbf{W}}(s)$ has minimum gain greater than $0 < \nu < \infty$ if there exists \mathbf{F} , \mathbf{G} , $\mathbf{Q} = \mathbf{Q}^\top > 0$, $\hat{\mathbf{P}} = \hat{\mathbf{P}}^\top = \begin{bmatrix} \mathbf{P}_1 & \mathbf{P}_1 \\ \mathbf{P}_1 & \mathbf{P}_2 \end{bmatrix} \geq 0$, and $\mathbf{P}_1 = \mathbf{P}_1^\top > 0$ such that

$$\hat{\mathbf{A}}\mathbf{Q} + \mathbf{Q}\hat{\mathbf{A}}^\top - \hat{\mathbf{B}}\mathbf{F} - \mathbf{F}^\top\hat{\mathbf{B}}^\top < 0, \quad (4.22)$$

$$\mathbf{P}_1\hat{\mathbf{A}} + \hat{\mathbf{A}}^\top\mathbf{P}_1 - \mathbf{G}\hat{\mathbf{C}} - \hat{\mathbf{C}}^\top\mathbf{G}^\top < 0, \quad (4.23)$$

$$\begin{bmatrix} \hat{\mathbf{M}}_{11} & \hat{\mathbf{M}}_{12} & \mathbf{G}\hat{\mathbf{D}}_w + \mathbf{P}_1\hat{\mathbf{B}}_w - \mathbf{C}_c^\top\mathbf{D}_c\hat{\mathbf{D}}_w \\ * & \hat{\mathbf{M}}_{22} & \mathbf{G}\hat{\mathbf{D}}_w + \mathbf{P}_2\hat{\mathbf{B}}_w - \hat{\mathbf{C}}_w^\top\mathbf{D}_c^\top\mathbf{D}_c\hat{\mathbf{D}}_w \\ & * & \nu^2\mathbf{1} - \hat{\mathbf{D}}_w^\top\mathbf{D}_c^\top\mathbf{D}_c\hat{\mathbf{D}}_w \end{bmatrix} \leq 0, \quad (4.24)$$

where $\hat{\mathbf{W}}(s)$ has a minimal state-space realization $(\hat{\mathbf{A}}_w, \hat{\mathbf{B}}_w, \hat{\mathbf{C}}_w, \hat{\mathbf{D}}_w)$, $\mathbf{F} = \mathbf{C}_c\mathbf{Q}$, $\mathbf{G} = \mathbf{P}_1\mathbf{B}_c$, $\hat{\mathbf{A}}_c = \hat{\mathbf{A}} - \hat{\mathbf{B}}\mathbf{C}_c$,

$$\begin{aligned} \hat{\mathbf{M}}_{11} &= \mathbf{P}_1\hat{\mathbf{A}}_c + \hat{\mathbf{A}}_c^\top\mathbf{P}_1 - \mathbf{G}(\hat{\mathbf{C}} - \hat{\mathbf{D}}\mathbf{C}_c) - (\hat{\mathbf{C}} - \hat{\mathbf{D}}\mathbf{C}_c)^\top\mathbf{G}^\top - \mathbf{C}_c^\top\mathbf{C}_c, \\ \hat{\mathbf{M}}_{12} &= \mathbf{P}_1\hat{\mathbf{A}}_w + \hat{\mathbf{A}}_c^\top\mathbf{P}_1 - (\hat{\mathbf{C}} - \hat{\mathbf{D}}\mathbf{C}_c)^\top\mathbf{G}^\top + \mathbf{G}\hat{\mathbf{C}}_w - \mathbf{C}_c^\top\mathbf{D}_c\hat{\mathbf{C}}_w, \\ \hat{\mathbf{M}}_{22} &= \mathbf{P}_2\hat{\mathbf{A}}_w + \hat{\mathbf{A}}_w^\top\mathbf{P}_2 + \mathbf{G}\mathbf{C}_w + \mathbf{C}_w^\top\mathbf{G}^\top - \hat{\mathbf{C}}_w^\top\mathbf{D}_c^\top\mathbf{D}_c\hat{\mathbf{C}}_w. \end{aligned}$$

Proof. The LMIs of (4.22) and (4.23) are equivalent to the matrix inequalities of (4.20) and (4.21) with the change of variables $\mathbf{F} = \mathbf{C}_c\mathbf{Q}$ and $\mathbf{G} = \mathbf{P}_1\mathbf{B}_c$. The LMI of (4.24) is equivalent to the matrix inequality of the Minimum Gain Lemma applied to the system $\mathbf{G}_c(s)\hat{\mathbf{W}}(s)$ with the Lyapunov variable $\hat{\mathbf{P}}$ and the change of variable $\mathbf{G} = \mathbf{P}_1\mathbf{B}_c$. A common Lyapunov variable \mathbf{P}_1 is used in both (4.23) and (4.24), which introduces additional conservatism, but yields a tractable LMI in the following controller synthesis method. \square

Assuming that $\mathbf{W}(s)$ is invertible, the choice $\hat{\mathbf{W}}(s) = \mathbf{W}^{-1}(s)$ gives a weighted \mathcal{H}_∞ norm that is equivalent to the weighted \mathcal{H}_∞ norm in the direct method.

Synthesis Method 4. *The controller synthesis method is performed in the following three steps.*

1. Select a feasible \mathbf{D}_c . A suitable choice is \mathbf{K} from the indirect static parallel feedforward method.
2. Fix \mathbf{D}_c , solve for \mathbf{F} and $\mathbf{Q} = \mathbf{Q}^\top > 0$ satisfying (4.22), and set $\mathbf{C}_c = \mathbf{F}\mathbf{Q}^{-1}$.
3. Fix \mathbf{C}_c and \mathbf{D}_c , and solve for \mathbf{G} , $\bar{\mathbf{P}} = \bar{\mathbf{P}}^\top \geq 0$, $\mathbf{P}_1 = \mathbf{P}_1^\top > 0$, and $0 < \nu < \infty$ that maximize $\mathcal{J}(\nu) = \nu$ subject to (4.23) and (4.24). Set $\mathbf{B}_c = \mathbf{P}_1^{-1}\mathbf{G}$, $\mathbf{A}_c =$

$$\hat{\mathbf{A}}_c - \mathbf{B}_c (\hat{\mathbf{C}} - \hat{\mathbf{D}}\mathbf{C}_c).$$

The parallel feedforward controller is obtained by inverting the dynamic output feedback controller using Lemma 2.38, and is given by the state-space representation $(\mathbf{A}_c - \mathbf{B}_c\mathbf{D}_c^{-1}\mathbf{C}_c, \mathbf{B}_c\mathbf{D}_c^{-1}, -\mathbf{D}_c^{-1}\mathbf{C}_c, \mathbf{D}_c^{-1})$.

4.4.3 Discussion

Similarly to the static parallel feedforward controller synthesis methods, the direct dynamic parallel feedforward controller synthesis method is iterative and requires the selection of an initial feasible controller. The controller must be the same order as the plant and is typically chosen to have a feedthrough matrix with either large positive or large negative eigenvalues. The indirect dynamic parallel feedforward controller synthesis method does not require an initial feasible controller, but does require an initial feasible controller feedthrough matrix and yields a observer-based controller that is the same order as the plant. For both the direct and indirect methods, it is possible to use the solution of the static parallel feedforward controller synthesis method as the initial feedthrough matrix.

The direct and indirect dynamic parallel feedforward controller synthesis methods require a weighting transfer matrix that is of the same order as the plant. This is due to the additional constraint added on the Lyapunov variable that is deliberately added to obtain tractable synthesis methods. An advantage of the indirect dynamic synthesis method is that it does not require iteration.

4.5 Numerical Example

A SISO numerical example is presented in this section to demonstrate the effectiveness of the proposed \mathcal{H}_∞ -optimal parallel feedforward controller synthesis methods. Although the synthesis methods are valid for MIMO systems, a simple SISO example is chosen since the \mathcal{H}_∞ -optimal static parallel feedforward controller can be found analytically, which provides a comparison for the results obtained with the proposed synthesis methods.

Consider the SISO transfer function

$$G(s) = \frac{s - 5}{s^2 + 3s + 2},$$

which has a nonminimum phase zero at $s = 5$. Suppose a static parallel feedforward

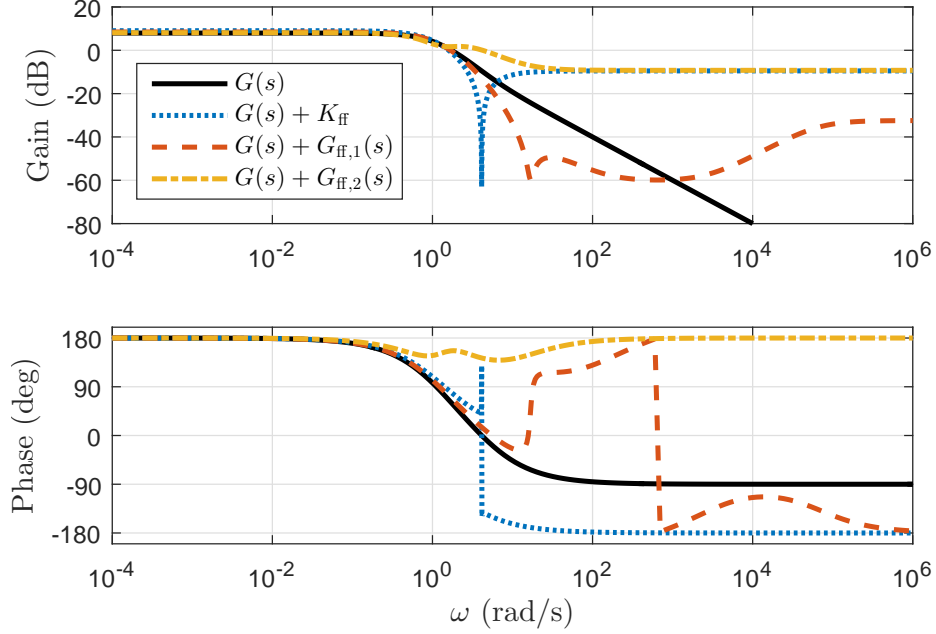


Figure 4.2: Bode plots of $G(s)$, $\bar{G}(s) = G(s) + k_{ff}$, $\bar{G}(s) = G(s) + G_{ff,1}(s)$, and $\bar{G}(s) = G(s) + G_{ff,2}(s)$. The magnitudes of $\bar{G}(s) = G(s) + G_{ff,1}(s)$ and $\bar{G}(s) = G(s) + G_{ff,2}(s)$ more closely match the magnitude of $G(s)$ at low frequencies compared to $\bar{G}(s) = G(s) + k_{ff}$, as a result of the chosen weighting functions $W_1(s) = 4 \times 10^{-8}(s + 500)^2 / (s + 1)^2$ and $W_2(s) = (s + 1)^2 / (s + 500)^2$.

controller, $G_{ff}(s) = k_{ff}$, is designed to render the augmented system,

$$\bar{G}(s) = G(s) + G_{ff}(s) = \frac{k_{ff}s^2 + (3k_{ff} + 1)s + 2k_{ff} - 5}{s^2 + 3s + 2},$$

minimum phase. If $0 < k_{ff} < \infty$, $\bar{G}(s)$ is minimum phase if and only if $k_{ff} > 2.5$. If $-\infty < k_{ff} < 0$, $\bar{G}(s)$ is minimum phase if and only if $k_{ff} < -1/3$. Therefore, the static parallel feedforward controller with smallest gain that renders $\bar{G}(s)$ minimum phase is $G_{ff}(s) = -1/3 - \epsilon$, where $0 < \epsilon < \infty$ is an arbitrarily small number that ensures $k_{ff} < -1/3$.

The static parallel feedforward controller synthesis methods presented in Section 4.3 are tested on this numerical example. For the direct method, an initial choice of $k_{ff,0} = -1 \times 10^6$ yields an optimal value of $k_{ff} = -0.335$, while $k_{ff,0} = 1 \times 10^6$ yields an optimal value of $k_{ff} = 2.503$. With the indirect method, an initial choice of $k_0 = -1 \times 10^{-6}$ gives an optimal value of $k_{ff} = -0.3333337$, while $k_0 = 1 \times 10^6$ gives an optimal value of $k_{ff} = 2.50000004$.

The dynamic parallel feedforward controller synthesis techniques from Section 4.4

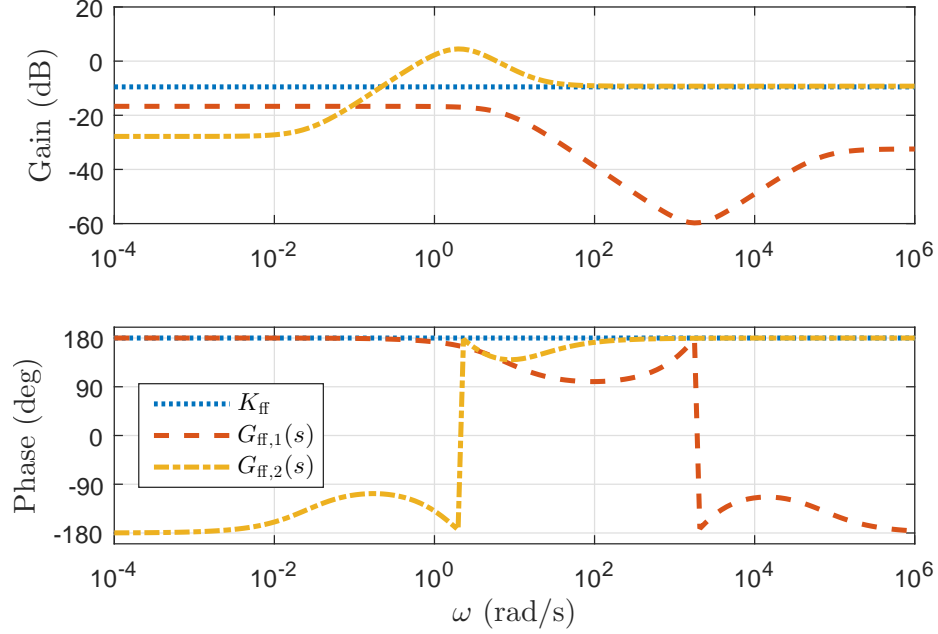


Figure 4.3: Bode plots of k_{ff} , $G_{ff,1}(s)$, and $G_{ff,2}(s)$. The gain of $G_{ff,1}(s)$ is the lowest of the three parallel feedforward controllers for all frequencies.

are implemented. The direct method uses a weighting transfer function of

$$W(s) = 10^{-8} \frac{(s + 500)^2}{(s + 1)^2},$$

and an initial controller of

$$G_{ff,0}(s) = -10 \frac{(s + 1)^2}{(s + 10)^2}.$$

The indirect method uses a weighting transfer function of

$$\hat{W}(s) = 10^3 \frac{(s + 1)^2}{(s + 500)^2},$$

and $D_c = -2.99$. These weighting transfer functions emphasize the importance that the difference between $\bar{G}(s)$ and $G(s)$ is small at frequencies below 1 rad/s. The weighting transfer function $\hat{W}(s)$ is chosen as $\hat{W}(s) = 10^{-4} \cdot W^{-1}(s)$ rather than simply $\hat{W}(s) = W^{-1}(s)$ to improve the numerical conditioning of the synthesis method. The scaling of the weighting transfer function is a tuning parameter that can be used to adjust the numerical conditioning of the optimization problem. The dynamic parallel

feedforward controller obtained with the direct method is

$$G_{\text{ff},1}(s) = -\frac{0.0239s^2 + 69.5s + 7.75 \times 10^4}{s^2 + 6.58 \times 10^4s + 5.30 \times 10^5},$$

and that obtained with the indirect method is

$$G_{\text{ff},2}(s) = -\frac{0.345s^2 + 6.13s + 0.161}{s^2 + 3.67s + 3.96}.$$

Bode plots of $G(s)$, $G(s) + k_{\text{ff}}$, $G(s) + G_{\text{ff},1}(s)$, and $G(s) + G_{\text{ff},2}(s)$ are shown in Figure 4.2, which illustrates that the dynamic parallel feedforward controllers are capable of rendering the augmented system minimum phase without perturbing the frequency response of the system at low frequencies. This is further reinforced in Figure 4.3, which includes Bode plots of k_{ff} , $G_{\text{ff},1}(s)$, and $G_{\text{ff},2}(s)$. The gain of $G_{\text{ff},1}$ is lower than k_{ff} over all frequencies, while the gain of $G_{\text{ff},2}$ is less than k_{ff} for frequencies below 0.1 rad/s, but then exceeds k_{ff} above this frequency. This is possibly due to the observer-based controller structure imposed on the controller when using the indirect method. The synthesis of the controllers in this numerical example is performed in MATLAB using YALMIP [64] and SDPT3 [65].

4.6 Closing Remarks

The parallel feedforward controller synthesis methods presented in this chapter render an open-loop asymptotically stable LTI system minimum phase using the parallel feedforward controller with the smallest \mathcal{H}_∞ norm or weighted \mathcal{H}_∞ norm. Both the static and dynamic parallel feedforward controllers can be synthesized using direct or indirect methods, which use different conditions to render the augmented system minimum phase. It was shown in a numerical example that dynamic parallel feedforward control can remove a plant's nonminimum phase zero, while causing little change to the output of the plant in a desired frequency band.

In future work it will be imperative to explicitly address the robustness of the proposed parallel feedforward controllers. A robust formulation of the controllers presented in this chapter is necessary in order to implement them on any physical system. A relatively simple extension to the controller synthesis methods presented in this chapter could be made using the Kharitonov-Bernstein-Haddad Theorem [66, 67], however, a more general robust parallel feedforward controller synthesis method would likely involve more sophisticated robust control techniques, such as \mathcal{H}_∞ control or the structured singular value.

Chapter 5

Linearly Combining Sensor Measurements Optimally to Enforce an SPR Transfer Matrix

5.1 Introduction

The characteristics of a dynamic system are greatly influenced by its inputs and outputs. When designing a feedback controller, the system inputs and outputs will determine the achievable performance and robustness of the closed-loop system. In order to ensure a desired level of closed-loop performance and/or robustness, it is beneficial to consider closed-loop system properties in the design stage when selecting sensors and actuators. The work of [18–21] considers the selection of sensor and actuator locations along with the design of feedback controllers such that the closed-loop \mathcal{H}_2 or \mathcal{H}_∞ norm of the system is minimized. These sensor selection schemes can also ensure robustness to model uncertainty [20] and sensor faults [21]. Other sensor selection strategies focus on closed-loop performance and/or robustness indirectly by considering open-loop system properties. For example, sensor selection can be performed to maximize the controllability and observability of the open-loop system [68–70], minimize parameter estimation error [71], and minimize the minimum real part of the open-loop system’s transmission zeros [69].

Rather than selecting the location of the system’s sensors and actuators, direct modification of the system’s output can be performed using either a static or dynamic compensator. This can yield an open-loop system with desirable properties, such as a system that is PR or SPR. The concept of positivity embedding was introduced

in [14, 17] for LTI systems, where the output of the system was modified to render it PR. By rendering the system PR, the task of designing a feedback controller that asymptotically stabilizes the closed-loop system is simplified, as any SPR controller will serve this purpose [72]. Further work makes use of this positivity embedding result to design feedback controllers [16] and observers [73], and investigates the issue of robust positivity embedding [15].

Motivated by the notion of sensor selection, the work in this chapter extends the positivity embedding results of [14, 17] to the selection of a linear combination of available LTI system sensor measurements that minimize either the \mathcal{H}_2 or \mathcal{H}_∞ norm of the difference between the new output and a specified desired system output. This process is described as optimal sensor interpolation rather than sensor selection, as it is a static linear combination of a fixed set of sensor measurements that is optimized instead of the location of sensors. The novelty of this work lies in the minimization of either the \mathcal{H}_2 or \mathcal{H}_∞ norm of the difference between the new system and a given desired system while rendering the new system SPR. The LMI-based optimal sensor interpolation algorithms presented in this chapter have practical uses for feedback and adaptive controller synthesis. In particular, once the system is rendered SPR, any PR controller in a negative feedback interconnection with the system will asymptotically stabilize the closed-loop system [72]. The new SPR system will also be minimum phase, which allows for the use of adaptive control techniques that have minimum phase or almost strictly positive real (ASPR) assumptions [13, 74].

The remaining sections of this chapter proceed as follows. Section 5.2 introduces important definitions, lemmas, and the problem statement, while the proposed optimal sensor interpolation algorithms are presented in Section 5.3. Numerical simulation results with the proposed sensor interpolation techniques are included in Section 5.4, which feature a single degree-of-freedom (DOF) mass-spring system and a two DOF flexible-joint serial robotic manipulator. Concluding remarks are given in Section 5.5.

5.2 Preliminaries

Definition 5.1 (Positive Real (PR) Transfer Matrix). A rational transfer matrix $\mathbf{G}(s) \in \mathbb{C}^{n \times n}$ is PR if

1. all elements of $\mathbf{G}(s)$ are analytic in $\text{Re}\{s\} > 0$, and
2. $\mathbf{G}^H(s) + \mathbf{G}(s) \geq 0$ in $\text{Re}\{s\} > 0$, or equivalently

- (a) the poles of $\mathbf{G}(s)$ on the imaginary axis are simple and have nonnegative-definite residues, and
- (b) the minimum Hermitian part of $\mathbf{G}(s)$, $\min_{\omega \in \mathbb{R}} (\mathbf{G}^H(j\omega) + \mathbf{G}(j\omega))$, is positive with $j\omega$ nor a pole of any element of $\mathbf{G}(j\omega)$.

Definition 5.2 (Strictly Positive Real (SPR) Transfer Matrix). An asymptotically stable rational transfer matrix $\mathbf{G}(s) \in \mathbb{C}^{n \times n}$ is SPR if $\mathbf{G}(s - \delta)$ is PR for some $0 < \delta < \infty$; that is, if

1. all elements of $\mathbf{G}(s)$ are analytic in $\text{Re}\{s\} \geq 0$,
2. the minimum Hermitian part of $\mathbf{G}(s)$, $\min_{\omega \in \mathbb{R}} (\mathbf{G}^H(j\omega) + \mathbf{G}(j\omega))$, is strictly positive, and
3. $\mathbf{Z} = \mathbf{G}^T(\infty) + \mathbf{G}(\infty) \geq 0$ or $\lim_{\omega \rightarrow \infty} \omega^2 (\mathbf{G}^H(j\omega) + \mathbf{G}(j\omega)) > 0$ if \mathbf{Z} is singular.

Lemma 5.3 (Kalman-Yakubovich-Popov (KYP) Lemma [40]). *Consider the LTI system*

$$\begin{aligned}\dot{\mathbf{x}}(t) &= \mathbf{A}\mathbf{x}(t) + \mathbf{B}\mathbf{u}(t), \\ \mathbf{y}(t) &= \mathbf{C}\mathbf{x}(t),\end{aligned}$$

where $\mathbf{x} \in \mathbb{R}^n$, $\mathbf{u}, \mathbf{y} \in \mathbb{R}^m$, the constant matrices are defined as $\mathbf{A} \in \mathbb{R}^{n \times n}$, $\mathbf{B} \in \mathbb{R}^{n \times m}$, and $\mathbf{C} \in \mathbb{R}^{m \times n}$, and $(\mathbf{A}, \mathbf{B}, \mathbf{C}, \mathbf{0})$ form a minimal state-space realization. The system is SPR if and only if there exists $\mathbf{P} \in \mathbb{R}^{n \times n}$, where $\mathbf{P} = \mathbf{P}^T > 0$ such that

$$\mathbf{P}\mathbf{A} + \mathbf{A}^T\mathbf{P} < 0, \tag{5.1}$$

$$\mathbf{P}\mathbf{B} = \mathbf{C}^T. \tag{5.2}$$

5.2.1 Problem Statement

Consider the LTI plant $\mathbf{G} : \mathcal{L}_{2e} \rightarrow \mathcal{L}_{2e}$, described by the transfer matrix $\mathbf{G}(s) = \mathbf{C}(s\mathbf{1} - \mathbf{A})^{-1}\mathbf{B} \in \mathbb{C}^{n_y \times n_u}$ and a minimal state-space realization

$$\begin{aligned}\dot{\mathbf{x}}(t) &= \mathbf{A}\mathbf{x}(t) + \mathbf{B}\mathbf{u}(t), \\ \mathbf{y}(t) &= \mathbf{C}\mathbf{x}(t),\end{aligned}$$

where $\mathbf{x}(t) \in \mathbb{R}^{n_x}$ contains the system states; $\mathbf{u}(t) \in \mathbb{R}^{n_u}$ is the system input; $\mathbf{y}(t) \in \mathbb{R}^{n_y}$ contains the available sensor measurements; $\mathbf{A} \in \mathbb{R}^{n_x \times n_x}$, $\mathbf{B} \in \mathbb{R}^{n_x \times n_u}$, and

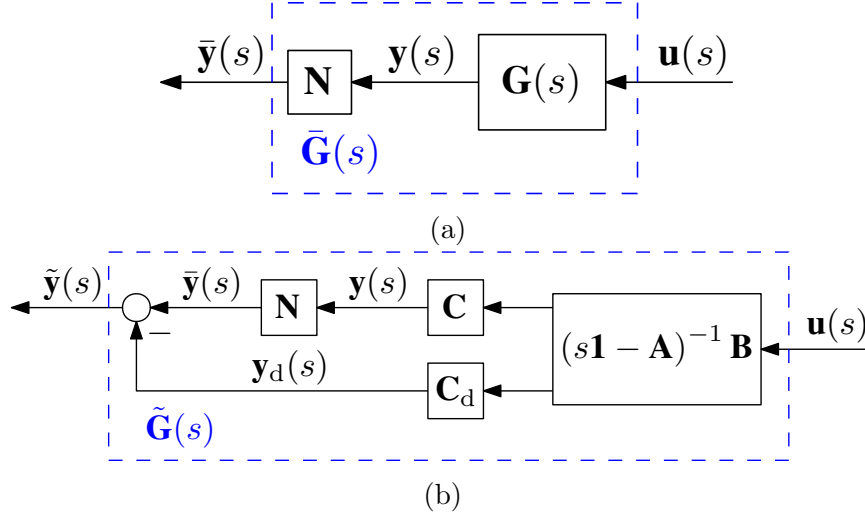


Figure 5.1: Block diagrams of (a) $\bar{\mathbf{G}}(s) = \mathbf{N}\mathbf{G}(s)$, the plant with interpolated sensor measurements, and (b) $\tilde{\mathbf{G}}(s) = \bar{\mathbf{G}}(s) - \mathbf{G}_d(s) = (\mathbf{N}\mathbf{C} - \mathbf{C}_d)(s\mathbf{1} - \mathbf{A})^{-1} \mathbf{B}$, the error between the plant with interpolated sensor measurements and the desired plant.

$\mathbf{C} \in \mathbb{R}^{n_y \times n_x}$ are constant matrices; and it is assumed that $n_u \leq n_y$. A desired system output is specified by $\mathbf{y}_d(t) = \mathbf{C}_d \mathbf{x}(t)$, where $\mathbf{C}_d \in \mathbb{R}^{n_u \times n_x}$, which yields a desired transfer matrix of $\mathbf{G}_d(s) = \mathbf{C}_d (s\mathbf{1} - \mathbf{A})^{-1} \mathbf{B} \in \mathbb{C}^{n_u \times n_u}$. The objective is to select a linear combination of the sensor measurements such that the new output of the system is as close as possible to the desired output, $\mathbf{y}_d(t)$, and the new transfer matrix is SPR. Specifically, the matrix $\mathbf{N} \in \mathbb{R}^{n_u \times n_y}$ is chosen to obtain the new system output $\bar{\mathbf{y}}(t) = \mathbf{N}\mathbf{y}(t) = \mathbf{N}\mathbf{C}\mathbf{x}(t)$ and the new transfer matrix $\bar{\mathbf{G}}(s) = \mathbf{N}\mathbf{G}(s) = \mathbf{N}\mathbf{C}(s\mathbf{1} - \mathbf{A})^{-1} \mathbf{B} \in \mathbb{C}^{n_u \times n_u}$, in such a manner that the \mathcal{H}_2 or \mathcal{H}_∞ norm of

$$\tilde{\mathbf{G}}(s) = \bar{\mathbf{G}}(s) - \mathbf{G}_d(s) = (\mathbf{N}\mathbf{C} - \mathbf{C}_d)(s\mathbf{1} - \mathbf{A})^{-1} \mathbf{B}$$

is minimized and $\bar{\mathbf{G}}(s)$ is SPR. Block diagrams of $\bar{\mathbf{G}}(s)$ and $\tilde{\mathbf{G}}(s)$ are provided in Figure 5.1.

5.3 Optimal Sensor Interpolation

This section presents two sensor interpolation techniques that render $\bar{\mathbf{G}}(s) = \mathbf{N}\mathbf{C}(s\mathbf{1} - \mathbf{A})^{-1} \mathbf{B}$ SPR, while minimizing either the \mathcal{H}_2 or the \mathcal{H}_∞ norm of $\tilde{\mathbf{G}}(s) = (\mathbf{N}\mathbf{C} - \mathbf{C}_d)(s\mathbf{1} - \mathbf{A})^{-1} \mathbf{B}$, where $\mathbf{G}_d(s) = \mathbf{C}_d (s\mathbf{1} - \mathbf{A})^{-1} \mathbf{B}$ is the desired transfer matrix. For $\bar{\mathbf{G}}(s)$ to be SPR, there must exist \mathbf{N} and $\mathbf{P} = \mathbf{P}^\top > 0$ satisfying (5.1) and

$$\mathbf{P}\mathbf{B} = \mathbf{C}^\top \mathbf{N}^\top. \quad (5.3)$$

5.3.1 \mathcal{H}_2 -Optimal Sensor Interpolation

The \mathcal{H}_2 norm of $\tilde{\mathbf{G}}(s)$ is the smallest value of $0 < \mu < \infty$ satisfying the LMIs of (2.5), (2.7), and

$$\begin{bmatrix} \mathbf{Q} & (\mathbf{N}\mathbf{C} - \mathbf{C}_d)^\top \\ * & \mathbf{Z} \end{bmatrix} > 0, \quad (5.4)$$

where $\mathbf{Q} = \mathbf{Q}^\top > 0$ and $\mathbf{Z} = \mathbf{Z}^\top > 0$.

The \mathcal{H}_2 -optimal interpolation of the sensor measurements is presented in the following algorithm.

Algorithm 1. Solve for \mathbf{N} , $\mathbf{P} = \mathbf{P}^\top > 0$, $\mathbf{Q} = \mathbf{Q}^\top > 0$, $\mathbf{Z} = \mathbf{Z}^\top > 0$, and $0 < \mu < \infty$ that minimize $\mathcal{J}_1(\mu) = \mu$ subject to (2.5), (2.7), (5.1), (5.3), and (5.4).

5.3.2 \mathcal{H}_∞ -Optimal Sensor Interpolation

The \mathcal{H}_∞ norm of $\tilde{\mathbf{G}}(s)$ is the smallest value of γ satisfying the LMI of the Bounded Real Lemma (Lemma 2.25) given by

$$\begin{bmatrix} \bar{\mathbf{Q}}\mathbf{A} + \mathbf{A}^\top\bar{\mathbf{Q}} & \bar{\mathbf{Q}}\mathbf{B} & (\mathbf{N}\mathbf{C} - \mathbf{C}_d)^\top \\ * & -\gamma\mathbf{1} & \mathbf{0} \\ * & * & -\gamma\mathbf{1} \end{bmatrix} < 0. \quad (5.5)$$

where $\bar{\mathbf{Q}} = \bar{\mathbf{Q}}^\top > 0$.

The \mathcal{H}_∞ -optimal interpolation of the sensor measurements is presented in the following algorithm.

Algorithm 2. Solve for \mathbf{N} , $\mathbf{P} = \mathbf{P}^\top > 0$, $\bar{\mathbf{Q}} = \bar{\mathbf{Q}}^\top < 0$, and $0 < \gamma < \infty$ that minimize $\mathcal{J}_2(\gamma) = \gamma$ subject to (5.1), (5.3), and (5.5).

5.3.3 Discussion

The \mathcal{H}_2 - and \mathcal{H}_∞ -optimal sensor interpolation algorithms presented in this section are convex optimization problems, as they involve linear objective functions, as well as linear equality and LMI constraints. As such, these optimal sensor interpolation algorithms can be easily solved using semidefinite programming software. The sensor interpolation algorithms can also be used to prove that no linear combination of sensor measurements yields an SPR transfer matrix from $\mathbf{u}(s)$ to $\bar{\mathbf{y}}(s)$, since the linear equality and LMI constraints used are necessary and sufficient conditions.

The minimum attainable \mathcal{H}_2 norm or \mathcal{H}_∞ norm of $\tilde{\mathbf{G}}(s) = \bar{\mathbf{G}}(s) - \mathbf{G}_d(s)$ is highly dependent on the desired transfer matrix $\mathbf{G}_d(s)$. For example, if $\mathbf{G}_d(s)$ has relative degree greater than one, it is unavoidable that $\tilde{\mathbf{G}}(s)$ have nonzero gain at high frequencies, since $\bar{\mathbf{G}}(s)$ must have a relative degree of one. Therefore, it is recommended to utilize these sensor interpolation methods with a desired $\mathbf{G}_d(s)$ that is “close” to being SPR. For example, a single-input single-output system whose Nyquist plot protrudes slightly into the left-half plane within a frequency band, or a multi-input multi-output system whose minimum Hermitian part is slightly negative within a frequency band.

A benefit of performing sensor interpolation to obtain a system that is SPR includes the ability to asymptotically stabilize the system in a negative feedback interconnection with any PR controller [72]. Additionally, an SPR system is minimum phase, which means that the performance limitations associated with nonminimum phase zeros can be avoided [51] and certain adaptive control techniques that have minimum phase requirement can be used [13, 74, 75].

5.4 Numerical Examples

The \mathcal{H}_2 - and \mathcal{H}_∞ -optimal sensor interpolation techniques from Section 5.3 are tested numerically on a single DOF mass-spring system and a two DOF flexible-joint manipulator. The numerical calculations in this section are performed in MATLAB using YALMIP [64] and SeDuMi [76].

5.4.1 Single DOF Mass-Spring System

Consider the mass-spring system, shown in Figure 5.2, whose dynamics are described by the linear equations of motion

$$\mathbf{M}\ddot{\mathbf{q}}(t) + \mathbf{D}\dot{\mathbf{q}}(t) + \mathbf{K}\mathbf{q}(t) = \hat{\mathbf{b}}f(t), \quad (5.6)$$

where $\mathbf{q}^\top(t) = [q_1(t) \quad q_2(t)]$, $\mathbf{D} = \text{diag}\{c_1, c_2\}$, $\mathbf{K} = \text{diag}\{k_1, k_2\}$,

$$\mathbf{M} = \begin{bmatrix} m_1 + m_2 & m_2 \\ m_2 & m_2 \end{bmatrix}, \quad \hat{\mathbf{b}} = \begin{bmatrix} 1 \\ 0 \end{bmatrix},$$

$q_1(t)$ is the elongation of the spring connected to the first mass relative to its unstretched length, $q_2(t)$ is the elongation of the spring connecting the first and second

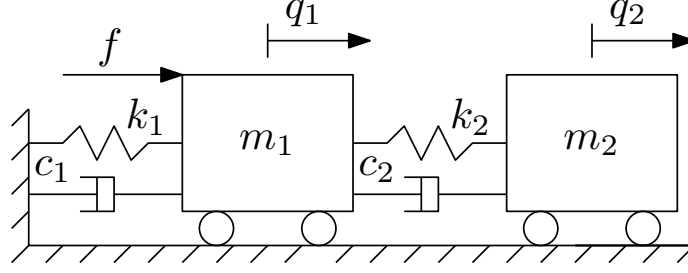


Figure 5.2: Schematic of the mass-spring system from the numerical example of Section 5.4.1.

masses relative to its unstretched length, $m_1 = 1$ kg is the first mass, $m_2 = 10$ kg is the second mass, $c_1 = 0.01$ N·s/m is the damping coefficient of the damper attached to the first mass, $c_2 = 0.01$ N·s/m is the damping coefficient of the damper between the masses, $k_1 = 1$ N/m is the stiffness coefficient of the spring attached to the first mass, $k_2 = 1$ N/m is the stiffness coefficient of the spring between the masses, and $f(t)$ is the force applied to the first mass in Newtons. The mass-spring system is very similar to the benchmark problem presented in [77], with the addition of a spring and damper attached to the first mass. The equations of motion of the system are written in state-space form as $\dot{\mathbf{x}}(t) = \mathbf{A}\mathbf{x}(t) + \mathbf{B}u(t)$, where $\mathbf{x}^\top(t) = [\mathbf{q}^\top(t) \quad \dot{\mathbf{q}}^\top(t)]$, $u(t) = f(t)$,

$$\mathbf{A} = \begin{bmatrix} \mathbf{0} & \mathbf{1} \\ -\mathbf{M}^{-1}\mathbf{K} & -\mathbf{M}^{-1}\mathbf{D} \end{bmatrix}, \quad \mathbf{B} = \begin{bmatrix} \mathbf{0} \\ \mathbf{M}^{-1}\hat{\mathbf{b}} \end{bmatrix}.$$

The desired system output is the velocity of the second mass, expressed by $y_d(t) = \begin{bmatrix} 0 & 0 & 1 & 1 \end{bmatrix} \mathbf{x}(t)$, and the velocities of the first and second masses are measured, which gives

$$\mathbf{y}(t) = \begin{bmatrix} 0 & 0 & 1 & 0 \\ 0 & 0 & 1 & 1 \end{bmatrix} \mathbf{x}(t).$$

The \mathcal{H}_2 and \mathcal{H}_∞ -optimal sensor interpolation techniques from Section 5.3 are implemented, yielding

$$\begin{aligned} \bar{y}_{\mathcal{H}_2}(t) &= \begin{bmatrix} 0 & 0 & 0.876 & 0.848 \end{bmatrix} \mathbf{x}(t), \\ \bar{y}_{\mathcal{H}_\infty}(t) &= \begin{bmatrix} 0 & 0 & 0.957 & 0.926 \end{bmatrix} \mathbf{x}(t). \end{aligned}$$

Bode plots of $G_d(s)$, $\bar{G}_{\mathcal{H}_2}(s)$, and $\bar{G}_{\mathcal{H}_\infty}(s)$ are provided in Figure 5.3. Bode plots of $\tilde{G}_{\mathcal{H}_2}(s) = \bar{G}_{\mathcal{H}_2}(s) - G_d(s)$ and $\tilde{G}_{\mathcal{H}_\infty}(s) = \bar{G}_{\mathcal{H}_\infty}(s) - G_d(s)$ are included in Figure 5.4. In Figure 5.3 it is shown that both methods yield an SPR system that is close to the desired system for frequencies below 0.3 rad/s, while the \mathcal{H}_∞ -optimal method

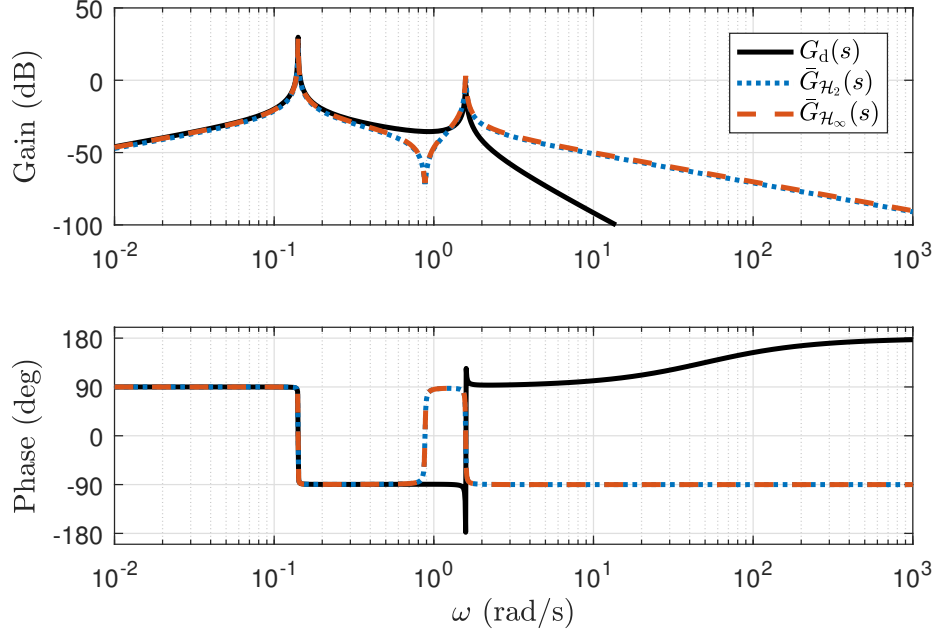


Figure 5.3: Bode plots of $G_d(s)$, $\bar{G}_{\mathcal{H}_2}(s)$, and $\bar{G}_{\mathcal{H}_\infty}(s)$ in the numerical example of Section 5.4.1. The gains of $\bar{G}_{\mathcal{H}_2}(s)$ and $\bar{G}_{\mathcal{H}_\infty}(s)$ closely match the gain of $G_d(s)$ at low frequencies. The Bode phase plot shows that $G_d(s)$ is not positive real, while $\bar{G}_{\mathcal{H}_2}(s)$ and $\bar{G}_{\mathcal{H}_\infty}(s)$ are.

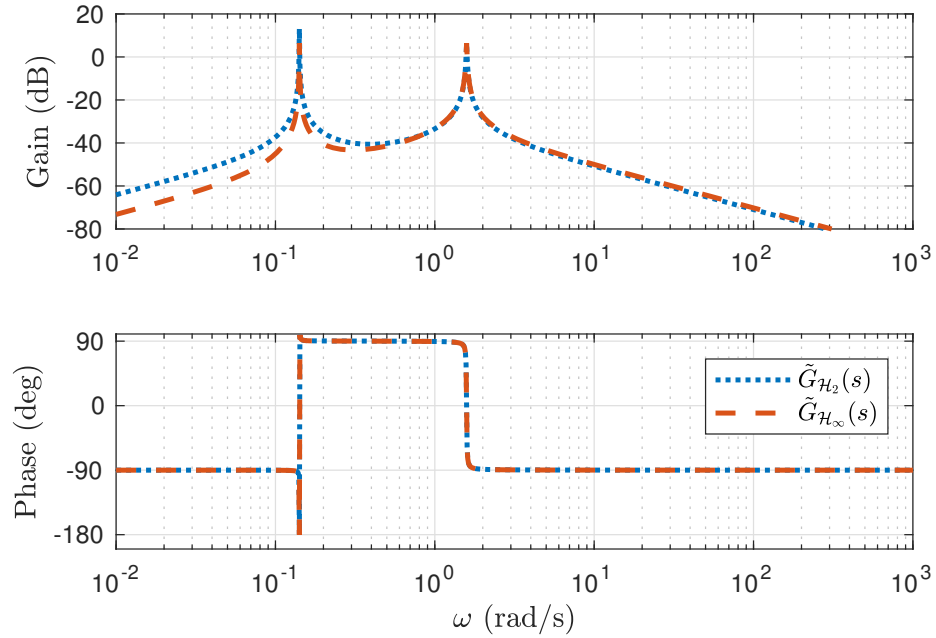


Figure 5.4: Bode plots of $\tilde{G}_{\mathcal{H}_2}(s) = \bar{G}_{\mathcal{H}_2}(s) - G_d(s)$ and $\tilde{G}_{\mathcal{H}_\infty}(s) = \bar{G}_{\mathcal{H}_\infty}(s) - G_d(s)$ in the numerical example of Section 5.4.1.

yields a system that is closer to the desired system, particularly at frequencies below 0.1 rad/s, as seen in Figure 5.4.

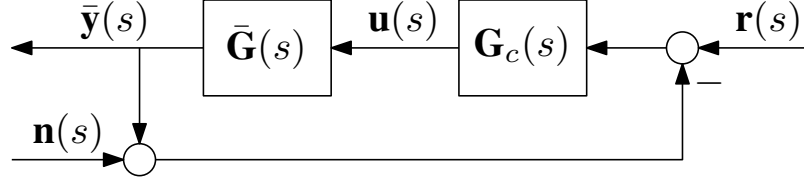


Figure 5.5: Block diagram of the system $\bar{\mathbf{G}}(s)$ in a negative feedback interconnection with a controller $\mathbf{G}_c(s)$, where $\mathbf{r}(s)$ is the reference signal that $\bar{\mathbf{y}}(s)$ should track and $\mathbf{n}(s)$ is measurement noise.

A closed-loop simulation is performed using the SPR-designed plants in a negative feedback interconnection with an SPR controller, as shown in Figure 5.5. It is important to note that although the system output $\bar{y}(t)$ is fed into the controller, it is in fact desired that the system output $y_d(t)$ track the reference signal $r(t)$. This reinforces the importance that $\bar{y}(t)$ match $y_d(t)$ as closely as possible in order to achieve acceptable tracking in the output $y_d(t)$. The desired velocity of the second mass is specified by

$$r(t) = 30 \left(\left(\frac{t}{t_f} \right)^2 - 2 \left(\frac{t}{t_f} \right)^3 + \left(\frac{t}{t_f} \right)^4 \right) r_f,$$

where $t_s(t) = t/t_f$, which is a smooth trajectory that is initially zero at $t = 0$ s, has a maximum value of $15/8r_f$ at $t = t_f/2$ and returns to zero at $t = t_f$. For this example, the trajectory parameters are chosen as $r_f = 1/6$ m/s and $t_f = 60$ s, and the reference trajectory is shifted ahead 20 s, as shown in Figure 5.6. This reference trajectory is purposefully chosen to be slow to ensure that its fundamental frequency falls below 0.3 rad/s, the frequency below which $\bar{y}(t)$ match $y_d(t)$ well. The SPR controller is defined as

$$G_c(s) = k \frac{s + a}{(s + b)(s + c)},$$

where $0 < a < b + c < \infty$ and $0 < k < \infty$ [40]. In this particular example the controller parameters are chosen as $k = 10^5$ N/m·s, $a = 10^{-1}$ 1/s, $b = 10^{-3}$ 1/s, and $c = 100$ 1/s. Measurement noise of $n(t) = 0.1 \sin(1000\pi t)$ m/s is also added to the signal $\bar{y}(t)$ is simulation. The closed-loop responses of the desired system output, $y_d(t)$, and the tracking error of the desired output, $y_d(t) - r(t)$, for both the \mathcal{H}_2 - and \mathcal{H}_∞ -optimal sensor interpolations are included in Figure 5.6, while the closed-loop responses of $\bar{y}(t)$ and the tracking error $\bar{y}(t) - r(t)$ for the same simulations are found in Figure 5.7.

The closed-loop simulation results in Figure 5.6 show that $y_d(t)$ does track the reference signal $r(t)$ with both sensor interpolation techniques, however, the track-

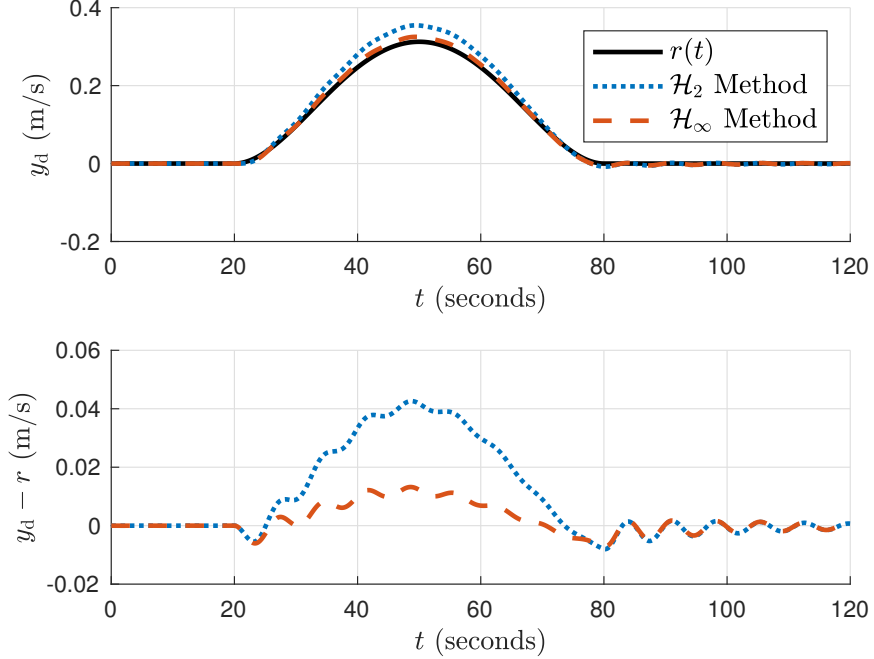


Figure 5.6: Closed-loop responses of $y_d(t)$ and the tracking error $y_d(t) - r(t)$ for both the \mathcal{H}_2 - and \mathcal{H}_∞ -optimal sensor interpolations in the numerical example of Section 5.4.1. The tracking error is less with the \mathcal{H}_∞ -optimal sensor interpolation during the nonzero portion of the reference trajectory, as the gain of $\tilde{G}_{\mathcal{H}_\infty}(s)$ is less than the gain of $\tilde{G}_{\mathcal{H}_2}(s)$ at lower frequencies.

ing error is less with the \mathcal{H}_∞ -optimal method. This is expected in this particular example, as the \mathcal{H}_∞ method yields a modified system that has gain closer to the gain of the desired system, especially at lower frequencies including the fundamental frequency of the reference trajectory. The tracking error $\bar{y}(t) - r(t)$ is quite small in both simulations in Figure 5.7, which shows that the larger tracking errors in Figure 5.6 are due to the difference between $y_d(t)$ and $\bar{y}(t)$ rather than a poorly tuned controller. Although the closed-loop tracking results with sensor interpolation include non-negligible tracking error, this is a substantial improvement over the attainable closed-loop performance when the output $y_d(t)$ is used directly for feedback control. The transfer matrix $G_d(s)$ in this particular example has relative degree 2 and its root locus plot has asymptotes in the open right-half plane (ORHP), which makes the closed-loop system severely gain limited and prevents the ability to perform output tracking. It is also worth noting that the chosen SPR feedback controller is very simple, which emphasizes the ease of synthesizing a feedback controller once the system is rendered SPR.

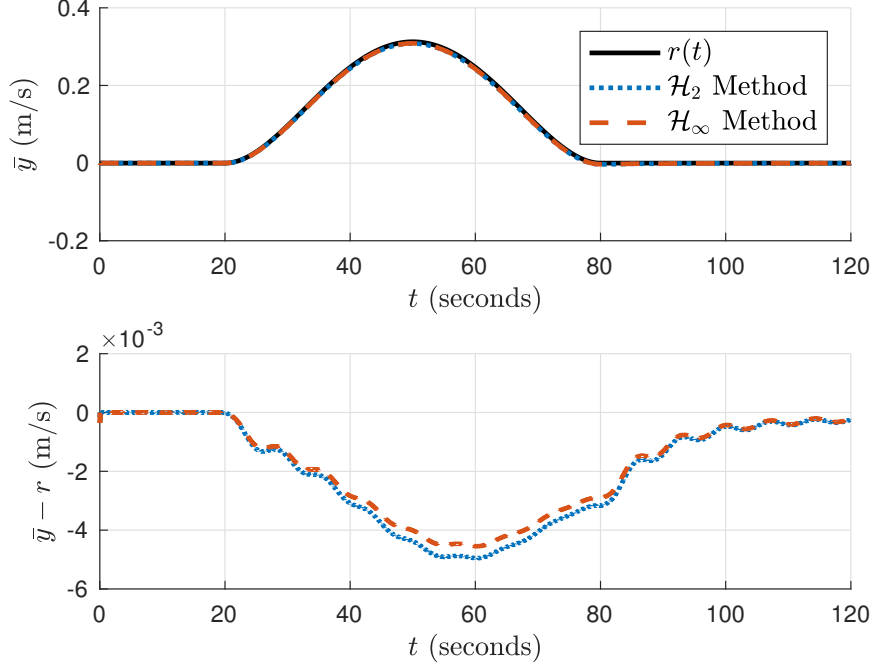


Figure 5.7: Closed-loop responses of $\bar{y}(t)$ and the tracking error $\bar{y}(t) - r(t)$ for both the \mathcal{H}_2 - and \mathcal{H}_∞ -optimal sensor interpolations in the numerical example of Section 5.4.1.

5.4.2 2 DOF Flexible-Joint Serial Manipulator

Consider a 2 DOF flexible-joint manipulator whose nonlinear equations of motion are described by [78]

$$\mathbf{M}(\mathbf{q}(t))\ddot{\mathbf{q}}(t) + \mathbf{D}\dot{\mathbf{q}}(t) + \mathbf{K}\mathbf{q}(t) = \hat{\mathbf{B}}\boldsymbol{\tau}(t) + \mathbf{f}_{\text{non}}(\mathbf{q}(t), \dot{\mathbf{q}}(t)), \quad (5.7)$$

where $\mathbf{q}^\top(t) = \begin{bmatrix} \boldsymbol{\theta}^\top(t) & \mathbf{q}_e^\top(t) \end{bmatrix} \in \mathbb{R}^4$ are the generalized coordinates, $\boldsymbol{\theta}(t) \in \mathbb{R}^2$ are the joint angles, $\mathbf{q}_e(t) \in \mathbb{R}^2$ are the elastic degrees of freedom, $\mathbf{M}(\mathbf{q}) = \mathbf{M}^\top(\mathbf{q}) > 0$, $\mathbf{D} = \mathbf{D}^\top \geq 0$, and $\mathbf{K} = \mathbf{K}^\top \geq 0$ are mass, damping, and stiffness matrices, $\hat{\mathbf{B}}^\top = \begin{bmatrix} \mathbf{1} & \mathbf{0} \end{bmatrix}$ is the input matrix, \mathbf{f}_{non} are the nonlinear inertial forces, and $\boldsymbol{\tau} \in \mathbb{R}^2$ are the joint torques.

The equations of motion in (5.7) are linearized about the equilibrium point $\bar{\mathbf{q}}^\top = \begin{bmatrix} 0^\circ & 45^\circ & 0^\circ & 0^\circ \end{bmatrix}$ and are given by $\dot{\mathbf{x}}(t) = \mathbf{A}\mathbf{x}(t) + \mathbf{B}\mathbf{u}(t)$, where $\mathbf{q}(t) = \bar{\mathbf{q}} + \delta\mathbf{q}(t)$, $\mathbf{x}^\top(t) = \begin{bmatrix} \delta\mathbf{q}^\top(t) & \delta\dot{\mathbf{q}}^\top(t) \end{bmatrix}$, $\mathbf{u}(t) = \boldsymbol{\tau}(t)$,

$$\mathbf{A} = \begin{bmatrix} \mathbf{0} & \mathbf{1} \\ -\mathbf{M}^{-1}(\bar{\mathbf{q}})\mathbf{K} & -\mathbf{M}^{-1}(\bar{\mathbf{q}})\mathbf{D} \end{bmatrix}, \quad \mathbf{B} = \begin{bmatrix} \mathbf{0} \\ \mathbf{M}^{-1}(\bar{\mathbf{q}})\hat{\mathbf{b}} \end{bmatrix},$$

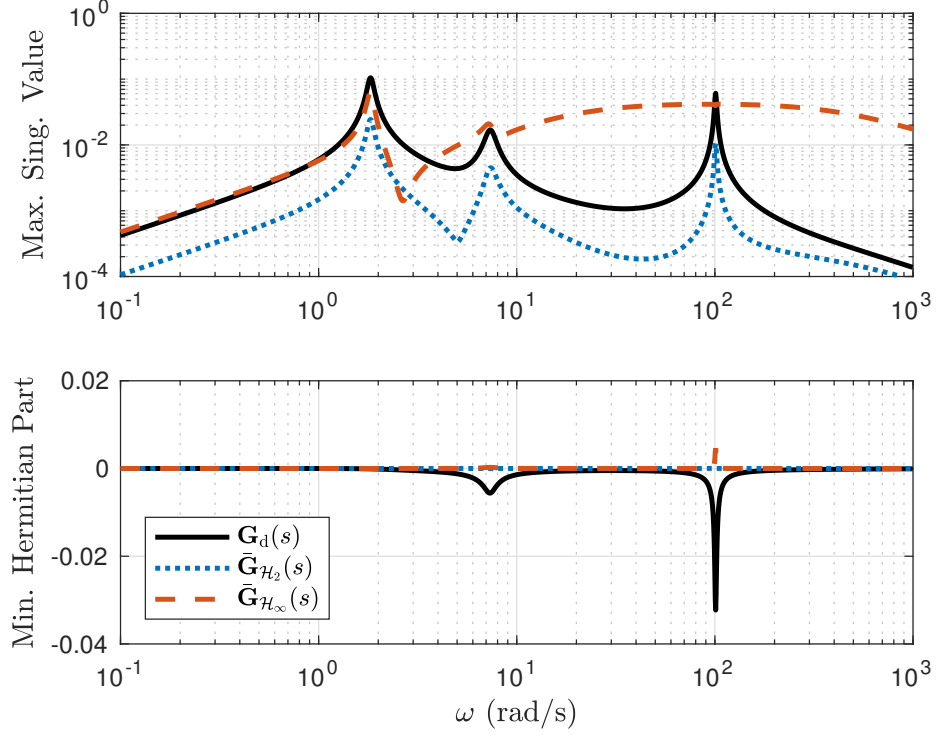


Figure 5.8: Plots of the maximum singular values and minimum Hermitian parts of $\mathbf{G}_d(s)$, $\bar{\mathbf{G}}_{\mathcal{H}_2}(s)$, and $\bar{\mathbf{G}}_{\mathcal{H}_\infty}(s)$ in the numerical example of Section 5.4.2. The gain of $\bar{\mathbf{G}}_{\mathcal{H}_\infty}(s)$ closely matches the gain of $\mathbf{G}_d(s)$ at low frequencies, whereas the gain of $\bar{\mathbf{G}}_{\mathcal{H}_2}(s)$ deviates less from the gain of $\mathbf{G}_d(s)$ compared to $\bar{\mathbf{G}}_{\mathcal{H}_\infty}(s)$ over all frequencies. The minimum Hermitian part plot shows that $\mathbf{G}_d(s)$ is not positive real, while $\bar{\mathbf{G}}_{\mathcal{H}_2}(s)$ and $\bar{\mathbf{G}}_{\mathcal{H}_\infty}(s)$ are.

$\mathbf{D} = \text{diag}\{0.45, 0.001, 0.05, 0.001\}$, $\mathbf{K} = \text{diag}\{0, 0, 9, 4\}$, and

$$\mathbf{M}(\bar{\mathbf{q}}) = \begin{bmatrix} 0.553 & 0.168 & 0.542 & 0.159 \\ 0.168 & 0.0916 & 0.168 & 0.0822 \\ 0.542 & 0.168 & 0.542 & 0.159 \\ 0.159 & 0.0822 & 0.159 & 0.0822 \end{bmatrix}.$$

The last two entries of the stiffness matrix \mathbf{K} represent the flexibility of the manipulator's elastic joints, while the first two entries are the result of an inner-loop proportional joint controller that has been pre-wrapped around the plant. The desired system output is the manipulator tip velocity, given by

$$\mathbf{y}_d(t) = \begin{bmatrix} \mathbf{0} & \mathbf{0} & \mathbf{J}_\theta(\bar{\mathbf{q}}) & \mathbf{J}_e(\bar{\mathbf{q}}) \end{bmatrix} \mathbf{x}(t),$$

where

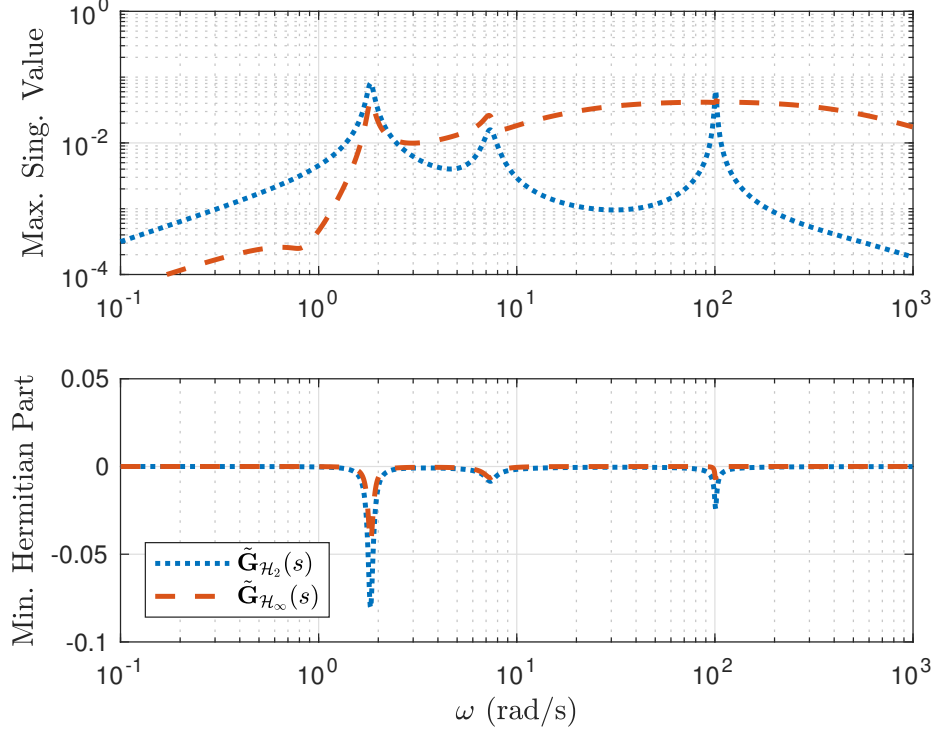


Figure 5.9: Plots of the maximum singular values and minimum Hermitian parts of $\tilde{\mathbf{G}}_{\mathcal{H}_2}(s) = \bar{\mathbf{G}}_{\mathcal{H}_2}(s) - \mathbf{G}_d(s)$ and $\tilde{\mathbf{G}}_{\mathcal{H}_\infty}(s) = \bar{\mathbf{G}}_{\mathcal{H}_\infty}(s) - \mathbf{G}_d(s)$.

$$\mathbf{J}_\theta(\bar{\mathbf{q}}) = \mathbf{J}_e(\bar{\mathbf{q}}) = \begin{bmatrix} -0.189 & -0.189 & -0.189 & -0.189 \\ 0.532 & 0.189 & 0.532 & 0.189 \end{bmatrix},$$

are the rigid and elastic Jacobians evaluated at $\bar{\mathbf{q}}$, respectively. The measurements available include the joint angular rates and the tip velocity, which are described by

$$\mathbf{y}(t) = \begin{bmatrix} \mathbf{0} & \mathbf{0} & \mathbf{1} & \mathbf{0} \\ \mathbf{0} & \mathbf{0} & \mathbf{J}_\theta(\bar{\mathbf{q}}) & \mathbf{J}_e(\bar{\mathbf{q}}) \end{bmatrix} \mathbf{x}(t).$$

The \mathcal{H}_2 - and \mathcal{H}_∞ -optimal sensor interpolation techniques from Section 5.3 are implemented, yielding $\bar{\mathbf{y}}_{\mathcal{H}_2}(t) = \mathbf{N}_{\mathcal{H}_2} \mathbf{C} \mathbf{x}(t)$ and $\bar{\mathbf{y}}_{\mathcal{H}_\infty}(t) = \mathbf{N}_{\mathcal{H}_\infty} \mathbf{C} \mathbf{x}(t)$, where

$$\mathbf{N}_{\mathcal{H}_2}(t) = \begin{bmatrix} -0.005 & -0.0007 & 0.045 & -0.083 \\ 0.0015 & 0.0021 & 0.171 & 0.327 \end{bmatrix},$$

$$\mathbf{N}_{\mathcal{H}_\infty}(t) = \begin{bmatrix} -0.122 & -0.0028 & 0.048 & -0.220 \\ 0.349 & 0.0007 & 0.270 & 0.699 \end{bmatrix}.$$

Plots of the maximum singular values and minimum Hermitian parts of $\mathbf{G}_d(s)$, $\bar{\mathbf{G}}_{\mathcal{H}_2}(s)$, and $\bar{\mathbf{G}}_{\mathcal{H}_\infty}(s)$ are provided in Figure 5.8, while the same plots of $\tilde{\mathbf{G}}_{\mathcal{H}_2}(s) = \bar{\mathbf{G}}_{\mathcal{H}_2}(s) -$

$\mathbf{G}_d(s)$ and $\tilde{\mathbf{G}}_{\mathcal{H}_\infty}(s) = \bar{\mathbf{G}}_{\mathcal{H}_\infty}(s) - \mathbf{G}_d(s)$ are included in Figure 5.9. In Figure 5.8 it is clear that both sensor interpolation techniques render the system SPR, while the \mathcal{H}_∞ -optimal method yields a system whose maximum singular value is closer to the desired system at lower frequencies and the \mathcal{H}_2 -optimal method yields a system whose maximum singular value is relatively close to the desired system over all frequencies. This is further reinforced in Figure 5.9, where it is shown that the maximum singular value of $\tilde{\mathbf{G}}_{\mathcal{H}_\infty}(s)$ is lower than that of $\tilde{\mathbf{G}}_{\mathcal{H}_2}(s)$ for frequencies lower than 2 rad/s, but higher than that of $\tilde{\mathbf{G}}_{\mathcal{H}_2}(s)$ for almost all frequencies higher than 2 rad/s.

A closed-loop simulation is performed using the SPR-designed plants in a negative feedback interconnection with an SPR controller, as shown in Figure 5.5. The desired tip velocity is specified by $\mathbf{r}^\top(t) = \begin{bmatrix} r_1(t) & r_2(t) \end{bmatrix}$, where

$$\begin{bmatrix} r_1(t) \\ r_2(t) \end{bmatrix} = 30 \left(\left(\frac{t}{t_f} \right)^2 - 2 \left(\frac{t}{t_f} \right)^3 + \left(\frac{t}{t_f} \right)^4 \right) \begin{bmatrix} r_{f1} \\ r_{f2} \end{bmatrix},$$

$t_s(t) = t/t_f$, $r_{f1} = -1/20$ m/s, $r_{f2} = 2/15$ m/s and $t_f = 60$ s, and the reference trajectory is shifted ahead by 20 s, as shown in Figure 5.10a. The SPR controller is chosen as

$$\mathbf{G}_c(s) = 2 \times 10^6 \frac{s + 10^{-1}}{(s + 10^{-3})(s + 10^2)} \begin{bmatrix} 1 & 0 \\ 0 & 2 \end{bmatrix}.$$

Measurement noise of $\mathbf{n}^\top(t) = 0.005 \begin{bmatrix} \sin(3000\pi t) & \sin(3000\pi t + 0.5) \end{bmatrix}$ m/s is also added to the signal $\bar{\mathbf{y}}(t)$ in simulation. The closed-loop responses of the desired output $\mathbf{y}_d^\top(t) = \begin{bmatrix} y_{d1}(t) & y_{d2}(t) \end{bmatrix}$ and the tracking error of the desired output $(\mathbf{y}_d(t) - \mathbf{r}(t))^\top = \begin{bmatrix} y_{d1}(t) - r_1(t) & y_{d2}(t) - r_2(t) \end{bmatrix}$ for both the \mathcal{H}_2 - and \mathcal{H}_∞ -optimal sensor interpolations are included in Figure 5.10, while plots of $\bar{\mathbf{y}}^\top(t) = \begin{bmatrix} \bar{y}_1(t) & \bar{y}_2(t) \end{bmatrix}$ and the tracking error $\bar{\mathbf{y}}(t) - \mathbf{r}(t) = \begin{bmatrix} \bar{y}_1(t) - r_1(t) & \bar{y}_2(t) - r_2(t) \end{bmatrix}$ for the same simulations are in Figure 5.11.

It is clear from Figure 5.10 that the tracking errors are smaller with the \mathcal{H}_∞ -optimal method compared to the \mathcal{H}_2 -optimal method. This is to be expected, as $\bar{\mathbf{G}}_{\mathcal{H}_\infty}(s)$ is a much better match for $\mathbf{G}_d(s)$ than $\bar{\mathbf{G}}_{\mathcal{H}_2}(s)$ at lower frequencies, which includes the fundamental frequency of the reference trajectory. Although it is not shown, the tracking error $\bar{\mathbf{y}}(t) - \mathbf{r}(t)$ is quite small, and much like the numerical results in Section 5.4.1, the noticeable tracking error in $\mathbf{y}_d(t) - \mathbf{r}(t)$ is due to the difference between $\bar{\mathbf{y}}(t)$ and $\mathbf{y}_d(t)$.

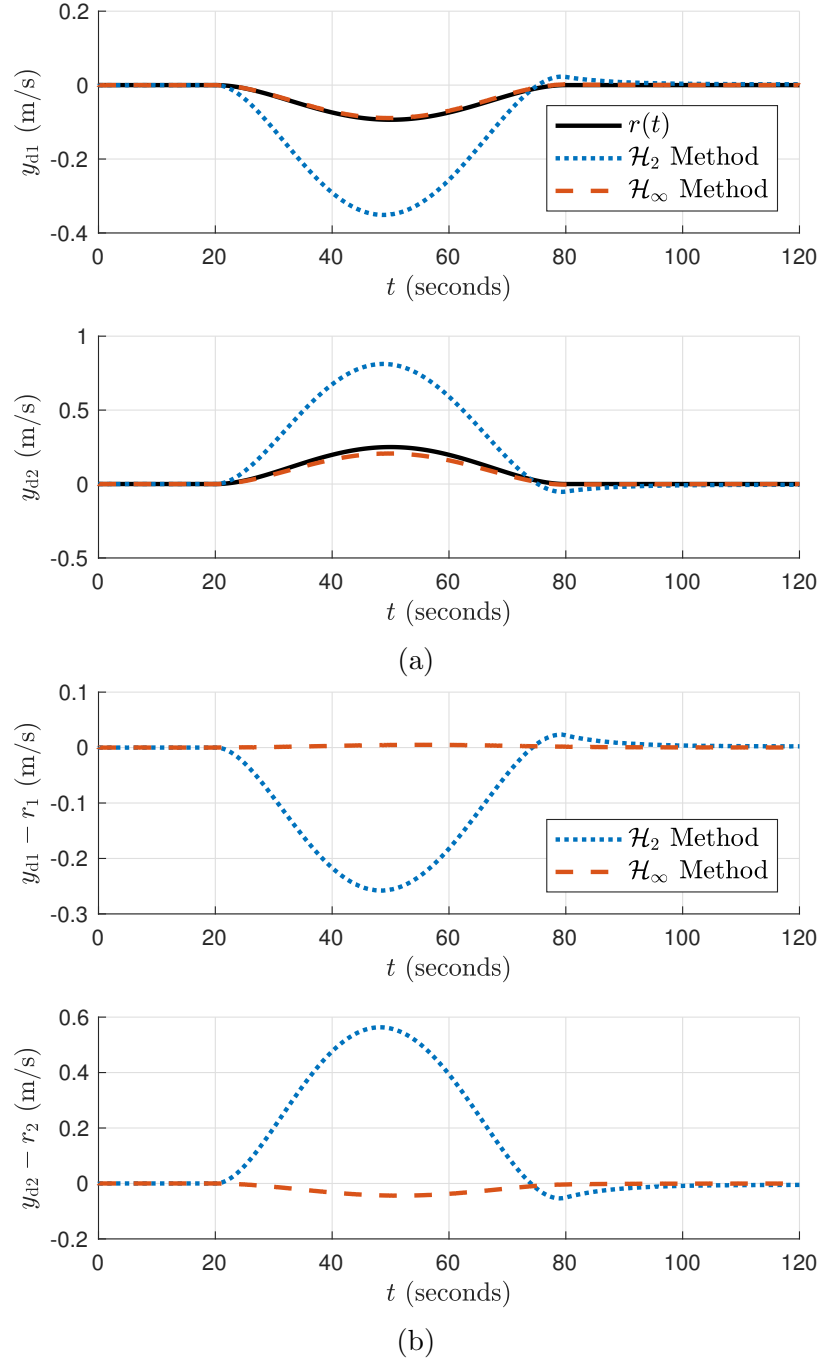


Figure 5.10: Closed-loop responses of (a) $y_{d1}(t)$ and $y_{d2}(t)$, and (b) the tracking errors $y_{d1}(t) - r_1(t)$ and $y_{d2}(t) - r_2(t)$ for both the \mathcal{H}_2 - and \mathcal{H}_∞ -optimal sensor interpolations in the numerical example of Section 5.4.2. The tracking error is less with the \mathcal{H}_∞ -optimal sensor interpolation during the nonzero portion of the reference trajectory, as the maximum singular value of $\bar{\mathbf{G}}_{\mathcal{H}_\infty}(s)$ more closely matches that of $\mathbf{G}_d(s)$ at lower frequencies than the maximum singular value of $\bar{\mathbf{G}}_{\mathcal{H}_2}(s)$ does.

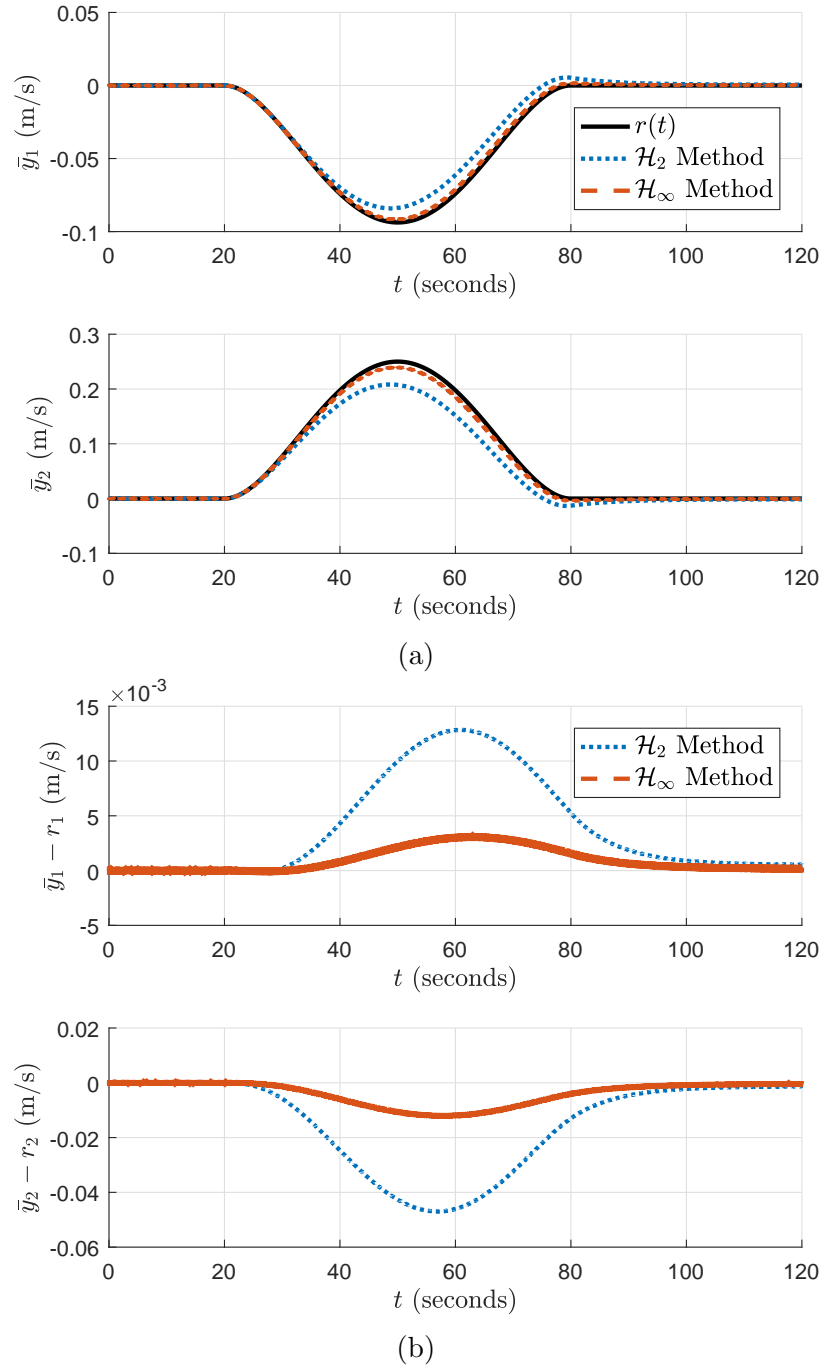


Figure 5.11: Closed-loop responses of (a) $\bar{y}_1(t)$ and $\bar{y}_2(t)$, and (b) the tracking errors $\bar{y}_1(t) - r_1(t)$ and $\bar{y}_2(t) - r_2(t)$ for both the \mathcal{H}_2 - and \mathcal{H}_∞ -optimal sensor interpolations in the numerical example of Section 5.4.2.

5.5 Closing Remarks

The sensor interpolation algorithms presented in this chapter render a system SPR by selecting a linear combination of available sensor measurements to be the

new system output. By minimizing either the \mathcal{H}_2 or \mathcal{H}_∞ norm of the difference between the new system and a specified desired system, it is possible to obtain an SPR system that has an output that is as close as possible to the desired output. The numerical examples demonstrated that the proposed sensor interpolation techniques can yield a new SPR plant whose gain is similar to that of a desired plant, and that satisfactory tracking of a reference signal is possible using a simple SPR controller in a feedback interconnection with the SPR plant.

Future work will include minimizing a weighted \mathcal{H}_2 or \mathcal{H}_∞ norm to obtain a system that closely resembles the desired system within a specified frequency band. This will be particularly useful, as the specific frequencies of the reference signal to be tracked can be targeted in the sensor interpolation algorithm.

Part III

The Large Gain Theorem

Chapter 6

Introduction to the Large Gain Theorem

6.1 Introduction

Input-output stability theorems provide a means for input-output stability properties of a feedback interconnection, such as the one shown in Figure 6.1, to be determined based on the input-output properties of the two systems within the feedback interconnection. In particular, the Large Gain Theorem is an input-output stability theorem based on the minimum gain properties of the two systems within a feedback interconnection. Although the Large Gain Theorem shares similarities with the well-known Small Gain Theorem, it is not well known and has been used in a very small number of applications [11, 12]. Limited understanding and awareness of the Large Gain Theorem is very likely due to a shortage of knowledge in the control systems community on minimum gain, whose properties were presented in detail in Chapter 3, the lack of an intuitive interpretation of this theorem, and the absence of concrete applications that make use of this theorem. The work presented in this part of the dissertation addresses these shortcomings of the Large Gain Theorem.

A proof of the Large Gain Theorem for LTI systems using the well-known Nyquist stability criterion is presented in Chapter 7, in an effort to increase understanding and awareness of this input-output stability result. Additional Large Gain Theorem-related stability results for LTI systems are also found in Chapter 7.

Due to its similarities with the Small Gain Theorem, it is natural to explore applications of the Small Gain Theorem as potential applications for the Large Gain Theorem. Chapter 8 presents a framework for the Large Gain Theorem to be used for

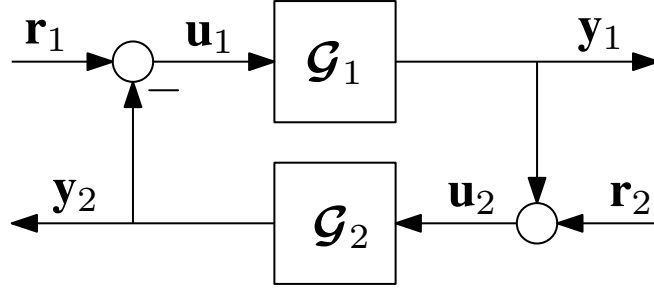


Figure 6.1: A negative feedback interconnection involving \mathcal{G}_1 and \mathcal{G}_2 .

robust control, which is arguably the most significant application the Small Gain Theorem. Robust full-state feedback and dynamic output feedback controller synthesis methods for robust stabilization, nominal performance, and robust performance are derived and tested numerically on a robust control benchmark problem in Chapter 9.

The remainder of this chapter formally presents the Small Gain Theorem and the Large Gain Theorem, followed by a brief discussion on how the Large Gain Theorem relates to the Small Gain Theorem and other input-output stability results.

6.2 The Large Gain Theorem

Theorem 6.1 (The Small Gain Theorem [30, 42]). *Consider the negative feedback interconnection of the causal systems $\mathcal{G}_1 : \mathcal{L}_{2e} \rightarrow \mathcal{L}_{2e}$ and $\mathcal{G}_2 : \mathcal{L}_{2e} \rightarrow \mathcal{L}_{2e}$, shown in Figure 6.1 and defined as*

$$\mathbf{y} = \begin{bmatrix} \mathbf{y}_1^\top & \mathbf{y}_2^\top \end{bmatrix}^\top, \quad \mathbf{y}_1 = \mathcal{G}_1 \mathbf{u}_1, \quad \mathbf{y}_2 = \mathcal{G}_2 \mathbf{u}_2,$$

$$\mathbf{r} = \begin{bmatrix} \mathbf{r}_1^\top & \mathbf{r}_2^\top \end{bmatrix}^\top, \quad \mathbf{u}_1 = \mathbf{r}_1 - \mathbf{y}_2, \quad \mathbf{u}_2 = \mathbf{r}_2 + \mathbf{y}_1.$$

If \mathcal{G}_1 and \mathcal{G}_2 have gains γ_1 and γ_2 , respectively, satisfying

$$0 < \gamma_1 \gamma_2 < 1,$$

then the closed-loop system, $\mathbf{y} = \mathbf{G}\mathbf{r}$, is input-output stable.

Theorem 6.2 (The Large Gain Theorem [8, 9]). *Consider the negative feedback interconnection of the causal systems $\mathcal{G}_1 : \mathcal{L}_{2e} \rightarrow \mathcal{L}_{2e}$ and $\mathcal{G}_2 : \mathcal{L}_{2e} \rightarrow \mathcal{L}_{2e}$, shown in*

Figure 6.1 and defined as

$$\begin{aligned}\mathbf{y} &= \begin{bmatrix} \mathbf{y}_1^\top & \mathbf{y}_2^\top \end{bmatrix}^\top, & \mathbf{y}_1 &= \mathcal{G}_1 \mathbf{u}_1, & \mathbf{y}_2 &= \mathcal{G}_2 \mathbf{u}_2, \\ \mathbf{r} &= \begin{bmatrix} \mathbf{r}_1^\top & \mathbf{r}_2^\top \end{bmatrix}^\top, & \mathbf{u}_1 &= \mathbf{r}_1 - \mathbf{y}_2, & \mathbf{u}_2 &= \mathbf{r}_2 + \mathbf{y}_1.\end{aligned}$$

If \mathcal{G}_1 and \mathcal{G}_2 have minimum gains ν_1 and ν_2 , respectively, satisfying

$$1 < \nu_1 \nu_2 < \infty,$$

then the closed-loop system, $\mathbf{y} = \mathcal{G}\mathbf{r}$, is input-output stable.

Proof. The following proof is adapted from [9]. To begin, the triangle inequality implies that

$$\|\mathbf{y}_1\|_{2T} = \|\mathbf{u}_2 - \mathbf{r}_2\|_{2T} \leq \|\mathbf{r}_2\|_{2T} + \|\mathbf{u}_2\|_{2T}, \quad (6.1)$$

$$\|\mathbf{y}_2\|_{2T} = \|\mathbf{r}_1 - \mathbf{u}_1\|_{2T} \leq \|\mathbf{r}_1\|_{2T} + \|\mathbf{u}_1\|_{2T}. \quad (6.2)$$

Applying the definition of minimum gain with the known minimum gains of each system, there exist $\beta_1 \in \mathbb{R}$ and $\beta_2 \in \mathbb{R}$ which depend only on the initial conditions, such that

$$\nu_1 \|\mathbf{u}_1\|_{2T} \leq \|\mathbf{y}_1\|_{2T} - \beta_1,$$

$$\nu_2 \|\mathbf{u}_2\|_{2T} \leq \|\mathbf{y}_2\|_{2T} - \beta_2.$$

Combining this with (6.1) and (6.2), and rearranging implies that

$$(\nu_1 \nu_2 - 1) \|\mathbf{y}_1\|_{2T} \leq \nu_1 \nu_2 \|\mathbf{r}_2\|_{2T} + \nu_1 \|\mathbf{r}_1\|_{2T} - \beta_1 - \nu_1 \beta_2,$$

$$(\nu_1 \nu_2 - 1) \|\mathbf{y}_2\|_{2T} \leq \nu_1 \nu_2 \|\mathbf{r}_1\|_{2T} + \nu_2 \|\mathbf{r}_2\|_{2T} - \beta_2 - \nu_2 \beta_2.$$

Recalling that $1 < \nu_1\nu_2 < \infty$, it is shown that

$$\begin{aligned}
\|\mathbf{y}\|_{2T} &\leq \|\mathbf{y}_1\|_{2T} + \|\mathbf{y}_2\|_{2T} \\
&\leq \frac{1}{\nu_1\nu_2 - 1} ((\nu_1\nu_2 + \nu_1) \|\mathbf{r}_1\|_{2T} + (\nu_1\nu_2 + \nu_2) \|\mathbf{r}_2\|_{2T}) + \beta \\
&\leq \frac{\nu_1\nu_2 + \max\{\nu_1, \nu_2\}}{\nu_1\nu_2 - 1} (\|\mathbf{r}_1\|_{2T} + \|\mathbf{r}_2\|_{2T}) + \beta \\
&\leq \frac{\nu_1\nu_2 + \max\{\nu_1, \nu_2\}}{\nu_1\nu_2 - 1} \sqrt{(\|\mathbf{r}_1\|_{2T} + \|\mathbf{r}_2\|_{2T})^2 + (\|\mathbf{r}_1\|_{2T} - \|\mathbf{r}_2\|_{2T})^2} + \beta \\
&= \frac{\nu_1\nu_2 + \max\{\nu_1, \nu_2\}}{\nu_1\nu_2 - 1} \sqrt{2(\|\mathbf{r}_1\|_{2T}^2 + \|\mathbf{r}_2\|_{2T}^2)} + \beta \\
&\leq \kappa \|\mathbf{r}\|_{2T} + \beta,
\end{aligned}$$

where

$$\begin{aligned}
\kappa &= \frac{\sqrt{2}(\nu_1\nu_2 + \max\{\nu_1, \nu_2\})}{\nu_1\nu_2 - 1}, \\
\beta &= -\frac{(1 + \nu_2)\beta_1 + (1 + \nu_1)\beta_2}{\nu_1\nu_2 - 1}.
\end{aligned}$$

Hence, \mathcal{G} maps any input $\mathbf{r} \in \mathcal{L}_2$ to an output $\mathbf{y} \in \mathcal{L}_2$, implying the closed-loop system is input-output stable. \square

Remark 6.3. The Small Gain Theorem and the Large Gain Theorem are also valid for positive feedback interconnections, since the negative sign associated with the feedback path can be lumped into \mathcal{G}_2 without affecting its gain.

Remark 6.4. The Large Gain Theorem may be satisfied when \mathcal{G}_1 , \mathcal{G}_2 , or \mathcal{G}_1 and \mathcal{G}_2 are unstable. This is different than the Small Gain Theorem that requires \mathcal{G}_1 and \mathcal{G}_2 be input-output stable. However, when \mathcal{G}_1 and \mathcal{G}_2 are LTI systems, the Large Gain Theorem requires that they are both minimum phase. There is no requirement with the Small Gain Theorem that \mathcal{G}_1 and \mathcal{G}_2 are minimum phase.

The Small Gain Theorem is somewhat intuitive in the sense that signals entering the negative feedback interconnection will become smaller as they pass through the feedback loop, since the loop gain is less than one. The Large Gain Theorem does not have a similar intuitive interpretation, which motivates the proof of the Large Gain Theorem using the well-known Nyquist stability criterion in Chapter 7.

The Small Gain Theorem and the Large Gain Theorem are special cases of the Extended Conic Sector Theorem. The Conic Sector Theorem, which itself is a special case of the Extended Conic Sector Theorem, contains the Small Gain Theorem as

a special case. The Large Gain Theorem involves an exterior conic property, and is therefore not a special case of the Conic Sector Theorem. Further details on the relation between input-output stability results can be found in [32, 37]

Chapter 7

Nyquist Interpretation of the Large Gain Theorem

7.1 Introduction

Feedback control is an engineering technology that realizes asymptotic stabilization, disturbance rejection, noise mitigation, and reduced sensitivity to uncertain parameters. Guaranteeing closed-loop asymptotic stability of a feedback interconnection is, arguably, the most important role feedback control plays, especially if the open-loop plant is nominally unstable. Depending on the known information of the systems in the feedback interconnection, denoted \mathcal{G}_1 and \mathcal{G}_2 in Figure 6.1, various stability results exist that can provide guarantees of closed-loop stability. For example, the Small Gain Theorem is a well-known stability result that guarantees the input-output stability of a negative feedback interconnection based on a condition involving gains of \mathcal{G}_1 and \mathcal{G}_2 . Alternatively, the Large Gain Theorem [8, 9], a formalization of the work in [38], is a relatively new and little-known stability result that guarantees the input-output stability of a negative feedback interconnection using lower bounds on the gains of \mathcal{G}_1 and \mathcal{G}_2 . The Large Gain Theorem addresses a limitation of the Small Gain Theorem by being able to assess the closed-loop input-output stability of negative feedback interconnections, where either \mathcal{G}_1 or \mathcal{G}_2 is unstable, or both \mathcal{G}_1 and \mathcal{G}_2 are unstable. This enables intriguing applications, such as the design of novel robust controllers [9, 11, 12], which is discussed in detail in Chapters 8 and 9. Despite its potential utility, only a limited number of Large Gain Theorem applications have been investigated, possibly due to the lack of familiar interpretations.

The objective of this chapter is to provide an interpretation of the Large Gain

Theorem for LTI systems using the well-known Nyquist stability criterion, which will help in making the Large Gain Theorem accessible to a wider audience. This is done by presenting five variations of Large Gain Theorem-based stability theorems for LTI systems, proofs of these theorems using the Nyquist stability criterion, and a comparison of the Small Gain Theorem and the Large Gain Theorem using Nyquist interpretations. Illustrative numerical examples are also included.

This chapter proceeds as follows. Preliminary definitions, results, and theorems are included in Section 7.2. Section 7.3 reviews a Nyquist interpretation of the Small Gain Theorem and presents five Large Gain Theorem stability theorems with proofs using the MIMO Nyquist stability criterion. Comparisons are also made between the Nyquist interpretations of the Large Gain Theorem and the Small Gain Theorem. Numerical examples of systems with nonzero minimum gain that satisfy the Large Gain Theorem and a simple robust stabilization example are given in Section 7.4, while Section 7.5 presents concluding remarks.

7.2 Preliminaries

Theorem 7.1 (Principle of the Argument [7]). *Let \mathcal{D} be a closed clockwise (CW) contour with no self intersections and $F(s)$ be a proper rational transfer function. Suppose $F(s)$ has no poles or zeros on \mathcal{D} , but \mathcal{D} encloses P poles and Z zeros of $F(s)$. The number of counter clockwise (CCW) encirclements of the origin of the $F(s)$ -plane is $\text{wno}\{F(s)\} = P - Z$.*

Theorem 7.2 (MIMO Nyquist stability criterion [79–81]). *Suppose $\mathbf{L}(s) = \mathbf{G}_1(s)\mathbf{G}_2(s)$ has $\bar{\eta}(\mathbf{L}(s))$ closed right-half plane (CRHP) poles counted according to the Smith-McMillan degree, and assume $\mathbf{L}(s)$ does not contain any unstable pole-zero cancellations. Construct the Nyquist plot of $-1 + \det(\mathbf{1} + \mathbf{L}(s))$, indenting into the left-half plane around poles on the imaginary axis when constructing the Nyquist contour. The feedback system is asymptotically stable if and only if the Nyquist plot of $-1 + \det(\mathbf{1} + \mathbf{L}(s))$ encircles the point $(-1, 0)$ exactly $\bar{\eta}(\mathbf{L}(s))$ times CCW (i.e., $\text{wno}\{\det(\mathbf{1} + \mathbf{L}(s))\} = \bar{\eta}(\mathbf{L}(s))$).*

7.3 Main Results

7.3.1 Motivation

Consider the negative feedback interconnection of $\mathcal{G}_1 : \mathcal{L}_{2e} \rightarrow \mathcal{L}_{2e}$ and $\mathcal{G}_2 : \mathcal{L}_{2e} \rightarrow \mathcal{L}_{2e}$, pictured in Figure 6.1. Assume \mathcal{G}_1 and \mathcal{G}_2 are causal LTI systems with transfer matrix representations $\mathbf{G}_1(s) \in \mathbb{C}^{n_{y_1} \times n_{u_1}}$ and $\mathbf{G}_2(s) \in \mathbb{C}^{n_{y_2} \times n_{u_2}}$, respectively, where $n_{y_1} = n_{u_2}$ and $n_{y_2} = n_{u_1}$. The goal of stability results, such as the Small Gain Theorem and the Large Gain Theorem, is to assess the stability of the feedback system using properties of $\mathbf{G}_1(s)$, $\mathbf{G}_2(s)$, $\mathbf{L}_1(s) = \mathbf{G}_1(s)\mathbf{G}_2(s) \in \mathbb{C}^{n_{y_1} \times n_{u_2}}$, and $\mathbf{L}_2(s) = \mathbf{G}_2(s)\mathbf{G}_1(s) \in \mathbb{C}^{n_{y_2} \times n_{u_1}}$. Nyquist interpretations of these stability theorems provide graphical means of understanding how they guarantee closed-loop asymptotic stability.

Although the input-output stability proof of the Large Gain Theorem in [9] directly implies asymptotic stability in the LTI case, which ensures that the MIMO Nyquist stability criterion is met, the proofs presented in this section do not rely on input-output stability theory and directly make use of the MIMO Nyquist stability criterion. The purpose of this is to present proofs that rely on more well-known theory and can be appreciated by a wider audience.

7.3.2 Large Gain Theorem Nyquist Interpretations

This section presents the main theoretical contributions of this chapter, which include stability theorems for LTI systems based on the Large Gain Theorem and proofs of these theorems using the MIMO Nyquist stability criterion.

Theorem 7.3. (*Large Gain Theorem for LTI SISO Systems*) *Consider the negative feedback interconnection involving the minimum phase transfer functions $G_1(s) \in \mathbb{C}$ and $G_2(s) \in \mathbb{C}$. The feedback interconnection is asymptotically stable if $1 < \nu_1 \nu_2 < \infty$, where ν_1 and ν_2 are minimum gains of $G_1(s)$ and $G_2(s)$, respectively.*

Proof. Since $1 < \nu_1 \nu_2 < \infty$, it is known from Lemma 3.8 that $1 < \nu_L < \infty$, where ν_L is a minimum gain of $L(s) = G_1(s)G_2(s)$. As a result of Lemma 3.4, $L(s)$ does not have any nonminimum phase zeros. Applying the Principle of the Argument with a contour \mathcal{D} that encircles the entire CRHP, $N_{\text{CCW},0} = P$ follows, where $N_{\text{CCW},0}$ is the number of CCW encirclements the Nyquist plot of $L(s)$ makes about the origin and P is the number of ORHP poles of $L(s)$. Since $1 < |L(j\omega)| < \infty$, the Nyquist plot of $L(s)$ cannot lie inside a unit disk centered at the origin and, as shown in Figure 7.1b,

any encirclements of the origin are also encirclements of the point $(-1, 0)$. To be clear, $N_{\text{CCW}, -1} = N_{\text{CCW}, 0} = P$, where $N_{\text{CCW}, -1}$ is the number of CCW encirclements about the point $(-1, 0)$. By the Nyquist Stability Criterion, the feedback system is asymptotically stable, since $N_{\text{CCW}, -1} = P$. \square

Theorem 7.4. (*Large Gain Theorem for LTI MIMO Systems*) Consider the negative feedback interconnection involving the minimum phase transfer matrices $\mathbf{G}_1(s) \in \mathbb{C}^{n_u \times n_y}$ and $\mathbf{G}_2(s) \in \mathbb{C}^{n_y \times n_u}$. The feedback interconnection is asymptotically stable if $1 < \nu_1 \nu_2 < \infty$, where ν_1 and ν_2 are minimum gains of $\mathbf{G}_1(s)$ and $\mathbf{G}_2(s)$, respectively.

Proof. It is known from Lemma 3.8 that $1 < \nu_L < \infty$, where $\nu_L = \nu_1 \nu_2$ is a minimum gain of $\mathbf{L}(s) = \mathbf{G}_1(s)\mathbf{G}_2(s)$, since $1 < \nu_1 \nu_2 < \infty$. The norm of the output of the SISO transfer function $H(s) = y(s)/u(s) = -1 + \det(\mathbf{1} + \mathbf{L}(s))$ is

$$\|y\|_{2T}^2 = \frac{1}{2\pi} \int_{-\infty}^{\infty} |H(j\omega)|^2 |u_T(j\omega)|^2 d\omega. \quad (7.1)$$

The term $|H(j\omega)|^2$ can be expanded as

$$\begin{aligned} |H(j\omega)|^2 &= H(-j\omega)H(j\omega), \\ &= (-1 + \det(\mathbf{1} + \mathbf{L}^H(j\omega))) (-1 + \det(\mathbf{1} + \mathbf{L}(j\omega))), \\ &= \det(\mathbf{1} + \mathbf{L}^H(j\omega) + \mathbf{L}(j\omega) + \mathbf{L}^H(j\omega)\mathbf{L}(j\omega)) \\ &\quad + 1 - \det(\mathbf{1} + \mathbf{L}^H(j\omega)) - \det(\mathbf{1} + \mathbf{L}(j\omega)). \end{aligned} \quad (7.2)$$

Using Minkowski's Inequality for determinants [82], it can be shown that

$$\begin{aligned} \det(\mathbf{1} + \mathbf{L}^H(j\omega) + \mathbf{L}(j\omega) + \mathbf{L}^H(j\omega)\mathbf{L}(j\omega)) &\geq \\ \det(\mathbf{1} + \mathbf{L}^H(j\omega)) + \det(\mathbf{1} + \mathbf{L}(j\omega)) + \det(\mathbf{L}^H(j\omega)\mathbf{L}(j\omega) - \mathbf{1}). \end{aligned}$$

This is substituted into (7.2) to obtain

$$\begin{aligned} |H(j\omega)|^2 &\geq 1 - \det(\mathbf{1} + \mathbf{L}^H(j\omega)) - \det(\mathbf{1} + \mathbf{L}(j\omega)) \\ &\quad + \det(\mathbf{1} + \mathbf{L}^H(j\omega)) + \det(\mathbf{1} + \mathbf{L}(j\omega)) + \det(\mathbf{L}^H(j\omega)\mathbf{L}(j\omega) - \mathbf{1}), \\ &= 1 + \det(\mathbf{L}^H(j\omega)\mathbf{L}(j\omega) - \mathbf{1}). \end{aligned} \quad (7.3)$$

Using properties of the determinant, eigenvalues, and singular values it can be shown

that

$$\begin{aligned}
\det(\mathbf{L}^H(j\omega)\mathbf{L}(j\omega) - \mathbf{1}) &= \prod_{i=1}^n \lambda_i\{\mathbf{L}^H(j\omega)\mathbf{L}(j\omega) - \mathbf{1}\}, \\
&= \prod_{i=1}^n (\lambda_i\{\mathbf{L}^H(j\omega)\mathbf{L}(j\omega)\} - 1), \\
&= \prod_{i=1}^n (\sigma_i^2\{\mathbf{L}(j\omega)\} - 1). \tag{7.4}
\end{aligned}$$

Substituting (7.4) into (7.3) yields $|H(j\omega)|^2 \geq 1 + \prod_{i=1}^n (\sigma_i^2\{\mathbf{L}(j\omega)\} - 1)$. Knowing that $\underline{\sigma}\{\mathbf{L}(j\omega)\} > 1$, this becomes $|H(j\omega)|^2 > 1$. Substituting this into (7.1) yields $\|y\|_{2T}^2 \geq \|u\|_{2T}^2$, which proves that $H(s) = -1 + \det(\mathbf{1} + \mathbf{L}(s))$ has a minimum gain of $\nu = 1$. From Lemma 3.7 and Lemma 3.4 it is concluded that $|-1 + \det(\mathbf{1} + \mathbf{L}(j\omega))| > 1$ and $H(s)$ has no nonminimum phase zeros.

Employing the Principle of the Argument with a contour \mathcal{D} that encircles the entire CHRP, it is known that $\text{wno}\{-1 + \det(\mathbf{1} + \mathbf{L}(s))\} = \bar{\eta}(-1 + \det(\mathbf{1} + \mathbf{L}(s)))$. In order to obtain $\text{wno}\{-1 + \det(\mathbf{1} + \mathbf{L}(s))\} = \bar{\eta}(\mathbf{L}(s))$, it is necessary to show that the poles of $-1 + \det(\mathbf{1} + \mathbf{L}(s))$ are identical to the poles of $\mathbf{L}(s)$. In order to prove this, the transfer matrix $\mathbf{L}(s)$ is written in terms of a minimal state-space representation as $\mathbf{L}(s) = \mathbf{C}_L(s\mathbf{1} - \mathbf{A}_L)^{-1}\mathbf{B}_L + \mathbf{D}_L$, where the poles of $\mathbf{L}(s)$ are the roots of $\det(s\mathbf{1} - \mathbf{A}_L)$. Substituting the state-space representation into $\det(\mathbf{1} + \mathbf{L}(s))$, knowing that $\mathbf{1} + \mathbf{D}_L$ is invertible due to the well-posedness of the feedback interconnection, and using determinant identities $\det(\mathbf{A}\mathbf{B}) = \det(\mathbf{A})\det(\mathbf{B}) \forall \mathbf{A}, \mathbf{B} \in \mathbb{R}^{n \times n}$ [48, Proposition 2.7.3, p. 113], $\det(\mathbf{A}^{-1}) = (\det(\mathbf{A}))^{-1}$ [48, Corollary 2.7.4, p. 113], and $\det(\mathbf{1} + \mathbf{A}\mathbf{B}) = \det(\mathbf{1} + \mathbf{B}\mathbf{A}) \forall \mathbf{A} \in \mathbb{R}^{n \times m}, \mathbf{B} \in \mathbb{R}^{m \times n}$ [48, Fact 2.14.2, p. 144] yields

$$\begin{aligned}
\det(\mathbf{1} + \mathbf{L}(s)) &= \det(\mathbf{1} + \mathbf{C}_L(s\mathbf{1} - \mathbf{A}_L)^{-1}\mathbf{B}_L + \mathbf{D}_L) \\
&= \det(\mathbf{1} + \mathbf{D}_L)\det(\mathbf{1} + (\mathbf{1} + \mathbf{D}_L)^{-1}\mathbf{C}_L(s\mathbf{1} - \mathbf{A}_L)^{-1}\mathbf{B}_L) \\
&= \det(\mathbf{1} + \mathbf{D}_L)\det(s\mathbf{1} - \mathbf{A}_L + \mathbf{B}_L(\mathbf{1} + \mathbf{D}_L)^{-1}\mathbf{C}_L)\det((s\mathbf{1} - \mathbf{A}_L)^{-1}) \\
&= \frac{\det(\mathbf{1} + \mathbf{D}_L)\det(s\mathbf{1} - \mathbf{A}_L + \mathbf{B}_L(\mathbf{1} + \mathbf{D}_L)^{-1}\mathbf{C}_L)}{\det(s\mathbf{1} - \mathbf{A}_L)}. \tag{7.5}
\end{aligned}$$

Subtracting 1 from both sides of (7.5) gives

$$-1 + \det(\mathbf{1} + \mathbf{L}(s)) = \frac{\det(\mathbf{1} + \mathbf{D}_L)\det(s\mathbf{1} - \mathbf{A}_L + \mathbf{B}_L(\mathbf{1} + \mathbf{D}_L)^{-1}\mathbf{C}_L) - \det(s\mathbf{1} - \mathbf{A}_L)}{\det(s\mathbf{1} - \mathbf{A}_L)}. \tag{7.6}$$

The numerator and the denominator of (7.6) are polynomials in s . The poles of $-1 + \det(\mathbf{1} + \mathbf{L}(s))$ are the roots of the denominator polynomial $\det(s\mathbf{1} - \mathbf{A}_L)$, which is identical to the characteristic polynomial of $\mathbf{L}(s)$. Therefore, the poles of $-1 + \det(\mathbf{1} + \mathbf{L}(s))$ are identical to the poles of $\mathbf{L}(s)$ and $\bar{\eta}(-1 + \det(\mathbf{1} + \mathbf{L}(s))) = \bar{\eta}(\mathbf{L}(s))$. From this it can be concluded that $\text{wno}\{-1 + \det(\mathbf{1} + \mathbf{L}(s))\} = \bar{\eta}(\mathbf{L}(s))$. Since $|-1 + \det(\mathbf{1} + \mathbf{L}(j\omega))| > 1$, the Nyquist plot of $-1 + \det(\mathbf{1} + \mathbf{L}(s))$ lies strictly outside a unit disk centered at the origin, which means that any encirclements of the origin are also encirclements of the point $(-1, 0)$. This proves that the Nyquist plot of $-1 + \det(\mathbf{1} + \mathbf{L}(s))$ encircles the point $(-1, 0)$ exactly $\bar{\eta}(\mathbf{L}(s))$ times in the CCW direction, and closed-loop asymptotic stability is guaranteed by the MIMO Nyquist stability criterion. \square

Remark 7.5. Note that there is no assumption that $\mathbf{G}_1(s)$ or $\mathbf{G}_2(s)$ are asymptotically stable in the statement of Theorem 7.4. However, the assumption that $\mathbf{G}_1(s)$ and $\mathbf{G}_2(s)$ have minimum gains satisfying $1 < \nu_1\nu_2 < \infty$ implies that both are minimum phase square systems. If $G_1(s)$ and $G_2(s)$ are SISO, then it is required that $G_1(s)$ and $G_2(s)$ be biproper transfer functions and their respective state-space representations have nonzero feedthrough term. If $\mathbf{G}_1(s)$ and $\mathbf{G}_2(s)$ are MIMO, then their respective transfer matrices must have \mathbf{D} matrices with singular values that are strictly greater than zero [9].

Theorem 7.6. *Consider the negative feedback interconnection of $\mathbf{G}_1(s) \in \mathbb{C}^{n_{y1} \times n_{u1}}$ and $\mathbf{G}_2(s) \in \mathbb{C}^{n_{y2} \times n_{u2}}$, the loop transfer matrices $\mathbf{L}_1(s) = \mathbf{G}_1(s)\mathbf{G}_2(s) \in \mathbb{C}^{n_{y1} \times n_{u2}}$ and $\mathbf{L}_2(s) = \mathbf{G}_2(s)\mathbf{G}_1(s) \in \mathbb{C}^{n_{y2} \times n_{u1}}$, and assume that $\mathbf{L}_1(s)$ and $\mathbf{L}_2(s)$ contain no unstable pole-zero cancellations. The feedback interconnection is asymptotically stable if $1 < \nu_L < \infty$, where $\nu_L = \max(\nu_{L_1}, \nu_{L_2})$, and ν_{L_1} and ν_{L_2} are minimum gains of $\mathbf{L}_1(s)$ and $\mathbf{L}_2(s)$, respectively.*

Proof. The proof of Theorem 7.6 is identical to the proof of Theorem 7.4 without the use of Lemma 3.8 in the first step of the proof and with $\mathbf{L}(s) = \mathbf{L}_1(s)$ if $\nu_L = \nu_{L_1}$ or $\mathbf{L}(s) = \mathbf{L}_2(s)$ if $\nu_L = \nu_{L_2}$. \square

Remark 7.7. In Theorem 7.6 the condition $1 < \nu_L < \infty$ implies that $\mathbf{L}_1(s)$ or $\mathbf{L}_2(s)$ is minimum phase. The transfer matrices $\mathbf{G}_1(s)$ and $\mathbf{G}_2(s)$ do not necessarily need to be minimum phase, as the transmission zeros of $\mathbf{G}_1(s)$ and $\mathbf{G}_2(s)$ are not necessarily the transmission zeros of $\mathbf{L}_1(s)$ or $\mathbf{L}_2(s)$. Additionally, since the minimum gain condition is placed directly on $\mathbf{L}_1(s)$ or $\mathbf{L}_2(s)$, there is no assumption that $\mathbf{G}_1(s)$ and $\mathbf{G}_2(s)$ are square systems. Theorem 7.4 is a special case of Theorem 7.6, where the

transfer matrices $\mathbf{G}_1(s)$ and $\mathbf{G}_2(s)$ each have non-zero minimum gain. Theorem 7.6 is particularly useful in the case where $\mathbf{G}_1(s)$ has nonminimum phase transmission zeros and $\mathbf{G}_2(s)$ has none, or vice-versa.

Theorem 7.8. *Consider the negative feedback interconnection of $\mathbf{G}_1(s) \in \mathbb{C}^{n_{y1} \times n_{u1}}$ and $\mathbf{G}_2(s) \in \mathbb{C}^{n_{y2} \times n_{u2}}$, and the loop transfer matrix $\mathbf{L}(s) = \mathbf{G}_1(s)\mathbf{G}_2(s) \in \mathbb{C}^{n_{y1} \times n_{u2}}$. Assume that $\mathbf{G}_1(s)\mathbf{G}_2(s)$ and $\mathbf{G}_2(s)\mathbf{G}_1(s)$ do not contain any unstable pole-zero cancellations and*

$$1 < \inf_{\omega \in \mathbb{R}^+} \max(\underline{\sigma}\{\mathbf{G}_1(j\omega)\mathbf{G}_2(j\omega)\}, \underline{\sigma}\{\mathbf{G}_2(j\omega)\mathbf{G}_1(j\omega)\}) < \infty. \quad (7.7)$$

The feedback connection is asymptotically stable if and only if $\text{wno}\{\det(\mathbf{L}(s))\} = \bar{\eta}(\mathbf{L}(s))$. Assuming $\det(\mathbf{L}(s)) \neq 0$, this condition is equivalent to the transmission zeros of $\mathbf{L}(s)$ being minimum phase.

Proof. A singular value inequality is first established for matrices $\mathbf{A} \in \mathbb{C}^{n \times m}$ and $\mathbf{B} \in \mathbb{R}^{m \times n}$. Assume without loss of generality that $n \leq m$ and recall that $\underline{\sigma}\{\mathbf{A} + \mathbf{B}\} \geq \underline{\sigma}\{\mathbf{A}\} - \bar{\sigma}\{\mathbf{B}\}$ [48, Corollary 9.6.9, p. 617]. For any matrix $\mathbf{C} \in \mathbb{R}^{n \times n}$, $\det(\mathbf{C}) = 0$ if and only if $\underline{\sigma}\{\mathbf{C}\} = 0$. Therefore, it follows that if $\underline{\sigma}\{\mathbf{AB}\} > 1$, then $|\det(\mathbf{AB} \pm \lambda\mathbf{1})| \geq \underline{\sigma}\{\mathbf{AB}\} - |\lambda| > 0$, $\forall \lambda \in [-1, 1]$. This inequality can be slightly refined. Recall that if $n = m$, then $\det(\mathbf{AB} \pm \mathbf{1}) = \det(\mathbf{BA} \pm \mathbf{1})$, and if $n < m$, then $\underline{\sigma}\{\mathbf{BA}\} = 0$. Consequently, $|\det(\mathbf{AB} \pm \mathbf{1})| > 0$ if $\max(\underline{\sigma}\{\mathbf{AB}\}, \underline{\sigma}\{\mathbf{BA}\}) > 1$. This singular value inequality implies that, by the assumption in (7.7), for all $\omega \in \mathbb{R}$ and $\lambda \in [-1, 1]$,

$$\det(\mathbf{L}(j\omega) \pm \lambda\mathbf{1}) \neq 0. \quad (7.8)$$

It follows from (7.8) that for all $\lambda \in [-1, 1]$, $\text{wno}\{\det(\mathbf{L}(s) \pm \mathbf{1})\} = \text{wno}\{\det(\mathbf{L}(s))\} = \bar{\eta}(\mathbf{L}(s))$. If these winding numbers were different, then there would exist $\lambda \in [-1, 1]$ and $\omega \in \mathbb{R}$ such that $\det(\mathbf{L}(j\omega) \pm \lambda\mathbf{1}) = 0$, a conclusion made impossible by (7.8). The result now follows from the Nyquist stability criterion, since asymptotic stability of the feedback interconnection is implied if and only if $\text{wno}\{\det(\mathbf{L}(s) \pm \mathbf{1})\} = \bar{\eta}(\mathbf{L}(s))$. \square

Remark 7.9. Theorem 7.8 is very similar to Theorem 7.6, but is presented in a slightly different manner to yield necessary and sufficient conditions for asymptotic closed-loop stability. Due to the necessary and sufficient condition stated in Theorem 7.8, it directly follows that the feedback interconnection described in Theorem 7.8 is unstable if and only if $\text{wno}\{\det(\mathbf{L}(s))\} = \bar{\eta}(\mathbf{L}(s))$. It is useful to note that when $\mathbf{G}_1(s)$ and

$\mathbf{G}_2(s)$ are square, the condition that $\mathbf{L}(s)$ has only minimum phase transmission zeros is equivalent to $\mathbf{G}_1(s)$ and $\mathbf{G}_2(s)$ having only minimum phase transmission zeros.

Theorem 7.10. *Consider the negative feedback interconnection involving the minimum phase square transfer matrices $\mathbf{G}_1(s) \in \mathbb{C}^{n_{y_1} \times n_{u_1}}$ and $\mathbf{G}_2(s) \in \mathbb{C}^{n_{y_2} \times n_{u_2}}$, where $n_{u_1} = n_{u_2} = n_{y_1} = n_{y_2}$. The feedback interconnection is asymptotically stable for all $\mathbf{G}_1(s)$ with minimum gain $0 < \nu_1 < \infty$ if and only if $1 < \nu_1 \nu_2 < \infty$, where ν_2 is a minimum gain of $\mathbf{G}_2(s)$.*

Proof. If $\mathbf{G}_1(s)$ and $\mathbf{G}_2(s)$ both are minimum phase, then the loop transfer matrix $\mathbf{L}(s) = \mathbf{G}_1(s)\mathbf{G}_2(s)$ will also be minimum phase and $\text{wno}\{\det(\mathbf{L}(s))\} = \bar{\eta}(\mathbf{L}(s))$. From Theorem 7.8, the feedback interconnection is asymptotically stable if and only if (7.7). Theorem 7.10 is to be true for all $\mathbf{G}_1(s)$ with minimum gain $0 < \nu_1 < \infty$, including $\mathbf{G}_1(s) = \nu_1 \mathbf{1}$. With this particular choice of $\mathbf{G}_1(s)$ it is shown that (7.7) becomes

$$\begin{aligned} 1 &< \inf_{\omega \in \mathbb{R}^+} \max(\underline{\sigma}\{\mathbf{G}_1(j\omega)\mathbf{G}_2(j\omega)\}, \underline{\sigma}\{\mathbf{G}_2(j\omega)\mathbf{G}_1(j\omega)\}) \\ &= \inf_{\omega \in \mathbb{R}^+} \max(\underline{\sigma}\{\nu_1 \mathbf{1}\mathbf{G}_2(j\omega)\}, \underline{\sigma}\{\mathbf{G}_2(j\omega)\nu_1 \mathbf{1}\}) \\ &= \nu_1 \inf_{\omega \in \mathbb{R}^+} \underline{\sigma}\{\mathbf{G}_2(j\omega)\}. \end{aligned} \quad (7.9)$$

Knowing that $\mathbf{G}_2(s)$ is minimum phase, $\nu_2 \leq \inf_{\omega \in \mathbb{R}^+} \underline{\sigma}\{\mathbf{G}_2(j\omega)\}$, which allows for (7.9) to be rewritten as

$$1 < \nu_1 \inf_{\omega \in \mathbb{R}^+} \underline{\sigma}\{\mathbf{G}_2(j\omega)\} \leq \nu_1 \nu_2,$$

which is the stability condition state in Theorem 7.10. \square

Remark 7.11. It is interesting to note that Theorems 7.3, 7.4, 7.6, 7.8, and 7.10 all hold for both negative and positive feedback interconnections of $\mathbf{G}_1(s)$ and $\mathbf{G}_2(s)$. This is immediate from the fact that transfer matrices $\mathbf{G}(s)$ and $-\mathbf{G}(s)$ have the same minimum gain. Additionally, these theorems can be satisfied by improper transfer matrices with nonzero minimum gain. This differs from the Small Gain Theorem, which can only be satisfied by proper transfer matrices. See [83] for additional details regarding the closed-loop stability and well posedness of improper transfer matrices.

7.3.3 Comparison of Large Gain Theorem and Small Gain Theorem Nyquist Interpretations

It will be shown that the conditions of the Small Gain Theorem imply the stipulations of the MIMO Nyquist stability criterion. This familiar result is presented because it parallels the novel MIMO Nyquist interpretation of the Large Gain Theorem presented in Section 7.3.2.

Consider the feedback system described in Section 7.3.1 involving the asymptotically stable transfer matrices $\mathbf{G}_1(s) \in \mathbb{C}^{n_{y1} \times n_{u1}}$ and $\mathbf{G}_2(s) \in \mathbb{C}^{n_{y2} \times n_{u2}}$, whose maximum gains satisfy $0 < \gamma_1 \gamma_2 < 1$. This implies that $0 < \gamma_L < 1$, where $\gamma_L = \sup_{\omega \in \mathbb{R}^+} \bar{\sigma}\{\mathbf{L}(j\omega)\}$ and $\mathbf{L}(s) = \mathbf{G}_1(s)\mathbf{G}_2(s)$. It will be shown in the contrapositive, using a proof adapted from [7], that if the conditions of the Small Gain Theorem hold, then $-1 + \det(\mathbf{1} + \mathbf{L}(s))$ does not encircle the point $(-1, 0)$, and closed-loop asymptotic stability is guaranteed by the first form of the MIMO Nyquist stability criterion. The contrapositive is proven by showing that if the Nyquist plot of $-1 + \det(\mathbf{1} + \mathbf{L}(s))$ does encircle the point $(-1, 0)$, then the maximum gain of $\mathbf{L}(s)$ must be greater than one.

If the Nyquist plot of $-1 + \det(\mathbf{1} + \mathbf{L}(s))$ does encircle the point $(-1, 0)$, then the shifted Nyquist plot $\det(\mathbf{1} + \mathbf{L}(s))$ does encircle the origin. From this, there must exist a gain $0 < \epsilon \leq 1$ and a frequency ω^* such that $\det(\mathbf{1} + \epsilon\mathbf{L}(j\omega^*)) = 0$. This is equivalent to $\prod_{i=1}^n \lambda_i\{\mathbf{1} + \epsilon\mathbf{L}(j\omega^*)\} = 0$ and $\prod_{i=1}^n (\epsilon\lambda_i\{\mathbf{L}(j\omega^*)\} + 1) = 0$. For at least one eigenvalue λ_i , the equality $\epsilon\lambda_i\{\mathbf{L}(j\omega^*)\} = -1$ must hold. Taking the absolute value of both sides of this leads to

$$|\epsilon| |\lambda_i\{\mathbf{L}(j\omega^*)\}| = 1. \quad (7.10)$$

Since $0 < \epsilon \leq 1$, (7.10) implies that $1 \leq |\lambda_i\{\mathbf{L}(j\omega^*)\}| \leq \sup_{\omega \in \mathbb{R}^+} \bar{\sigma}\{\mathbf{L}(j\omega)\} = \gamma_L$, which gives the desired result of $1 \leq \gamma_L$. From this it can be concluded that the condition of the Small Gain Theorem, $0 < \gamma_L < 1$, can only hold if those of the MIMO Nyquist stability criterion also hold.

When satisfying the Small Gain Theorem, the Nyquist plot of $-1 + \det(\mathbf{1} + \mathbf{L}(s))$ must lie within a unit disk centered at the origin in the Small Gain Theorem, as pictured in Figure 7.1a. When satisfying the Large Gain Theorem, as stated in Theorem 7.4, 7.6, 7.8, or 7.10, the Nyquist plot of $-1 + \det(\mathbf{1} + \mathbf{L}(s))$ must lie outside a unit disk centered at the origin in the Large Gain Theorem, as shown in in Figure 7.1b. This highlights the complementary nature of the Large Gain Theorem and the Small Gain Theorem. Moreover, the Small Gain Theorem cannot account for an unstable

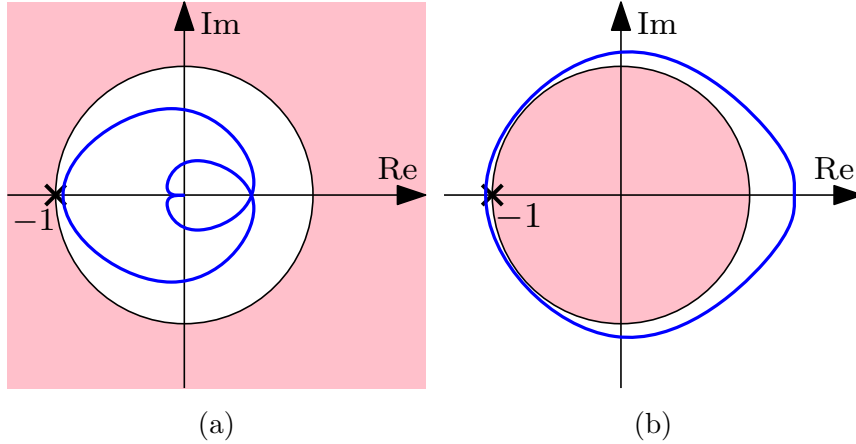


Figure 7.1: Plots of the regions (shaded pink) that the Nyquist plot of $-1 + \det(\mathbf{1} + \mathbf{L}(s))$ cannot lie based on the conditions set forth in the (a) Small Gain Theorem and (b) Large Gain Theorem. Example Nyquist plots of $-1 + \det(\mathbf{1} + \mathbf{L}(s))$ that satisfy these theorems are illustrated in blue. Note that the Nyquist plot of $-1 + \det(\mathbf{1} + \mathbf{L}(s))$ in (b) could also lie to the right or the left of the unit disk, and does not necessarily encircle the point $(-1, 0)$.

$\mathbf{L}(s)$ and the Large Gain Theorem cannot account for a nonminimum phase $\mathbf{L}(s)$. It can also be shown that if $\mathbf{L}(s)$ has minimum gain satisfying $1 < \nu_L < \infty$, then the Nyquist plot of $\det(\mathbf{L}(s))$ will be strictly outside a unit disk centered at the origin, as a consequence of $\underline{\sigma}^n\{\mathbf{A}\} \leq |\det(\mathbf{A})|$ for $\mathbf{A} \in \mathbb{C}^{n \times n}$ [48, p. 356]. . Similarly, if $\mathbf{L}(s)$ has maximum gain satisfying $0 < \gamma_L < 1$, then the Nyquist plot of $\det(\mathbf{L}(s))$ will be strictly inside a unit disk centered at the origin, since $|\det(\mathbf{A})| \leq \bar{\sigma}^n\{\mathbf{A}\}$ for $\mathbf{A} \in \mathbb{C}^{n \times n}$ [48, p. 356].

7.4 Numerical Examples

Numerical examples are provided in this section that demonstrate the use of the theorems presented in Section 7.3, including a simple example illustrating the use of the Large Gain Theorem for robust stabilization.

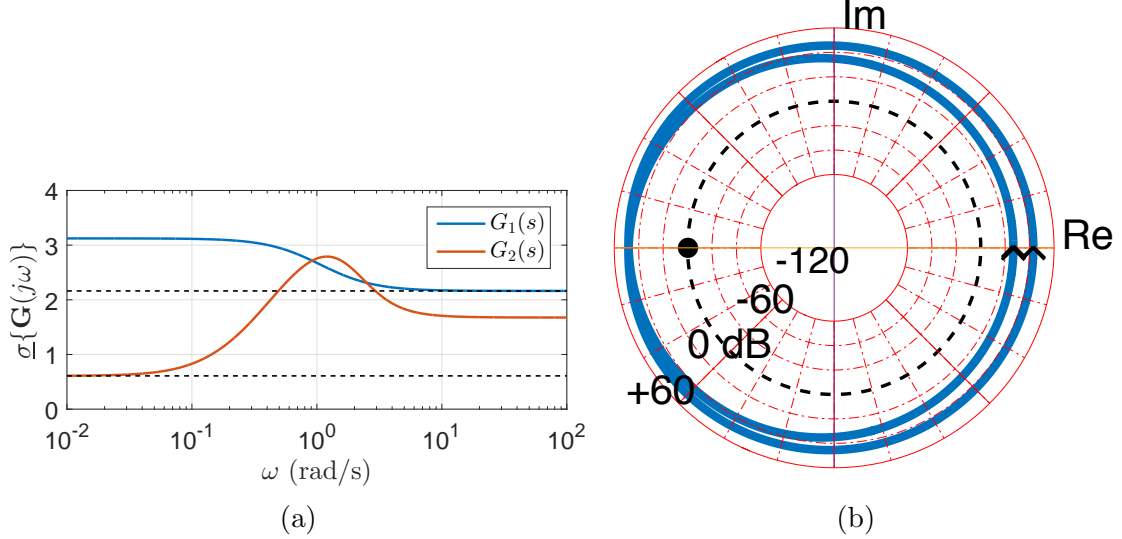


Figure 7.2: (a) Plots of the minimum singular value of $\mathbf{G}_1(s)$ and $\mathbf{G}_2(s)$ versus frequency with $k = 1$ in Example 7.12. Black dashed lines represent $\nu^* = \inf_{\omega \in \mathbb{R}^+} \underline{\sigma}\{\mathbf{G}(j\omega)\}$ of each system. (b) Nyquist plots of $-1 + \det(\mathbf{1} + \mathbf{L}(s))$ for Example 7.12 with $k = 1$. The Nyquist plots are generated on a logarithmic scale, where the gridlines are red, except for the 0 dB gridline, which is a black dashed line [84]. The point $(-1, 0)$ is labeled by a black circular marker.

7.4.1 Large Gain Theorem with LTI MIMO Systems

Example 7.12. Consider the MIMO transfer matrices

$$\mathbf{G}_1(s) = k \begin{bmatrix} \frac{2s+5}{s-1} & 1 \\ -1 & \frac{4s+3}{s-1} \end{bmatrix}, \quad (7.11)$$

$$\mathbf{G}_2(s) = \begin{bmatrix} \frac{2s^2+15s+4}{s^2+2s+2} & -\frac{s+1}{s+2} \\ \frac{7s-3}{s+1} & \frac{3s^2+10s+2}{s^2+3s+1} \end{bmatrix}, \quad (7.12)$$

where $k = 1$. Plots of the minimum singular values of $\mathbf{G}_1(s)$ and $\mathbf{G}_2(s)$ are shown in Figure 7.2a. It can be seen in Figure 7.2a that $\mathbf{G}_1(s)$ has a least conservative minimum gain of $\nu_1^* = 2.16$, while $\mathbf{G}_2(s)$ has a least conservative minimum gain of $\nu_2^* = 0.61$. Note that the Minimum Gain Lemma (Lemma 3.9) can be used to numerically solve for ν_1^* and ν_2^* .

Consider the loop transfer matrices $\mathbf{L}_1(s) = \mathbf{G}_1(s)\mathbf{G}_2(s)$ and $\mathbf{L}_2(s) = \mathbf{G}_2(s)\mathbf{G}_1(s)$. The feedback system shown in Figure 6.1, with \mathcal{G}_1 replaced by $\mathbf{G}_1(s)$ and \mathcal{G}_2 replaced by $\mathbf{G}_2(s)$, is asymptotically stable by Theorem 7.4, since $1 < \nu_1^*\nu_2^* < \infty$, with a lower gain margin of 2.38 dB. Asymptotic stability of the feedback interconnection is also guaranteed by Theorem 7.6, since $\mathbf{L}_1(s)$ and $\mathbf{L}_2(s)$ have least conservative minimum

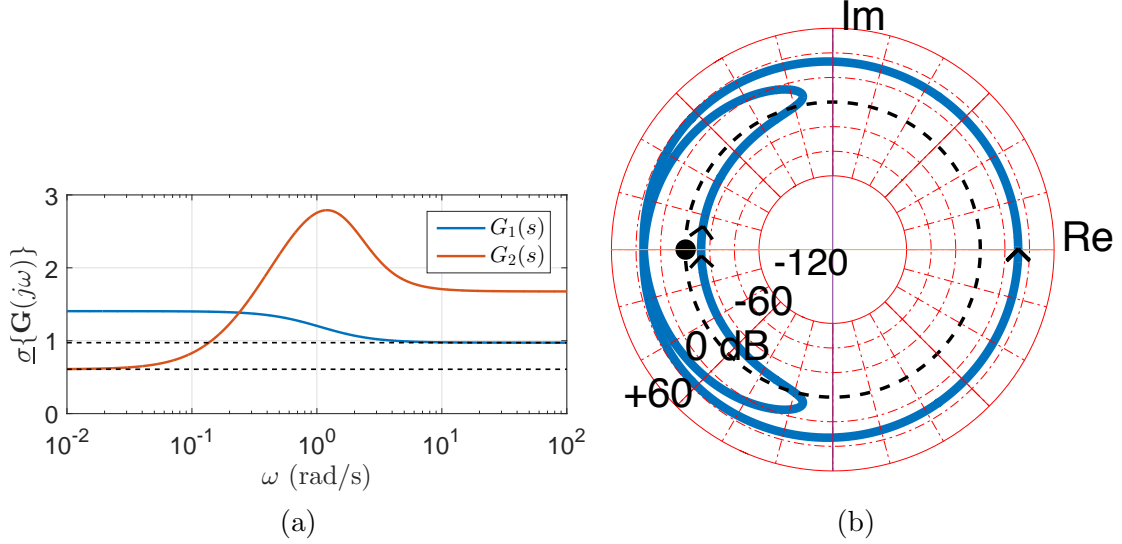


Figure 7.3: (a) Plots of the minimum singular value of $\mathbf{G}_1(s)$ and $\mathbf{G}_2(s)$ versus frequency with $k = 0.45$ in Example 7.13. Black dashed lines represent $\nu^* = \inf_{\omega \in \mathbb{R}^+} \underline{\sigma}\{\mathbf{G}(j\omega)\}$ of each system. (b) Nyquist plots of $-1 + \det(\mathbf{1} + \mathbf{L}(s))$ for Example 7.13 with $k = 0.45$. The Nyquist plots are generated on a logarithmic scale, where the gridlines are red, except for the 0 dB gridline, which is a black dashed line [84]. The point $(-1, 0)$ is labeled by a black circular marker.

gains of $\nu_{L_1}^* = 2.47$ and $\nu_{L_2}^* = 2.14$, respectively, and $\nu_L = 2.47$. Using Theorem 7.6 or Theorem 7.8, the feedback system has a lower gain margin of 7.85 dB. The open-loop transfer matrices $\mathbf{L}_1(s)$ and $\mathbf{L}_2(s)$ have one CRHP pole and their Nyquist plot, shown in Figure 7.2b, has one CCW encirclement of $(-1, 0)$. Closed-loop asymptotic stability is guaranteed by the MIMO Nyquist stability criterion, since the number of CCW encirclements of the point $(-1, 0)$ is equal to $\bar{\eta}(\mathbf{L}_1(s)) = \bar{\eta}(\mathbf{L}_2(s))$. In this example, closed-loop input-output stability is not guaranteed by the Small Gain Theorem, since $\mathbf{G}_1(s)$ is unstable. This highlights the usefulness of the Large Gain Theorem in assessing closed-loop stability when the open-loop system is unstable or has a large \mathcal{H}_∞ norm.

Example 7.13. Consider the MIMO transfer matrices in (7.11) and (7.12), where $k = 0.45$. Plots of the minimum singular values of $\mathbf{G}_1(s)$ and $\mathbf{G}_2(s)$ are shown in Figure 7.3a. It can be seen in Figure 7.3a that $\mathbf{G}_1(s)$ has a least conservative minimum gain of $\nu_1^* = 0.97$, while $\mathbf{G}_2(s)$ has a least conservative minimum gain of $\nu_2^* = 0.61$.

The feedback system shown in Figure 6.1, with \mathcal{G}_1 replaced by $\mathbf{G}_1(s)$ and \mathcal{G}_2 replaced by $\mathbf{G}_2(s)$, cannot be proven asymptotically stable by Theorem 7.4, since $\nu_1^* \nu_2^* = 0.59$. The loop transfer matrices $\mathbf{L}_1(s)$ and $\mathbf{L}_2(s)$ have least conservative

minimum gains of $\nu_{L_1}^* = 1.11$ and $\nu_{L_2}^* = 0.97$, respectively, yielding $\nu_L = 1.11$. From this, it can be concluded using Theorem 7.6 that the closed-loop system is asymptotically stable with a lower gain margin of 0.92 dB. This highlights the importance of using $\nu_L = \max(\nu_{L_1}^*, \nu_{L_2}^*)$ rather than $\nu_{L_1}^*$ or $\nu_{L_2}^*$ individually, as no assessment of stability can be made using Theorem 7.6 solely using minimum gain of $\mathbf{L}_2(s)$. Closed-loop asymptotic stability with a lower gain margin of 0.92 dB is also concluded from Theorem 7.8. Both open-loop transfer matrices $\mathbf{L}_1(s)$ and $\mathbf{L}_2(s)$ have two CRHP poles and their Nyquist plot, shown in Figure 7.3b, have two CCW encirclements of $(-1, 0)$. Closed-loop asymptotic stability is guaranteed by the MIMO Nyquist stability criterion, since the number of CCW encirclements of the point $(-1, 0)$ is equal to $\bar{\eta}(\mathbf{L}_1(s)) = \bar{\eta}(\mathbf{L}_2(s))$.

Example 7.14. Consider the MIMO transfer matrices

$$\mathbf{G}_3(s) = \begin{bmatrix} \frac{s-1}{s+5} & 1 \end{bmatrix}, \quad \mathbf{G}_4(s) = \begin{bmatrix} 1 \\ \frac{s+7}{s+5} \end{bmatrix},$$

where

$$L_3(s) = \mathbf{G}_3(s)\mathbf{G}_4(s) = \frac{2s+6}{s+5}, \quad \mathbf{L}_4(s) = \mathbf{G}_4(s)\mathbf{G}_3(s) = \begin{bmatrix} \frac{s-1}{s+5} & 1 \\ \frac{s^2+6s-7}{s^2+10s+25} & \frac{s+7}{s+5} \end{bmatrix}.$$

The minimum gains of $\mathbf{G}_3(s)$ and $\mathbf{L}_4(s)$ are $\nu_3 = \nu_{L_4} = 0$, and the least conservative minimum gains of $\mathbf{G}_4(s)$ and $L_3(s)$ are $\nu_4^* = 7/5$ and $\nu_{L_3}^* = 6/5$, respectively. The feedback system shown in Figure 6.1, with \mathcal{G}_1 replaced by $\mathbf{G}_3(s)$ and \mathcal{G}_2 replaced by $\mathbf{G}_4(s)$, is not proven to be asymptotically stable by Theorem 7.4, since $\nu_3 = 0$. However, asymptotic stability of the feedback interconnection is guaranteed by Theorem 7.6 and Theorem 7.8, since $1 < \nu_L < \infty$ with $\nu_L = \nu_{L_3}^* = 6/5$ and $L_3(s)$ has only a minimum phase zero. The feedback system has a lower gain margin of 1.58 dB. This example illustrates the benefit of examining the minimum gain of $L_3(s)$ in Theorem 7.6 and Theorem 7.8, rather than using the minimum gain of $\mathbf{G}_3(s)$ and $\mathbf{G}_4(s)$ separately with Theorem 7.4.

7.4.2 Robust Stabilization Example

Example 7.15. Consider the robust stabilization of the uncertain LTI SISO system

$$G_p(s) = \frac{y(s)}{u(s)} = \frac{\delta s^2 + (1 + \delta + \delta b)s + (\delta - 1)b}{(s+1)(s-b)},$$

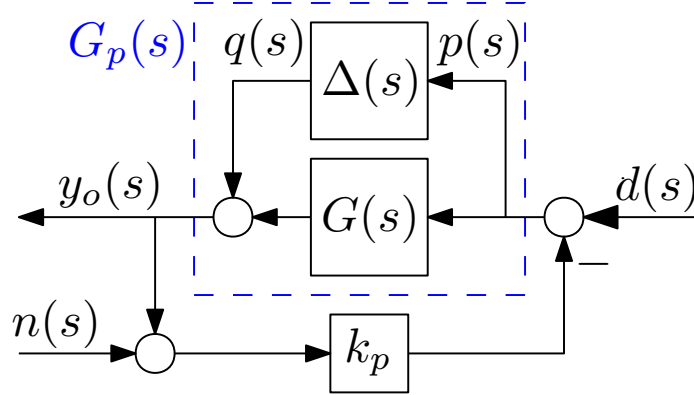


Figure 7.4: Block diagram of the system considered in the robust control Example 7.15.

where $1 < |\delta| < \infty$ and $0 < b < \infty$. The system can be described by the nominal model $G(s) = \frac{1}{s+1}$ and the uncertainty block $\Delta(s) = \delta \frac{s+b}{s-b}$, where $1 < |\Delta(s)| < \infty$ ($1 < \nu_\Delta < \infty$) and $G_p(s) = G(s) + \Delta(s)$. A proportional controller of the form $u(s) = -k_p y(s)$, where $0 < k_p < \infty$, is designed to robustly stabilize the unstable open-loop system. A block diagram of the system architecture is shown in Figure 7.4. In this example, the exogenous signals are $\mathbf{w}^\top(s) = \begin{bmatrix} d(s) & n(s) \end{bmatrix}$ and the performance signal is $z(s) = y_o(s)$. Although more sophisticated controllers could be considered, a proportional controller is chosen for simplicity.

Combining the feedback controller with the nominal plant model yields the block diagrams in Figure 7.5. The resulting nominal closed-loop transfer function from $p(s)$ to $q(s)$ is $G_{\text{CL}qp}(s) = -k_p \frac{s+1}{s+1+k_p}$, which can be shown to have minimum gain $1 < \nu_{\text{CL}qp} < \infty$ if $1 < k_p < \infty$. Robust stabilization is guaranteed by the Large Gain Theorem, as $1 < \nu_\Delta \nu_{\text{CL}qp} < \infty$. The Nyquist plot of $L(s) = G_{\text{CL}qp}(s)\Delta(s)$ is presented in Figure 7.6 for $k_p = 2$, $\delta = 1.1$, and $k = 5$ rad/s. The Nyquist plot of $L(s)$ satisfies the Nyquist stability criterion by encircling the point $(-1, 0)$ exactly $\bar{\eta}(\mathbf{L}(s)) = 1$ times in the CCW direction. It can be shown that the nominal closed-loop transfer functions from the exogenous inputs $d(s)$ and $n(s)$ to the output $y_o(s)$ are given by $G_{\text{CL}y_o d}(s) = \frac{1}{s+1+k_p}$ and $G_{\text{CL}y_o n}(s) = \frac{k_p}{s+1+k_p}$, respectively. Both $G_{\text{CL}y_o d}(s)$ and $G_{\text{CL}y_o n}(s)$ are strictly proper, which means they have zero minimum gain, underlining the fact that there is no minimum gain constraint on the performance channel.

This example provided a simple demonstration of the use of the Large Gain Theorem for robust stabilization. An in-depth treatment of robust stabilization with the Large Gain Theorem is found in Chapter 8, which also discusses the use of the Large Gain Theorem for nominal performance and robust performance problems. The

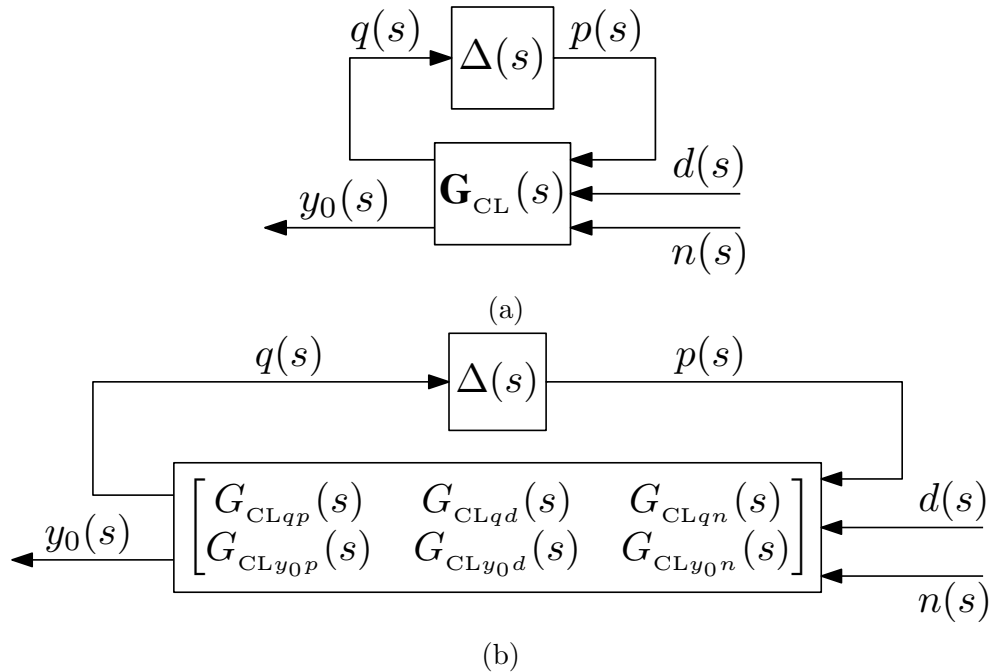


Figure 7.5: Block diagrams used in Example 7.15 of (a) the nominal closed-loop system in a feedback interconnection with the uncertainty $\Delta(s)$ and (b) the nominal closed-loop system in a feedback interconnection with the uncertainty $\Delta(s)$, where the contents of the transfer matrix $\mathbf{G}_{CL}(s)$ have been expanded.

synthesis of feedback controllers for robust stabilization, nominal performance, and robust performance with the Large Gain Theorem is the topic of Chapter 9.

7.5 Closing Remarks

This chapter presented an overview of the Large Gain Theorem, including LTI stability theorems with proofs using the familiar Nyquist stability criterion, a Nyquist comparison to the Small Gain Theorem, and numerical examples. It was shown that the MIMO Nyquist plot of an LTI system satisfying the Large Gain Theorem lies strictly outside a circle of unit radius centered at the origin and is guaranteed to make the correct number of encirclements of the point $(-1, 0)$ due to the fact that the loop transfer matrix is minimum phase.

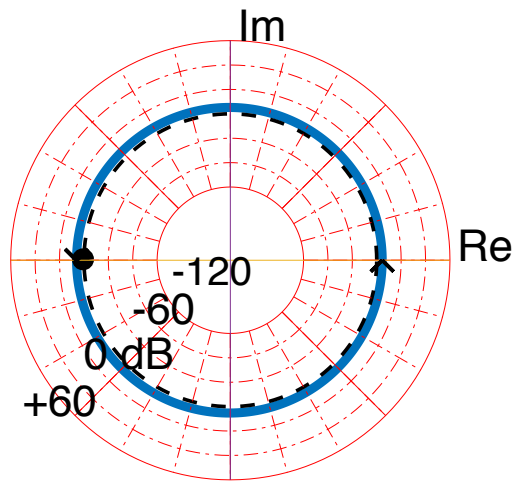


Figure 7.6: Nyquist plot of the transfer function $L(s) = G_{CLqp}(s)\Delta(s)$ in Example 7.15, where $k_p = 2$, $\delta = 1.1$ and $b = 5$ rad/s. Notice that the Nyquist plot encircles the point $(-1, 0)$ once in the CCW direction, which corresponds to the number of CRHP poles of $L(s)$. The Nyquist plots are generated on a logarithmic scale, where the gridlines are red, except for the 0 dB gridline, which is a black dashed line [84]. The point $(-1, 0)$ is labeled by a black circular marker.

Chapter 8

Robust Control with the Large Gain Theorem

8.1 Introduction

The presence of plant uncertainty is an unavoidable issue that must be considered in the design of robust feedback controllers. Mathematical models never perfectly capture the dynamics of a given system, which leads to inevitable plant uncertainty. Controllers must be designed with this uncertainty in mind in order to guarantee the robust stability and/or robust performance of the closed-loop system. An array of stability theorems and robust control techniques are available to design robust controllers, and the choice of a suitable technique will depend heavily on the nature of the uncertainty being considered. For example, if the gain of the uncertainty model has a sufficiently small upper bound, then the Small Gain Theorem and robust \mathcal{H}_∞ control will most likely yield satisfactory results [39, 49, 85, 86]. Other classes of uncertainty, such as polytopic [87–90] or polynomial [91, 92] uncertainty have robust controller synthesis methods specifically tailored for them. One particular class of uncertainty that lacks a suitable robust control technique, is the case where the uncertainty model has a nonzero lower bound on its gain and possibly a very large upper bound on its gain. For this class of uncertainty, robust controllers designed using the Small Gain Theorem may be overly conservative. Moreover, if the uncertainty model is itself unstable, then the Small Gain Theorem is not applicable at all. This issue can sometimes be overcome by reformulating the problem with a modification or conversion of the uncertainty model into an alternative form [85, pp. 51–81], [86, p. 315], but this may lead to complications or a loss of physical meaning.

The Large Gain Theorem, introduced in [8] and extended in [9], is an input-output stability theorem that can directly accommodate a feedback interconnection involving unstable systems using the notion of minimum gain. The implications of this theorem include the ability to design robust controllers for systems that previously led to unnecessary conservatism when robustly stabilized, could not be robustly stabilized, or required significant manipulation and reformulation in order to realize robust stabilization. The Large Gain Theorem and the Small Gain Theorem provide guarantees of robust input-output stability using different information about the uncertainty, which in some situations allows for controllers designed with the Large Gain Theorem to outperform controllers designed with the Small Gain Theorem. Preliminary robust feedforward controller designs using the Large Gain Theorem are found in [11, 12] for specific classes of nonlinear systems.

This chapter presents the framework in which the Large Gain Theorem can be used for the robust control of systems whose uncertainty has nonzero minimum gain, specifically to solve robust stabilization, nominal performance, and robust performance problems. In particular, it is shown that a robust stability problem posed using the Large Gain Theorem is equivalent to a robust stabilization problem using the Small Gain Theorem, the notion of nominal performance when the uncertainty has nonzero minimum gain is introduced, and a novel concept of robust performance is defined when using the Large Gain Theorem. A structured singular value for robust stabilization with structured uncertainty that has nonzero minimum gain is discussed as well. The novelty of performing robust control with the Large Gain Theorem lies in the fact that it can robustly stabilize systems subject to uncertainty that has large gain and may even be itself unstable. This is not an entirely new concept, as topological results do exist in the literature that can be exploited to design controllers that robustly stabilize systems with unstable uncertainty [83, 93–95]. However, the robust control framework presented in this chapter accomplishes this using a more systematic approach that directly parallels \mathcal{H}_∞ control and the Small Gain Theorem.

The remaining sections of this chapter proceed as follows. Section 8.2 presents the notion of robust stabilization using the Large Gain Theorem and how it is equivalent to robust stabilization using the Small Gain Theorem. The nominal performance problem within a Large Gain Theorem framework is included in Section 8.3. Section 8.4 introduces a new type of robust performance based on the Large Gain Theorem, while summarizing remarks are given in Section 8.5.

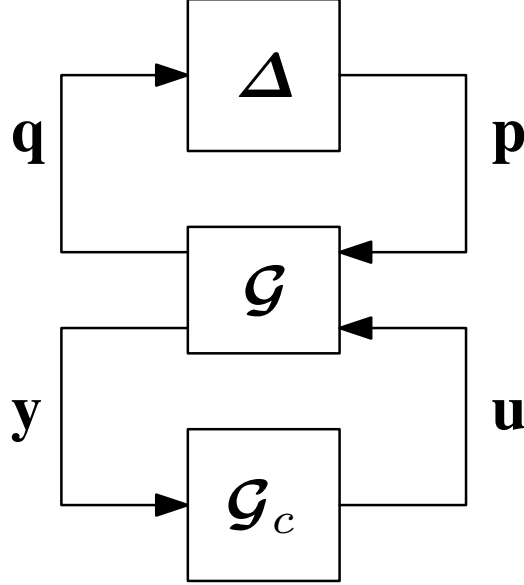


Figure 8.1: Feedback interconnection involving the nominal plant \mathcal{G} , the controller \mathcal{G}_c , and the uncertainty Δ .

8.2 Robust Stabilization

Consider the block diagram in Figure 8.1, which involves feedback interconnections of a nominal plant $\mathcal{G} : \mathcal{L}_{2e} \rightarrow \mathcal{L}_{2e}$, an uncertainty block $\Delta : \mathcal{L}_{2e} \rightarrow \mathcal{L}_{2e}$, and a controller $\mathcal{G}_c : \mathcal{L}_{2e} \rightarrow \mathcal{L}_{2e}$. The objective of robust stabilization is to design a controller \mathcal{G}_c such that the closed-loop system is input-output stable for all $\Delta \in S_u$, where S_u is the set of all possible uncertainties. In this chapter, either the Small Gain Theorem or the Large Gain Theorem is used to guarantee robust input-output stability, which restricts the set of uncertainty considered to

$$S_u : \{\Delta : \mathcal{L}_{2e} \rightarrow \mathcal{L}_{2e} \mid \|\Delta\|_\infty \leq \gamma_\Delta, \gamma_\Delta \in \mathbb{R}_{>0}\},$$

or

$$S_u : \{\Delta : \mathcal{L}_{2e} \rightarrow \mathcal{L}_{2e} \mid \Delta \text{ has minimum gain } \nu_\Delta, \nu_\Delta \in \mathbb{R}_{>0}\}.$$

In order to invoke either the Small Gain Theorem or Large Gain Theorem, it is convenient to combine the nominal plant with the controller to yield $\mathcal{G}_{\text{CLQP}} : \mathcal{L}_{2e} \rightarrow \mathcal{L}_{2e}$, as shown in the block diagram of Figure 8.2.

It is often the case that the nominal plant and the controller are LTI systems. In this situation, the nominal plant $\mathbf{G} : \mathcal{L}_{2e} \rightarrow \mathcal{L}_{2e}$ is represented by a minimal

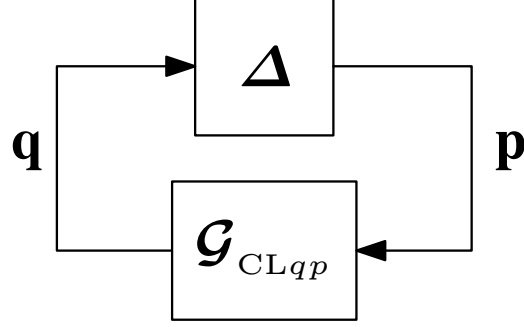


Figure 8.2: Feedback interconnection involving the nominal closed-loop system \mathcal{G}_{CLqp} and the uncertainty Δ .

state-space realization

$$\dot{\mathbf{x}}(t) = \mathbf{A}\mathbf{x}(t) + \mathbf{B}_2\mathbf{u}(t) + \mathbf{B}_3\mathbf{p}(t), \quad (8.1)$$

$$\mathbf{y}(t) = \mathbf{C}_2\mathbf{x}(t) + \mathbf{D}_{22}\mathbf{u}(t) + \mathbf{D}_{23}\mathbf{p}(t), \quad (8.2)$$

$$\mathbf{q}(t) = \mathbf{C}_3\mathbf{x}(t) + \mathbf{D}_{32}\mathbf{u}(t) + \mathbf{D}_{33}\mathbf{p}(t), \quad (8.3)$$

and the controller $\mathbf{G}_c : \mathcal{L}_{2e} \rightarrow \mathcal{L}_{2e}$ is represented by a minimal state-space realization

$$\dot{\mathbf{x}}_c(t) = \mathbf{A}_c\mathbf{x}_c(t) + \mathbf{B}_c\mathbf{u}_c(t),$$

$$\mathbf{y}_c(t) = \mathbf{C}_c\mathbf{x}_c(t) + \mathbf{D}_c\mathbf{u}_c(t).$$

The nominal closed-loop system $\mathbf{G}_{CLqp} : \mathcal{L}_{2e} \rightarrow \mathcal{L}_{2e}$ is then represented by a state-space realization

$$\dot{\mathbf{x}}_{CL}(t) = \mathbf{A}_{CL}\mathbf{x}_{CL}(t) + \mathbf{B}_{CL3}\mathbf{p}(t),$$

$$\mathbf{q}(t) = \mathbf{C}_{CL3}\mathbf{x}_{CL}(t) + \mathbf{D}_{CL33}\mathbf{p}(t),$$

where $\mathbf{x}_{CL}^\top(t) = \begin{bmatrix} \mathbf{x}^\top(t) & \mathbf{x}_c^\top(t) \end{bmatrix}$,

$$\mathbf{A}_{CL} = \begin{bmatrix} \mathbf{A} + \mathbf{B}_2\mathbf{D}_c\tilde{\mathbf{D}}^{-1}\mathbf{C}_2 & \mathbf{B}_2 \left(\mathbf{1} + \mathbf{D}_c\tilde{\mathbf{D}}^{-1}\mathbf{D}_{22} \right) \mathbf{C}_c \\ \mathbf{B}_c\tilde{\mathbf{D}}^{-1}\mathbf{C}_2 & \mathbf{A}_c + \mathbf{B}_c\tilde{\mathbf{D}}^{-1}\mathbf{D}_{22}\mathbf{C}_c \end{bmatrix}, \quad (8.4)$$

$$\mathbf{B}_{CL3} = \begin{bmatrix} \mathbf{B}_3 + \mathbf{B}_2\mathbf{D}_c\tilde{\mathbf{D}}^{-1}\mathbf{D}_{23} \\ \mathbf{B}_c\tilde{\mathbf{D}}^{-1}\mathbf{D}_{23} \end{bmatrix}, \quad (8.5)$$

$$\mathbf{C}_{CL3} = \begin{bmatrix} \mathbf{C}_3 + \mathbf{D}_{32}\mathbf{D}_c\tilde{\mathbf{D}}^{-1}\mathbf{C}_2 & \mathbf{D}_{32} \left(\mathbf{1} + \mathbf{D}_c\tilde{\mathbf{D}}^{-1}\mathbf{D}_{22} \right) \mathbf{C}_c \end{bmatrix}, \quad (8.6)$$

$$\mathbf{D}_{CL33} = \mathbf{D}_{33} + \mathbf{D}_{32}\mathbf{D}_c\tilde{\mathbf{D}}^{-1}\mathbf{D}_{23}, \quad (8.7)$$

and $\tilde{\mathbf{D}} = \mathbf{1} - \mathbf{D}_{22}\mathbf{D}_c$. For the case when $\mathbf{D}_{22} = \mathbf{0}$, the closed-loop state-space matrices simplify to

$$\begin{aligned}\mathbf{A}_{\text{CL}} &= \begin{bmatrix} \mathbf{A} + \mathbf{B}_2\mathbf{D}_c\mathbf{C}_2 & \mathbf{B}_2\mathbf{C}_c \\ \mathbf{B}_c\mathbf{C}_2 & \mathbf{A}_c \end{bmatrix}, \\ \mathbf{B}_{\text{CL}3} &= \begin{bmatrix} \mathbf{B}_3 + \mathbf{B}_2\mathbf{D}_c\mathbf{D}_{23} \\ \mathbf{B}_c\mathbf{D}_{23} \end{bmatrix}, \\ \mathbf{C}_{\text{CL}3} &= \begin{bmatrix} \mathbf{C}_3 + \mathbf{D}_{32}\mathbf{D}_c\mathbf{C}_2 & \mathbf{D}_{32}\mathbf{C}_c \end{bmatrix}, \\ \mathbf{D}_{\text{CL}33} &= \mathbf{D}_{33} + \mathbf{D}_{32}\mathbf{D}_c\mathbf{D}_{23}.\end{aligned}$$

The closed-loop transfer matrix from $\mathbf{p}(s)$ to $\mathbf{q}(s)$ is $\mathbf{G}_{\text{CL}qp}(s) = \mathbf{C}_{\text{CL}3}(s\mathbf{1} - \mathbf{A}_{\text{CL}})\mathbf{B}_{\text{CL}3} + \mathbf{D}_{\text{CL}33}$, which is the transfer matrix of interest when performing robust stabilization.

The following sections present the conditions for robust stabilization using the Small Gain Theorem and the Large Gain Theorem, as well as the equivalence between the two stability results.

8.2.1 Robust Stabilization with the Small Gain Theorem and the Structured Singular Value

Assume that the uncertainty $\mathbf{\Delta}$ has gain that is upper bounded by $0 < \gamma_{\Delta} < \infty$. In this case, robust input-output stability of the closed-loop system is guaranteed by the Small Gain Theorem provided that an upper bound on the gain of $\mathcal{G}_{\text{CL}qp}$, given by $\gamma_{\text{CL}qp}$, satisfies $0 < \gamma_{\Delta}\gamma_{\text{CL}qp} < 1$. When the nominal plant and the controller are LTI systems, this is equivalent to the \mathcal{H}_{∞} norm of $\mathbf{G}_{\text{CL}qp}(s)$, given by $\gamma_{\text{CL}qp}$, satisfying $0 < \gamma_{\Delta}\gamma_{\text{CL}qp} < 1$. An \mathcal{H}_{∞} robust LTI controller can be synthesized using a number of state-space techniques [49, 96, 97] to satisfy the Small Gain Theorem and robustly stabilize the closed-loop system.

The Small Gain Theorem is well-suited for unstructured uncertainty, which is uncertainty that may be a fully populated matrix when $\mathbf{\Delta}$ is MIMO. However, when $\mathbf{\Delta}$ has a block-diagonal structure, the Small Gain Theorem is a conservative robust input-output stability condition, which may artificially limit the set of uncertainty for which the closed-loop system is robustly input-output stable or yield an incorrect conclusion that the closed-loop system is not robustly input-output stable. When the uncertainty block has structure and is represented by a complex diagonal matrix $\mathbf{\Delta}_s(s)$, the structured singular value [98–100] can be used to obtain a non-conservative robust stability condition.

The concept of the structured singular value is a generalization of the Small Gain Theorem robust stability condition for an LTI $\mathbf{G}_{\text{CL}qp}(s)$ and complex unstructured $\mathbf{\Delta}(s)$, which states that assuming $\mathbf{G}_{\text{CL}qp}(s)$ and $\mathbf{\Delta}(s)$ are asymptotically stable transfer matrices, the closed-loop system is asymptotically stable for all $\mathbf{\Delta}(s)$ satisfying $\|\mathbf{\Delta}\|_\infty \leq \gamma_\Delta$ if and only if $\bar{\sigma}\{\mathbf{G}_{\text{CL}qp}(j\omega)\} < 1/\gamma_\Delta, \forall \omega \in \mathbb{R}$ [7, p. 303]. To quantify the smallest destabilizing structured complex $\mathbf{\Delta}_s(s)$, the structured singular value of the transfer matrix $\mathbf{M}(s)$ with respect to the structured complex perturbation $\mathbf{\Delta}_s(s)$, evaluated at $s_0 \in \mathbb{C}$ is defined as

$$\mu_{\Delta_s}\{\mathbf{M}(s_0)\} = [\min\{\bar{\sigma}\{\mathbf{\Delta}_s(s_0)\} : \det(\mathbf{1} - \mathbf{M}(s_0)\mathbf{\Delta}_s(s_0)) = 0, \mathbf{\Delta}_s(s_0) \text{ structured}\}]^{-1}.$$

A generalized Small Gain Theorem using the structured singular value states that assuming $\mathbf{G}_{\text{CL}qp}(s)$ and $\mathbf{\Delta}_s(s)$ are asymptotically stable transfer matrices, the closed-loop system is asymptotically stable for all $\mathbf{\Delta}_s(s)$ satisfying $\|\mathbf{\Delta}_s\|_\infty \leq \gamma_\Delta$ if and only if $\mu_{\Delta_s}\{\mathbf{G}_{\text{CL}qp}(j\omega)\} < 1/\gamma_\Delta, \forall \omega \in \mathbb{R}$ [7, p. 314]. This stability condition can be used to synthesize robust controllers with little conservatism using a synthesis method known as *DK*-iteration or μ -synthesis [101, 102].

8.2.2 Robust Stabilization with the Large Gain Theorem and the Structured Minimum Singular Value

Assume that the uncertainty $\mathbf{\Delta}$ is square and has gain that is lower bounded by $0 < \nu_\Delta < \infty$. In this case, robust input-output stability of the closed-loop system is guaranteed by the Large Gain Theorem provided that a minimum gain of $\mathcal{G}_{\text{CL}qp}$, given by $\nu_{\text{CL}qp}$, satisfies $1 < \nu_\Delta \nu_{\text{CL}qp} < \infty$. When the nominal plant and the controller are LTI systems, this is equivalent to a minimum gain of $\mathbf{G}_{\text{CL}qp}(s)$, given by $\nu_{\text{CL}qp}$, satisfying $1 < \nu_\Delta \nu_{\text{CL}qp} < \infty$. The synthesis of a robustly stabilizing LTI controller using the Large Gain Theorem is presented in Section 9.4.1 of Chapter 9. The requirement that $\mathbf{\Delta}$ be square comes from the need for $\mathbf{\Delta}$ and $\mathcal{G}_{\text{CL}qp}$ to both have nonzero minimum gain. A system whose output has dimension greater than the dimension of its input has a minimum gain of zero, so in order to prevent this case and for $\mathbf{\Delta}$ and $\mathcal{G}_{\text{CL}qp}$ to have compatible dimensions it is required that they be square. Additionally, in order for the transfer matrix $\mathbf{G}_{\text{CL}qp}(s)$ to have nonzero minimum gain that potentially satisfies $1 < \nu_\Delta \nu_{\text{CL}qp} < \infty$ it is required that $\mathbf{D}_{\text{CL}33}$ be invertible.

Theorem 8.1. *Assuming that $\mathbf{\Delta}$ and $\mathbf{D}_{\text{CL}33}$ are square and invertible, robust stabilization using the Large Gain Theorem is equivalent to robust stabilization using the Small Gain Theorem with uncertainty of $\bar{\mathbf{\Delta}} = \mathbf{\Delta}^{-1}$ and a nominal closed-loop system*

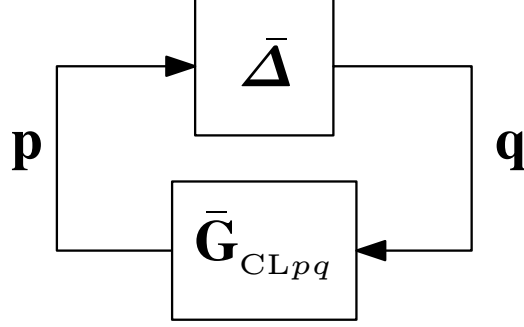


Figure 8.3: Feedback interconnection involving the inverted nominal closed-loop system $\bar{\mathbf{G}}_{\text{CL}pq} = \mathbf{G}_{\text{CL}qp}^{-1}$ and the uncertainty $\bar{\Delta} = \Delta^{-1}$.

$\bar{\mathbf{G}}_{\text{CL}pq} = \mathbf{G}_{\text{CL}qp}^{-1}$, as shown in Figure 8.3. The inverted system $\bar{\mathbf{G}}_{\text{CL}pq}$ has a state-space realization

$$\begin{aligned}\dot{\mathbf{x}}_{\text{CL}}(t) &= \bar{\mathbf{A}}_{\text{CL}} \mathbf{x}_{\text{CL}}(t) + \bar{\mathbf{B}}_{\text{CL}3} \mathbf{q}(t), \\ \mathbf{p}(t) &= \bar{\mathbf{C}}_{\text{CL}3} \mathbf{x}_{\text{CL}}(t) + \bar{\mathbf{D}}_{\text{CL}33} \mathbf{q}(t),\end{aligned}$$

where

$$\begin{aligned}\bar{\mathbf{A}}_{\text{CL}} &= \mathbf{A}_{\text{CL}} - \mathbf{B}_{\text{CL}3} \mathbf{D}_{\text{CL}33}^{-1} \mathbf{C}_{\text{CL}3}, \\ \bar{\mathbf{B}}_{\text{CL}3} &= \mathbf{B}_{\text{CL}3} \mathbf{D}_{\text{CL}33}^{-1}, \\ \bar{\mathbf{C}}_{\text{CL}3} &= -\mathbf{D}_{\text{CL}33}^{-1} \mathbf{C}_{\text{CL}3}, \\ \bar{\mathbf{D}}_{\text{CL}33} &= \mathbf{D}_{\text{CL}33}^{-1}.\end{aligned}$$

Proof. The uncertainty is inverted to obtain $\mathbf{q} = \bar{\Delta} \mathbf{p}$. This changes the plant's robustness input channel to \mathbf{q} and the robustness output channel to \mathbf{p} . The system $\mathbf{G}_{\text{CL}pq}$ is inverted using Lemma 2.38 to obtain $\mathbf{p} = \bar{\mathbf{G}}_{\text{CL}pq} \mathbf{q}$. From Lemma 3.3, it is known that the \mathcal{H}_∞ norm of $\bar{\Delta}$ is $\gamma_{\bar{\Delta}} = \nu_{\Delta}^{*-1}$ and the \mathcal{H}_∞ norm of $\bar{\mathbf{G}}_{\text{CL}pq}$ is $\gamma_{\text{CL}\bar{p}\bar{q}} = \nu_{\text{CL}qp}^{*-1}$, where ν_{Δ}^* and $\nu_{\text{CL}qp}^*$ are the least conservative minimum gains of Δ and $\mathbf{G}_{\text{CL}qp}$, respectively. If the original feedback interconnection of Δ and $\mathbf{G}_{\text{CL}qp}$ satisfies the Large Gain Theorem with $1 < \nu_{\Delta}^* \nu_{\text{CL}qp}^* < \infty$, then equivalently $1 < \gamma_{\bar{\Delta}}^{-1} \gamma_{\text{CL}\bar{p}\bar{q}}^{-1} < \infty$. Inverting this expression yields $0 < \gamma_{\bar{\Delta}} \gamma_{\text{CL}\bar{p}\bar{q}} < 1$, which is the input-output robust stability condition of the Small Gain Theorem involving the feedback interconnection of $\bar{\Delta}$ and $\bar{\mathbf{G}}_{\text{CL}pq}$. It can be analogously proven that if the feedback interconnection of Δ and $\mathbf{G}_{\text{CL}qp}$ satisfies the Small Gain Theorem then the feedback interconnection of $\bar{\Delta}$ and $\bar{\mathbf{G}}_{\text{CL}pq}$ satisfies the Large Gain Theorem. \square

Remark 8.2. The system inversion detailed in Theorem 8.1 can be performed prior to controller synthesis. Inverting the open-loop state-space equations in (8.1), (8.2), and (8.3) gives

$$\dot{\mathbf{x}}(t) = (\mathbf{A} - \mathbf{B}_3 \mathbf{D}_{33}^{-1} \mathbf{C}_3) \mathbf{x}(t) + (\mathbf{B}_2 - \mathbf{B}_3 \mathbf{D}_{33}^{-1} \mathbf{D}_{32}) \mathbf{u}(t) + \mathbf{B}_3 \mathbf{D}_{33}^{-1} \mathbf{q}(t), \quad (8.8)$$

$$\mathbf{y}(t) = (\mathbf{C}_2 - \mathbf{D}_{23} \mathbf{D}_{33}^{-1} \mathbf{C}_3) \mathbf{x}(t) + (\mathbf{D}_{22} - \mathbf{D}_{23} \mathbf{D}_{33}^{-1} \mathbf{D}_{32}) \mathbf{u}(t) + \mathbf{D}_{23} \mathbf{D}_{33}^{-1} \mathbf{q}(t), \quad (8.9)$$

$$\mathbf{p}(t) = -\mathbf{D}_{33}^{-1} \mathbf{C}_3 \mathbf{x}(t) - \mathbf{D}_{33}^{-1} \mathbf{D}_{32} \mathbf{u}(t) + \mathbf{D}_{33}^{-1} \mathbf{q}(t), \quad (8.10)$$

The state-space equations in (8.8), (8.9), and (8.10) can be used to convert between robust controller synthesis using the Large Gain Theorem and the Small Gain Theorem. It is interesting to note that even if $\mathbf{D}_{22} = \mathbf{0}$, the inverted open-loop system may have a nonzero feedthrough matrix from $\mathbf{u}(s)$ to $\mathbf{y}(s)$, as shown in (8.9).

Remark 8.3. A controller synthesized such that the feedback interconnection of $\mathbf{\Delta}$ and $\mathcal{G}_{\text{CL}qp}$ satisfies the Small Gain Theorem will also ensure that the feedback interconnection of $\bar{\mathbf{\Delta}}$ and $\bar{\mathcal{G}}_{\text{CL}pq}$ satisfies the Large Gain Theorem provided $\mathbf{\Delta}$ and $\mathcal{G}_{\text{CL}qp}$ are square and invertible, or vice versa. This is because the inversion of the robustness feedback interconnection does not change the definitions of the control input or measurement output channels.

Remark 8.4. As stated in Theorem 8.1, the equivalence between robust stabilization with the Small Gain Theorem and the Large Gain Theorem requires that $\mathbf{D}_{\text{CL}33}$ be invertible. It is very possible that $\mathbf{D}_{\text{CL}33}$ not be invertible, for example, if \mathbf{D}_{33} is non-invertible and $\mathbf{D}_{32} = \mathbf{0}$, $\mathbf{D}_{23} = \mathbf{0}$, or $\mathbf{D}_c = \mathbf{0}$, then $\mathbf{D}_{\text{CL}33}$ will not be invertible. When this case arises, it is still possible to convert a robust stabilization problem with the Small Gain Theorem into a robust stabilization problem with the Large Gain Theorem with the aid of a loop transformation [40, pp. 174–177]. Consider the case when $\mathbf{D}_{33} = \mathbf{0}$, $\mathbf{D}_{32} = \mathbf{0}$, $\mathbf{D}_{23} = \mathbf{0}$, or $\mathbf{D}_c = \mathbf{0}$, which results in $\mathbf{D}_{\text{CL}33} = \mathbf{D}_{33} = \mathbf{0}$. A new invertible feedthrough term $\hat{\mathbf{D}}_{33}$ can be added with a loop transformation, as shown in Figure 8.4, such that $\hat{\mathbf{q}}(t) = \mathbf{q}(t) + \hat{\mathbf{D}}_{33} \mathbf{p}(t) = \mathbf{C}_{\text{CL}3} \mathbf{x}_{\text{CL}}(t) + \hat{\mathbf{D}}_{33} \mathbf{p}(t)$ and the uncertainty block is redefined as $\hat{\mathbf{\Delta}} = \mathbf{\Delta} \cdot \left(\mathbf{1} + \hat{\mathbf{D}}_{33} \cdot \mathbf{\Delta} \right)^{-1}$, which leads to $\mathbf{p} = \hat{\mathbf{\Delta}} \hat{\mathbf{q}}$. The upper bound on the gain of $\hat{\mathbf{\Delta}}$ will most likely be different than the upper bound on the gain of $\mathbf{\Delta}$, but this difference can be minimized by choosing a small, yet invertible $\hat{\mathbf{D}}_{33}$. The system can now be inverted to obtain an equivalent robust stabilization problem with the Large Gain Theorem.

As discussed in Section 8.2.1, the robust input-output stability condition of the Small Gain Theorem is conservative when $\mathbf{\Delta}$ has a block-diagonal structure. The

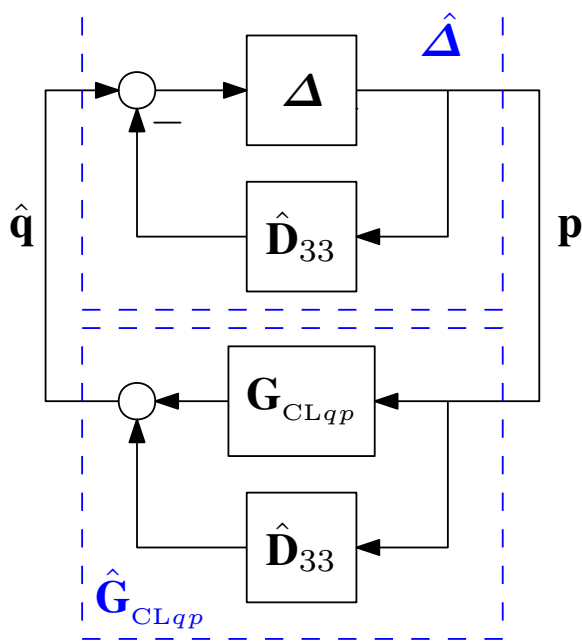


Figure 8.4: Feedback interconnection involving the nominal closed-loop system $\hat{\mathbf{G}}_{\text{CL}qp}$ and the uncertainty $\hat{\Delta}$, where a loop transformation with $\hat{\mathbf{D}}_{33}$ has been performed.

same concept applies when using the Large Gain Theorem for robust stability with a structured Δ that has nonzero minimum gain. In order to eliminate this conservatism, a new structured singular value suitable for structured Δ with nonzero minimum gain is to be defined. To this end, the structured minimum singular value, $\underline{\mu}$, is defined for LTI systems subject to complex structured uncertainty as follows.

Definition 8.5 (Structured Minimum Singular Value). The structured minimum singular value of the transfer matrix $\mathbf{M}(s)$ with respect to the structured complex perturbation $\Delta_s(s)$, evaluated at $s_0 \in \mathbb{C}$ is defined as

$$\underline{\mu}_{\Delta_s}\{\mathbf{M}(s_0)\} = [\max\{\underline{\sigma}\{\Delta_s(s_0)\} : \det(\mathbf{1} - \mathbf{M}(s_0)\Delta_s(s_0)) = 0, \Delta_s(s_0) \text{ structured}\}]^{-1},$$

which is a measure of the largest destabilizing structured uncertainty.

This definition leads to a non-conservative robust stability condition for structured uncertainty with nonzero minimum gain.

Theorem 8.6 (Robust Stability with Minimum Gain Structured Uncertainty). *Assume that the transfer matrix $\mathbf{G}_{\text{CL}qp}(s)$ is minimum phase. The closed-loop system is asymptotically stable for all Δ_s with minimum gain $0 < \nu_{\Delta_s} < \infty$ if and only if $1/\nu_{\Delta_s} < \underline{\mu}_{\Delta_s}\{\mathbf{G}_{\text{CL}qp}(j\omega)\}$, $\forall \omega \in \mathbb{R}$.*

Proof. Since $\mathbf{G}_{\text{CL}qp}(s)$ and $\mathbf{\Delta}_s(s)$ are square minimum phase transfer matrices, it is known that $\mathbf{G}_{\text{CL}qp}(s)\mathbf{\Delta}_s(s)$ is minimum phase and the Nyquist plot of $-1 + \det(\mathbf{1} - \mathbf{G}_{\text{CL}qp}(s)\mathbf{\Delta}_s(s))$ will circle the origin exactly $\bar{\eta}(\mathbf{G}_{\text{CL}qp}(s)\mathbf{\Delta}_s(s))$ times and the Nyquist plot of $\det(\mathbf{1} - \mathbf{G}_{\text{CL}qp}(s)\mathbf{\Delta}_s(s))$ will circle the point $(1, 0)$ exactly $\bar{\eta}(\mathbf{G}_{\text{CL}qp}(s)\mathbf{\Delta}_s(s))$ times. If $1/\nu_{\Delta_s} < \underline{\mu}_{\Delta_s}\{\mathbf{G}_{\text{CL}qp}(j\omega)\}$ for all frequencies, then $\det(\mathbf{1} - \mathbf{G}_{\text{CL}qp}(s)\mathbf{\Delta}_s(s)) = 0$ for $\mathbf{\Delta}_s$ with minimum gain less than ν_{Δ_s} and the Nyquist plot encircles the origin exactly $\bar{\eta}(\mathbf{G}_{\text{CL}qp}(s)\mathbf{\Delta}_s(s))$ times for all $\mathbf{\Delta}_s$ with minimum ν_{Δ_s} . This satisfies the Nyquist stability criterion and guarantees asymptotic stability of the closed-loop system. \square

Although the concept of the structured minimum singular value and robust stability using the structured minimum singular value are presented in this chapter, the properties of $\underline{\mu}$ and details related to the calculation of $\underline{\mu}$ are not formally developed. As such, the robust controller synthesis methods presented in Chapter 9 are based on the Large Gain Theorem, even in the presence of structured uncertainty. Further work is required to make the structured minimum singular value a practical tool for analysis and controller synthesis.

Remark 8.7. The conditions placed on $\mathbf{\Delta}$ when directly using the Large Gain Theorem to guarantee robust input-output stability are significantly different than those placed on $\mathbf{\Delta}$ when using other stability theorems, such as the Small Gain Theorem. In particular, the nonzero minimum gain constraint on $\mathbf{\Delta}$ ensures that the nominal plant never fully captures the uncertain plant. Although this concept is very different from existing robust control formulations, it does have practical benefits. For example, an accurate model of the plant may have properties that make it difficult to design a robustly stabilizing controller (e.g., nonminimum phase zeros, nonlinearities, unstable modes, etc.). In these cases, the undesirable properties may be lumped into $\mathbf{\Delta}$, thereby purposely perturbing the plant model in order to obtain a nominal model that is easier to use for robust controller synthesis. Another use of $\mathbf{\Delta}$ with nonzero minimum gain is that it can directly accommodate parametric uncertainty with a single-sided bound (i.e., $\nu_\delta < \delta < \infty$ or $-\infty < \delta < -\nu_\delta$).

It is worth noting that $\mathbf{\Delta}$ cannot represent a time delay when using the Large Gain Theorem for robust stability, and therefore does not satisfy the conditions of w -stability [103, 104]. The intuition behind this is the fact that a linear approximation of a time delay is nonminimum phase, and therefore has a minimum gain of zero.

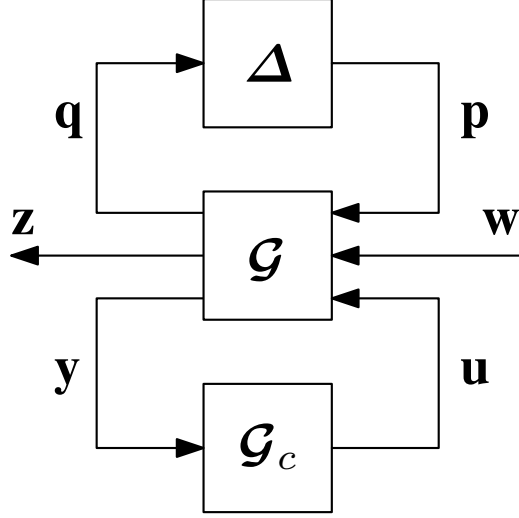


Figure 8.5: Feedback interconnection involving the nominal plant \mathcal{G} , the controller \mathcal{G}_c , and the uncertainty Δ , with the exogenous input signal \mathbf{w} and the performance output signal \mathbf{z} .

8.3 Nominal Performance

When solely performing robust stabilization, there is no measure of closed-loop performance. One method to characterize closed-loop performance is by the nominal performance of the closed-loop system without any uncertainty. To this end, consider a performance output signal of the plant, $\mathbf{z}(t)$, and an exogenous input signal, $\mathbf{w}(t)$, as shown in Figure 8.5. When the nominal plant is an LTI system, it has a minimal state-space realization

$$\dot{\mathbf{x}}(t) = \mathbf{A}\mathbf{x}(t) + \mathbf{B}_1\mathbf{w}(t) + \mathbf{B}_2\mathbf{u}(t) + \mathbf{B}_3\mathbf{p}(t), \quad (8.11)$$

$$\mathbf{z}(t) = \mathbf{C}_1\mathbf{x}(t) + \mathbf{D}_{11}\mathbf{w}(t) + \mathbf{D}_{12}\mathbf{u}(t) + \mathbf{D}_{13}\mathbf{p}(t), \quad (8.12)$$

$$\mathbf{y}(t) = \mathbf{C}_2\mathbf{x}(t) + \mathbf{D}_{21}\mathbf{w}(t) + \mathbf{D}_{22}\mathbf{u}(t) + \mathbf{D}_{23}\mathbf{p}(t), \quad (8.13)$$

$$\mathbf{q}(t) = \mathbf{C}_3\mathbf{x}(t) + \mathbf{D}_{31}\mathbf{w}(t) + \mathbf{D}_{32}\mathbf{u}(t) + \mathbf{D}_{33}\mathbf{p}(t). \quad (8.14)$$

Combining the nominal plant and the controller yields $\mathcal{G}_{\text{CL}} : \mathcal{L}_{2e} \rightarrow \mathcal{L}_{2e}$, as shown in Figure 8.6. A typical statement of nominal performance when Δ has gain upper bounded by $0 < \gamma_\Delta < \infty$ is that $\|\mathcal{G}_{\text{CL}zw}\|_\infty < \gamma_P$ when Δ is zero, where $\mathcal{G}_{\text{CL}zw}$ is the mapping from $\mathbf{w}(t)$ to $\mathbf{z}(t)$. When the nominal plant and the controller are LTI systems, the uncertain system is described by the block diagram in Figure 8.7 and

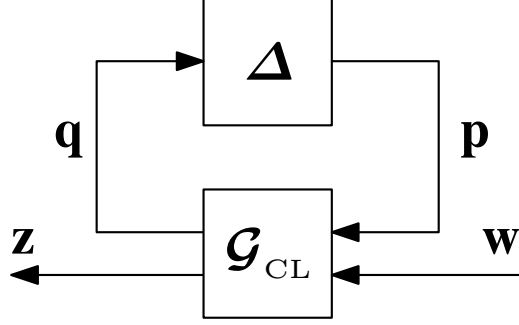


Figure 8.6: Feedback interconnection involving the nominal closed-loop system \mathbf{G}_{CL} and the uncertainty Δ , with the exogenous input signal \mathbf{w} and the performance output signal \mathbf{z} .

the nominal closed-loop system \mathbf{G}_{CL} has a state-space realization

$$\dot{\mathbf{x}}_{CL}(t) = \mathbf{A}_{CL} \mathbf{x}_{CL}(t) + \mathbf{B}_{CL1} \mathbf{w}(t) + \mathbf{B}_{CL3} \mathbf{p}(t), \quad (8.15)$$

$$\mathbf{z}(t) = \mathbf{C}_{CL1} \mathbf{x}_{CL}(t) + \mathbf{D}_{CL11} \mathbf{w}(t) + \mathbf{D}_{CL13} \mathbf{p}(t), \quad (8.16)$$

$$\mathbf{q}(t) = \mathbf{C}_{CL3} \mathbf{x}_{CL}(t) + \mathbf{D}_{CL31} \mathbf{w}(t) + \mathbf{D}_{CL33} \mathbf{p}(t), \quad (8.17)$$

where $\mathbf{C}_{CL1} = \begin{bmatrix} \mathbf{C}_1 + \mathbf{D}_{12} \tilde{\mathbf{D}}^{-1} \mathbf{D}_c \mathbf{C}_2 & \mathbf{D}_{12} \tilde{\mathbf{D}}^{-1} \mathbf{C}_c \end{bmatrix}$, $\mathbf{D}_{CL11} = \mathbf{D}_{11} + \mathbf{D}_{12} \tilde{\mathbf{D}}^{-1} \mathbf{D}_c \mathbf{D}_{21}$, $\mathbf{D}_{CL13} = \mathbf{D}_{13} + \mathbf{D}_{12} \tilde{\mathbf{D}}^{-1} \mathbf{D}_c \mathbf{D}_{23}$, $\mathbf{D}_{CL31} = \mathbf{D}_{31} + \mathbf{D}_{32} \tilde{\mathbf{D}}^{-1} \mathbf{D}_c \mathbf{D}_{21}$,

$$\mathbf{B}_{CL1} = \begin{bmatrix} \mathbf{B}_1 + \mathbf{B}_2 \tilde{\mathbf{D}}^{-1} \mathbf{D}_c \mathbf{D}_{21} \\ \mathbf{B}_c \left(\mathbf{1} + \mathbf{D}_{22} \tilde{\mathbf{D}}^{-1} \mathbf{D}_c \right) \mathbf{D}_{21} \end{bmatrix},$$

and $\mathbf{x}_{CL}(t)$, \mathbf{A}_{CL} , \mathbf{B}_{CL3} , \mathbf{C}_{CL3} , \mathbf{D}_{CL33} , and $\tilde{\mathbf{D}}$ are defined in Section 8.2. For the case with $\mathbf{D}_{22} = \mathbf{0}$, the state-space matrices simplify to $\mathbf{C}_{CL1} = \begin{bmatrix} \mathbf{C}_1 + \mathbf{D}_{12} \mathbf{D}_c \mathbf{C}_2 & \mathbf{D}_{12} \mathbf{C}_c \end{bmatrix}$, $\mathbf{D}_{CL11} = \mathbf{D}_{11} + \mathbf{D}_{12} \mathbf{D}_c \mathbf{D}_{21}$, $\mathbf{D}_{CL13} = \mathbf{D}_{13} + \mathbf{D}_{12} \mathbf{D}_c \mathbf{D}_{23}$, $\mathbf{D}_{CL31} = \mathbf{D}_{31} + \mathbf{D}_{32} \mathbf{D}_c \mathbf{D}_{21}$, and

$$\mathbf{B}_{CL1} = \begin{bmatrix} \mathbf{B}_1 + \mathbf{B}_2 \mathbf{D}_c \mathbf{D}_{21} \\ \mathbf{B}_c \mathbf{D}_{21} \end{bmatrix}.$$

When the uncertainty is zero, the closed-loop transfer matrix from $\mathbf{w}(s)$ to $\mathbf{z}(s)$ is given by $\mathbf{G}_{CLzw}(s) = \mathbf{C}_{CL1} (s\mathbf{1} - \mathbf{A}_{CL})^{-1} \mathbf{B}_{CL1} + \mathbf{D}_{CL11}$, which is typically the transfer matrix considered for nominal performance.

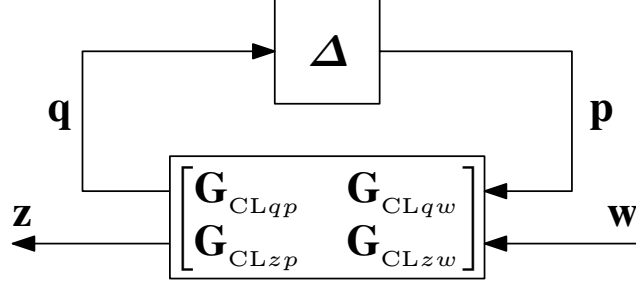


Figure 8.7: Feedback interconnection involving the LTI nominal closed-loop system \mathbf{G}_{CL} and the uncertainty Δ , with the exogenous input signal \mathbf{w} and the performance output signal \mathbf{z} .

8.3.1 Nominal Performance with the Small Gain Theorem

Assume that the uncertainty Δ has gain that is upper bounded by $0 < \gamma_{\Delta} < \infty$. In this case, nominal performance is achieved if $\|\mathcal{G}_{CLzw}\|_{\infty} < \gamma_P$, where $0 < \gamma_P$ is a specified target performance. This is simply an \mathcal{H}_{∞} control problem, for which there are many controller synthesis methods [49, 96, 97]. If it is desired to minimize the \mathcal{H}_{∞} norm of \mathcal{G}_{CLzw} , this becomes an \mathcal{H}_{∞} -optimal control problem. In the case where the plant and controller are LTI systems, it is the \mathcal{H}_{∞} norm of the transfer matrix $\mathbf{G}_{CLzw}(s) = \mathbf{C}_{CL1}(s\mathbf{1} - \mathbf{A}_{CL})^{-1}\mathbf{B}_{CL1} + \mathbf{D}_{CL1}$ that is of interest.

8.3.2 Nominal Performance with the Large Gain Theorem

A particularity of the case when Δ has nonzero minimum gain, is that the uncertainty is never zero and \mathcal{G}_{CLzw} does not represent the nominal closed-loop system, as the uncertain system will never be identical to \mathcal{G}_{CLzw} . As such, a robust control problem with this type of uncertainty, which is directly suitable for robust stabilization using the Large Gain Theorem, will lead to a nominal performance problem that is slightly different from that obtained in Section 8.3.1. It is shown in the following theorem for an LTI plant \mathbf{G}_{CLzw} and controller \mathbf{G}_c that provided Δ has no finite upper bound on its gain, the nominal performance problem can be formulated by inverting the uncertainty and the plant in a similar manner to Theorem 8.1. A similar inversion procedure is possible for the general case where \mathcal{G}_{CLzw} and \mathcal{G}_c are operators, but it is more more complicated and abstract, and therefore is not presented in this section.

Theorem 8.8. *Assuming that Δ and \mathbf{D}_{CL33} are square and invertible, and Δ^{-1} has a minimum gain of zero, nominal performance of the closed-loop system is given by*

the \mathcal{H}_∞ norm of the the transfer matrix $\bar{\mathbf{G}}_{\text{CL}zw}(s)$ with state-space realization

$$\dot{\mathbf{x}}_{\text{CL}}(t) = \bar{\mathbf{A}}_{\text{CL}} \mathbf{x}_{\text{CL}}(t) + \bar{\mathbf{B}}_{\text{CL}1} \mathbf{w}(t), \quad (8.18)$$

$$\mathbf{z}(t) = \bar{\mathbf{C}}_{\text{CL}1} \mathbf{x}_{\text{CL}}(t) + \bar{\mathbf{D}}_{\text{CL}11} \mathbf{w}(t), \quad (8.19)$$

where

$$\begin{aligned} \bar{\mathbf{A}}_{\text{CL}} &= \mathbf{A}_{\text{CL}} - \mathbf{B}_{\text{CL}3} \mathbf{D}_{\text{CL}33}^{-1} \mathbf{C}_{\text{CL}3}, \\ \bar{\mathbf{B}}_{\text{CL}1} &= \mathbf{B}_{\text{CL}1} - \mathbf{B}_{\text{CL}3} \mathbf{D}_{\text{CL}33}^{-1} \mathbf{D}_{\text{CL}31}, \\ \bar{\mathbf{C}}_{\text{CL}1} &= \mathbf{C}_{\text{CL}1} - \mathbf{D}_{\text{CL}13} \mathbf{D}_{\text{CL}33}^{-1} \mathbf{C}_{\text{CL}3}, \\ \bar{\mathbf{D}}_{\text{CL}11} &= \mathbf{D}_{\text{CL}11} - \mathbf{D}_{\text{CL}13} \mathbf{D}_{\text{CL}33}^{-1} \mathbf{D}_{\text{CL}31}. \end{aligned}$$

Proof. The uncertainty is inverted to obtain $\mathbf{q} = \bar{\Delta} \mathbf{p}$, where $\bar{\Delta} = \Delta^{-1}$ has a minimum gain of zero. This changes the plant's robustness input channel to \mathbf{q} and the robustness output channel to \mathbf{p} . Rearranging (8.17) yields

$$\mathbf{p}(t) = -\mathbf{D}_{\text{CL}33}^{-1} \mathbf{C}_{\text{CL}3} \mathbf{x}_{\text{CL}}(t) - \mathbf{D}_{\text{CL}33}^{-1} \mathbf{D}_{\text{CL}31} \mathbf{w}(t) + \mathbf{D}_{\text{CL}33}^{-1} \mathbf{q}(t). \quad (8.20)$$

Substituting the expression for $\mathbf{p}(t)$ from (8.20) into (8.15) and (8.16), and setting $\bar{\Delta}$ to zero gives the state-space realization in (8.18) and (8.19), which is the nominal closed-loop system without uncertainty. \square

Following the inversion in Theorem 8.8, nominal performance is achieved by ensuring the \mathcal{H}_∞ norm of the transfer matrix $\bar{\mathbf{G}}_{\text{CL}zw}(s) = \bar{\mathbf{C}}_{\text{CL}1} (s\mathbf{I} - \bar{\mathbf{A}}_{\text{CL}})^{-1} \bar{\mathbf{B}}_{\text{CL}1} + \bar{\mathbf{D}}_{\text{CL}11}$ is less than a specified value.

Remark 8.9. The inversion performed in Theorem 8.8 to obtain the nominal closed-loop system can be performed prior to controller synthesis. Performing the inversion on the open-loop state-space equations in (8.11), (8.12), (8.13) and (8.14) gives

$$\begin{aligned} \dot{\mathbf{x}}(t) &= (\mathbf{A} - \mathbf{B}_3 \mathbf{D}_{33}^{-1} \mathbf{C}_3) \mathbf{x}(t) + (\mathbf{B}_1 - \mathbf{B}_3 \mathbf{D}_{33}^{-1} \mathbf{D}_{31}) \mathbf{w}(t) \\ &\quad + (\mathbf{B}_2 - \mathbf{B}_3 \mathbf{D}_{33}^{-1} \mathbf{D}_{32}) \mathbf{u}(t) + \mathbf{B}_3 \mathbf{D}_{33}^{-1} \mathbf{q}(t), \end{aligned} \quad (8.21)$$

$$\begin{aligned} \mathbf{z}(t) &= (\mathbf{C}_1 - \mathbf{D}_{13} \mathbf{D}_{33}^{-1} \mathbf{C}_3) \mathbf{x}(t) + (\mathbf{D}_{11} - \mathbf{D}_{13} \mathbf{D}_{33}^{-1} \mathbf{D}_{31}) \mathbf{w}(t) \\ &\quad + (\mathbf{D}_{12} - \mathbf{D}_{13} \mathbf{D}_{33}^{-1} \mathbf{D}_{32}) \mathbf{u}(t) + \mathbf{D}_{13} \mathbf{D}_{33}^{-1} \mathbf{q}(t), \end{aligned} \quad (8.22)$$

$$\begin{aligned} \mathbf{y}(t) &= (\mathbf{C}_2 - \mathbf{D}_{23} \mathbf{D}_{33}^{-1} \mathbf{C}_3) \mathbf{x}(t) + (\mathbf{D}_{21} - \mathbf{D}_{23} \mathbf{D}_{33}^{-1} \mathbf{D}_{31}) \mathbf{w}(t) \\ &\quad + (\mathbf{D}_{22} - \mathbf{D}_{23} \mathbf{D}_{33}^{-1} \mathbf{D}_{32}) \mathbf{u}(t) + \mathbf{D}_{23} \mathbf{D}_{33}^{-1} \mathbf{q}(t), \end{aligned} \quad (8.23)$$

$$\mathbf{p}(t) = -\mathbf{D}_{33}^{-1} \mathbf{C}_3 \mathbf{x}(t) - \mathbf{D}_{33}^{-1} \mathbf{D}_{31} \mathbf{w}(t) - \mathbf{D}_{33}^{-1} \mathbf{D}_{32} \mathbf{u}(t) + \mathbf{D}_{33}^{-1} \mathbf{q}(t), \quad (8.24)$$

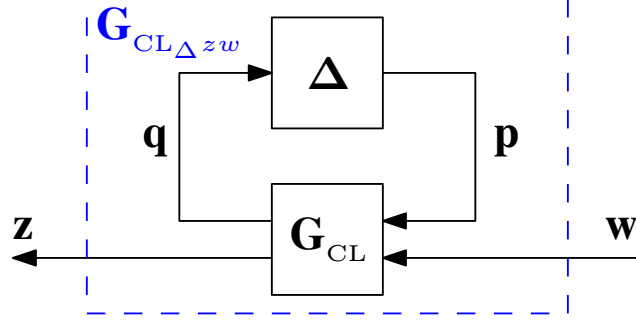


Figure 8.8: Feedback interconnection involving the LTI nominal closed-loop system \mathbf{G}_{CL} and the uncertainty Δ , which when combined yield the uncertain closed-loop system $\mathbf{G}_{\text{CL}\Delta zw}$.

The state-space equations in (8.21), (8.22), (8.23), and (8.24) can be used to synthesize a controller for nominal performance when the uncertainty Δ has nonzero minimum gain and requires inversion to recover the nominal system without uncertainty.

Remark 8.10. If the gain of Δ has both a nonzero lower bound and a finite upper bound, then the notion of nominal performance is not clear, as both the original plant and the inverted plant will always differ from the uncertain plant. In this case, it may be suitable to set either Δ or $\bar{\Delta}$ to zero, or lump some value of uncertainty gain that is between the upper and lower gain bounds of Δ into the plant and consider this the nominal plant.

8.4 Robust Performance

The robust performance problem involves guaranteeing certain performance criteria for all possible uncertainty within a specified set. Within the context of the Small Gain Theorem for LTI systems, the performance criterion is typically a guarantee that the \mathcal{H}_∞ norm of the uncertain closed-loop transfer matrix

$$\begin{aligned} \mathbf{G}_{\text{CL}\Delta zw}(s) &= \mathcal{F}_u(\mathbf{G}_{\text{CL}}(s), \Delta(s)) \\ &= \mathbf{G}_{\text{CL}zw}(s) + \mathbf{G}_{\text{CL}zp}(s)\Delta(s) (\mathbf{1} - \mathbf{G}_{\text{CL}qp}(s)\Delta(s))^{-1} \mathbf{G}_{\text{CL}qw}(s), \end{aligned}$$

shown in Figure 8.8, remains less than $0 < \gamma_P < \infty$ for all Δ satisfying $\|\Delta\|_\infty \leq \gamma_\Delta$. The term $\mathcal{F}_u(\mathbf{G}_{\text{CL}}(s), \Delta(s))$ represents an upper linear fractional transformation (LFT) [7, pp. 543–544],[105]. This definition of robust performance is not well-suited for systems whose uncertainty has a nonzero minimum gain, where the Large Gain Theorem is to be used to provide a guarantee of robustness. In this case, a new

definition of robust performance is adopted related to minimum gain of the uncertain closed-loop transfer matrix $\mathbf{G}_{\text{CL}\Delta zw}(s)$ and its minimum phase properties. Within this section, the uncertainty $\Delta(s)$ is restricted to a transfer matrix, since robust performance with the Large Gain Theorem is concerned with a minimum phase constraint on the uncertain closed-loop transfer matrix $\mathbf{G}_{\text{CL}\Delta zw}(s)$.

8.4.1 Robust Performance with the Small Gain Theorem and the Structured Singular Value

The robust performance problem considered in this section is to design a controller such that the \mathcal{H}_∞ norm of the uncertain closed-loop system $\mathbf{G}_{\text{CL}\Delta zw}$ remains less than $0 < \gamma_P < \infty$ for all Δ satisfying $\|\Delta\|_\infty \leq \gamma_\Delta$. It is known that this problem can be transformed into an equivalent robust stabilization problem involving the nominal closed-loop system \mathbf{G}_{CL} and the augmented uncertainty block $\tilde{\Delta} = \text{diag}\{\Delta, \Delta_P\}$ shown in Figure 8.9, where Δ_P is a full matrix whose maximum singular value determines the maximum allowable \mathcal{H}_∞ norm of $\mathbf{G}_{\text{CL}\Delta zw}$ [7, p. 317]. Using the Small Gain Theorem, robust stability, and therefore robust performance, can be guaranteed if $0 < \gamma_{\tilde{\Delta}}\gamma_{\text{CL}}$, where γ_{CL} is the \mathcal{H}_∞ norm of \mathbf{G}_{CL} . This robust stabilization problem will always have structured uncertainty since $\tilde{\Delta}$ has a block-diagonal structure. As a result, the Small Gain Theorem is a conservative robust stability condition and the structured singular value should be used to assess robust stability without conservatism.

8.4.2 Robust Performance with the Large Gain Theorem and the Structured Minimum Singular Value

Robust performance in the traditional sense (i.e., guaranteeing an upper bound on the \mathcal{H}_∞ norm of $\mathbf{G}_{\text{CL}\Delta zw}$) is quite a difficult problem when using the Large Gain Theorem. The Small Gain Theorem involves the \mathcal{H}_∞ norm of two system within a feedback interconnection, in particular, $\tilde{\Delta}$ and \mathbf{G}_{CL} when solving the robust performance problem. Conveniently, the maximum singular value of \mathbf{G}_{CL} can be related to a guaranteed bound on the \mathcal{H}_∞ norm of $\mathbf{G}_{\text{CL}\Delta zw}$, which allows the Small Gain Theorem or the structured singular value to be used to solve the robust performance problem. Conversely, the Large Gain Theorem involves minimum gain and not the \mathcal{H}_∞ norm, which makes it difficult to provide any guarantee on the \mathcal{H}_∞ norm of $\mathbf{G}_{\text{CL}\Delta zw}$. If it is desired to solve the robust performance problem in the traditional sense, it is recommended to invert the problem as shown in Theorem 8.1 and use a technique

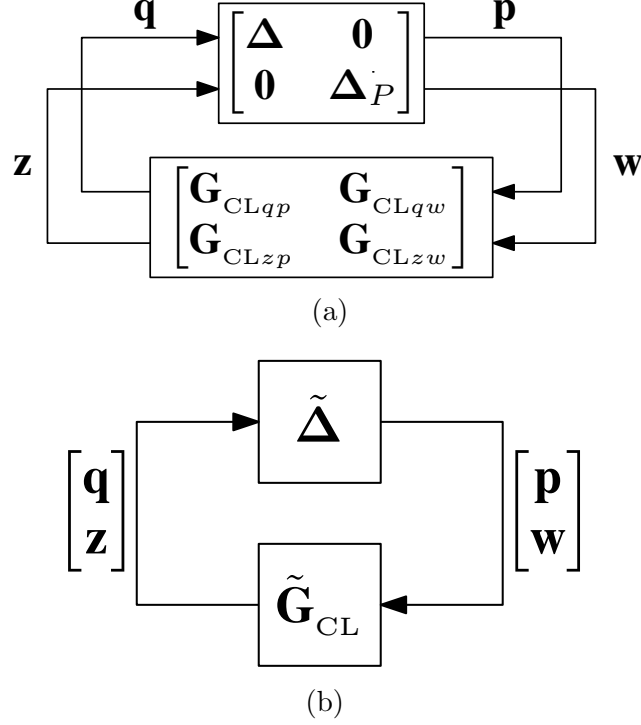


Figure 8.9: Equivalent feedback interconnections of $\tilde{\mathbf{G}}_{\text{CL}}$ and $\tilde{\Delta}$ used for robust performance, where the contents of $\tilde{\mathbf{G}}_{\text{CL}}$ and $\tilde{\Delta}$ are expanded in (a) and written compactly in (b).

such as DK -iteration.

A different type of robust performance that is more relevant to the Large Gain Theorem is guaranteeing a lower bound on the least conservative minimum gain of $\mathbf{G}_{\text{CL}\Delta zw}$. On the surface this may not appear to be a useful robust performance criterion, however, if it is possible to guarantee that $\mathbf{G}_{\text{CL}\Delta zw}$ has nonzero minimum gain, from Lemma 3.5 it is implied that $\mathbf{G}_{\text{CL}\Delta zw}$ is minimum phase. With this definition of robust performance in mind, consider the following theorem.

Theorem 8.11. *The uncertain closed-loop system $\mathbf{G}_{\text{CL}\Delta zw}$ has minimum gain strictly greater than $\nu_{\Delta_P}^{-1}$ for all Δ with minimum gain $0 < \nu_{\Delta} < \infty$ if $1 < \nu_{\text{CL}}\nu_{\tilde{\Delta}} < \infty$, where $\tilde{\Delta} = \text{diag}\{\Delta, \Delta_P\}$, Δ_P has minimum gain $0 < \nu_{\Delta_P} < \infty$, $0 < \nu_{\tilde{\Delta}} < \infty$ is a minimum gain of $\tilde{\Delta}$, and $0 < \nu_{\text{CL}} < \infty$ is a minimum gain of \mathbf{G}_{CL} .*

Proof. The proof of Theorem 8.11 is very similar to the proof that shows the traditional robust performance problem is equivalent to a robust stabilization problem, which can be found in a number of references [7, 39]. In the interest of completeness, an adapted proof is presented here.

If the condition $1 < \nu_{\text{CL}}\nu_{\tilde{\Delta}} < \infty$ is satisfied, then asymptotic stability of the

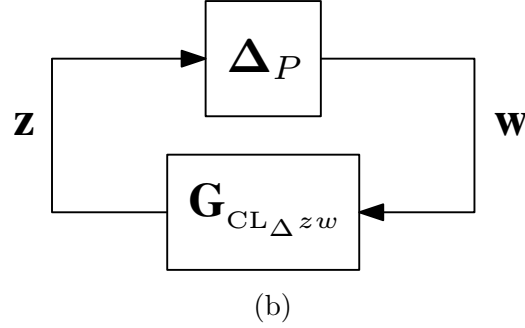
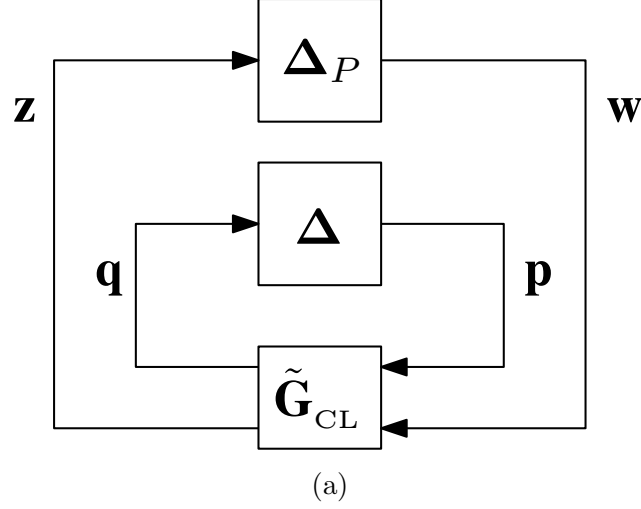


Figure 8.10: Equivalent feedback interconnections of (a) $\mathbf{G}_{\text{CL}\Delta zw}$ and Δ_P and (b) $\tilde{\mathbf{G}}_{\text{CL}}$, Δ , and Δ_P used for the proof of Theorem 8.11.

feedback interconnection involving \mathbf{G}_{CL} and $\tilde{\Delta}$, shown in Figure 8.9b, is guaranteed by the Large Gain Theorem. This feedback interconnection is equivalent to the feedback interconnections in Figure 8.10a and Figure 8.10b, which implies that the feedback interconnection of $\mathbf{G}_{\text{CL}\Delta zw}$ and Δ_P in Figure 8.10b is asymptotically stable. Since Δ_P has minimum gain $0 < \nu_{\Delta_P} < \infty$, it is known from Theorem 7.10 that $\mathbf{G}_{\text{CL}\Delta zw}$ has minimum gain strictly greater than $\nu_{\Delta_P}^{-1}$. \square

Corollary 8.12. *The uncertain closed-loop transfer matrix $\mathbf{G}_{\text{CL}\Delta zw}(s)$ is minimum phase if $1 < \nu_{\text{CL}}\nu_{\tilde{\Delta}} < \infty$, where $\tilde{\Delta} = \text{diag}\{\Delta, \Delta_P\}$, Δ_P has nonzero minimum gain, $0 < \nu_{\tilde{\Delta}} < \infty$ is a minimum gain of $\tilde{\Delta}$, and $0 < \nu_{\text{CL}} < \infty$ is a minimum gain of $\mathbf{G}_{\text{CL}\Delta zw}$.*

Proof. The proof of Corollary 8.12 amounts to combining the results of Theorem 8.11 and Lemma 3.5. \square

Remark 8.13. It was shown in Theorem 8.11 that robust performance with the Large Gain Theorem is equivalent to a robust stabilization problem with the Large Gain Theorem. From Theorem 8.1, it is known that a robust stabilization problem with the Large Gain Theorem can be converted into a robust stabilization problem with the Small Gain Theorem, therefore it is possible to convert a robust performance problem with the Large Gain Theorem into a robust stabilization problem or a robust performance problem with the Small Gain Theorem.

Similarly to the use of the Small Gain Theorem for robust performance, the conditions stated in Theorem 8.11 and Corollary 8.12 are conservative, as they do not account for the structure in the combined uncertainty block $\tilde{\Delta}$. As discussed in Section 8.2.2, a structured minimum singular value is required to assess robust stability without conservatism when the uncertainty block has structure, which is also needed for robust performance to remove the conservatism of Theorem 8.11 and Corollary 8.12. A structured singular value approach to robust performance guaranteeing a lower bound on the closed-loop system's minimum gain or a closed-loop minimum phase transfer matrix would follow the same approach outlined in Theorem 8.11 and Corollary 8.12, but would use the structured singular value to assess robust stability rather than the Large Gain Theorem.

Remark 8.14. Robust performance with the Large Gain Theorem is related to the location of the zeros of the uncertain closed-loop transfer matrix $\mathbf{G}_{\text{CL}_{\Delta zw}}(s)$. It is known that the closed-loop zeros of a servo loop with a feedback controller will include the open-loop zeros of the servo loop [106], as feedback control does not affect the location of zeros. Because of this, designing a feedback controller for robust performance with the Large Gain Theorem may be quite difficult if the open-loop transfer matrix $\mathbf{G}_{zw}(s)$ is nonminimum phase. It is not necessarily impossible to accomplish this with feedback control, as the generalized plant need not represent a servo loop, but it may be difficult. Parallel feedforward control, which was discussed in Chapter 4, is quite capable of placing zeros. The generalized plant framework used in this chapter is not exclusive to feedback controller, and in fact can accommodate the case of a parallel feedforward controller or even a two DOF controller composed of parallel feedforward and feedback components. In general, performing Large Gain Theorem-based robust performance is best suited for a controller that has a feedforward component, as it will be better equipped to adjust the zeros of the closed-loop system.

8.4.3 Robust Performance with a Mixed Structured Singular Value

The robust stability and robust performance problems presented in Sections 8.2.2 and 8.4.2 using the Large Gain Theorem are only valid for systems whose uncertainty has nonzero minimum gain. It was shown in Theorem 8.1 that after inversion of the uncertainty and the plant robust stabilization with the Large Gain Theorem is equivalent to robust stabilization with the Small Gain Theorem. It was also discussed in Remark 8.13 that since robust performance with the Large Gain Theorem is solved as a robust stabilization problem, it can be inverted to a robust performance problem using the Large Gain Theorem or the structured singular value. However, consider the case where it is desired that the uncertain closed-loop transfer matrix be minimum phase and have an \mathcal{H}_∞ norm less than some specified value. In this situation it may be possible to invert a portion of the uncertainty block and the plant to yield a traditional robust performance problem or a robust performance problem with the Large Gain Theorem, but this may be difficult or impossible depending on the problem. Ideally, a robust performance problem could be formulated that simultaneously places conditions on the closed-loop system's \mathcal{H}_∞ norm and minimum gain, which would ultimately be a robust stabilization problem with uncertainty whose sub-blocks have either lower or upper bounds on gain. In order to solve this new robust performance problem without conservatism, a mixed structured singular value is needed that incorporates Small Gain Theorem and Large Gain Theorem concepts. This would yield a significant advancement over current robust performance capabilities, and will be interesting topic of future work.

8.5 Closing Remarks

This chapter outlined the capabilities of the Large Gain Theorem for robust control, in particular its ability to solve robust stabilization and nominal performance problems, as well as a new type of robust performance problem. It was shown how robust stabilization using the Large Gain Theorem is equivalent to robust stabilization using the Small Gain Theorem after inversion of the uncertainty and the plant. This provides a means to convert from one stability theorem to the other, depending on which is more convenient for a given problem. The concept of a structured minimum singular value was introduced as a means to assess robust stability without conservatism when the uncertainty has nonzero minimum gain and structure. A mixed structured singular value was also discussed that would be used when certain portions of the uncertainty block have a lower bound on their gain and others have

an upper bound on their gain, which could help solve a robust performance problem that guarantees a lower and upper bound on the gain of the closed-loop system.

Mathematical formalizations of the structured minimum singular value and the mixed structured singular value are to be developed in future work, which will be largely based on the properties of the well-known structured singular value.

Chapter 9

Robust Controller Synthesis using the Large Gain Theorem

9.1 Introduction

The use of the Small Gain Theorem is prevalent in robust control, which has made the Small Gain Theorem an indispensable tool for robust control engineers to synthesize robust controllers. Robust \mathcal{H}_∞ control is capable of solving a wide variety of robust control problems, including robust stabilization, nominal performance, and robust performance, with many suitable controller synthesis methods [49, 96, 97]. More advanced controller synthesis techniques based on the structured singular value, such as DK -iteration or μ -synthesis [101, 102], provide a guarantee of robust stability using a principle similar to the Small Gain Theorem, but with less conservatism when the uncertainty has structure. Robust control using the Small Gain Theorem or the structured singular value is practical when the gain of the uncertainty has a known upper bound that is relatively small. When the upper bound on the gain of the uncertainty is quite large, which does appear in practical examples such as aeroelastic systems [107, 108], it may still be possible to synthesize a robust controller using the Small Gain Theorem or DK -iteration. Such a controller may lead to conservative results compared to the use of other stability theorems or uncertainty models, such as positive real [109, 110], passive [111], or interior conic [112] uncertainty modeling.

A framework for robust control using the Large Gain Theorem is presented in Chapter 8, which features input-output stability conditions that can be used to solve the robust stabilization, nominal performance, and robust performance problems when faced with uncertainty that has a nonzero lower bound on its gain, also known

as uncertainty with nonzero minimum gain. In situations where the uncertainty has large upper and lower bounds on its gain, performing robust control with the Large Gain Theorem may lead to less conservative results than the Small Gain Theorem, as each stability theorem will use different bounds on the uncertainty for a guarantee of robustness. The robust performance problem posed with the Large Gain Theorem is different than the traditional robust performance problem, as it is concerned with a guarantee of a lower bound on the least conservative minimum gain of the uncertain closed-loop system, rather than an upper bound on the \mathcal{H}_∞ norm of this system. By guaranteeing the uncertain LTI closed-loop system has nonzero minimum gain, it is guaranteed that its transfer matrix is minimum phase, which is a robust performance criterion that is not enforceable using the Small Gain Theorem. It is also shown in Chapter 8 that a system whose uncertainty has a minimum gain of zero can be transformed into an equivalent system whose uncertainty has nonzero minimum gain using a loop transformation and inversion, making the Large Gain Theorem applicable on any uncertain system where the Small Gain Theorem is applicable.

In this chapter, robust controller synthesis methods using the Large Gain Theorem are presented based on the theory in Chapter 8. In particular, full-state feedback and dynamic output feedback controller synthesis methods are provided for robust stabilization, robust stabilization and nominal performance, and robust performance problems. The synthesis methods make use of LMI constraints, which lead to tractable optimization problems using semidefinite programming. A numerical robust control benchmark problem from [77] is used to compare the proposed controller synthesis methods using the Large Gain Theorem to robust \mathcal{H}_∞ controller synthesis methods using the Small Gain Theorem. The novel contributions of this chapter are the aforementioned robust controller synthesis methods using the Large Gain Theorem and the first numerical testing of Large Gain Theorem-based robust controllers on a physically meaningful system.

The remainder of this chapter proceeds with a statement of the robust control problems considered in Section 9.2. Full-state feedback controller synthesis methods are developed in Section 9.3, which includes solutions to the robust stabilization, nominal performance, and robust performance problems using the Large Gain Theorem. Dynamic feedback controller synthesis methods are presented in Section 9.4. Numerical examples with the proposed controller synthesis methods are found in Section 9.5 and concluding remarks are given in Section 9.6.

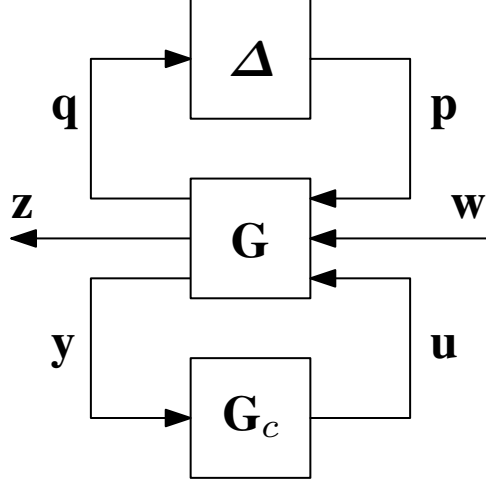


Figure 9.1: Feedback interconnection involving the nominal plant \mathbf{G} , the controller \mathbf{G}_c , and the uncertainty Δ .

9.2 Problem Statement

Consider an LTI system, $\mathbf{G} : \mathcal{L}_{2e} \rightarrow \mathcal{L}_{2e}$, shown in Figure 9.1, with a minimal state-space realization given by

$$\dot{\mathbf{x}}(t) = \mathbf{A}\mathbf{x}(t) + \mathbf{B}_1\mathbf{w}(t) + \mathbf{B}_2\mathbf{u}(t) + \mathbf{B}_3\mathbf{p}(t), \quad (9.1)$$

$$\mathbf{z}(t) = \mathbf{C}_1\mathbf{x}(t) + \mathbf{D}_{11}\mathbf{w}(t) + \mathbf{D}_{12}\mathbf{u}(t) + \mathbf{D}_{13}\mathbf{p}(t), \quad (9.2)$$

$$\mathbf{y}(t) = \mathbf{C}_2\mathbf{x}(t) + \mathbf{D}_{21}\mathbf{w}(t) + \mathbf{D}_{22}\mathbf{u}(t) + \mathbf{D}_{23}\mathbf{p}(t), \quad (9.3)$$

$$\mathbf{q}(t) = \mathbf{C}_3\mathbf{x}(t) + \mathbf{D}_{31}\mathbf{w}(t) + \mathbf{D}_{32}\mathbf{u}(t) + \mathbf{D}_{33}\mathbf{p}(t), \quad (9.4)$$

where it is assumed that $(\mathbf{A}, \mathbf{B}_2)$ is controllable and $(\mathbf{A}, \mathbf{C}_2)$ is observable. The system is subject to uncertainty Δ with a known minimum gain of $0 < \nu_\Delta < \infty$. The objective is to design a feedback controller, $\mathbf{G}_c : \mathcal{L}_{2e} \rightarrow \mathcal{L}_{2e}$, such that one of the following problems is solved.

1. **Robust Stabilization:** The closed-loop system is robustly input-output stable subject to the uncertainty Δ .
2. **Robust Stabilization and Nominal Performance:** The closed-loop system is robustly input-output stable subject to the uncertainty Δ and the \mathcal{H}_∞ norm of the nominal closed-loop system transfer matrix from $\mathbf{w}(s)$ to $\mathbf{z}(s)$ is less than a specified value.
3. **Robust Performance:** The closed-loop system is robustly input-output stable

subject to the uncertainty $\Delta(s)$ and the least conservative minimum gain of the uncertain closed-loop system transfer matrix from $\mathbf{w}(s)$ to $\mathbf{z}(s)$ is greater than a specified value. If the least conservative minimum gain of the uncertain closed-loop system transfer matrix from $\mathbf{w}(s)$ to $\mathbf{z}(s)$ is greater than zero, then the transfer matrix is minimum phase.

9.3 Full-State Feedback Controller Synthesis

This section presents synthesis methods for a full-state feedback controller of the form $\mathbf{u}(t) = \mathbf{K}\mathbf{x}(t)$ to solve robust stabilization, robust stabilization and nominal performance, and robust performance problems using the Large Gain Theorem. For the synthesis of robust full-state feedback controllers, it is assumed that the minimum singular value of the matrix \mathbf{D}_{33} is greater than $1/\nu_\Delta$ (i.e., $\mathbf{D}_{33}^\top \mathbf{D}_{33} \geq 1/\nu_\Delta^2 \mathbf{1}$). The condition on the minimum singular value of \mathbf{D}_{33} relates to the input-output stability condition of the Large Gain Theorem, the statement of the Minimum Gain Lemma, and the inability of full-state feedback to change the \mathbf{D}_{33} matrix of the closed-loop system. Since a full-state measurement is assumed to be available, $\mathbf{C}_2 = \mathbf{1}$, $\mathbf{D}_{21} = \mathbf{0}$, $\mathbf{D}_{22} = \mathbf{0}$, and $\mathbf{D}_{23} = \mathbf{0}$ in (9.3).

Substituting $\mathbf{u}(t) = -\mathbf{K}\mathbf{x}(t)$ into the state-space equations of (9.1), (9.2), (9.4) yields the nominal closed-loop system, \mathbf{G}_{CL} , with state-space realization

$$\dot{\mathbf{x}}(t) = \mathbf{A}_{\text{CL}} \mathbf{x}(t) + \mathbf{B}_1 \mathbf{w}(t) + \mathbf{B}_3 \mathbf{p}(t), \quad (9.5)$$

$$\mathbf{z}(t) = \mathbf{C}_{\text{CL}1} \mathbf{x}(t) + \mathbf{D}_{11} \mathbf{w}(t) + \mathbf{D}_{13} \mathbf{p}(t), \quad (9.6)$$

$$\mathbf{q}(t) = \mathbf{C}_{\text{CL}3} \mathbf{x}(t) + \mathbf{D}_{31} \mathbf{w}(t) + \mathbf{D}_{33} \mathbf{p}(t), \quad (9.7)$$

where $\mathbf{A}_{\text{CL}} = \mathbf{A} - \mathbf{B}_2 \mathbf{K}$, $\mathbf{C}_{\text{CL}1} = \mathbf{C}_1 - \mathbf{D}_{12} \mathbf{K}$, and $\mathbf{C}_{\text{CL}3} = \mathbf{C}_3 - \mathbf{D}_{32} \mathbf{K}$. The nominal closed-loop transfer matrix, $\mathbf{G}_{\text{CL}}(s)$, is defined as

$$\begin{bmatrix} \mathbf{q}(s) \\ \mathbf{z}(s) \end{bmatrix} = \underbrace{\begin{bmatrix} \mathbf{G}_{\text{CL}qp}(s) & \mathbf{G}_{\text{CL}qw}(s) \\ \mathbf{G}_{\text{CL}zp}(s) & \mathbf{G}_{\text{CL}zw}(s) \end{bmatrix}}_{\mathbf{G}_{\text{CL}}(s)} \begin{bmatrix} \mathbf{p}(s) \\ \mathbf{w}(s) \end{bmatrix}.$$

A block diagram of the nominal closed-loop system \mathbf{G}_{CL} and the uncertainty Δ is found in Figure 8.7.

9.3.1 Robust Stabilization

In order to guarantee robust input-output stability of the closed-loop system using the Large Gain Theorem, the full-state feedback gain \mathbf{K} is to be chosen such that the transfer matrix $\mathbf{G}_{\text{CL}qp}(s) = \mathbf{C}_{\text{CL}3} (s\mathbf{1} - \mathbf{A}_{\text{CL}})^{-1} \mathbf{B}_3 + \mathbf{D}_{33}$ has minimum gain $0 < \nu_{\text{CL}qp} < \infty$ satisfying $1 < \nu_{\Delta} \nu_{\text{CL}qp} < \infty$. The Minimum Gain Lemma (Lemma 3.9) is employed to determine a minimum gain of $\mathbf{G}_{\text{CL}qp}(s)$, which is any value of $0 < \nu_{\text{CL}qp} < \infty$ satisfying

$$\begin{bmatrix} \mathbf{P}\mathbf{A}_{\text{CL}} + \mathbf{A}_{\text{CL}}^{\top} \mathbf{P} - \mathbf{C}_{\text{CL}3}^{\top} \mathbf{C}_{\text{CL}3} & \mathbf{P}\mathbf{B}_3 - \mathbf{C}_{\text{CL}3}^{\top} \mathbf{D}_{33} \\ * & \nu_{\text{CL}qp}^2 \mathbf{1} - \mathbf{D}_{33}^{\top} \mathbf{D}_{33} \end{bmatrix} \leq 0, \quad (9.8)$$

with $\mathbf{P} = \mathbf{P}^{\top} \geq 0$. Since $\mathbf{G}_{\text{CL}qp}(s)$ is square, the matrix inequality in (9.8) is a necessary and sufficient condition for minimum gain. Unfortunately, the term $-\mathbf{C}_{\text{CL}3}^{\top} \mathbf{C}_{\text{CL}3}$ in (9.8) makes the synthesis of \mathbf{K} difficult, as it leads to a BMI that cannot be directly transformed into an LMI. Using the Modified Minimum Gain Lemma (Lemma 3.11), a sufficient condition for $\mathbf{G}_{\text{CL}qp}(s)$ to have a minimum gain $0 \leq \nu_{\text{CL}qp} < \infty$ is for there to exist $\mathbf{P} = \mathbf{P}^{\top} \geq 0$ such that

$$\begin{bmatrix} \mathbf{P}\mathbf{A}_{\text{CL}} + \mathbf{A}_{\text{CL}}^{\top} \mathbf{P} & \mathbf{P}\mathbf{B}_3 - \mathbf{C}_{\text{CL}3}^{\top} \mathbf{D}_{33} \\ * & \nu_{\text{CL}qp}^2 \mathbf{1} - \mathbf{D}_{33}^{\top} \mathbf{D}_{33} \end{bmatrix} \leq 0. \quad (9.9)$$

Expanding (9.9) with the expressions for \mathbf{A}_{CL} and $\mathbf{C}_{\text{CL}3}$ yields

$$\begin{bmatrix} \mathbf{P}\mathbf{A} + \mathbf{A}^{\top} \mathbf{P} - \mathbf{P}\mathbf{B}_2 \mathbf{K} - \mathbf{K}^{\top} \mathbf{B}_2^{\top} \mathbf{P} & \mathbf{P}\mathbf{B}_3 - \mathbf{C}_3^{\top} \mathbf{D}_{33} + \mathbf{K}^{\top} \mathbf{D}_{32}^{\top} \mathbf{D}_{33} \\ * & \nu_{\text{CL}qp}^2 \mathbf{1} - \mathbf{D}_{33}^{\top} \mathbf{D}_{33} \end{bmatrix} \leq 0. \quad (9.10)$$

Lemma 9.1. *The transfer matrix $\mathbf{G}_{\text{CL}qp}(s) = \mathbf{C}_{\text{CL}3} (s\mathbf{1} - \mathbf{A}_{\text{CL}})^{-1} \mathbf{B}_3 + \mathbf{D}_{33}$ has minimum gain $0 < \nu_{\text{CL}qp} < \infty$ if there exists $\mathbf{Q} = \mathbf{Q}^{\top} > 0$ and $\mathbf{F} = \mathbf{K}\mathbf{Q}$ such that*

$$\begin{bmatrix} \mathbf{A}\mathbf{Q} + \mathbf{Q}\mathbf{A}^{\top} - \mathbf{B}_2 \mathbf{F} - \mathbf{F}^{\top} \mathbf{B}_2^{\top} & \mathbf{B}_3 - \mathbf{Q}\mathbf{C}_3^{\top} \mathbf{D}_{33} + \mathbf{F}^{\top} \mathbf{D}_{32}^{\top} \mathbf{D}_{33} \\ * & \nu_{\text{CL}qp}^2 \mathbf{1} - \mathbf{D}_{33}^{\top} \mathbf{D}_{33} \end{bmatrix} \leq 0. \quad (9.11)$$

Proof. The restriction $\mathbf{P} = \mathbf{P}^{\top} > 0$ is deliberately added to the Modified Minimum Gain Lemma, which still yields a sufficient minimum gain condition. The congruence transformation $\mathbf{W} = \text{diag}\{\mathbf{P}^{-1}, \mathbf{1}\}$ [7, pp. 521–522] is performed on (9.10) (i.e., the matrix inequality in (9.10) is left multiplied by \mathbf{W}^{\top} and right multiplied by \mathbf{W}). A change of variables is defined as $\mathbf{Q} = \mathbf{P}^{-1}$ and $\mathbf{F} = \mathbf{K}\mathbf{Q}$, which yields the LMI of (9.11). Aside from enforcing $\mathbf{P} = \mathbf{P}^{\top} > 0$, (9.10) and (9.11) are equivalent, but due to this restriction it is concluded that (9.11) \implies (9.10), which is a sufficient minimum gain

condition. □

The following controller synthesis method guarantees the robust input-output stability of the uncertain closed-loop system by ensuring that the Large Gain Theorem is satisfied with $1 < \nu_{\Delta} \nu_{\text{CL}qp} < \infty$.

Synthesis Method 5 (Robust Stability with Full-State Feedback). *Solve for $\mathbf{Q} = \mathbf{Q}^T > 0$, \mathbf{F} , and $0 < \nu_{\text{CL}qp}^2 < \infty$ satisfying $1 < \nu_{\Delta}^2 \nu_{\text{CL}qp}^2 < \infty$ and the LMI of (9.11). The controller gain is recovered by $\mathbf{K} = \mathbf{F}\mathbf{Q}^{-1}$.*

If it is desired to guarantee robust closed-loop input-output stability with the largest margin possible, the objective function $\mathcal{J}(\nu_{\text{CL}qp}^2) = \nu_{\text{CL}qp}^2$ is to be maximized when performing Synthesis Method 5.

9.3.2 Robust Stabilization and Nominal Performance

The controller synthesis method derived in the previous section only provides a means to robustly stabilize the uncertain system without any consideration of closed-loop performance. In this section, the nominal performance of the closed-loop system is explicitly considered when synthesizing a full-state feedback controller in addition to the task of ensuring the closed-loop system is robustly input-output stable.

Using Theorem 8.8 and assuming that $\mathbf{\Delta}^{-1}$ has a minimum gain of zero, the nominal closed-loop transfer matrix from $\mathbf{w}(s)$ to $\mathbf{z}(s)$ without uncertainty is given by $\bar{\mathbf{G}}_{\text{CL}zw}(s) = \bar{\mathbf{C}}_{\text{CL}1} (s\mathbf{1} - \bar{\mathbf{A}}_{\text{CL}})^{-1} \bar{\mathbf{B}}_1 + \bar{\mathbf{D}}_{11}$, where

$$\begin{aligned} \bar{\mathbf{A}}_{\text{CL}} &= \mathbf{A} - \mathbf{B}_3 \mathbf{D}_{33}^{-1} \mathbf{C}_3 - (\mathbf{B}_2 - \mathbf{B}_3 \mathbf{D}_{33}^{-1} \mathbf{D}_{32}) \mathbf{K}, \\ \bar{\mathbf{B}}_1 &= \mathbf{B}_1 - \mathbf{B}_3 \mathbf{D}_{33}^{-1} \mathbf{D}_{31}, \end{aligned} \tag{9.12}$$

$$\begin{aligned} \bar{\mathbf{C}}_{\text{CL}1} &= \mathbf{C}_1 - \mathbf{D}_{13} \mathbf{D}_{33}^{-1} \mathbf{C}_3 - (\mathbf{D}_{12} - \mathbf{D}_{13} \mathbf{D}_{33}^{-1} \mathbf{D}_{32}) \mathbf{K}, \\ \bar{\mathbf{D}}_{11} &= \mathbf{D}_{11} - \mathbf{D}_{13} \mathbf{D}_{33}^{-1} \mathbf{D}_{31}. \end{aligned} \tag{9.13}$$

The \mathcal{H}_{∞} norm of $\bar{\mathbf{G}}_{\text{CL}zw}(s)$ is the minimum value of $0 < \gamma_{\text{CL}z\bar{w}} < \infty$ that satisfies the matrix inequality of the Bounded Real Lemma (Lemma 2.25), given by

$$\begin{bmatrix} \bar{\mathbf{P}}\bar{\mathbf{A}}_{\text{CL}} + \bar{\mathbf{A}}_{\text{CL}}^T \bar{\mathbf{P}} & \bar{\mathbf{P}}\bar{\mathbf{B}}_1 & \bar{\mathbf{C}}_{\text{CL}1}^T \\ * & -\gamma_{\text{CL}z\bar{w}} \mathbf{1} & \bar{\mathbf{D}}_{11}^T \\ * & * & -\gamma_{\text{CL}z\bar{w}} \mathbf{1} \end{bmatrix} < 0, \tag{9.14}$$

where $\bar{\mathbf{P}} = \bar{\mathbf{P}}^\top > 0$. Substituting the expressions for $\bar{\mathbf{A}}_{\text{CL}}$ and $\bar{\mathbf{C}}_{\text{CL}3}$ into (9.14) yields

$$\begin{bmatrix} \bar{\mathbf{P}}\bar{\mathbf{A}} - \bar{\mathbf{P}}\bar{\mathbf{B}}_2\mathbf{K} + \bar{\mathbf{A}}^\top\bar{\mathbf{P}} - \mathbf{K}^\top\bar{\mathbf{B}}_2^\top\bar{\mathbf{P}} & \bar{\mathbf{P}}\bar{\mathbf{B}}_1 & \bar{\mathbf{C}}_1^\top - \mathbf{K}^\top\bar{\mathbf{D}}_{12}^\top \\ * & -\gamma_{\text{CL}\bar{z}\bar{w}}\mathbf{1} & \bar{\mathbf{D}}_{11}^\top \\ * & * & -\gamma_{\text{CL}\bar{z}\bar{w}}\mathbf{1} \end{bmatrix} < 0, \quad (9.15)$$

where

$$\bar{\mathbf{A}} = \mathbf{A} - \mathbf{B}_3\mathbf{D}_{33}^{-1}\mathbf{C}_3, \quad (9.16)$$

$$\bar{\mathbf{B}}_2 = \mathbf{B}_2 - \mathbf{B}_3\mathbf{D}_{33}^{-1}\mathbf{D}_{32},$$

$$\bar{\mathbf{C}}_1 = \mathbf{C}_1 - \mathbf{D}_{13}\mathbf{D}_{33}^{-1}\mathbf{C}_3, \quad (9.17)$$

$$\bar{\mathbf{D}}_{12} = \mathbf{D}_{12} - \mathbf{D}_{13}\mathbf{D}_{33}^{-1}\mathbf{D}_{32}. \quad (9.18)$$

Lemma 9.2. *The \mathcal{H}_∞ norm of the transfer matrix $\bar{\mathbf{G}}_{\text{CL}zw}(s) = \bar{\mathbf{C}}_{\text{CL}1}(s\mathbf{1} - \bar{\mathbf{A}}_{\text{CL}})^{-1}\bar{\mathbf{B}}_1 + \bar{\mathbf{D}}_{11}$ is less than or equal to $0 < \gamma_{\text{CL}\bar{z}\bar{w}} < \infty$ if there exists $\bar{\mathbf{Q}} = \bar{\mathbf{Q}}^\top > 0$ and $\bar{\mathbf{F}} = \mathbf{K}\bar{\mathbf{Q}}$ such that*

$$\begin{bmatrix} \bar{\mathbf{A}}\bar{\mathbf{Q}} + \bar{\mathbf{Q}}\bar{\mathbf{A}}^\top - \bar{\mathbf{B}}_2\bar{\mathbf{F}} - \bar{\mathbf{F}}^\top\bar{\mathbf{B}}_2^\top & \bar{\mathbf{B}}_1 & \bar{\mathbf{Q}}\bar{\mathbf{C}}_1^\top - \bar{\mathbf{F}}^\top\bar{\mathbf{D}}_{12}^\top \\ * & -\gamma_{\text{CL}\bar{z}\bar{w}}\mathbf{1} & \bar{\mathbf{D}}_{11}^\top \\ * & * & -\gamma_{\text{CL}\bar{z}\bar{w}}\mathbf{1} \end{bmatrix} < 0. \quad (9.19)$$

Proof. Performing the congruence transformation $\bar{\mathbf{W}} = \text{diag}\{\bar{\mathbf{P}}^{-1}, \mathbf{1}, \mathbf{1}\}$ on (9.15) and defining the variables $\bar{\mathbf{Q}} = \bar{\mathbf{P}}^{-1}$ and $\bar{\mathbf{F}} = \mathbf{K}\bar{\mathbf{Q}}$ gives the LMI of (9.19). It is concluded that (9.15) \iff (9.19) and the \mathcal{H}_∞ norm of $\bar{\mathbf{G}}_{\text{CL}zw}(s)$ is less than or equal to $\gamma_{\text{CL}\bar{z}\bar{w}}$. \square

The following full-state controller synthesis method guarantees the robust input-output stability of the uncertain closed-loop system and ensures that the \mathcal{H}_∞ norm of $\bar{\mathbf{G}}_{\text{CL}zw}(s)$ is less than $0 < \gamma_{\text{CL}\bar{z}\bar{w},d} < \infty$.

Synthesis Method 6 (Robust Stability and Nominal Performance with Full-State Feedback). *Solve for $\mathbf{Q} = \mathbf{Q}^\top > 0$, \mathbf{F} , $0 < \nu_{\text{CL}}^2 < \infty$, and $0 < \gamma_{\text{CL}\bar{z}\bar{w}} < \infty$ satisfying $1 < \nu_\Delta^2 \nu_{\text{CL}}^2$, $\gamma_{\text{CL}\bar{z}\bar{w}} < \gamma_{\text{CL}\bar{z}\bar{w},d}$, and the LMIs of (9.11) and (9.19), where $\bar{\mathbf{Q}} = \mathbf{Q}$ and $\bar{\mathbf{F}} = \mathbf{F}$. The controller gain is recovered by $\mathbf{K} = \mathbf{F}\mathbf{Q}^{-1}$.*

If it is desired to minimize the \mathcal{H}_∞ norm of $\bar{\mathbf{G}}_{\text{CL}zw}(s)$ while ensuring robust closed-loop input-output stability, the objective function $\mathcal{J}(\gamma_{\text{CL}\bar{z}\bar{w}}) = \gamma_{\text{CL}\bar{z}\bar{w}}$ is to be minimized when performing Synthesis Method 6.

9.3.3 Robust Performance

As discussed in Section 8.4.2, robust performance with the Large Gain Theorem is capable of robustly guaranteeing a lower bound on the least conservative minimum gain of the uncertain closed-loop transfer matrix defined with an upper LFT as

$$\begin{aligned}\mathbf{G}_{\text{CL}\Delta zw}(s) &= \mathcal{F}_u(\mathbf{G}_{\text{CL}}(s), \mathbf{\Delta}(s)) \\ &= \mathbf{G}_{\text{CL}zw}(s) + \mathbf{G}_{\text{CL}zp}(s)\mathbf{\Delta}(s) (\mathbf{1} - \mathbf{G}_{\text{CL}qp}(s)\mathbf{\Delta}(s))^{-1} \mathbf{G}_{\text{CL}qw}(s),\end{aligned}$$

which can be used to provide a guarantee that $\mathbf{G}_{\text{CL}\Delta zw}(s)$ is minimum phase. A full-state feedback controller that solves the robust performance problem is presented in this section.

The closed-loop plant with the full-state feedback controller is defined by the state-space equations in (9.5), (9.6), (9.7). It is assumed that $\mathbf{\Delta}$ is LTI and can be written as a transfer matrix $\mathbf{\Delta}(s)$. As outlined in Section 8.4.2, this is converted into the robust stabilization of the feedback interconnection involving $\tilde{\mathbf{\Delta}} = \text{diag}\{\mathbf{\Delta}, \mathbf{\Delta}_P\}$ and \mathbf{G}_{CL} , whose state-space equations are redefined as

$$\begin{aligned}\dot{\mathbf{x}}(t) &= \mathbf{A}_{\text{CL}}\mathbf{x}(t) + \tilde{\mathbf{B}}_3 \begin{bmatrix} \mathbf{p}(t) \\ \mathbf{w}(t) \end{bmatrix}, \\ \begin{bmatrix} \mathbf{q}(t) \\ \mathbf{z}(t) \end{bmatrix} &= \tilde{\mathbf{C}}_{\text{CL}3}\mathbf{x}(t) + \tilde{\mathbf{D}}_{33} \begin{bmatrix} \mathbf{p}(t) \\ \mathbf{w}(t) \end{bmatrix},\end{aligned}$$

where

$$\tilde{\mathbf{B}}_3 = \begin{bmatrix} \mathbf{B}_3 & \mathbf{B}_1 \end{bmatrix}, \quad \tilde{\mathbf{C}}_{\text{CL}3} = \begin{bmatrix} \mathbf{C}_{\text{CL}3} \\ \mathbf{C}_{\text{CL}1} \end{bmatrix} = \underbrace{\begin{bmatrix} \mathbf{C}_3 \\ \mathbf{C}_1 \end{bmatrix}}_{\tilde{\mathbf{C}}_3} - \underbrace{\begin{bmatrix} \mathbf{D}_{32} & \mathbf{D}_{12} \end{bmatrix}}_{\tilde{\mathbf{D}}_{32}} \mathbf{K}, \quad \tilde{\mathbf{D}}_{33} = \begin{bmatrix} \mathbf{D}_{33} & \mathbf{D}_{31} \\ \mathbf{D}_{13} & \mathbf{D}_{11} \end{bmatrix}.$$

Lemma 9.3. *The uncertain closed-loop transfer matrix $\mathbf{G}_{\text{CL}\Delta zw}(s)$ has minimum gain $0 < \nu_{\Delta_P}^{-1} < \infty$ for all $\mathbf{\Delta}$ with minimum gain $0 < \nu_{\Delta} < \infty$ if there exists $\mathbf{Q} = \mathbf{Q}^T > 0$, $\mathbf{F} = \mathbf{K}\mathbf{Q}$, and $0 < \nu_{\text{CL}} < \infty$ such that $1 < \nu_{\tilde{\Delta}}\nu_{\text{CL}} < \infty$ and*

$$\begin{bmatrix} \mathbf{A}\mathbf{Q} + \mathbf{Q}\mathbf{A}^T - \mathbf{B}_2\mathbf{F} - \mathbf{F}^T\mathbf{B}_2^T & \tilde{\mathbf{B}}_3 - \mathbf{Q}\tilde{\mathbf{C}}_3^T\tilde{\mathbf{D}}_{33} + \mathbf{F}^T\tilde{\mathbf{D}}_{32}^T\tilde{\mathbf{D}}_{33} \\ * & \nu_{\text{CL}}^2 \mathbf{1} - \tilde{\mathbf{D}}_{33}^T\tilde{\mathbf{D}}_{33} \end{bmatrix} \leq 0, \quad (9.20)$$

where $\tilde{\mathbf{\Delta}} = \text{diag}\{\mathbf{\Delta}, \mathbf{\Delta}_P\}$, $\mathbf{\Delta}_P$ has minimum gain $0 < \nu_{\Delta_P} < \infty$, and $0 < \nu_{\tilde{\Delta}} < \infty$ is a minimum gain of $\tilde{\mathbf{\Delta}}$.

Proof. From Lemma 9.1, the LMI in (9.20) is a sufficient condition for \mathbf{G}_{CL} to have minimum gain ν_{CL} . If this minimum gain satisfies $1 < \nu_{\tilde{\Delta}} \nu_{\text{CL}} < \infty$, then the feedback interconnection of \mathbf{G}_{CL} and $\tilde{\Delta}$ satisfies the Large Gain Theorem and it is known that $\mathbf{G}_{\text{CL}\Delta zw}(s)$ has minimum gain $0 < \nu_{\Delta P}^{-1} < \infty$ from Theorem 8.11. \square

Synthesis Method 7 (Robust Performance with Full-State Feedback). *Choose Δ_P to have minimum gain $0 < \nu_{\Delta P} < \infty$, preferably such that $0 < \nu_{\Delta} \leq \nu_{\Delta P} < \infty$, and define $\tilde{\Delta} = \text{diag}\{\Delta, \Delta_P\}$. Solve for $\mathbf{Q} = \mathbf{Q}^T > 0$, \mathbf{F} , and $0 < \nu_{\text{CL}}^2 < \infty$ satisfying $1 < \nu_{\tilde{\Delta}}^2 \nu_{\text{CL}}^2 < \infty$ and the LMI of (9.20), where $0 < \nu_{\tilde{\Delta}} < \infty$ is a minimum gain of $\tilde{\Delta}$. The controller gain is recovered by $\mathbf{K} = \mathbf{F}\mathbf{Q}^{-1}$.*

Performing Synthesis Method 7 with $0 < \nu_{\Delta P} < \infty$ ensures that $\mathbf{G}_{\text{CL}\Delta zw}(s)$ has nonzero minimum gain and is minimum phase.

Remark 9.4. When considering robust performance with $\nu_{\Delta P}^* \neq \nu_{\Delta}^*$, the controller synthesized with Synthesis Method 7 may be unnecessarily conservative, as $\nu_{\tilde{\Delta}}^*$, which is used for the robust performance condition, will be less than either $\nu_{\Delta P}^*$ or ν_{Δ}^* . In this case, it is useful to normalize the uncertainty block such that $\nu_{\tilde{\Delta}}^* = 1$ represents the limits of both Δ and Δ_P . This can be done by using $\mathbf{W}\mathbf{G}_{\text{CL}}$ instead of simply \mathbf{G}_{CL} in Lemma 9.3 and Synthesis Method 7, where $\mathbf{W} = \text{diag}\{\nu_{\Delta}^*, \nu_{\Delta P}^*\}$, which yields $\tilde{\Delta} = \text{diag}\{1/\nu_{\Delta}^* \Delta, 1/\nu_{\Delta P}^* \Delta_P\}$ and $\nu_{\tilde{\Delta}}^* = 1$.

9.4 Dynamic Feedback Controller Synthesis

Robust dynamic output feedback controller synthesis methods are presented in this section to solve robust stabilization and robust performance problems using the Large Gain Theorem. Although no general synthesis method is presented for the robust stabilization and nominal performance problem, a synthesis method is presented that is applicable to a special case of the problem.

9.4.1 Robust Stabilization

In order to guarantee robust input-output stability of the closed-loop system using the Large Gain Theorem, the dynamic output feedback controller \mathbf{G}_c is to be designed such that the transfer matrix $\mathbf{G}_{\text{CL}qp}(s) = \mathbf{C}_{\text{CL}3} (s\mathbf{I} - \mathbf{A}_{\text{CL}})^{-1} \mathbf{B}_{\text{CL}3} + \mathbf{D}_{\text{CL}33}$ has minimum gain $0 < \nu_{\text{CL}qp} < \infty$ satisfying $1 < \nu_{\Delta} \nu_{\text{CL}qp} < \infty$. The Minimum Gain Lemma is employed to determine a minimum gain of $\mathbf{G}_{\text{CL}qp}(s)$, which is any value of $0 < \nu_{\text{CL}qp} <$

∞ satisfying

$$\begin{bmatrix} \mathbf{P}\mathbf{A}_{\text{CL}} + \mathbf{A}_{\text{CL}}^{\text{T}}\mathbf{P} - \mathbf{C}_{\text{CL3}}^{\text{T}}\mathbf{C}_{\text{CL3}} & \mathbf{P}\mathbf{B}_{\text{CL3}} - \mathbf{C}_{\text{CL3}}^{\text{T}}\mathbf{D}_{\text{CL33}} \\ * & \nu_{\text{CLqp}}^2 \mathbf{1} - \mathbf{D}_{\text{CL33}}^{\text{T}}\mathbf{D}_{\text{CL33}} \end{bmatrix} \leq 0 \quad (9.21)$$

with $\mathbf{P} = \mathbf{P}^{\text{T}} \geq 0$, where \mathbf{A}_{CL} , \mathbf{B}_{CL3} , \mathbf{C}_{CL3} , and \mathbf{D}_{CL33} are defined in (8.4), (8.5), (8.6) and (8.7). The transfer matrix $\mathbf{G}_{\text{CLqp}}(s)$ is square, which makes the matrix inequality in (9.21) a necessary and sufficient condition for minimum gain. The matrix inequality of (9.21) is not an LMI in the design variables \mathbf{A}_c , \mathbf{B}_c , \mathbf{C}_c , and \mathbf{D}_c , so it must be transformed in order to yield a tractable controller synthesis method. An extensive transformation of the matrix inequality is performed, which is inspired by the change of variables in [97], to obtain the following synthesis method. Details of the transformation are found in the Appendix.

Synthesis Method 8 (Robust Stability with Dynamic Output Feedback). *Perform the following iterative steps.*

1. Set $\mathbf{X}_0 = \mathbf{1}$, $\mathbf{Y}_0 = \mathbf{0}$, $\mathbf{Z}_0 = \mathbf{0}$ and set $k = 0$.

2. Fix \mathbf{X}_k , \mathbf{Y}_k , \mathbf{Z}_k , and solve for $\mathbf{A}_{n,k}$, $\mathbf{B}_{n,k}$, $\mathbf{C}_{n,k}$, $\mathbf{D}_{n,k}$, $\mathbf{P}_{1,k} = \mathbf{P}_{1,k}^{\text{T}} > 0$, $\mathbf{Q}_{1,k} = \mathbf{Q}_{1,k}^{\text{T}} > 0$, and $0 < \nu_{\text{CLqp},k}^2 < \infty$ that maximize $\mathcal{J}(\nu_{\text{CLqp},k}^2) = \nu_{\text{CLqp},k}^2$ subject to

$$\begin{bmatrix} \mathbf{M}_{11} & \mathbf{M}_{12} & \mathbf{M}_{13} & \mathbf{Y}_k^{\text{T}} \\ * & \mathbf{M}_{22} & \mathbf{M}_{23} & \mathbf{Z}_k^{\text{T}} \\ * & * & \mathbf{M}_{33} & \mathbf{X}_k^{\text{T}} \\ * & * & * & -\mathbf{1} \end{bmatrix} < 0, \quad (9.22)$$

$$\begin{bmatrix} \mathbf{P}_{1,k} & \mathbf{1} \\ * & \mathbf{Q}_{1,k} \end{bmatrix} > 0, \quad (9.23)$$

where

$$\begin{aligned}
\mathbf{M}_{11} &= \mathbf{A}\mathbf{Q}_{1,k} + \mathbf{Q}_{1,k}\mathbf{A}^\top + \mathbf{B}_2\mathbf{C}_{n,k} + \mathbf{C}_{n,k}^\top\mathbf{B}_2^\top \\
&\quad - \mathbf{Y}_k^\top (\mathbf{C}_3\mathbf{Q}_{1,k} + \mathbf{D}_{32}\mathbf{C}_{n,k}) - (\mathbf{C}_3\mathbf{Q}_{1,k} + \mathbf{D}_{32}\mathbf{C}_{n,k})^\top \mathbf{Y}_k \\
\mathbf{M}_{12} &= \mathbf{A} + \mathbf{A}_{n,k}^\top + \mathbf{B}_2\mathbf{D}_{n,k}\mathbf{C}_2 - \mathbf{Y}_k^\top (\mathbf{C}_3 + \mathbf{D}_{32}\mathbf{D}_{n,k}\mathbf{C}_2) - (\mathbf{C}_3\mathbf{Q}_{1,k} + \mathbf{D}_{32}\mathbf{C}_{n,k})^\top \mathbf{Z}_k, \\
\mathbf{M}_{22} &= \mathbf{P}_{1,k}\mathbf{A} + \mathbf{A}^\top\mathbf{P}_{1,k} + \mathbf{B}_{n,k}\mathbf{C}_2 + \mathbf{C}_2^\top\mathbf{B}_{n,k}^\top \\
&\quad - \mathbf{Z}_k^\top (\mathbf{C}_3 + \mathbf{D}_{32}\mathbf{D}_{n,k}\mathbf{C}_2) - (\mathbf{C}_3 + \mathbf{D}_{32}\mathbf{D}_{n,k}\mathbf{C}_2)^\top \mathbf{Z}_k. \\
\mathbf{M}_{13} &= \mathbf{B}_3 + \mathbf{B}_2\mathbf{D}_{n,k}\mathbf{D}_{23} - (\mathbf{C}_3\mathbf{Q}_{1,k} + \mathbf{D}_{32}\mathbf{C}_{n,k})^\top \mathbf{X}_k - \mathbf{Y}_k^\top (\mathbf{D}_{33} + \mathbf{D}_{32}\mathbf{D}_{n,k}\mathbf{D}_{23}), \\
\mathbf{M}_{23} &= \mathbf{P}_{1,k}\mathbf{B}_3 + \mathbf{B}_{n,k}\mathbf{D}_{23} - (\mathbf{C}_3 + \mathbf{D}_{32}\mathbf{D}_{n,k}\mathbf{C}_2)^\top \mathbf{X}_k - \mathbf{Z}_k^\top (\mathbf{D}_{33} + \mathbf{D}_{32}\mathbf{D}_{n,k}\mathbf{D}_{23}), \\
\mathbf{M}_{33} &= \nu_{\text{CLqp},k}^2 \mathbf{1} - (\mathbf{D}_{33} + \mathbf{D}_{32}\mathbf{D}_{n,k}\mathbf{D}_{23})^\top \mathbf{X}_k - \mathbf{X}_k^\top (\mathbf{D}_{33} + \mathbf{D}_{32}\mathbf{D}_{n,k}\mathbf{D}_{23}).
\end{aligned}$$

3. Fix $\mathbf{A}_{n,k}$, $\mathbf{B}_{n,k}$, $\mathbf{C}_{n,k}$, $\mathbf{D}_{n,k}$, $\mathbf{P}_{1,k} = \mathbf{P}_{1,k}^\top > 0$, $\mathbf{Q}_{1,k} = \mathbf{Q}_{1,k}^\top > 0$, and solve for \mathbf{X}_k , \mathbf{Y}_k , \mathbf{Z}_k , and $0 < \nu_{\text{CLqp},k}^2 < \infty$ that maximize $\mathcal{J}(\nu_{\text{CLqp},k}^2) = \nu_{\text{CLqp},k}^2$ subject to (9.22).

4. If $1 < \nu_{\Delta}^2 \nu_{\text{CLqp},k}^2 < \infty$ is satisfied or $\left| \nu_{\text{CLqp},k}^2 - \nu_{\text{CLqp},k-1}^2 \right|$ is less than a specified tolerance, end. Otherwise, set $k = k + 1$ and repeat Steps 2) and 3).

The controller is recovered by

$$\mathbf{A}_c = \mathbf{A}_K - \mathbf{B}_c (\mathbf{1} - \mathbf{D}_{22}\mathbf{D}_c)^{-1} \mathbf{D}_{22}\mathbf{C}_c, \quad (9.24)$$

$$\mathbf{B}_c = \mathbf{B}_K (\mathbf{1} - \mathbf{D}_{22}\mathbf{D}_c), \quad (9.25)$$

$$\mathbf{C}_c = (\mathbf{1} - \mathbf{D}_c\mathbf{D}_{22}) \mathbf{C}_K, \quad (9.26)$$

$$\mathbf{D}_c = (\mathbf{1} + \mathbf{D}_K\mathbf{D}_{22})^{-1} \mathbf{D}_K, \quad (9.27)$$

where

$$\begin{bmatrix} \mathbf{A}_K & \mathbf{B}_K \\ \mathbf{C}_K & \mathbf{D}_K \end{bmatrix} = \begin{bmatrix} \mathbf{P}_{2,k} & \mathbf{P}_{1,k}\mathbf{B}_2 \\ \mathbf{0} & \mathbf{1} \end{bmatrix}^{-1} \left(\begin{bmatrix} \mathbf{A}_{n,k} & \mathbf{B}_{n,k} \\ \mathbf{C}_{n,k} & \mathbf{D}_{n,k} \end{bmatrix} - \begin{bmatrix} \mathbf{P}_{1,k}\mathbf{A}\mathbf{Q}_{1,k} & \mathbf{0} \\ \mathbf{0} & \mathbf{0} \end{bmatrix} \right) \begin{bmatrix} \mathbf{Q}_{2,k}^\top & \mathbf{0} \\ \mathbf{C}_2\mathbf{Q}_{1,k} & \mathbf{1} \end{bmatrix}^{-1},$$

and the matrices $\mathbf{P}_{2,k}$ and $\mathbf{Q}_{2,k}$ satisfy $\mathbf{P}_{2,k}\mathbf{Q}_{2,k} = \mathbf{1} - \mathbf{P}_{1,k}\mathbf{Q}_{1,k}$. The matrices $\mathbf{P}_{2,k}$ and $\mathbf{Q}_{2,k}$ can be found by solving a matrix decomposition problem, such as an LU decomposition, or simply choosing $\mathbf{P}_{2,k} = \mathbf{1}$ and $\mathbf{Q}_{2,k} = \mathbf{1} - \mathbf{P}_{1,k}\mathbf{Q}_{1,k}$.

A feasible solution to the robust stabilization problem is obtained if Synthesis Method 8 ends with $1 < \nu_{\Delta}^2 \nu_{\text{CLqp},k}^2 < \infty$ satisfied.

9.4.2 Robust Stabilization and Nominal Performance

The robust control problem of robust stabilization and nominal performance when the uncertainty has nonzero minimum gain is difficult with dynamic output feedback control. The change of variables used to obtain a tractable controller synthesis method for robust stabilization involved defining \mathbf{A}_κ , \mathbf{B}_κ , and \mathbf{C}_κ as functions of \mathbf{B}_2 and \mathbf{C}_2 . Following the inversion procedure to obtain the nominal performance transfer matrix in Section 8.3.2, the new matrices $\bar{\mathbf{B}}_2 = \mathbf{B}_2 - \mathbf{B}_3\mathbf{D}_{33}^{-1}\mathbf{D}_{32}$ and $\bar{\mathbf{C}}_2 = \mathbf{C}_2 - \mathbf{D}_{23}\mathbf{D}_{33}^{-1}\mathbf{C}_3$ are in general different from \mathbf{B}_2 and \mathbf{C}_3 . In order to satisfy both the Minimum Gain Lemma for robust stability and the Bounded Real Lemma for nominal performance with the same controller, the change of variables must be identical, which is not possible when $\bar{\mathbf{B}}_2 \neq \mathbf{B}_2$ and $\bar{\mathbf{C}}_2 \neq \mathbf{C}_2$. It may be possible to solve this problem using a projection-based controller synthesis method, as in [39, 49], but this is beyond the scope of the work in this dissertation.

In the case where $\bar{\mathbf{B}}_2 = \mathbf{B}_2$, $\bar{\mathbf{C}}_2 = \mathbf{C}_2$ and Δ^{-1} has a minimum gain of zero, the following controller synthesis method can be performed to ensure that the \mathcal{H}_∞ norm of the closed-loop transfer matrix from $\mathbf{w}(s)$ to $\mathbf{z}(s)$ without uncertainty is less than $0 < \gamma_{\text{CL}\bar{z}\bar{w},d} < \infty$. The synthesis method involves the inverted state-space matrices $\bar{\mathbf{A}}$, $\bar{\mathbf{B}}_1$, $\bar{\mathbf{C}}_1$, $\bar{\mathbf{D}}_{11}$, $\bar{\mathbf{D}}_{12}$ defined in (9.12), (9.13), (9.16), (9.17), and (9.18), as well as the matrices $\bar{\mathbf{D}}_{21} = \mathbf{D}_{21} - \mathbf{D}_{23}\mathbf{D}_{33}^{-1}\mathbf{D}_{31}$ and $\bar{\mathbf{D}}_{22} = \mathbf{D}_{22} - \mathbf{D}_{23}\mathbf{D}_{33}^{-1}\mathbf{D}_{32}$.

Synthesis Method 9 (Robust Stability and Nominal Performance with Dynamic Output Feedback). *Perform the following iterative steps.*

1. Set $\mathbf{X}_0 = \mathbf{1}$, $\mathbf{Y}_0 = \mathbf{0}$, $\mathbf{Z}_0 = \mathbf{0}$ and set $k = 0$.
2. Fix \mathbf{X}_k , \mathbf{Y}_k , \mathbf{Z}_k , and solve for $\mathbf{A}_{n,k}$, $\mathbf{B}_{n,k}$, $\mathbf{C}_{n,k}$, $\mathbf{D}_{n,k}$, $\mathbf{P}_{1,k} = \mathbf{P}_{1,k}^\top > 0$, $\mathbf{Q}_{1,k} = \mathbf{Q}_{1,k}^\top > 0$, $0 < \nu_{\text{CLqp},k}^2 < \infty$, and $0 < \gamma_{\text{CL}\bar{z}\bar{w},k} < \infty$ that maximize $\mathcal{J}(\nu_{\text{CLqp},k}^2) = \nu_{\text{CLqp},k}^2$ subject to (9.22), (9.23), $\gamma_{\text{CL}\bar{z}\bar{w},k} < \gamma_{\text{CL}\bar{z}\bar{w},d}$, and

$$\begin{bmatrix} \mathbf{N}_{11} & \bar{\mathbf{A}} + \mathbf{A}_{n,k}^\top + \mathbf{B}_2\mathbf{D}_{n,k}\mathbf{C}_2 & \bar{\mathbf{B}}_1 + \mathbf{B}_2\mathbf{D}_{n,k}\mathbf{D}_{21} & \mathbf{Q}_{1,k}^\top\bar{\mathbf{C}}_1^\top + \mathbf{C}_{n,k}^\top\bar{\mathbf{D}}_{12}^\top \\ * & \mathbf{N}_{22} & \mathbf{P}_{1,k}\mathbf{B}_1 + \mathbf{B}_{n,k}\bar{\mathbf{D}}_{21} & \bar{\mathbf{C}}_1^\top + \mathbf{C}_2^\top\mathbf{D}_{n,k}^\top\bar{\mathbf{D}}_{12}^\top \\ * & * & -\gamma_{\text{CL}\bar{z}\bar{w}}\mathbf{1} & \bar{\mathbf{D}}_{11}^\top + \bar{\mathbf{D}}_{21}^\top\mathbf{D}_{n,k}^\top\bar{\mathbf{D}}_{12}^\top \\ * & * & * & -\gamma_{\text{CL}\bar{z}\bar{w}}\mathbf{1} \end{bmatrix} < 0, \quad (9.28)$$

where $\mathbf{N}_{11} = \bar{\mathbf{A}}\mathbf{Q}_{1,k} + \mathbf{Q}_{1,k}\bar{\mathbf{A}}^\top + \mathbf{B}_2\mathbf{C}_{n,k} + \mathbf{C}_{n,k}^\top\mathbf{B}_2^\top$ and $\mathbf{N}_{22} = \mathbf{P}_{1,k}\bar{\mathbf{A}} + \bar{\mathbf{A}}^\top\mathbf{P}_{1,k} + \mathbf{B}_{n,k}\mathbf{C}_2 + \mathbf{C}_2^\top\mathbf{B}_{n,k}^\top$.

3. Fix $\mathbf{A}_{n,k}$, $\mathbf{B}_{n,k}$, $\mathbf{C}_{n,k}$, $\mathbf{D}_{n,k}$, $\mathbf{P}_1 = \mathbf{P}_1^\top > 0$, $\mathbf{Q}_{1,k} = \mathbf{Q}_{1,k}^\top > 0$, and solve for \mathbf{X}_k , \mathbf{Y}_k ,

\mathbf{z}_k , and $0 < \nu_{\text{CL}qp,k}^2 < \infty$, and $0 < \gamma_{\text{CL}zw} < \infty$ that maximize $\mathcal{J}(\nu_{\text{CL}qp,k}^2) = \nu_{\text{CL}qp,k}^2$ subject to (9.22), $\gamma_{\text{CL}\bar{z}\bar{w}} < \gamma_{\text{CL}\bar{z}\bar{w},d}$, and (9.28).

4. If $1 < \nu_{\Delta}^2 \nu_{\text{CL}qp,k}^2 < \infty$ is satisfied or $\left| \nu_{\text{CL}qp,k}^2 - \nu_{\text{CL}qp,k-1}^2 \right|$ is less than a specified tolerance, end. Otherwise, set $k = k + 1$ and repeat Steps 2) and 3).

The controller is recovered as done in (9.24), (9.25), (9.26), and (9.27).

A feasible solution to the robust stabilization and nominal performance problem is only obtained if Synthesis Method 9 ends with $1 < \nu_{\Delta}^2 \nu_{\text{CL}qp,k}^2 < \infty$ satisfied.

9.4.3 Robust Performance

Robust performance with the Large Gain Theorem provides a guarantee of a lower bound on the least conservative minimum gain of the uncertain closed-loop system $\mathbf{G}_{\text{CL}\Delta zw}$ for all Δ with minimum gain $0 < \nu_{\Delta} < \infty$. As shown in Section 8.4.2, this robust performance problem can be converted into the robust stabilization of a feedback interconnection involving $\tilde{\Delta} = \text{diag}\{\Delta, \Delta_P\}$ and \mathbf{G}_{CL} , whose state-space equations are

$$\begin{aligned} \dot{\mathbf{x}}(t) &= \mathbf{A}_{\text{CL}} \mathbf{x}(t) + \tilde{\mathbf{B}}_{\text{CL}3} \begin{bmatrix} \mathbf{p}(t) \\ \mathbf{w}(t) \end{bmatrix}, \\ \begin{bmatrix} \mathbf{q}(t) \\ \mathbf{z}(t) \end{bmatrix} &= \tilde{\mathbf{C}}_{\text{CL}3} \mathbf{x}(t) + \tilde{\mathbf{D}}_{\text{CL}33} \begin{bmatrix} \mathbf{p}(t) \\ \mathbf{w}(t) \end{bmatrix}. \end{aligned}$$

The state-space matrices $\tilde{\mathbf{B}}_{\text{CL}3}$, $\tilde{\mathbf{C}}_{\text{CL}3}$, and $\tilde{\mathbf{D}}_{\text{CL}33}$ are functions of the matrices $\tilde{\mathbf{B}}_3$, $\tilde{\mathbf{C}}_3$, $\tilde{\mathbf{D}}_{32}$, and $\tilde{\mathbf{D}}_{33}$, which were defined in Section 9.3.3, as well as the matrix

$$\tilde{\mathbf{D}}_{32} = \begin{bmatrix} \mathbf{D}_{32} \\ \mathbf{D}_{12} \end{bmatrix}.$$

Robust input-output stability of this feedback interconnection is guaranteed by the Large Gain Theorem provided $1 < \nu_{\tilde{\Delta}} \nu_{\text{CL}} < \infty$, where $\nu_{\tilde{\Delta}}$ is a minimum gain of $\tilde{\Delta}$ and ν_{CL} is a minimum gain of \mathbf{G}_{CL} . Robust input-output stability of the feedback interconnection ensures that the least conservative minimum gain of $\mathbf{G}_{\text{CL}\Delta zw}$ is greater than $\nu_{\Delta_P}^{-1}$, where $0 < \nu_{\Delta_P} < \infty$ is a minimum gain of Δ_P . The following controller synthesis method for robust performance is based on Synthesis Method 8 for robust stabilization.

Synthesis Method 10 (Robust Performance with Dynamic Output Feedback). *Perform the following iterative steps.*

1. Set $\mathbf{X}_0 = \mathbf{1}$, $\mathbf{Y}_0 = \mathbf{0}$, $\mathbf{Z}_0 = \mathbf{0}$ and set $k = 0$.
2. Fix \mathbf{X}_k , \mathbf{Y}_k , \mathbf{Z}_k , and solve for $\mathbf{A}_{n,k}$, $\mathbf{B}_{n,k}$, $\mathbf{C}_{n,k}$, $\mathbf{D}_{n,k}$, $\mathbf{P}_{1,k} = \mathbf{P}_{1,k}^\top > 0$, $\mathbf{Q}_{1,k} = \mathbf{Q}_{1,k}^\top > 0$, and $0 < \nu_{\text{CL},k}^2 < \infty$ that maximize $\mathcal{J}(\nu^2) = \nu_{\text{CL},k}^2$ subject to (9.22) and (9.23) where the terms in (9.22) are redefined as

$$\begin{aligned} \mathbf{M}_{11} &= \mathbf{A}\mathbf{Q}_{1,k} + \mathbf{Q}_{1,k}\mathbf{A}^\top + \mathbf{B}_2\mathbf{C}_n + \mathbf{C}_n^\top\mathbf{B}_2^\top \\ &\quad - \mathbf{Y}_k^\top \left(\tilde{\mathbf{C}}_3\mathbf{Q}_{1,k} + \tilde{\mathbf{D}}_{32}\mathbf{C}_n \right) - \left(\tilde{\mathbf{C}}_3\mathbf{Q}_{1,k} + \tilde{\mathbf{D}}_{32}\mathbf{C}_n \right)^\top \mathbf{Y}_k \\ \mathbf{M}_{12} &= \mathbf{A} + \mathbf{A}_n^\top + \mathbf{B}_2\mathbf{D}_n\mathbf{C}_2 - \mathbf{Y}_k^\top \left(\tilde{\mathbf{C}}_3 + \tilde{\mathbf{D}}_{32}\mathbf{D}_n\mathbf{C}_2 \right) - \left(\tilde{\mathbf{C}}_3\mathbf{Q}_{1,k} + \tilde{\mathbf{D}}_{32}\mathbf{C}_n \right)^\top \mathbf{Z}_k, \\ \mathbf{M}_{22} &= \mathbf{P}_{1,k}\mathbf{A} + \mathbf{A}^\top\mathbf{P}_{1,k} + \mathbf{B}_n\mathbf{C}_2 + \mathbf{C}_2^\top\mathbf{B}_n^\top \\ &\quad - \mathbf{Z}_k^\top \left(\tilde{\mathbf{C}}_3\mathbf{Q}_{1,k} + \tilde{\mathbf{D}}_{32}\mathbf{C}_n \right) - \left(\tilde{\mathbf{C}}_3\mathbf{Q}_{1,k} + \tilde{\mathbf{D}}_{32}\mathbf{C}_n \right)^\top \mathbf{Z}_k. \\ \mathbf{M}_{13} &= \tilde{\mathbf{B}}_3 + \mathbf{B}_2\mathbf{D}_n\tilde{\mathbf{D}}_{23} - \left(\tilde{\mathbf{C}}_3\mathbf{Q}_{1,k} + \tilde{\mathbf{D}}_{32}\mathbf{C}_n \right)^\top \mathbf{X}_k - \mathbf{Y}_k^\top \left(\tilde{\mathbf{D}}_{33} + \tilde{\mathbf{D}}_{32}\mathbf{D}_n\tilde{\mathbf{D}}_{23} \right), \\ \mathbf{M}_{23} &= \mathbf{P}_{1,k}\tilde{\mathbf{B}}_3 + \mathbf{B}_n\tilde{\mathbf{D}}_{23} - \left(\tilde{\mathbf{C}}_3 + \tilde{\mathbf{D}}_{32}\mathbf{D}_n\mathbf{C}_2 \right)^\top \mathbf{X}_k - \mathbf{Z}_k^\top \left(\tilde{\mathbf{D}}_{33} + \tilde{\mathbf{D}}_{32}\mathbf{D}_n\tilde{\mathbf{D}}_{23} \right), \\ \mathbf{M}_{33} &= \nu_{\text{CL},k}^2 \mathbf{1} - \left(\tilde{\mathbf{D}}_{33} + \tilde{\mathbf{D}}_{32}\mathbf{D}_n\tilde{\mathbf{D}}_{23} \right)^\top \mathbf{X}_k - \mathbf{X}_k^\top \left(\tilde{\mathbf{D}}_{33} + \tilde{\mathbf{D}}_{32}\mathbf{D}_n\tilde{\mathbf{D}}_{23} \right). \end{aligned}$$

3. Fix $\mathbf{A}_{n,k}$, $\mathbf{B}_{n,k}$, $\mathbf{C}_{n,k}$, $\mathbf{D}_{n,k}$, $\mathbf{P}_{1,k} = \mathbf{P}_{1,k}^\top > 0$, $\mathbf{Q}_{1,k} = \mathbf{Q}_{1,k}^\top > 0$, and solve for \mathbf{X}_k , \mathbf{Y}_k , \mathbf{Z}_k , and $0 < \nu_{\text{CL},k}^2 < \infty$ that maximize $\mathcal{J}(\nu_{\text{CL},k}^2) = \nu_{\text{CL},k}^2$ subject to (9.22), where the terms in (9.22) are defined in Step 2.
4. If $1 < \nu_{\Delta}^2 \nu_{\text{CL},k}^2 < \infty$ is satisfied, where $0 < \nu_{\Delta} < \infty$ is a minimum gain of $\tilde{\Delta}$, or $\left| \nu_{\text{CL},k}^2 - \nu_{\text{CL},k-1}^2 \right|$ is less than a specified tolerance, end. Otherwise, set $k = k + 1$ and repeat Steps 2) and 3).

The controller is recovered as done in (9.24), (9.25), (9.26), and (9.27).

If Synthesis Method 10 yields a feasible dynamic output feedback controller (i.e., the synthesis method ends with $1 < \nu_{\Delta}^2 \nu_{\text{CL},k}^2 < \infty$) for a nonzero minimum gain $\nu_{\Delta P}$, the uncertain closed-loop transfer matrix $\mathbf{G}_{\text{CL}_{\Delta zw}}(s)$ is minimum phase for all Δ with minimum gain $0 < \nu_{\Delta} < \infty$.

As discussed in Remark 9.4 for robust performance with full-state feedback, normalization of the uncertainty is necessary to limit the conservatism of Synthesis Method 10.

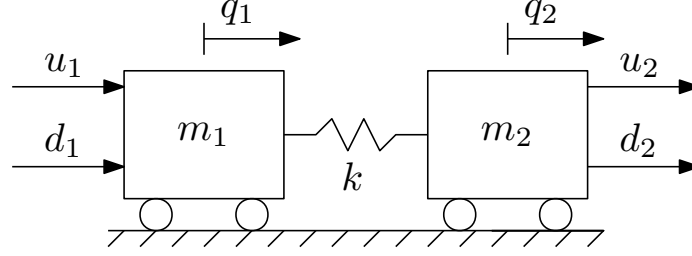


Figure 9.2: Schematic of the mass-spring system from the numerical example of Section 9.5

9.5 Numerical Example

Consider the single DOF mass-spring system shown in Figure 9.2. It is similar to the mass-spring system in the numerical example of Section 5.4.1, but with a rigid-body mode, without any damping, and with absolute coordinates instead of relative coordinates. This example is taken from the benchmark problem for robust control design found in [77]. The equations of motion of the system in state-space form are given by

$$\dot{\mathbf{x}}(t) = \begin{bmatrix} 0 & 0 & 1 & 0 \\ 0 & 0 & 0 & 1 \\ -k/m_1 & k/m_1 & 0 & 0 \\ k/m_2 & -k/m_2 & 0 & 0 \end{bmatrix} \mathbf{x}(t) + \begin{bmatrix} 0 & 0 \\ 0 & 0 \\ 1/m_1 & 0 \\ 0 & 1/m_2 \end{bmatrix} \mathbf{d}(t) + \begin{bmatrix} 0 & 0 \\ 0 & 0 \\ 1/m_1 & 0 \\ 0 & 1/m_2 \end{bmatrix} \mathbf{u}(t),$$

where the state is $\mathbf{x}^\top(t) = [q_1(t) \ q_2(t) \ \dot{q}_1(t) \ \dot{q}_2(t)]$, the control input is $\mathbf{u}^\top(t) = [u_1(t) \ u_2(t)]$, the disturbance is $\mathbf{d}^\top(t) = [d_1(t) \ d_2(t)]$, $q_1(t)$ is the position of the first mass m_1 , $q_2(t)$ is the position of the second mass m_2 , k is the stiffness coefficient of the spring between the masses, $u_1(t)$ is the force applied to the first mass, $u_2(t)$ is the force applied to the second mass, $d_1(t)$ is the disturbance force acting on the first mass, and $d_2(t)$ is the disturbance force acting on the second mass. A measurement of the position of the second mass is available, given by the expression

$$y(t) = q_2(t) + n(t) = \begin{bmatrix} 0 & 1 & 0 & 0 \end{bmatrix} \mathbf{x}(t) + n(t),$$

where $n(t)$ is measurement noise.

The nominal system is given by $m_1 = m_2 = 1$ kg and a stiffness coefficient of $k = 1$ N/m. The stiffness coefficient is uncertain, but known to be 0.5 N/m $\leq k \leq 2$ N/m, and as a result can be written as $k = k_0 + \Delta k$, where k_0 is a nominal

value that is not necessarily $k_0 = 1$ N/m and Δk represents the uncertainty in the stiffness coefficient. The stiffness coefficient uncertainty is only present in the system's equations of motion, which can be rewritten as [113–115]

$$\dot{\mathbf{x}}(t) = (\mathbf{A} + \mathbf{B}_3 \Delta k \mathbf{C}_3) \mathbf{x}(t) + \mathbf{B}_1 \mathbf{w}(t) + \mathbf{B}_2 \mathbf{u}(t),$$

where $\mathbf{w}^\top(t) = [d_1(t) \ d_2(t) \ n(t)]$, $\mathbf{C}_3 = [1 \ -1 \ 0 \ 0]$,

$$\mathbf{A} = \begin{bmatrix} 0 & 0 & 1 & 0 \\ 0 & 0 & 0 & 1 \\ -k_0/m_1 & k_0/m_1 & 0 & 0 \\ k_0/m_2 & -k_0/m_2 & 0 & 0 \end{bmatrix}, \quad \mathbf{B}_1 = \begin{bmatrix} 0 & 0 & 0 \\ 0 & 0 & 0 \\ 1/m_1 & 0 & 0 \\ 0 & 1/m_2 & 0 \end{bmatrix},$$

$$\mathbf{B}_2 = \begin{bmatrix} 0 & 0 \\ 0 & 0 \\ 1/m_1 & 0 \\ 0 & 1/m_2 \end{bmatrix}, \quad \mathbf{B}_3 = \begin{bmatrix} 0 \\ 0 \\ -1/m_1 \\ 1/m_2 \end{bmatrix}.$$

Defining $p(t) = \Delta k q(t)$, the generalized plant \mathbf{G} with uncertainty is written as

$$\dot{\mathbf{x}}(t) = \mathbf{A}\mathbf{x}(t) + \mathbf{B}_1 \mathbf{w}(t) + \mathbf{B}_2 \mathbf{u}(t) + \mathbf{B}_3 p(t), \quad (9.29)$$

$$z(t) = \mathbf{C}_1 \mathbf{x}(t) + \mathbf{D}_{11} \mathbf{w}(t), \quad (9.30)$$

$$y(t) = \mathbf{C}_2 \mathbf{x}(t) + \mathbf{D}_{21} \mathbf{w}(t), \quad (9.31)$$

$$q(t) = \mathbf{C}_3 \mathbf{x}(t), \quad (9.32)$$

where $\mathbf{C}_2 = [0 \ 1 \ 0 \ 0]$, $\mathbf{D}_{21} = [0 \ 0 \ 1]$, $\mathbf{C}_1 = [0 \ 1 \ 0 \ 0]$, and $\mathbf{D}_{11} = [0.01 \ 0 \ 0]$. The performance signal is the position of the first mass with a small feedforward from the disturbance force acting on the first mass. The feedforward term \mathbf{D}_{11} is added to allow for a feasible robust performance problem when using the Large Gain Theorem in Sections 9.5.3 and 9.5.4 when considering robust performance. For the purposes of this example, the feedforward term is arbitrarily chosen, but could in fact be optimally synthesized using one of the synthesis methods from Chapter 4. In order to make a fair comparison, the feedforward term is also included when considering robust performance with the Small Gain Theorem, although the term is not necessary to solve the robust performance problem in this case.

The value of k_0 can be chosen such that $|\Delta k| \leq \gamma_\Delta$ for 0.5 N/m $\leq k \leq 2$ N/m. Choosing $k_0 = 1.25$ N/m for this particular example leads to $|\Delta k| \leq 0.75$ N/m. The

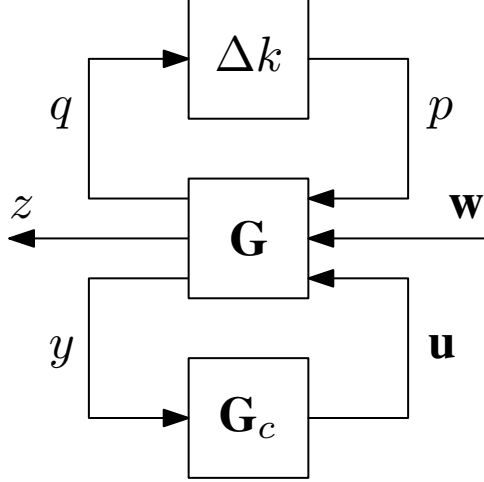


Figure 9.3: Block diagram of the generalized plant \mathbf{G} and uncertainty Δk in the numerical example of Section 9.5.

generalized plant defined by (9.29), (9.30), (9.31), (9.32), and the uncertainty Δk are suitable for robust control with the Small Gain Theorem, since the magnitude of Δk has an upper bound. In order to yield a robust control problem suitable for the Large Gain Theorem, the uncertainty and the generalized plant must be inverted, which is not directly possible since $D_{33} = 0$ in this example. A loop transformation [40, pp. 174–177] is applied to the uncertainty and the generalized plant, which yields a new uncertainty block $\Delta \hat{k} = \Delta k / (1 + \Delta k D_{33})$ and a new robustness channel output $\hat{q}(t) = \mathbf{C}_3 \mathbf{x}(t) + D_{33} p(t)$, giving $p(t) = \Delta \hat{k} \hat{q}(t)$ as shown in Figure 9.4. The uncertain system obtained after performing the loop transformation is equivalent to the original system, with only the signal $\hat{q}(t)$ differing from the original signal $q(t)$. Assuming that $0 < D_{33} < 1$ and knowing $|\Delta k| \leq \gamma_\Delta$, the gain of the new uncertainty is bounded by $|\Delta \hat{k}| \leq \gamma_\Delta / (1 - \gamma_\Delta D_{33})$. Choosing $D_{33} = 0.1$ and $k_0 = 1.25$ N/m yields $|\Delta \hat{k}| \leq 0.811$. The selection of D_{33} is made such that $0 < D_{33} |\Delta \hat{k}| < 1$, which is a necessary condition for a robustly stabilizing controller to be synthesized using the Small Gain Theorem or with the Large Gain Theorem after inversion in this particular example since $\mathbf{D}_{23} = \mathbf{0}$, $\mathbf{D}_{32} = \mathbf{0}$, and $D_{\text{CL}33} = D_{33} + \mathbf{D}_{32} \mathbf{D}_c \mathbf{D}_{23} = D_{33}$.

The uncertainty and generalized plant are inverted as shown in Figure 9.5, yielding

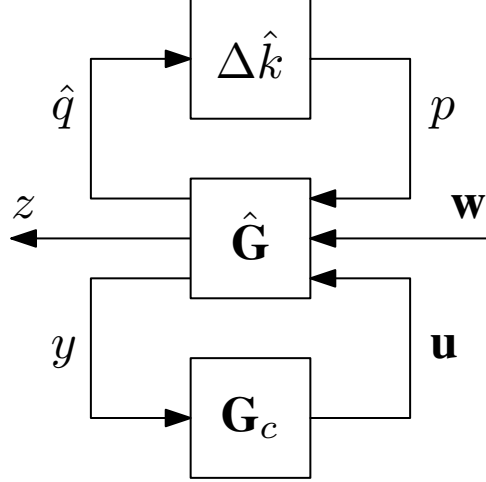


Figure 9.4: Block diagram of the generalized plant $\hat{\mathbf{G}}$ and uncertainty $\Delta\hat{k} = \Delta k / (1 + \Delta k D_{33})$ following a loop transformation in the numerical example of Section 9.5.

$\Delta\bar{k} = \Delta\hat{k}^{-1}$ and a generalized plant $\bar{\mathbf{G}}$ with state-space realization

$$\dot{\mathbf{x}}(t) = (\mathbf{A} - \mathbf{B}_3 D_{33}^{-1} \mathbf{C}_3) \mathbf{x}(t) + \mathbf{B}_1 \mathbf{w}(t) + \mathbf{B}_2 \mathbf{u}(t) + \mathbf{B}_3 D_{33}^{-1} \hat{q}(t), \quad (9.33)$$

$$z(t) = \mathbf{C}_1 \mathbf{x}(t) + \mathbf{D}_{11} \mathbf{w}(t), \quad (9.34)$$

$$y(t) = \mathbf{C}_2 \mathbf{x}(t) + \mathbf{D}_{21} \mathbf{w}(t), \quad (9.35)$$

$$p(t) = -D_{33}^{-1} \mathbf{C}_3 \mathbf{x}(t) + D_{33}^{-1} \hat{q}(t), \quad (9.36)$$

where $\hat{q}(t) = \Delta\bar{k}p(t)$ and $|\Delta\bar{k}| \geq (1 - \gamma_\Delta D_{33}) / \gamma_\Delta = 1.23$. The uncertainty and generalized plant are now in a form that is suitable for the Large Gain Theorem.

In the following sections, the generalized plant \mathbf{G} , whose state-space equations are defined in (9.29), (9.30), (9.31), (9.32), and the generalized plant $\bar{\mathbf{G}}$, whose state-space equations are defined in (9.33), (9.34), (9.35), (9.36), are used to solve the robust stabilization and robust performance problems using \mathcal{H}_∞ robust control techniques and the Large Gain Theorem-based controller synthesis methods from Sections 9.3 and 9.4. Both full-state feedback and dynamic output feedback controllers are implemented in the numerical examples. Although a full-state feedback robust stabilization and nominal performance controller synthesis method was presented in Section 9.3.2, robust stabilization and nominal performance is not considered in this numerical example as a general dynamic feedback controller synthesis method is lacking for this problem and robust performance is considered for this example, which is typically a more practical result.

The numerical calculations of this section are performed in MATLAB using YALMIP [64],

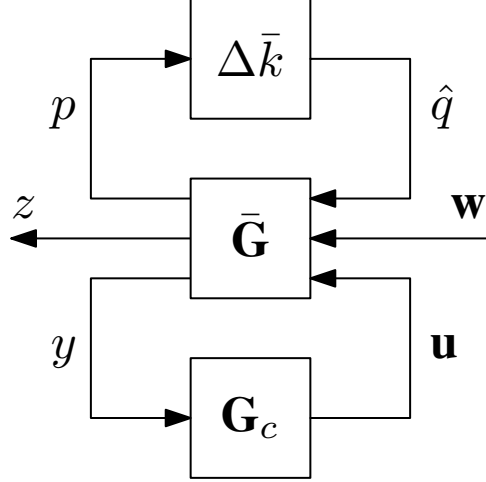


Figure 9.5: Block diagram of the inverted generalized plant $\bar{\mathbf{G}}$ and uncertainty $\Delta\bar{k} = \Delta\hat{k}^{-1}$ in the numerical example of Section 9.5.

SDPT3 [65], SeDuMi [76], and MOSEK [116].

9.5.1 Robust Stabilization with Full-State Feedback

Robust stabilization with full-state feedback using either the Small Gain Theorem or Large Gain Theorem is considered in this section.

When performing robust stabilization using the Small Gain Theorem, a full-state feedback controller is to be designed such that the transfer matrix $\mathbf{G}_{\text{CL}qp}(s) = \mathbf{C}_{\text{CL}3}(s\mathbf{1} - \mathbf{A}_{\text{CL}})^{-1}\mathbf{B}_3$ has an \mathcal{H}_∞ norm less than $1/\gamma_\Delta = 4/3$. Using the LMI \mathcal{H}_∞ controller synthesis method from [49], a robust full-state feedback controller is synthesized as

$$\mathbf{K}_{\mathcal{H}_\infty} = \begin{bmatrix} 2.91 & -1.90 & 1.74 & -1.70 \\ -0.76 & 2.33 & -0.016 & 1.73 \end{bmatrix},$$

yielding a closed-loop \mathcal{H}_∞ norm of $\gamma_{\text{CL}qp} = 0.32$ and an upper gain margin of 4.1 using the Small Gain Theorem. It is shown numerically by gridding the space of possible values of k that the closed-loop system is robustly stable for $-2.05 \text{ N/m} \leq k < \infty$. In order to maximize the closed-loop system's stability margin, the same controller synthesis method is performed such that the \mathcal{H}_∞ norm of $\mathbf{G}_{\text{CL}qp}(s)$ is minimized, giving

$$\mathbf{K}_{\mathcal{H}_\infty}^* = 10^2 \cdot \begin{bmatrix} 9.19 \times 10^5 & -9.19 \times 10^5 & 2.49 & -2.49 \\ -9.19 \times 10^5 & 9.19 \times 10^5 & -2.47 & 2.49 \end{bmatrix},$$

a closed-loop \mathcal{H}_∞ norm of $\gamma_{\text{CL}qp} = 2.97 \times 10^{-7}$, and an upwards gain margin of 4.49×10^6 using the Small Gain Theorem. It is shown numerically that the closed-loop system

Table 9.1: Robustness properties of the closed-loop system with full-state feedback designed for robust stabilization in Section 9.5.1, including the gain margin for robust stability using either the Small Gain Theorem or Large Gain Theorem and the range of k for which the closed-loop system is asymptotically stable.

Method	Gain Margin	Asymptotically Stable
Small Gain	4.1	$-2.05 \leq k < \infty$
Large Gain	12.0	$-539 \leq k < \infty$
Optimal Small Gain	4.49×10^6	$-9.19 \times 10^7 \leq k < \infty$
Optimal Large Gain	12.3	$-6.42 \times 10^8 \leq k < \infty$

is robustly stable for $-9.19 \times 10^7 \text{ N/m} \leq k < \infty$. The robustness properties of the closed-loop system with $\mathbf{K}_{\mathcal{H}\infty}$ and $\mathbf{K}_{\mathcal{H}\infty}^*$ are summarized in Table 9.1.

When performing robust stabilization using the Large Gain Theorem, a full-state feedback controller is to be designed such that the transfer matrix $\bar{\mathbf{G}}_{\text{CL}p\hat{q}}(s) = \bar{\mathbf{C}}_{\text{CL}3} (s\mathbf{1} - \bar{\mathbf{A}}_{\text{CL}})^{-1} \bar{\mathbf{B}}_3 + \bar{\mathbf{D}}_{33}$ has minimum gain greater than $1/\nu_{\bar{\Delta}} = 0.811$. Performing Synthesis Method 5 gives

$$\mathbf{K}_{\nu} = \begin{bmatrix} 5.41 \times 10^2 & -5.40 \times 10^2 & 6.65 & -6.01 \\ -5.37 \times 10^2 & 5.39 \times 10^2 & -5.52 & 6.64 \end{bmatrix},$$

a least conservative minimum gain of $\nu_{\text{CL}p\hat{q}}^* = 9.70$, and a lower gain margin of 12.0. Numerically it is shown that the closed-loop system is robustly stable for $-539.5 \text{ N/m} \leq k < \infty$. Synthesis Method 5 is performed again with the maximization of the objective function $\mathcal{J}(\nu_{\text{CL}p\hat{q}}) = \nu_{\text{CL}p\hat{q}}$, yielding

$$\mathbf{K}_{\nu}^* = 10^4 \cdot \begin{bmatrix} 6.43 \times 10^4 & -6.43 \times 10^4 & 4.69 & -4.69 \\ -6.43 \times 10^4 & 6.43 \times 10^4 & -4.69 & 4.69 \end{bmatrix},$$

a least conservative minimum gain of $\nu_{\text{CL}p\hat{q}}^* = 10$, and a lower gain margin of 12.3. Numerically it is shown that the closed-loop system is robustly stable for $-6.42 \times 10^8 \text{ N/m} \leq k < \infty$. The robustness properties of the closed-loop system with \mathbf{K}_{ν} and \mathbf{K}_{ν}^* are summarized in Table 9.1.

9.5.2 Robust Stabilization with Dynamic Output Feedback

Robust stabilization with dynamic output feedback using both the Small Gain Theorem and Large Gain Theorem is considered in this section. The control input $u_2(t)$ is not used in the design of the dynamic output feedback controllers, in an effort

Table 9.2: Robustness properties of the closed-loop system with dynamic output feedback designed for robust stabilization in Section 9.5.2, including the gain margin for robust stability using either the Small Gain Theorem or Large Gain Theorem and the range of k for which the closed-loop system is asymptotically stable.

Method	Gain Margin	Asymptotically Stable
Small Gain	1.10	$0.301 \leq k \leq 3.376$
Large Gain	1.19	$0.171 \leq k \leq 15.94$
Optimal Small Gain	1.66	$0.01 \leq k \leq 2.917$
Optimal Large Gain	1.29	$0.003 \leq k \leq 2.664$

to replicated the robust stabilization benchmark problem in [77].

When performing robust stabilization using the Small Gain Theorem, a dynamic output feedback controller is to be designed such that the transfer matrix $\mathbf{G}_{\text{CL}qp}(s) = \mathbf{C}_{\text{CL}3} (s\mathbf{1} - \mathbf{A}_{\text{CL}})^{-1} \mathbf{B}_{\text{CL}3}$ has an \mathcal{H}_∞ norm less than $1/\gamma_\Delta = 4/3$. Following the LMI \mathcal{H}_∞ controller synthesis method in [97], a dynamic output feedback controller is synthesized as

$$G_{c,\mathcal{H}_\infty}(s) = \frac{-182.8s^3 + 661.5s^2 - 66s - 14.31}{s^4 + 8.24s^3 + 73.24s^2 + 198.9s + 504.7},$$

yielding a closed-loop \mathcal{H}_∞ norm of $\gamma_{\text{CL}qp} = 1.21$ and an upper gain margin of 1.10 using the Small Gain Theorem. It is shown numerically that the closed-loop system is robustly stable for $0.301 \text{ N/m} \leq k \leq 3.376 \text{ N/m}$. In order to maximize the closed-loop system's stability margin, the same controller synthesis method is performed such that the \mathcal{H}_∞ norm of $\mathbf{G}_{\text{CL}qp}(s)$ is minimized, giving

$$G_{c,\mathcal{H}_\infty}^*(s) = \frac{-3.24 \times 10^8 s^3 + 9.13 \times 10^7 s^2 - 3.70 \times 10^3 s - 4.11}{s^4 + 61.66s^3 + 3.36 \times 10^4 s^2 + 7.42 \times 10^5 s + 4.65 \times 10^7},$$

a closed-loop \mathcal{H}_∞ norm of $\gamma_{\text{CL}qp} = 0.8$, and an upwards gain margin of 1.66 using the Small Gain Theorem. It is shown numerically that the closed-loop system is robustly stable for $0.01 \text{ N/m} \leq k \leq 2.917 \text{ N/m}$. The robustness properties of the closed-loop system with $G_{c,\mathcal{H}_\infty}(s)$ and $G_{c,\mathcal{H}_\infty}^*(s)$ are summarized in Table 9.2.

When performing robust stabilization using the Large Gain Theorem, a dynamic output feedback controller is to be designed such that the transfer matrix $\bar{\mathbf{G}}_{\text{CL}pq}(s) = \bar{\mathbf{C}}_{\text{CL}3} (s\mathbf{1} - \bar{\mathbf{A}}_{\text{CL}})^{-1} \bar{\mathbf{B}}_{\text{CL}3} + \bar{\mathbf{D}}_{\text{CL}33}$ has minimum gain greater than $1/\nu_\Delta = 0.811$. Performing Synthesis Method 8 gives

$$G_{c,\nu}(s) = \frac{-1.63 \times 10^5 s^3 + 6.38 \times 10^5 s^2 - 3.36 \times 10^3 s + 188.5}{s^4 + 30.04s^3 + 2.76 \times s^2 + 2.49 \times 10^4 s + 3.41 \times 10^5},$$

a least conservative minimum gain of $\nu_{\text{CL}p\hat{q}}^* = 0.971$, and a lower gain margin of 1.19. Numerically it is shown that the closed-loop system is robustly stable for $0.171 \text{ N/m} \leq k \leq 15.94 \text{ N/m}$. Synthesis Method 8 is performed again with the maximization of the objective function $\mathcal{J}(\nu_{\text{CL}p\hat{q}}) = \nu_{\text{CL}p\hat{q}}$, yielding

$$G_{c,\nu}^*(s) = \frac{-5.43 \times 10^9 s^3 + 1.22 \times 10^9 s^2 - 3.27 \times 10^4 s - 29.73}{s^4 + 210.2s^3 + 2.21 \times 10^5 s^2 + 5.69 \times 10^6 s + 6.21 \times 10^8},$$

a least conservative minimum gain of $\nu_{\text{CL}p\hat{q}}^* = 1.04$, and a lower gain margin of 1.29. Numerically it is shown that the closed-loop system is robustly stable for $0.003 \text{ N/m} \leq k \leq 2.664 \text{ N/m}$. The robustness properties of the closed-loop system with $G_{c,\nu}(s)$ and $G_{c,\nu}^*(s)$ are summarized in Table 9.2.

9.5.3 Robust Performance with Full-State Feedback

Robust performance with full-state feedback using both the Small Gain Theorem and Large Gain Theorem is considered in this section. Both control inputs are used with the full-state feedback controllers, as done in the robust stabilization example with full-state feedback.

When using the Small Gain Theorem for robust performance, the objective is to design a full-state feedback controller that guarantees the \mathcal{H}_∞ norm of the transfer function given by $G_{\text{CL}\Delta zw}(s)$ is less than a prescribed value, $0 < \gamma_P < \infty$ for all $|\Delta k| \leq \gamma_\Delta$. As described in Section 8.4, this can be transformed into a robust stabilization problem by augmenting the uncertainty block with a performance block. To reduce conservatism, the structured singular value and DK -iteration should be used to synthesize the controller. However, in order to make a fair comparison to robust performance with the Large Gain Theorem, the Small Gain Theorem and robust \mathcal{H}_∞ control is used instead. In this case, a full-state feedback controller is to be designed such that the transfer matrix $\mathbf{W}\tilde{\mathbf{G}}_{\text{CL}qp}(s) = \mathbf{W}\tilde{\mathbf{C}}_{\text{CL}3}(s\mathbf{1} - \mathbf{A}_{\text{CL}})^{-1}\tilde{\mathbf{B}}_{\text{CL}3}$ has an \mathcal{H}_∞ norm less than 1, where $\mathbf{W} = \text{diag}\{0.75, 1/\gamma_P\}$ is a weighting matrix used to normalize the uncertainty block and $\gamma_P = 0.5$. Using the LMI \mathcal{H}_∞ controller synthesis method from [49], a full-state feedback controller is synthesized as

$$\mathbf{K}_{\mathcal{H}_\infty} = \begin{bmatrix} 2.56 & -1.74 & 2.33 & -1.61 \\ 0.56 & 8.98 & 0.33 & 2.68 \end{bmatrix},$$

where $\mathbf{W}\tilde{\mathbf{G}}_{\text{CL}qp}(s)$ has an \mathcal{H}_∞ norm of $\gamma_{\text{CL}qp} = 0.32$ and an upper gain margin of 3.08 using the Small Gain Theorem. From the Small Gain Theorem, this means

Table 9.3: Robustness properties of the closed-loop system with full-state feedback designed for robust performance in Section 9.5.3, including the gain margin (GM) for robust performance using either the Small Gain Theorem or Large Gain Theorem, the range of k for which the closed-loop system is asymptotically stable (AS), the range of k for which $\|\mathbf{G}_{\text{CL}\Delta zw}\|_\infty < 0.5$, and the range of k for which $\mathbf{G}_{\text{CL}\Delta zw}(s)$ is minimum phase.

Method	GM	AS	$\ \mathbf{G}_{\text{CL}\Delta zw}\ _\infty < 0.5$	$\mathbf{G}_{\text{CL}\Delta zw}(s)$ Min. Phase
Small Gain	3.08	$-2.29 \leq k < \infty$	$-1.81 \leq k < \infty$	$103.7 \leq k < \infty$
Large Gain	2.00	$-1073 \leq k < \infty$	$-1071 \leq k < \infty$	$-1071 \leq k < \infty$

that $\mathbf{K}_{\mathcal{H}_\infty}$ is robust to roughly three times the specified uncertainty and the closed-loop transfer function $G_{\text{CL}\Delta zw}(s)$ has an \mathcal{H}_∞ norm less than $\gamma_P/3.08 = 0.162$ for up to $|\Delta k| \leq 3.08\gamma_\Delta = 2.31$. It is shown numerically that the closed-loop system is robustly stable for $-2.29 \text{ N/m} \leq k < \infty$ and $G_{\text{CL}\Delta zw}(s)$ has an \mathcal{H}_∞ norm less than $\gamma_P = 0.5$ for $-1.81 \text{ N/m} \leq k < \infty$. It is also shown numerically that the transfer function $G_{\text{CL}\Delta zw}(s)$ is minimum phase for $103.7 \text{ N/m} \leq k < \infty$, which is well outside of the region where the closed-loop system is robustly stable. When considering robust performance with the Small Gain Theorem there is no guarantee that the closed-loop system is minimum phase, so this is a valid result. The robustness properties of the closed-loop system with $\mathbf{K}_{\mathcal{H}_\infty}$ are summarized in Table 9.3.

When using the Large Gain Theorem for robust performance, a feedback controller is to be designed such that the transfer function $G_{\text{CL}\Delta zw}(s)$ is minimum phase for all $|\Delta k| \leq \gamma_\Delta$ or $|\Delta \bar{k}| \geq \nu_\Delta$. The transfer function $G_{\text{CL}\Delta zw}(s)$ is minimum phase if it has minimum gain greater than $0 < \nu_P < \infty$. This is converted into a robust stabilization problem, which amounts to synthesizing a full-state feedback controller such that the transfer function $\bar{\mathbf{W}}\tilde{\mathbf{G}}_{\text{CL}p\hat{q}}(s) = \bar{\mathbf{W}}\tilde{\mathbf{C}}_3(s\mathbf{1} - \bar{\mathbf{A}}_{\text{CL}})^{-1}\tilde{\mathbf{B}}_3 + \bar{\mathbf{W}}\tilde{\mathbf{D}}_{33}$ has minimum gain greater than 1, where $\bar{\mathbf{W}} = \text{diag}\{1.233, 1/\nu_P\}$ is a weighting matrix used to normalize the uncertainty block, $\nu_P = 0.005$, $\bar{\mathbf{A}}_{\text{CL}} = \mathbf{A} - \mathbf{B}_3 D_{33}^{-1} \mathbf{C}_3 - \mathbf{B}_2 \mathbf{K}$,

$$\tilde{\mathbf{C}}_3 = \begin{bmatrix} \mathbf{C}_1 \\ -D_{33}^{-1} \mathbf{C}_3 \end{bmatrix}, \quad \tilde{\mathbf{B}}_3 = \begin{bmatrix} \mathbf{B}_1 & \mathbf{B}_3 D_{33}^{-1} \end{bmatrix}, \quad \tilde{\mathbf{D}}_{33} = \begin{bmatrix} D_{11w_1} & 0 \\ 0 & D_{33}^{-1} \end{bmatrix}.$$

Performing Synthesis Method 7 gives

$$\mathbf{K}_\nu = \begin{bmatrix} 1.08 \times 10^3 & -7.20 \times 10^2 & 11.82 & -0.48 \\ -1.4 \times 10^2 & 4.45 \times 10^4 & -2.63 & 38.69 \end{bmatrix},$$

where $\bar{\mathbf{W}}\tilde{\mathbf{G}}_{\text{CL}p\hat{q}}(s)$ has a least conservative minimum gain of $\nu_{\text{CL}p\hat{q}}^* = 2.00$, and a lower gain margin of 2.00 using the Large Gain Theorem. From the Large Gain Theorem, this means that \mathbf{K}_ν is robust to two times the specified uncertainty and the closed-loop transfer function $G_{\text{CL}\Delta zw}(s)$ has minimum gain greater than $2\nu_P = 0.01$ for up to $|\Delta\bar{k}| \geq \nu_{\bar{\Delta}}/2 = 0.616$. It is shown numerically that the closed-loop system is robustly stable for $-1073 \text{ N/m} \leq k < \infty$, and the transfer function $G_{\text{CL}\Delta zw}(s)$ has minimum gain greater than $\nu_P = 0.005$ and is minimum phase for $-1071 \text{ N/m} \leq k < \infty$. The robustness properties of the closed-loop system with \mathbf{K}_ν are summarized in Table 9.3.

The full-state feedback controller synthesized using the Large Gain Theorem was able to provide a guarantee that $G_{\text{CL}\Delta zw}(s)$ be minimum phase for all $|\Delta k| \leq 0.75 \text{ N/m}$, which was not accomplished by the full-state feedback controller synthesized using the Small Gain Theorem. This is not to say that a controller synthesized using the Small Gain Theorem is unable to render the transfer function $G_{\text{CL}\Delta zw}(s)$ minimum phase, but there is no constraint in the robust performance problem with the Small Gain Theorem to enforce this, which highlights the benefit of robust performance with the Large Gain Theorem.

Numerical simulations are performed with the full-state feedback controllers designed using the Small Gain Theorem and the Large Gain Theorem for robust performance. The uncertain closed-loop systems are given a unit step disturbance $d_1(t) = 1 \cdot 1(t)$, where $1(t)$ is the Heaviside step function, for a range of values of k . Figure 9.6 plots the closed-loop responses of $x_2(t)$, as well as the inputs $u_1(t)$ and $u_2(t)$ for 20 sampled values of k in the range $0.5 \text{ N/m} \leq k \leq 2 \text{ N/m}$ with $\mathbf{K}_{\mathcal{H}\infty}$ and \mathbf{K}_ν . The same plots are generated in Figure 9.7 for $-1.81 \text{ N/m} \leq k \leq 12.5 \text{ N/m}$ with $\mathbf{K}_{\mathcal{H}\infty}$ and in Figure 9.7 for $-1071 \text{ N/m} \leq k \leq 12.5 \text{ N/m}$ with \mathbf{K}_ν . The upper limits on the ranges of k considered in Figures 9.7 and 9.8 are based on the numerical limits for which the closed-loop system satisfies the performance objectives, with 12.5 N/m chosen as the upper limit instead of an infinite bound.

9.5.4 Robust Performance with Dynamic Output Feedback

Robust performance with dynamic output feedback using both the Small Gain Theorem and Large Gain Theorem is considered in this section. For this particular example, the robust performance problem is significantly more challenging than the robust stabilization problem, particularly when the Small Gain Theorem or the Large Gain Theorem is used instead of the structured singular value or the structured minimum singular value. For this reason, both control inputs are used instead of the single control input used with the dynamic output feedback controller for robust

Table 9.4: Robustness properties of the closed-loop system with dynamic output feedback designed for robust performance in Section 9.5.4, including the gain margin (GM) for robust performance using either the Small Gain Theorem or Large Gain Theorem, the range of k for which the closed-loop system is asymptotically stable (AS), the range of k for which $\|\mathbf{G}_{\text{CL}\Delta zw}\|_\infty < 0.5$, and the range of k for which $\mathbf{G}_{\text{CL}\Delta zw}(s)$ is minimum phase.

Method	GM	AS	$\ \mathbf{G}_{\text{CL}\Delta zw}\ _\infty < 0.5$	$\mathbf{G}_{\text{CL}\Delta zw}(s)$ Min. Phase
Small Gain	1.04	$0.003 \leq k \leq 3.017$	$0.023 \leq k \leq 2.946$	$864.3 \leq k < \infty$
Large Gain	1.30	$0.001 \leq k \leq 12.21$	$0.001 \leq k \leq 12.21$	$0.001 \leq k \leq 12.21$

stabilization.

When using the Small Gain Theorem for robust performance, a dynamic output feedback controller is to be synthesized that guarantees the \mathcal{H}_∞ norm of the transfer function $G_{\text{CL}\Delta zw}(s)$ is less than $0 < \gamma_P < \infty$ for all $|\Delta k| \leq \gamma_\Delta$. The robust performance problem is transformed into a robust stabilization problem and normalized, yielding the condition that the transfer matrix $\mathbf{W}\tilde{\mathbf{G}}_{\text{CL}qp}(s)$ has an \mathcal{H}_∞ norm less than 1, where $\mathbf{W} = \text{diag}\{0.75, 1/\gamma_P\}$ is a weighting matrix used to normalize the uncertainty block and $\gamma_P = 0.5$. Using the LMI \mathcal{H}_∞ controller synthesis method from [97], a dynamic output feedback controller is synthesized as

$$\mathbf{G}_{c,\mathcal{H}_\infty}(s) = \begin{bmatrix} \frac{-5.91 \times 10^4 s^4 - 9214 s^3 - 3.26 \times 10^4 s^2 - 3.04 \times 10^5 s + 2.50 \times 10^4}{s^4 + 16.97 s^3 + 641.7 s^2 + 1058 s + 2.17 \times 10^4} \\ \frac{11.33 s^4 - 3121 s^3 - 1.09 \times 10^4 s^2 - 9.59 \times 10^4 s - 2.61 \times 10^5}{s^4 + 16.97 s^3 + 641.7 s^2 + 1058 s + 2.17 \times 10^4} \end{bmatrix},$$

where $\mathbf{W}\tilde{\mathbf{G}}_{\text{CL}qp}(s)$ has an \mathcal{H}_∞ norm of $\gamma_{\text{CL}qp} = 0.96$ and an upper gain margin of 1.04 using the Small Gain Theorem. From the Small Gain Theorem, this means that $\mathbf{G}_c(s)$ is robust to slightly more than the specified uncertainty and the closed-loop transfer function $G_{\text{CL}\Delta zw}(s)$ has an \mathcal{H}_∞ norm less than $\gamma_P/1.04 = 0.48$ for up to $|\Delta k| \leq 1.042\gamma_\Delta = 0.78$. It is shown numerically that the closed-loop system is robustly stable for $0.03 \text{ N/m} \leq k \leq 3.017 \text{ N/m}$ and $G_{\text{CL}\Delta zw}(s)$ has an \mathcal{H}_∞ norm less than $\gamma_P = 0.5$ for $0.023 \text{ N/m} \leq k \leq 2.946 \text{ N/m}$. It is also shown numerically that the transfer function $G_{\text{CL}\Delta zw}(s)$ is minimum phase for $864.3 \text{ N/m} \leq k < \infty \text{ N/m}$, which is well outside of the region where the closed-loop system is robustly stable. The robustness properties of the closed-loop system with $\mathbf{G}_{c,\mathcal{H}_\infty}(s)$ are summarized in Table 9.4.

When using the Large Gain Theorem for robust performance, a feedback controller is to be designed such that the transfer function $G_{\text{CL}\Delta zw}(s)$ is minimum phase

for all $|\Delta k| \leq \gamma_\Delta$ or equivalently $|\Delta \bar{k}| \geq \nu_\Delta$. The transfer function $G_{\text{CL}_{\Delta zw}}(s)$ is minimum phase if it has minimum gain greater than $0 < \nu_P < \infty$. This is converted into a robust stabilization problem, which amounts to synthesizing a full-state feedback controller such that the transfer function $\bar{\mathbf{W}}\tilde{\mathbf{G}}_{\text{CL}_{p\hat{q}}}(s) = \bar{\mathbf{W}}\tilde{\mathbf{C}}_3 (s\mathbf{1} - \bar{\mathbf{A}}_{\text{CL}})^{-1} \tilde{\mathbf{B}}_3 + \bar{\mathbf{W}}\tilde{\mathbf{D}}_{33}$ has minimum gain greater than 1, where $\bar{\mathbf{W}} = \text{diag}\{1.233, 1/\nu_P\}$ is a weighting matrix used to normalize the uncertainty block and $\nu_P = 0.005$. Performing Synthesis Method 10 gives

$$\mathbf{G}_{c,\nu}(s) = \left[\begin{array}{c} \frac{-1.53 \times 10^5 s^4 - 2.60 \times 10^{12} s^3 - 7.13 \times 10^{14} s^2 - 3.92 \times 10^{19} s - 9.96 \times 10^{18}}{s^4 + 1892 s^3 + 3.33 \times 10^7 s^2 + 3.36 \times 10^{11} s + 1.72 \times 10^{14}} \\ \frac{-1.00 \times 10^6 s^4 + 3.05 \times 10^{11} s^3 - 1.09 \times 10^{14} s^2 - 1.96 \times 10^{16} s - 7.12 \times 10^{18}}{s^4 + 1892 s^3 + 3.33 \times 10^7 s^2 + 3.36 \times 10^{11} s + 1.72 \times 10^{14}} \end{array} \right],$$

where $\bar{\mathbf{W}}\tilde{\mathbf{G}}_{\text{CL}_{p\hat{q}}}(s)$ has a least conservative minimum gain of $\nu_{\text{CL}_{p\hat{q}}}^* = 1.30$, and a lower gain margin of 1.30 using the Large Gain Theorem. From the Large Gain Theorem, this means that $\mathbf{G}_c(s)$ is robust to 1.3 times the specified uncertainty and the closed-loop transfer function $G_{\text{CL}_{\Delta zw}}(s)$ has minimum gain greater than $1.3\nu_P = 0.013$ for up to $|\Delta \bar{k}| \geq \nu_\Delta/1.3 = 0.948$. It is shown numerically that the closed-loop system is robustly stable for $0.001 \text{ N/m} \leq k \leq 12.211 \text{ N/m}$, and the transfer function $G_{\text{CL}_{\Delta zw}}(s)$ has minimum gain greater than $\nu_P = 0.005$ for $0.513 \text{ N/m} \leq k \leq 4.715 \text{ N/m}$ and is minimum phase for $0.001 \text{ N/m} \leq k \leq 12.211 \text{ N/m}$. The robustness properties of the closed-loop system with $\mathbf{G}_{c,\nu}(s)$ are summarized in Table 9.4.

Similarly to Section 9.5.3, numerical simulations are performed with the dynamic output feedback controllers designed using the Small Gain Theorem and the Large Gain Theorem for robust performance. The uncertain closed-loop systems are again given a unit step disturbance $d_1(t) = 1 \cdot 1(t)$ for a range of values of k . Figure 9.9 plots the closed-loop responses of $x_2(t)$, as well as the inputs $u_1(t)$ and $u_2(t)$ for 20 sampled values of k in the range $0.5 \leq k \leq 2$ with $\mathbf{G}_{c,\mathcal{H}_\infty}(s)$ and $\mathbf{G}_{c,\nu}(s)$ without the presence of measurement noise. Figure 9.10 includes the same plots for $0.023 \text{ N/m} \leq k \leq 22.946 \text{ N/m}$ with $\mathbf{G}_{c,\mathcal{H}_\infty}(s)$, while Figure 9.10 has the same plots for $0.001 \text{ N/m} \leq k \leq 12.211 \text{ N/m}$ with $\mathbf{G}_{c,\nu}(s)$. Once again, the ranges of k considered in Figures 9.10 and 9.11 are based on the numerical limits for which the closed-loop system satisfies the performance objectives. The numerical simulations from Figure 9.9 are performed again with measurement noise of $n(t) = 0.001 \sin(200\pi t) \text{ m/s}$, with results presented in Figure 9.12.

9.5.5 Discussion

The results of robust stabilization with the Small Gain Theorem and the Large Gain Theorem summarized in Tables 9.1 and 9.2 indicate similar closed-loop robustness properties. When using full-state feedback that maximizes the robustness gain margin, the Small Gain Theorem gives a much higher robust stability guarantee via the gain margin, but a slightly smaller range of k that yields an asymptotically stable closed-loop system. The gain margin when using the Large Gain Theorem is limited by the feedthrough matrix D_{33} which could be chosen larger if a larger gain margin is desired. When using dynamic output feedback for robust stabilization, it is shown in Table 9.2 that once again the controller synthesized with the Large Gain Theorem yields a slightly smaller gain margin than the Small Gain Theorem's controller when designed to maximize robustness. The numerically-determined range of asymptotically stable k is also slightly larger with the Small Gain Theorem in this case. Nonetheless, both methods are fully capable of robustly stabilizing the closed-loop system for initially specified range $0.5 \text{ N/m} \leq k \leq 2 \text{ N/m}$.

Tables 9.3 and 9.4 presents results of robust performance with the Small Gain Theorem and the Large Gain Theorem. The robustness properties of these closed-loop systems are difficult to compare, as the controllers are designed to solve different robust performance problems. When using full-state feedback and the Small Gain Theorem, the robust performance gain margin is 3.08 and the range in which robust performance specifications are met is $-1.81 \text{ N/m} \leq k < \infty$, and $\mathbf{G}_{\text{CL}\Delta zw}(s)$ is minimum phase for $103.7 \text{ N/m} \leq k < \infty$. With the Large Gain Theorem, the full-state feedback controller yields a gain margin of 2.00, and the closed-loop system meets the robust performance specifications for $-1071 \text{ N/m} \leq k < \infty$ and $\mathbf{G}_{\text{CL}\Delta zw}(s)$ has an \mathcal{H}_∞ norm less than 0.5 in this same range. Interestingly, the full-state feedback controller design with the Large Gain Theorem meets the robust performance specifications of both the Small Gain Theorem and the Large Gain Theorem for $-1071 \text{ N/m} \leq k < \infty$, while the controller designed with the Small Gain Theorem meets these specifications outside the useful range of k . Numerical simulation results in Figure 9.6 demonstrate that the Large Gain Theorem yields consistent closed-loop system responses for values of $0.5 \text{ N/m} \leq k \leq 2 \text{ N/m}$, while the closed-loop system responses with the Small Gain Theorem are much more varied. The responses with the Small Gain Theorem also feature nonminimum phase behavior, in that the response of $x_2(t)$ initially moves in the negative direction before moving in the positive direction to reach its steady-state value. This behavior is not present in the simulations with the Large Gain Theorem-designed controller, as it is guaranteed to be minimum phase. Figures 9.7

and 9.8 reinforce these observations for the ranges of k in which the respective robust performance specifications are met.

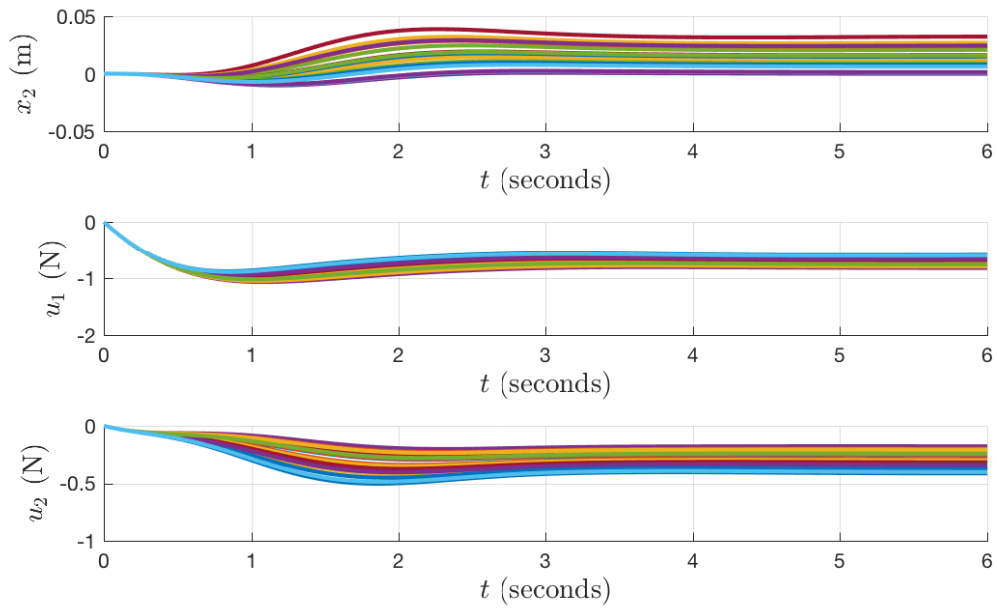
The results of robust performance with dynamic output feedback control are summarized in Table 9.4, where it is shown that a robust performance gain margin of 1.04 is obtained with the Small Gain Theorem, robust specifications are met for $0.023 \text{ N/m} \leq k \leq 2.946 \text{ N/m}$, and the $\mathbf{G}_{\text{CL}\Delta zw}(s)$ is minimum phase for $846.3 \text{ N/m} \leq k < \infty$. The Large Gain Theorem yields a gain margin of 1.30, meets robust specifications for $0.001 \text{ N/m} \leq k \leq 12.211 \text{ N/m}$, and $\mathbf{G}_{\text{CL}\Delta zw}(s)$ has an \mathcal{H}_∞ norm less than 0.5 in the same range. Again, the controller designed with the Large Gain Theorem meets the robust specifications of both the Small Gain Theorem and Large Gain Theorem, while the controller designed with the Small Gain Theorem does not. Similarly to the full-state feedback control results, numerical simulation results without measurement noise in Figure 9.9 demonstrate that the Large Gain Theorem gives closed-loop system responses that are much more consistent than the Small Gain Theorem for values of $0.5 \text{ N/m} \leq k \leq 2 \text{ N/m}$. The responses with the Small Gain Theorem do present any qualitative nonminimum phase behavior, even though $\mathbf{G}_{\text{CL}\Delta zw}(s)$ is nonminimum phase for $0.5 \text{ N/m} \leq k \leq 2 \text{ N/m}$. Figures 9.10 and 9.11 plots the closed-loop responses for the maximum ranges of k in which the respective robust performance specifications are met. Performance with the Small Gain Theorem-designed controller degrades significantly as k approaches the limits of this range in Figure 9.11. It is seen in Figure 9.12b that in the presence of measurement noise the control inputs with the Large Gain Theorem-designed controller are extremely large and unrealistic. The performance variable $z(t)$ is not chosen to be a function of the control inputs to limit the control effort, therefore this is completely reasonable based on the specified problem. Moreover, robust performance with the Large Gain Theorem is not well-equipped to handle limitations on control effort even if the performance variable is a function of the control inputs, as it is not capable of limiting the closed-loop \mathcal{H}_∞ norm. In order to satisfy such a performance specification and also guarantee $\mathbf{G}_{\text{CL}\Delta zw}(s)$ is minimum phase, the mixed structured singular value discussed in Section 8.4.3 is required.

9.6 Closing Remarks

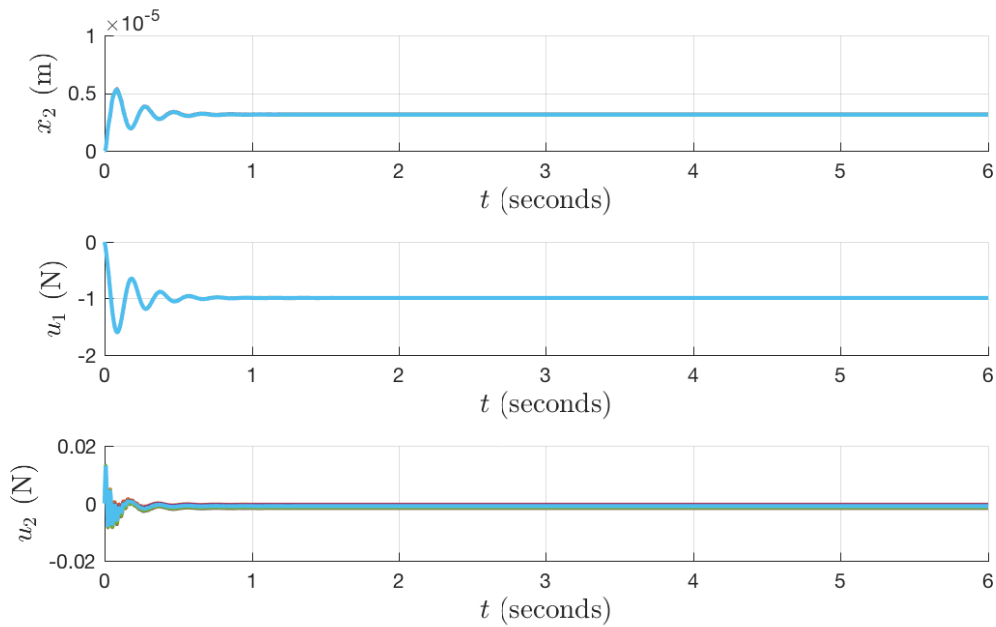
Full-state feedback and dynamic output feedback LMI-based controller synthesis methods were presented in this chapter that solve the robust stabilization, robust stabilization and nominal performance, and robust performance problems. The robust controllers were tested numerically on a robust control benchmark problem and com-

pared to robust \mathcal{H}_∞ controllers synthesized using the Small Gain Theorem. These numerical examples mark the first known use of the Large Gain Theorem for robust control of a physically-meaningful example. The robust controllers synthesized using the Large Gain Theorem exhibit similar robustness properties to the robust controllers synthesized using the Small Gain Theorem, except when used for robust performance, where the Large Gain Theorem-based robust controllers are capable of guaranteeing the uncertain closed-loop transfer matrix is minimum phase and the Small Gain Theorem-based robust controllers are not. Robust performance is arguably the most useful application of robust control with the Large Gain Theorem, as it solves a robust performance problem that could not previously be solved with the Small Gain Theorem.

Future work will include developing robust controller synthesis methods using the structured minimum singular value and the mixed structured singular value, which will most likely bear similarities to DK -iteration. The synthesis of parallel feed-forward controllers and two degree-of-freedom controllers when considering robust performance will also be explored, which will allow for robust performance using the Large Gain Theorem to be applied to a wider variety of systems.



(a)



(b)

Figure 9.6: Closed-loop response of $x_2(t)$ and the control inputs $u_1(t)$ and $u_2(t)$ for $0.5 \leq k \leq 2$ with full-state feedback controllers designed using the (a) Small Gain Theorem and (b) the Large Gain Theorem for robust performance in Section 9.5.3.

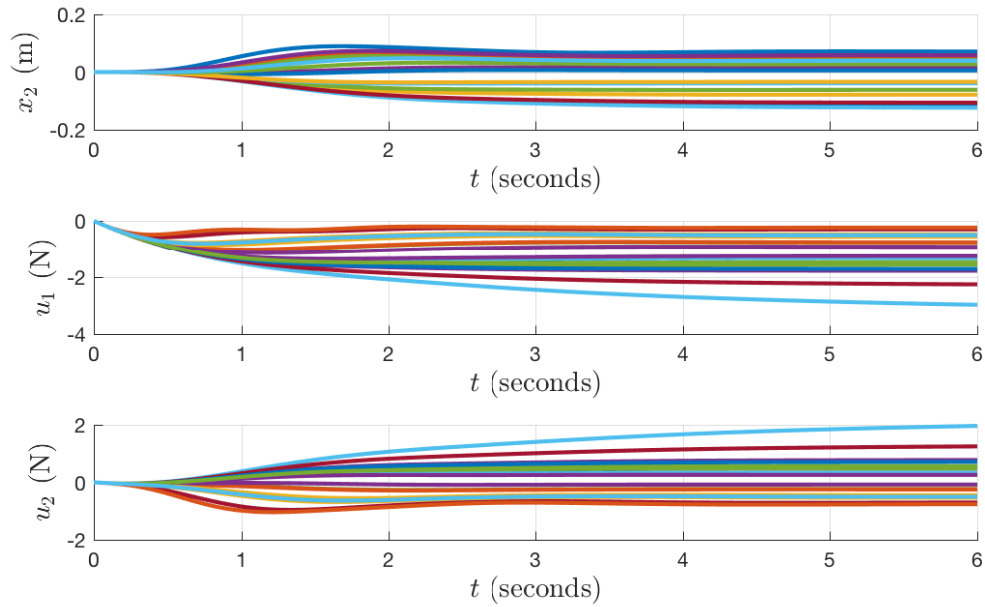


Figure 9.7: Closed-loop response of $x_2(t)$ and the control inputs $u_1(t)$ and $u_2(t)$ for $-1.81 \leq k \leq 12.5$ with a full-state feedback controller designed using the Small Gain Theorem for robust performance in Section 9.5.3.

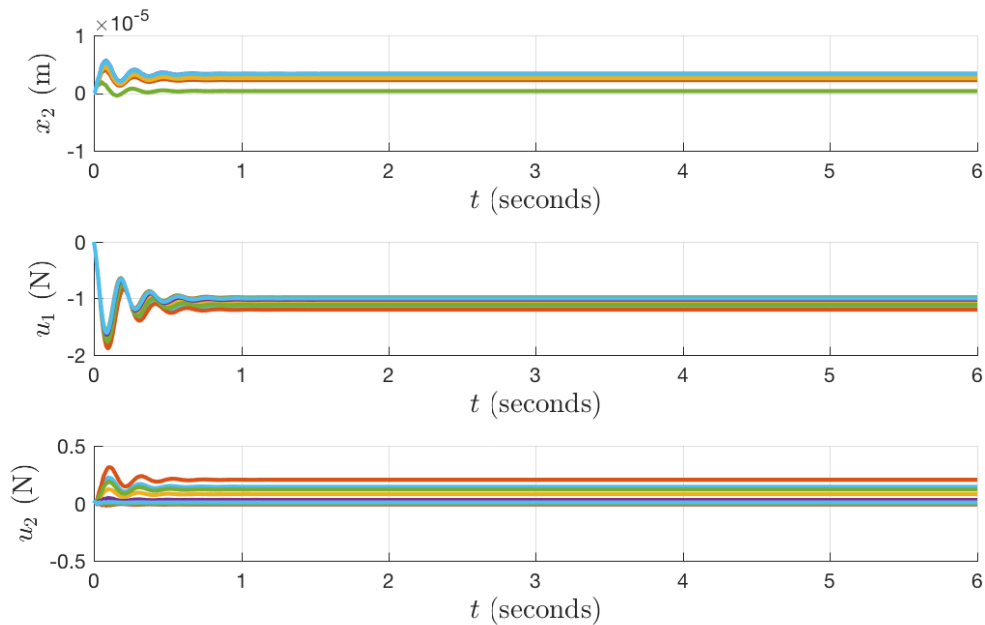
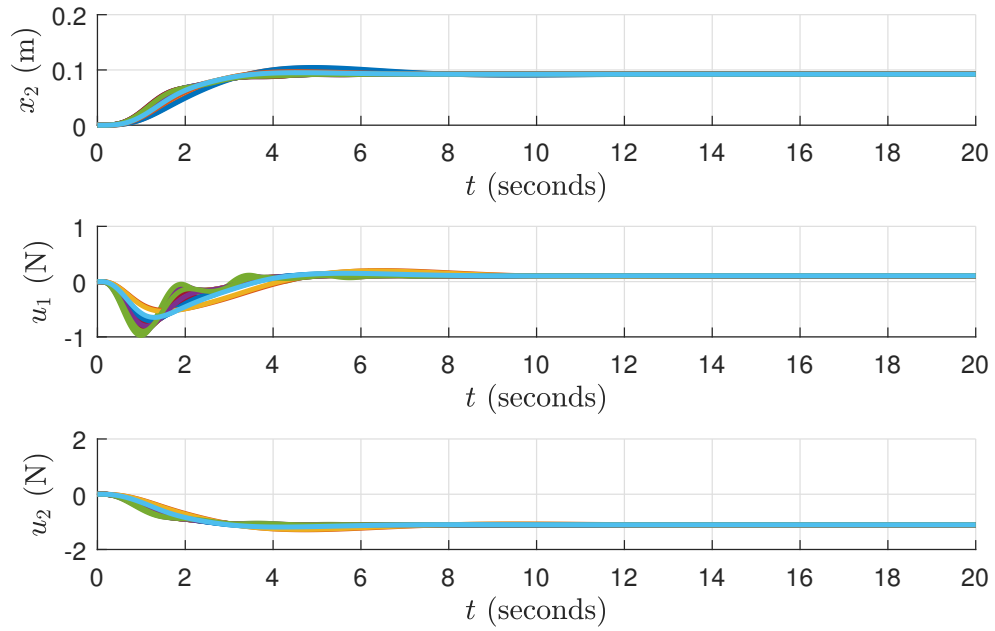
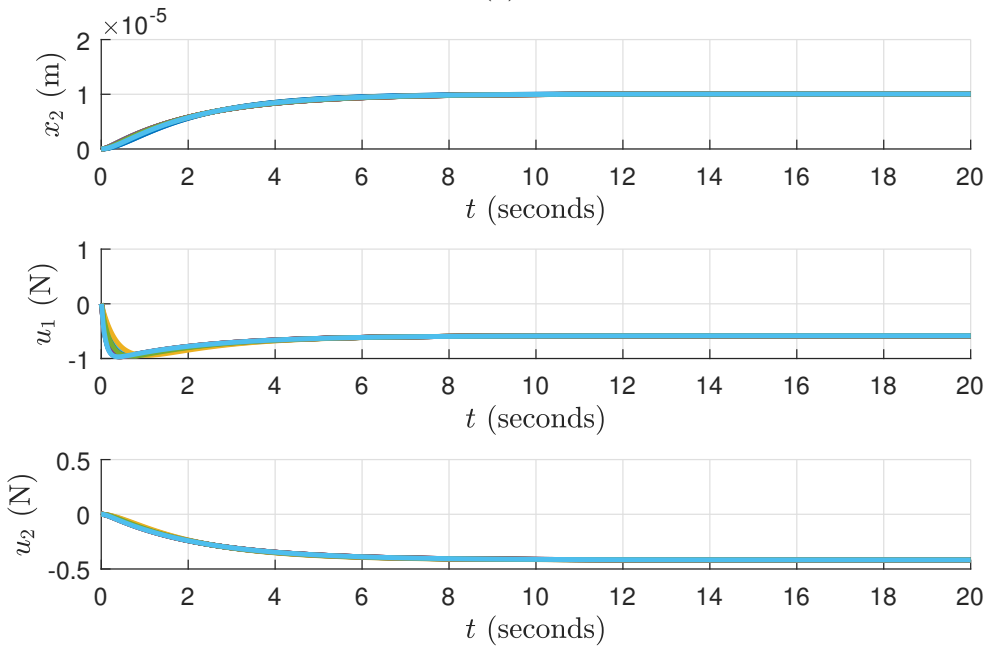


Figure 9.8: Closed-loop response of $x_2(t)$ and the control inputs $u_1(t)$ and $u_2(t)$ for $-1071 \leq k \leq 12.5$ with a full-state feedback controller designed using the Large Gain Theorem for robust performance in Section 9.5.3.



(a)



(b)

Figure 9.9: Closed-loop response of $x_2(t)$ and the control inputs $u_1(t)$ and $u_2(t)$ for $0.5 \leq k \leq 2$ with dynamic output feedback controllers designed using the (a) Small Gain Theorem and (b) the Large Gain Theorem for robust performance in Section 9.5.4.

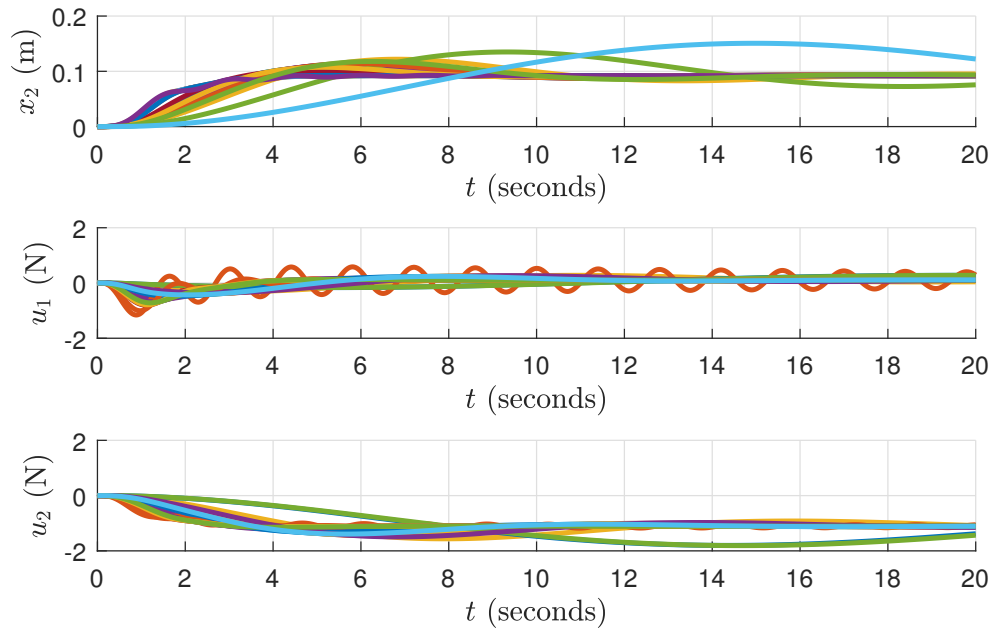


Figure 9.10: Closed-loop response of $x_2(t)$ and the control inputs $u_1(t)$ and $u_2(t)$ for $0.023 \leq k \leq 2.946$ with a dynamic output feedback controller designed using the Small Gain Theorem for robust performance in Section 9.5.4.

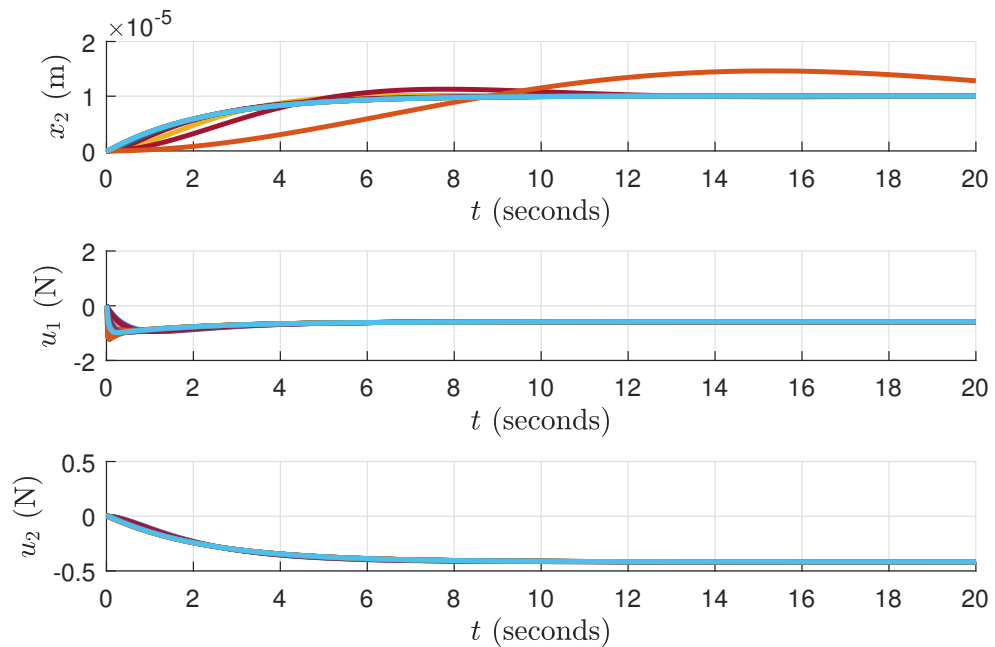
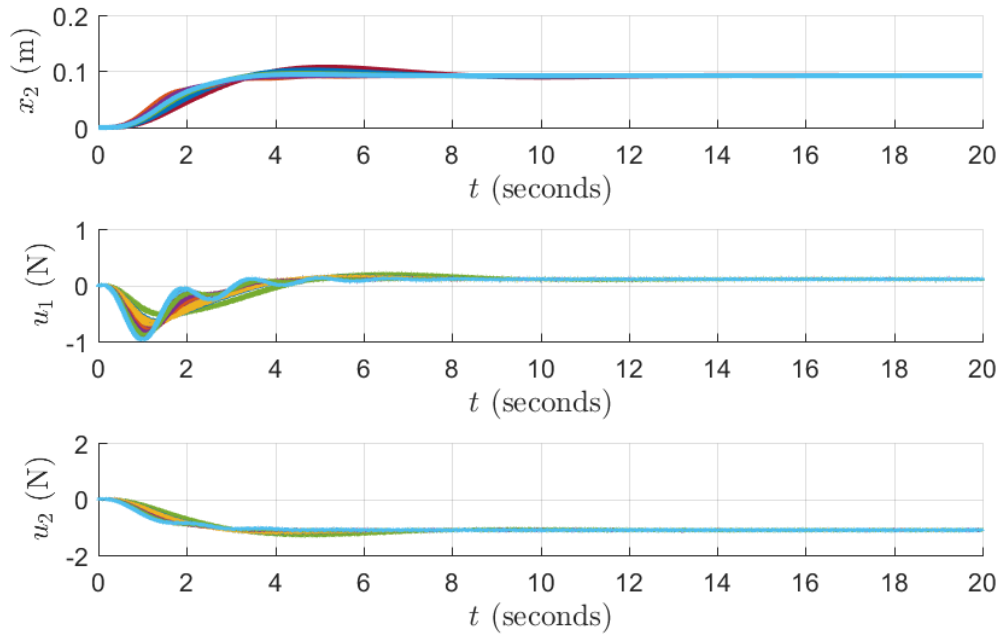
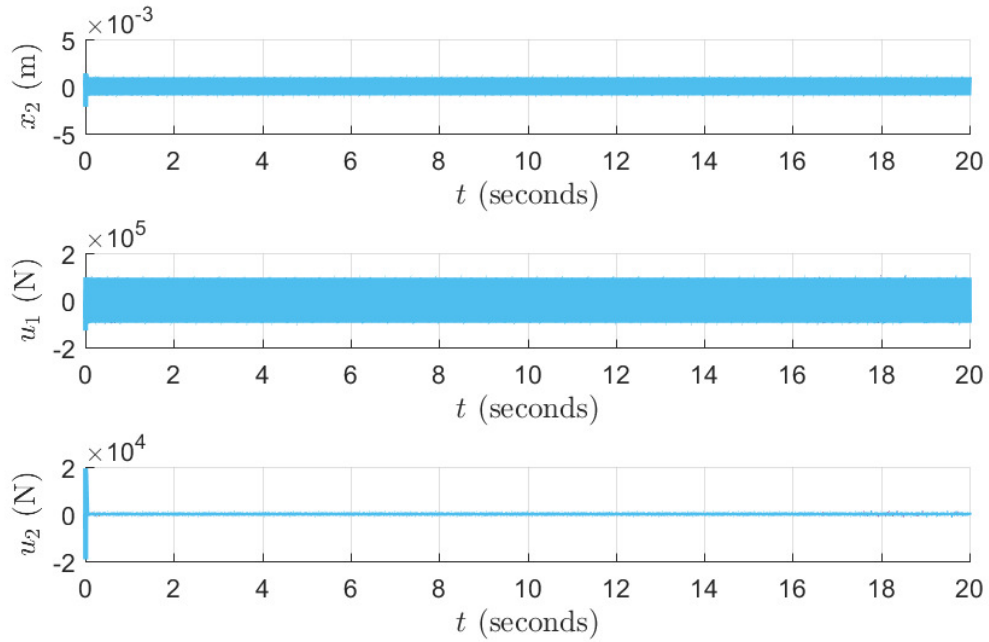


Figure 9.11: Closed-loop response of $x_2(t)$ and the control inputs $u_1(t)$ and $u_2(t)$ for $0.001 \leq k \leq 12.21$ with a dynamic output feedback controller designed using the Large Gain Theorem for robust performance in Section 9.5.4.



(a)



(b)

Figure 9.12: Closed-loop response of $x_2(t)$ and the control inputs $u_1(t)$ and $u_2(t)$ for $0.5 \leq k \leq 2$ and measurement noise of $n(t) = 0.001 \sin(200\pi t)$ with dynamic output feedback controllers designed using the (a) Small Gain Theorem and (b) the Large Gain Theorem for robust performance in Section 9.5.4.

Part IV
Conclusion

Chapter 10

Closing Remarks and Future Work

This dissertation considers the broad topics of optimal output modification and robust control. Briefly, the main contributions of this dissertation are related to

1. the properties of minimum gain,
2. the synthesis of \mathcal{H}_∞ -optimal parallel feedforward controllers using minimum gain,
3. a method to linearly combine sensor measurements to obtain an SPR transfer matrix in an \mathcal{H}_2 - or \mathcal{H}_∞ -optimal manner,
4. a Nyquist stability criterion proof of the Large Gain Theorem for LTI systems,
5. a framework for robust control with the Large Gain Theorem, and
6. full-state and dynamic output feedback robust controller synthesis methods with the Large Gain Theorem.

A complete list of novel contributions found in this dissertation and publications resulting from this research is found in the Preface. These contributions mark theoretical and practical advancements to the areas of optimal output modification, input-output stability theory, and robust control.

Despite the advancements made in this dissertation, there is much room for improvement and future work. Suggestions for future extensions to the research presented in this dissertation are detailed as follows.

Minimum Gain and Optimal Output Modification

Building upon the \mathcal{H}_∞ -optimal parallel feedforward controller synthesis methods in Chapter 4, an optimal robust parallel feedforward control formulation is a promising avenue of future research. A parallel feedforward controller solving this problem would

yield an augmented system that is robustly minimum phase and as close as possible to the original system. As discussed in Chapter 4, a somewhat simple extension to robust parallel feedforward control would involve state-space interval uncertainty. A more general extension to robust parallel feedforward control may be found using the robust performance problem described in Chapter 9. Robust performance with the Large Gain Theorem is capable of robustly guaranteeing that the closed-loop performance transfer matrix is minimum phase, which may be tailored specifically for the purposes of parallel feedforward control. Mathematical development of a structured minimum singular value or a mixed structured singular value would be useful in reducing conservatism in this context.

The \mathcal{H}_2 - and \mathcal{H}_∞ -optimal linear combination of sensor measurements to yield an SPR transfer matrix in Chapter 5 shows promising results on numerical examples of a noncolocated mass-spring system and a flexible joint robotic manipulator. A potential extension of this work is the incorporation of weighting transfer matrices in the minimization of the \mathcal{H}_2 or \mathcal{H}_∞ norms, which would minimize the difference between the modified system output and the desired system output within specified bands of frequency. The sensor interpolation techniques would also greatly benefit from a robust formulation that guarantees the transfer matrix obtained is SPR subject to model uncertainty. This would most likely be possible for systems subject to uncertainty that is PR, by using the stability result in [72].

The Large Gain Theorem

Following the advances made in this dissertation regarding the use of the Large Gain Theorem for robust control in Chapters 8 and 9, the remaining challenges are mostly computational in nature. In particular, an efficient method to compute the structured minimum singular value is to be developed and further details regarding the mixed singular value are to be determined. The structured minimum singular value would allow for the new minimum phase robust performance criterion to be enforced without conservatism in a wide range of practical situations, while the mixed structured singular value would enable the robust control of systems subject to uncertainty that has some components with nonzero minimum gain and some that have an upper bound on its gain.

Experimental validation of robust controllers designed using the Large Gain Theorem or the structured minimum singular value would help demonstrate the ability of these controllers in practice. Since it was shown in Chapter 8 that the Large Gain Theorem is applicable on any problem suitable for the Small Gain Theorem, there

are many options for experimental test platforms, including a number of aerospace and robotic systems.

In summary, the Large Gain Theorem can provide robustness guarantees that are not possible with other stability results, including the Small Gain Theorem. This dissertation has provided the first steps towards making the Large Gain Theorem a practical tool for robust control, but further contributions will be required in order to fully complete this task.

Appendix

Appendix

Derivation of Dynamic Output Feedback Controller Synthesis for Robust Stabilization using the Large Gain Theorem

This appendix presents details of the transformations performed on the matrix inequality of (9.21) in Chapter 9 to yield the LMIs used for robust stabilization with dynamic output feedback control in Synthesis Method 8. These transformations are largely based on those used for the LMI synthesis of an \mathcal{H}_∞ -optimal dynamic output feedback controller in [97]. Details of the transformations found in [97] are clearly explained in the course notes of Dr. Sanjay Lall at Stanford University and Dr. Matthew Peet at Arizona State University, which were also used as inspiration in the derivation of the following matrix inequality transformations.

The matrix inequality in (9.21), given by

$$\begin{bmatrix} \mathbf{P}\mathbf{A}_{\text{CL}} + \mathbf{A}_{\text{CL}}^T \mathbf{P} - \mathbf{C}_{\text{CL}3}^T \mathbf{C}_{\text{CL}3} & \mathbf{P}\mathbf{B}_{\text{CL}3} - \mathbf{C}_{\text{CL}3}^T \mathbf{D}_{\text{CL}33} \\ * & \nu_{\text{CL}qp}^2 \mathbf{1} - \mathbf{D}_{\text{CL}33}^T \mathbf{D}_{\text{CL}33} \end{bmatrix} \leq 0 \quad (\text{A.1})$$

with $\mathbf{P} = \mathbf{P}^T \geq 0$, which ensures that the transfer matrix $\mathbf{G}_{\text{CL}qp}(s)$ has minimum gain $0 < \nu_{\text{CL}qp} < \infty$, where the nominal closed-loop state-space matrices are defined

in (8.4), (8.5), (8.6) and (8.7) as

$$\mathbf{A}_{\text{CL}} = \begin{bmatrix} \mathbf{A} + \mathbf{B}_2 \mathbf{D}_c \tilde{\mathbf{D}}^{-1} \mathbf{C}_2 & \mathbf{B}_2 \left(\mathbf{1} + \mathbf{D}_c \tilde{\mathbf{D}}^{-1} \mathbf{D}_{22} \right) \mathbf{C}_c \\ \mathbf{B}_c \tilde{\mathbf{D}}^{-1} \mathbf{C}_2 & \mathbf{A}_c + \mathbf{B}_c \tilde{\mathbf{D}}^{-1} \mathbf{D}_{22} \mathbf{C}_c \end{bmatrix}, \quad (\text{A.2})$$

$$\mathbf{B}_{\text{CL3}} = \begin{bmatrix} \mathbf{B}_3 + \mathbf{B}_2 \mathbf{D}_c \tilde{\mathbf{D}}^{-1} \mathbf{D}_{23} \\ \mathbf{B}_c \tilde{\mathbf{D}}^{-1} \mathbf{D}_{23} \end{bmatrix}, \quad (\text{A.3})$$

$$\mathbf{C}_{\text{CL3}} = \begin{bmatrix} \mathbf{C}_3 + \mathbf{D}_{32} \mathbf{D}_c \tilde{\mathbf{D}}^{-1} \mathbf{C}_2 & \mathbf{D}_{32} \left(\mathbf{1} + \mathbf{D}_c \tilde{\mathbf{D}}^{-1} \mathbf{D}_{22} \right) \mathbf{C}_c \end{bmatrix}, \quad (\text{A.4})$$

$$\mathbf{D}_{\text{CL33}} = \mathbf{D}_{33} + \mathbf{D}_{32} \mathbf{D}_c \tilde{\mathbf{D}}^{-1} \mathbf{D}_{23}, \quad (\text{A.5})$$

and $\tilde{\mathbf{D}} = \mathbf{1} - \mathbf{D}_{22} \mathbf{D}_c$.

The matrix inequality of (A.1) is equivalently written as

$$\begin{bmatrix} \mathbf{P} \mathbf{A}_{\text{CL}} + \mathbf{A}_{\text{CL}}^T \mathbf{P} & \mathbf{P} \mathbf{B}_{\text{CL3}} \\ * & \nu_{\text{CL}qp}^2 \mathbf{1} \end{bmatrix} - \begin{bmatrix} \mathbf{C}_{\text{CL3}}^T \\ \mathbf{D}_{\text{CL33}}^T \end{bmatrix} \begin{bmatrix} \mathbf{C}_{\text{CL3}} & \mathbf{D}_{\text{CL33}} \end{bmatrix} \leq 0. \quad (\text{A.6})$$

Applying Young's relation to the term $\begin{bmatrix} \mathbf{C}_{\text{CL3}}^T \\ \mathbf{D}_{\text{CL33}}^T \end{bmatrix} \begin{bmatrix} \mathbf{C}_{\text{CL3}} & \mathbf{D}_{\text{CL33}} \end{bmatrix}$ gives the matrix inequality

$$\begin{bmatrix} \mathbf{P} \mathbf{A}_{\text{CL}} + \mathbf{A}_{\text{CL}}^T \mathbf{P} - \mathbf{Y}_{\text{CL}}^T \mathbf{C}_{\text{CL3}} - \mathbf{C}_{\text{CL3}}^T \mathbf{Y}_{\text{CL}} & \mathbf{P} \mathbf{B}_{\text{CL3}} - \mathbf{C}_{\text{CL3}}^T \mathbf{X} - \mathbf{Y}_{\text{CL}}^T \mathbf{D}_{\text{CL33}} & \mathbf{Y}_{\text{CL}}^T \\ * & \nu_{\text{CL}qp}^2 \mathbf{1} - \mathbf{X}^T \mathbf{D}_{\text{CL33}} - \mathbf{D}_{\text{CL33}}^T \mathbf{X} & \mathbf{X}^T \\ * & * & -\mathbf{1} \end{bmatrix} \leq 0, \quad (\text{A.7})$$

which implies the matrix inequality in (A.6). The matrix \mathbf{Y}_{CL} is parameterized as

$$\mathbf{Y}_{\text{CL}} = \bar{\mathbf{Y}} \mathbf{P}. \quad (\text{A.8})$$

Substituting (A.8) into (A.7) gives

$$\begin{bmatrix} \hat{\mathbf{M}}_{11} & \mathbf{P} \left(\mathbf{B}_{\text{CL3}} - \bar{\mathbf{Y}}^T \mathbf{D}_{\text{CL33}} \right) - \mathbf{C}_{\text{CL3}}^T \mathbf{X} & \mathbf{P} \bar{\mathbf{Y}}^T \\ * & \nu_{\text{CL}qp}^2 \mathbf{1} - \mathbf{X}^T \mathbf{D}_{\text{CL33}} - \mathbf{D}_{\text{CL33}}^T \mathbf{X} & \mathbf{X}^T \\ * & * & -\mathbf{1} \end{bmatrix} \leq 0, \quad (\text{A.9})$$

where $\hat{\mathbf{M}}_{11} = \mathbf{P} \left(\mathbf{A}_{\text{CL}} - \bar{\mathbf{Y}}^T \mathbf{C}_{\text{CL3}} \right) + \left(\mathbf{A}_{\text{CL}} - \bar{\mathbf{Y}}^T \mathbf{C}_{\text{CL3}} \right)^T \mathbf{P}$.

A first change of variables to simplify an algebraic loop is performed as

$$\begin{aligned}\mathbf{A}_K &= \mathbf{A}_c + \mathbf{B}_c (\mathbf{1} - \mathbf{D}_{22}\mathbf{D}_c)^{-1} \mathbf{D}_{22}\mathbf{C}_c, \\ \mathbf{B}_K &= \mathbf{B}_c (\mathbf{1} - \mathbf{D}_{22}\mathbf{D}_c)^{-1}, \\ \mathbf{C}_K &= (\mathbf{1} - \mathbf{D}_c\mathbf{D}_{22})^{-1} \mathbf{C}_c, \\ \mathbf{D}_K &= \mathbf{D}_c (\mathbf{1} - \mathbf{D}_{22}\mathbf{D}_c)^{-1},\end{aligned}$$

which when substituted into (A.2), (A.3), (A.4) and (A.5) yields

$$\mathbf{A}_{\text{CL}} = \begin{bmatrix} \mathbf{A} + \mathbf{B}_2\mathbf{D}_K\mathbf{C}_2 & \mathbf{B}_2\mathbf{C}_K \\ \mathbf{B}_K\mathbf{C}_2 & \mathbf{A}_K \end{bmatrix}, \quad (\text{A.10})$$

$$\mathbf{B}_{\text{CL3}} = \begin{bmatrix} \mathbf{B}_3 + \mathbf{B}_2\mathbf{D}_K\mathbf{D}_{23} \\ \mathbf{B}_K\mathbf{D}_{23} \end{bmatrix}, \quad (\text{A.11})$$

$$\mathbf{C}_{\text{CL3}} = \begin{bmatrix} \mathbf{C}_3 + \mathbf{D}_{32}\mathbf{D}_K\mathbf{C}_2 & \mathbf{D}_{32}\mathbf{C}_K \end{bmatrix}, \quad (\text{A.12})$$

$$\mathbf{D}_{\text{CL33}} = \mathbf{D}_{33} + \mathbf{D}_{32}\mathbf{D}_K\mathbf{D}_{23}. \quad (\text{A.13})$$

Note that the simplification $(\mathbf{1} + \mathbf{D}_c(\mathbf{1} - \mathbf{D}_{22}\mathbf{D}_c)^{-1}\mathbf{D}_{22})\mathbf{C}_c = (\mathbf{1} - \mathbf{D}_c\mathbf{D}_{22})^{-1}\mathbf{C}_c = \mathbf{C}_K$ is made using the identity in [48, Fact 2.16.17]. The reverse change of variables, which is needed following the controller synthesis method to recover the controller, is given by

$$\begin{aligned}\mathbf{A}_c &= \mathbf{A}_K - \mathbf{B}_c (\mathbf{1} - \mathbf{D}_{22}\mathbf{D}_c)^{-1} \mathbf{D}_{22}\mathbf{C}_c, \\ \mathbf{B}_c &= \mathbf{B}_K (\mathbf{1} - \mathbf{D}_{22}\mathbf{D}_c), \\ \mathbf{C}_c &= (\mathbf{1} - \mathbf{D}_c\mathbf{D}_{22}) \mathbf{C}_K, \\ \mathbf{D}_c &= (\mathbf{1} + \mathbf{D}_K\mathbf{D}_{22})^{-1} \mathbf{D}_K.\end{aligned}$$

Next, the matrices $\mathbf{P} = \mathbf{P}^\top > 0$ and $\mathbf{Q} = \mathbf{P}^{-1}$ are defined as

$$\mathbf{P} = \begin{bmatrix} \mathbf{P}_1 & \mathbf{P}_2 \\ \mathbf{P}_2^\top & \mathbf{P}_3 \end{bmatrix}, \quad \mathbf{Q} = \begin{bmatrix} \mathbf{Q}_1 & \mathbf{Q}_2 \\ \mathbf{Q}_2^\top & \mathbf{Q}_3 \end{bmatrix}.$$

Lemma A.1 ([39, 49]). *Given $\mathbf{P}_1 = \mathbf{P}_1^\top > 0$ and $\mathbf{Q}_1 = \mathbf{Q}_1^\top > 0$, the matrices \mathbf{P} and*

\mathbf{Q} can be constructed to satisfy $\mathbf{PQ} = \mathbf{1}$, $\mathbf{P} = \mathbf{P}^\top > 0$, and $\mathbf{Q} = \mathbf{Q}^\top > 0$ provided

$$\begin{bmatrix} \mathbf{P}_1 & \mathbf{1} \\ * & \mathbf{Q}_1 \end{bmatrix} \geq 0, \quad (\text{A.14})$$

$$\mathbf{P}_2 \mathbf{P}_2^\top = \mathbf{P}_1 - \mathbf{Q}_1^{-1}, \quad (\text{A.15})$$

where

$$\mathbf{P} = \begin{bmatrix} \mathbf{P}_1 & \mathbf{P}_2 \\ * & \mathbf{1} \end{bmatrix}, \quad (\text{A.16})$$

$$\mathbf{Q} = \begin{bmatrix} \mathbf{Q}_1 & -\mathbf{Q}_1 \mathbf{P}_2 \\ * & \mathbf{P}_2^\top \mathbf{Q}_1 \mathbf{P}_2 + \mathbf{1} \end{bmatrix}. \quad (\text{A.17})$$

That is, $((\text{A.14}) \wedge (\text{A.15})) \implies (\mathbf{PQ} = \mathbf{1} \wedge \mathbf{P} = \mathbf{P}^\top > 0 \wedge \mathbf{Q} = \mathbf{Q}^\top > 0)$. It is also known that $((\text{A.14}) \wedge (\text{A.15}))$ implies that the matrices

$$\mathbf{Q}_{\text{CL}} = \begin{bmatrix} \mathbf{Q}_1 & \mathbf{1} \\ \mathbf{Q}_2^\top & \mathbf{0} \end{bmatrix}, \quad \mathbf{P}_{\text{CL}} = \begin{bmatrix} \mathbf{1} & \mathbf{0} \\ \mathbf{P}_1 & \mathbf{P}_2 \end{bmatrix}$$

are full rank.

Using the parameterizations in (A.16) and (A.17), it is shown that

$$\mathbf{Q}_{\text{CL}}^\top \mathbf{P} = \begin{bmatrix} \mathbf{Q}_1 & \mathbf{Q}_2 \\ \mathbf{1} & \mathbf{0} \end{bmatrix} \begin{bmatrix} \mathbf{P}_1 & \mathbf{P}_2 \\ \mathbf{P}_2^\top & \mathbf{P}_3 \end{bmatrix} = \begin{bmatrix} \mathbf{1} & \mathbf{0} \\ \mathbf{P}_1 & \mathbf{P}_2 \end{bmatrix} = \mathbf{P}_{\text{CL}}. \quad (\text{A.18})$$

Knowing that \mathbf{Q}_{CL} is full rank, a congruence transformation is performed on (A.9) with $\mathbf{W} = \text{diag}\{\mathbf{Q}_{\text{CL}}, \mathbf{1}, \mathbf{1}, \mathbf{1}\}$. Defining $\bar{\mathbf{Y}} = [\mathbf{Y}_1 \quad \mathbf{Y}_2]$ and substituting in the closed-loop state-space matrices from (A.10), (A.11), (A.12) and (A.13), the result of the congruence transformation is

$$\begin{bmatrix} \bar{\mathbf{M}}_{11} & \bar{\mathbf{M}}_{12} & \bar{\mathbf{M}}_{13} & \mathbf{Y}_1^\top \\ * & \bar{\mathbf{M}}_{22} & \bar{\mathbf{M}}_{23} & \mathbf{P}_1 \mathbf{Y}_1^\top + \mathbf{P}_2 \mathbf{Y}_2^\top \\ * & * & \bar{\mathbf{M}}_{33} & \mathbf{X}^\top \\ * & * & * & -\mathbf{1} \end{bmatrix} \leq 0, \quad (\text{A.19})$$

where

$$\begin{aligned}
\bar{\mathbf{M}}_{11} &= \mathbf{A}\mathbf{Q}_1 + \mathbf{Q}_1\mathbf{A} + \mathbf{B}_2 (\mathbf{D}_K \mathbf{C}_2 \mathbf{Q}_1 + \mathbf{C}_K \mathbf{Q}_2^\top) + (\mathbf{D}_K \mathbf{C}_2 \mathbf{Q}_1 + \mathbf{C}_K \mathbf{Q}_2^\top)^\top \mathbf{B}_2^\top \\
&\quad - \mathbf{Y}_1^\top (\mathbf{C}_3 \mathbf{Q}_1 + \mathbf{D}_{32} (\mathbf{D}_K \mathbf{C}_2 \mathbf{Q}_1 + \mathbf{C}_K \mathbf{Q}_2^\top)) \\
&\quad - (\mathbf{C}_3 \mathbf{Q}_1 + \mathbf{D}_{32} (\mathbf{D}_K \mathbf{C}_2 \mathbf{Q}_1 + \mathbf{C}_K \mathbf{Q}_2^\top))^\top \mathbf{Y}_1, \\
\bar{\mathbf{M}}_{12} &= \mathbf{A} + \mathbf{B}_2 \mathbf{D}_K \mathbf{C}_2 + \left((\mathbf{D}_K \mathbf{C}_2 \mathbf{Q}_1 + \mathbf{C}_K \mathbf{Q}_2^\top)^\top \mathbf{B}_2^\top + \mathbf{Q}_1 \mathbf{A}^\top \right) \mathbf{P}_1 \\
&\quad + (\mathbf{Q}_1 \mathbf{C}_2^\top \mathbf{B}_K^\top + \mathbf{Q}_2 \mathbf{A}_K^\top) \mathbf{P}_2^\top - \mathbf{Y}_1^\top \mathbf{C}_3 - \mathbf{D}_{32} \mathbf{D}_K \mathbf{C}_2 \\
&\quad - (\mathbf{C}_3 \mathbf{Q}_1 + \mathbf{D}_{32} (\mathbf{D}_K \mathbf{C}_2 \mathbf{Q}_1 + \mathbf{C}_K \mathbf{Q}_2^\top))^\top (\mathbf{P}_1 \mathbf{Y}_1^\top + \mathbf{P}_2 \mathbf{Y}_2^\top)^\top, \\
\bar{\mathbf{M}}_{22} &= \mathbf{P}_1 \mathbf{A} + \mathbf{A}^\top \mathbf{P}_1 + (\mathbf{P}_1 \mathbf{B}_2 \mathbf{D}_K + \mathbf{P}_2 \mathbf{B}_K) \mathbf{C}_2 + \mathbf{C}_2^\top (\mathbf{P}_1 \mathbf{B}_2 \mathbf{D}_K + \mathbf{P}_2 \mathbf{B}_K)^\top \\
&\quad - (\mathbf{P}_1 \mathbf{Y}_1^\top + \mathbf{P}_2 \mathbf{Y}_2^\top) (\mathbf{C}_3 + \mathbf{D}_{32} \mathbf{D}_K \mathbf{C}_2) - (\mathbf{C}_3 + \mathbf{D}_{32} \mathbf{D}_K \mathbf{C}_2)^\top (\mathbf{P}_1 \mathbf{Y}_1^\top + \mathbf{P}_2 \mathbf{Y}_2^\top)^\top, \\
\bar{\mathbf{M}}_{13} &= \mathbf{B}_3 + \mathbf{B}_2 \mathbf{D}_K \mathbf{D}_{23} - (\mathbf{C}_3 \mathbf{Q}_1 + \mathbf{D}_{32} (\mathbf{D}_K \mathbf{C}_2 \mathbf{Q}_1 + \mathbf{C}_K \mathbf{Q}_2^\top))^\top \mathbf{X} \\
&\quad - \mathbf{Y}_1^\top (\mathbf{D}_{33} + \mathbf{D}_{32} \mathbf{D}_K \mathbf{D}_{23}), \\
\bar{\mathbf{M}}_{23} &= \mathbf{P}_1 \mathbf{B}_3 + (\mathbf{P}_1 \mathbf{B}_2 \mathbf{D}_K + \mathbf{P}_2 \mathbf{B}_K) \mathbf{D}_{23} - (\mathbf{C}_3^\top + \mathbf{C}_2^\top \mathbf{D}_K^\top \mathbf{D}_{32}^\top) \mathbf{X} \\
&\quad - (\mathbf{P}_1 \mathbf{Y}_1^\top + \mathbf{P}_2 \mathbf{Y}_2^\top) (\mathbf{D}_{33} + \mathbf{D}_{32} \mathbf{D}_K \mathbf{D}_{23}), \\
\bar{\mathbf{M}}_{33} &= \nu_{\text{CL}qp}^2 \mathbf{1} - (\mathbf{D}_{33} + \mathbf{D}_{32} \mathbf{D}_K \mathbf{D}_{23})^\top \mathbf{X} - \mathbf{X}^\top (\mathbf{D}_{33} + \mathbf{D}_{32} \mathbf{D}_K \mathbf{D}_{23}),
\end{aligned}$$

and the simplification of (A.18) is used. Another change of variables is performed as $\mathbf{Y} = \mathbf{Y}_1$, $\mathbf{Z} = \mathbf{P}_1 \mathbf{Y}_1^\top + \mathbf{P}_2 \mathbf{Y}_2^\top$, $\mathbf{D}_n = \mathbf{D}_K$,

$$\begin{aligned}
\mathbf{B}_n &= \mathbf{P}_1 \mathbf{B}_2 \mathbf{D}_K + \mathbf{P}_2 \mathbf{B}_K, \\
\mathbf{C}_n &= \mathbf{D}_K \mathbf{C}_2 \mathbf{Q}_1 + \mathbf{C}_K \mathbf{Q}_2^\top, \\
\mathbf{A}_n &= \mathbf{P}_1 (\mathbf{A} \mathbf{Q}_1 + \mathbf{B}_2 \mathbf{C}_n) + \mathbf{P}_2 (\mathbf{B}_K \mathbf{C}_2 \mathbf{Q}_1 + \mathbf{A}_K \mathbf{Q}_2^\top)
\end{aligned}$$

The change of variables can also be written as

$$\begin{bmatrix} \mathbf{A}_n & \mathbf{B}_n \\ \mathbf{C}_n & \mathbf{D}_n \end{bmatrix} = \begin{bmatrix} \mathbf{P}_2 & \mathbf{P}_1 \mathbf{B}_2 \\ \mathbf{0} & \mathbf{1} \end{bmatrix} \begin{bmatrix} \mathbf{A}_K & \mathbf{B}_K \\ \mathbf{C}_K & \mathbf{D}_K \end{bmatrix} \begin{bmatrix} \mathbf{Q}_2^\top & \mathbf{0} \\ \mathbf{C}_2 \mathbf{Q}_1 & \mathbf{1} \end{bmatrix} + \begin{bmatrix} \mathbf{P}_1 \mathbf{A} \mathbf{Q}_1 & \mathbf{0} \\ \mathbf{0} & \mathbf{0} \end{bmatrix}, \quad (\text{A.20})$$

$$\begin{bmatrix} \mathbf{Y}^\top \\ \mathbf{Z}^\top \end{bmatrix} = \begin{bmatrix} \mathbf{1} & \mathbf{0} \\ \mathbf{P}_1 & \mathbf{P}_2 \end{bmatrix} \begin{bmatrix} \mathbf{Y}_1^\top \\ \mathbf{Y}_2^\top \end{bmatrix}. \quad (\text{A.21})$$

Substituting the change of variables into (A.19) yields

$$\begin{bmatrix} \mathbf{M}_{11} & \mathbf{M}_{12} & \mathbf{M}_{13} & \mathbf{Y}^\top \\ * & \mathbf{M}_{22} & \mathbf{M}_{23} & \mathbf{Z}^\top \\ * & * & \mathbf{M}_{33} & \mathbf{X}^\top \\ * & * & * & -\mathbf{1} \end{bmatrix} \leq 0, \quad (\text{A.22})$$

where

$$\begin{aligned} \mathbf{M}_{11} &= \mathbf{A}\mathbf{Q}_1 + \mathbf{Q}_1\mathbf{A} + \mathbf{B}_2\mathbf{C}_n + \mathbf{C}_n^\top\mathbf{B}_2^\top - \mathbf{Y}^\top(\mathbf{C}_3\mathbf{Q}_1 + \mathbf{D}_{32}\mathbf{C}_n) - (\mathbf{C}_3\mathbf{Q}_1 + \mathbf{D}_{32}\mathbf{C}_n)^\top\mathbf{Y}, \\ \mathbf{M}_{12} &= \mathbf{A} + \mathbf{B}_2\mathbf{D}_K\mathbf{C}_2 + \mathbf{A}_n^\top - \mathbf{Y}^\top\mathbf{C}_3 - \mathbf{D}_{32}\mathbf{D}_K\mathbf{C}_2 - (\mathbf{C}_3\mathbf{Q}_1 + \mathbf{D}_{32}\mathbf{C}_n)^\top\mathbf{Z}^\top, \\ \mathbf{M}_{22} &= \mathbf{P}_1\mathbf{A} + \mathbf{A}^\top\mathbf{P}_1 + \mathbf{B}_n\mathbf{C}_2 + \mathbf{C}_2^\top\mathbf{B}_n^\top - \mathbf{Z}(\mathbf{C}_3 + \mathbf{D}_{32}\mathbf{D}_K\mathbf{C}_2) \\ &\quad - (\mathbf{C}_3 + \mathbf{D}_{32}\mathbf{D}_K\mathbf{C}_2)^\top\mathbf{Z}^\top, \\ \mathbf{M}_{13} &= \mathbf{B}_3 + \mathbf{B}_2\mathbf{D}_K\mathbf{D}_{23} - (\mathbf{C}_3\mathbf{Q}_1 + \mathbf{D}_{32}\mathbf{C}_n)^\top\mathbf{X} - \mathbf{Y}^\top(\mathbf{D}_{33} + \mathbf{D}_{32}\mathbf{D}_K\mathbf{D}_{23}), \\ \mathbf{M}_{23} &= \mathbf{P}_1\mathbf{B}_3 + \mathbf{B}_n\mathbf{D}_{23} - (\mathbf{C}_3^\top + \mathbf{C}_2^\top\mathbf{D}_K^\top\mathbf{D}_{32}^\top)\mathbf{X} - \mathbf{Z}(\mathbf{D}_{33} + \mathbf{D}_{32}\mathbf{D}_K\mathbf{D}_{23}), \\ \mathbf{M}_{33} &= \nu_{CLqp}^2\mathbf{1} - (\mathbf{D}_{33} + \mathbf{D}_{32}\mathbf{D}_K\mathbf{D}_{23})^\top\mathbf{X} - \mathbf{X}^\top(\mathbf{D}_{33} + \mathbf{D}_{32}\mathbf{D}_K\mathbf{D}_{23}). \end{aligned}$$

The matrix inequality in (A.22) is identical to the matrix inequality in (9.22), without the subscript k on the design variables.

The reverse of the change of variables in (A.20) is necessary to be able to recover the original controller. Assuming that \mathbf{B}_2 and \mathbf{C}_2 are full rank, the matrices

$$\begin{bmatrix} \mathbf{P}_2 & \mathbf{P}_1\mathbf{B}_2 \\ \mathbf{0} & \mathbf{1} \end{bmatrix} \text{ and } \begin{bmatrix} \mathbf{Q}_2^\top & \mathbf{0} \\ \mathbf{C}_2\mathbf{Q}_1 & \mathbf{1} \end{bmatrix}$$

are full rank and invertible using the result of Lemma A.1. Multiplying (A.20) by the inverses of these matrices, the reverse change of variables for the controller state-space matrices is given by

$$\begin{bmatrix} \mathbf{A}_K & \mathbf{B}_K \\ \mathbf{C}_K & \mathbf{D}_K \end{bmatrix} = \begin{bmatrix} \mathbf{P}_2 & \mathbf{P}_1\mathbf{B}_2 \\ \mathbf{0} & \mathbf{1} \end{bmatrix}^{-1} \left(\begin{bmatrix} \mathbf{A}_n & \mathbf{B}_n \\ \mathbf{C}_n & \mathbf{D}_n \end{bmatrix} - \begin{bmatrix} \mathbf{P}_1\mathbf{A}\mathbf{Q}_1 & \mathbf{0} \\ \mathbf{0} & \mathbf{0} \end{bmatrix} \right) \begin{bmatrix} \mathbf{Q}_2^\top & \mathbf{0} \\ \mathbf{C}_2\mathbf{Q}_1 & \mathbf{1} \end{bmatrix}^{-1}.$$

The reverse change of variables of (A.21) is

$$\begin{bmatrix} \mathbf{Y}_1^\top \\ \mathbf{Y}_2^\top \end{bmatrix} = \begin{bmatrix} \mathbf{1} & \mathbf{0} \\ \mathbf{P}_1 & \mathbf{P}_2 \end{bmatrix}^{-1} \begin{bmatrix} \mathbf{Y}^\top \\ \mathbf{Z}^\top \end{bmatrix},$$

where the inverse of $\begin{bmatrix} \mathbf{1} & \mathbf{0} \\ \mathbf{P}_1 & \mathbf{P}_2 \end{bmatrix}$ is known to exist from Lemma A.1.

The matrix inequalities used for controller synthesis are summarized as (A.14) and (A.22). The LMI of (A.14) ensures that the design variables \mathbf{P}_1 and \mathbf{Q}_1 yield matrices \mathbf{P} and \mathbf{Q} that satisfy Lemma A.1. The matrix inequality of (A.22) is a sufficient condition for minimum gain provided (A.14) is satisfied. Unfortunately, (A.22) is not an LMI in the design variables $\mathbf{P}_1 = \mathbf{P}_1^\top > 0$, $\mathbf{Q}_1 = \mathbf{Q}_1^\top > 0$, \mathbf{A}_n , \mathbf{B}_n , \mathbf{C}_n , \mathbf{D}_n , \mathbf{X} , \mathbf{Y} , \mathbf{Z} , and ν_{CLqp}^2 . Because of this, an iterative method is proposed in Synthesis Method 8 that involves solving an LMI in each step to find a value of ν_{CLqp}^2 that satisfies the robust stabilization condition of the Large Gain Theorem. Synthesis Method 10 for robust performance makes use of the same matrix inequality transformations on the Minimum Gain Lemma presented in this appendix. Synthesis Method 9 uses the same matrix inequalities as Synthesis Method 8, as well as the matrix inequalities found in [97] based on the Bounded Real Lemma.

Bibliography

Bibliography

- [1] R. J. Caverly and J. R. Forbes, “Robust controller design using the large gain theorem: The full-state feedback case,” in *American Control Conference*, (Boston, MA), pp. 3832–3837, July 2016.
- [2] R. J. Caverly and J. R. Forbes, “Regional pole and zero placement with static output feedback via the modified minimum gain lemma,” in *American Control Conference*, (Seattle, WA), pp. 364–369, 2017.
- [3] R. J. Caverly, R. Pates, L. J. Bridgeman, and J. R. Forbes, “MIMO Nyquist interpretation of the large gain theorem,” *International Journal of Control*, 2018. Under review.
- [4] R. J. Caverly and J. R. Forbes, “Nyquist interpretation of the large gain theorem,” *IFAC-PapersOnLine*, vol. 50, no. 1, pp. 3606–3611, 2017.
- [5] R. J. Caverly and J. R. Forbes, “ \mathcal{H}_∞ -optimal parallel feedforward control using minimum gain,” *IEEE Control Systems Letters*, 2018. Under review.
- [6] R. J. Caverly and J. R. Forbes, “Linearly combining sensor measurements optimally to enforce an SPR transfer matrix,” in *IEEE Conference on Control Technology and Applications*, (Copenhagen, Denmark), 2018. Under review.
- [7] S. Skogestad and I. Postlethwaite, *Multivariable Feedback Control: Analysis and Design*. Wiley-Interscience, 2 ed., 2005.
- [8] V. Zahedzadeh, H. J. Marquez, and T. Chen, “On the input-output stability of nonlinear systems: Large gain theorem,” in *American Control Conference*, (Seattle, WA), pp. 3440–3445, 2008.
- [9] L. J. Bridgeman and J. R. Forbes, “The minimum gain lemma,” *International Journal of Robust and Nonlinear Control*, vol. 25, no. 14, pp. 2515–2531, 2015.
- [10] V. Zahedzadeh, *Gain Analysis and Stability of Nonlinear Systems*. PhD thesis, University of Alberta, 2009.
- [11] N. Vasegh and A. Ghaderi, “Stabilizing a class of nonlinear systems by applying large gain theorem,” in *International Conference on System Theory, Control and Computing*, (Sinaia, Romania), pp. 1–4, 2012.

- [12] A. Ghaderi and N. Vasegh, "Input-output stabilizing controller synthesis for SISO T-S fuzzy systems by applying large gain theorem," *International Journal of Fuzzy Systems*, vol. 18, no. 4, pp. 550–556, 2016.
- [13] I. Barkana, "Parallel feedforward and simplified adaptive control," *International Journal of Adaptive Control and Signal Processing*, vol. 1, no. 2, pp. 95–109, 1987.
- [14] F. C. Lee, H. Flashner, and M. G. Safonov, "Positivity embedding for noncollocated nonsquare flexible structures," in *American Control Conference*, (Baltimore, MD), pp. 267–271, 1994.
- [15] F. C. Lee, H. Flashner, and M. G. Safonov, "An LMI approach to positivity embedding," in *American Control Conference*, (Seattle, WA), pp. 2081–2085, 1995.
- [16] F. C. Lee, H. Flashner, and M. G. Safonov, "Positivity-based control system synthesis using alternating LMIs," in *American Control Conference*, (Seattle, WA), pp. 1469–1473, 1995.
- [17] F. C. Lee, H. Flashner, and M. G. Safonov, "Positivity embedding for noncollocated and nonsquare flexible systems," *Applied Mathematics and Computation*, vol. 70, no. 2–3, pp. 233–246, 1995.
- [18] J. L. van Niekerk and B. H. Tongue, "Optimal positioning of sensors and actuators using closed-loop norms," *IFAC Proceedings Volumes*, vol. 29, no. 1, pp. 7600–7605, 1996.
- [19] G. J. Balas and P. M. Young, "Sensor selection via closed-loop control objectives," *IEEE Transactions on Control Systems Technology*, vol. 7, no. 6, pp. 692–705, 1999.
- [20] C. P. Moreno, H. Pfifer, and G. J. Balas, "Actuator and sensor selection for robust control of aeroservoelastic systems," in *American Control Conference*, (Chicago, IL), pp. 1899–1904, 2015.
- [21] K. Michail, A. C. Zolotas, and R. M. Goodall, "Optimised sensors selection for control and fault tolerance of electromagnetic suspension systems: A robust loop shaping approach," *ISA Transactions*, vol. 53, no. 1, pp. 97–109, 2014.
- [22] P. Misra and R. V. Patel, "Transmission zero assignment in linear multivariable systems - part I: Square systems," in *Conference on Decision and Control*, (Austin, TX), pp. 1310–1311, 1988.
- [23] S. Roy, J. A. Torres, and M. Xue, "Sensor and actuator placement for zero-shaping in dynamical networks," in *IEEE Conference on Decision and Control*, (Las Vegas, NV), pp. 1745–1750, 2016.

- [24] R. J. Caverly and J. R. Forbes, “Zero shaping of nonminimum phase aircraft dynamics,” in *AIAA Guidance, Navigation, and Control Conference, AIAA SciTech Forum*, (Kissimmee, FL), p. 601, 2018.
- [25] R. V. Patel and P. Misra, “Transmission zero assignment in linear multivariable systems - part II: The general case,” in *American Control Conference*, (Chicago, IL), pp. 644–648, 1992.
- [26] Z. Qu, D. Wiese, A. M. Annaswamy, and E. Lavretsky, “Squaring-up method in the presence of transmission zeros,” *IFAC P. Ser.*, vol. 47, no. 3, pp. 4164 – 4169, 2014. 19th IFAC World Congress.
- [27] E. Lavretsky and K. A. Wise, *Robust and Adaptive Control with Aerospace Applications*. London, UK: Springer-Verlag, 2013.
- [28] C. J. Damaren, “Passivity analysis for flexible multilink space manipulators,” *Journal of Guidance, Control, and Dynamics*, vol. 18, no. 2, pp. 272–279, 1995.
- [29] C. J. Damaren, “On the dynamics and control of flexible multibody systems with closed loops,” *International Journal of Robotics Research*, vol. 19, no. 3, pp. 238–253, 2000.
- [30] G. Zames, “On the input-output stability of time-varying nonlinear feedback systems parts I & II,” *IEEE Transactions on Automatic Control*, vol. 11, no. 2, pp. 229–231, 1966.
- [31] I. W. Sandberg, “On the \mathcal{L}_2 -boundedness of solutions of nonlinear functional equations,” *The Bell System Technical Journal*, vol. 43, no. 4, pp. 1581–1599, 1964.
- [32] L. J. Bridgeman and J. R. Forbes, “A comparative study of input-output stability results,” *IEEE Transactions on Automatic Control*, vol. 63, no. 2, pp. 463–476, 2018.
- [33] M. Vidyasagar, “ \mathcal{L}_2 -stability of interconnected systems using a reformulation of the Passivity Theorem,” *IEEE Transactions on Circuits and Systems*, vol. 24, no. 11, pp. 637–645, 1977.
- [34] J. Bao and P. L. Lee, *Process Control: The Passive Systems Approach*. London, UK: Springer-Verlag, 2007.
- [35] N. Sakamoto and M. Suzuki, “ γ -passive system and its phase property and synthesis,” *IEEE Transactions on Automatic Control*, vol. 41, no. 6, pp. 859–865, 1996.
- [36] S. Gupta, “Robust stability analysis using LMIs: Beyond small gain and passivity,” *International Journal of Robust and Nonlinear Control*, vol. 6, no. 9–10, pp. 953–968, 1996.

- [37] L. J. Bridgeman and J. R. Forbes, “The extended conic sector theorem,” *IEEE Transactions on Automatic Control*, vol. 61, no. 7, pp. 1931–1937, 2016.
- [38] T. T. Georgiou, M. Khammash, and A. Megretski, “On a large-gain theorem,” *Systems & Control Letters*, vol. 32, no. 4, pp. 231–234, 1997.
- [39] G. E. Dullerud and F. Paganini, *A Course in Robust Control Theory: A Convex Approach*. No. 36 in Texts in Applied Mathematics, New York, NY: Springer, 2000.
- [40] H. J. Marquez, *Nonlinear Control Systems: Analysis and Design*. Hoboken, NJ: Wiley, 2003.
- [41] A. J. Van der Schaft, *\mathcal{L}_2 -gain and passivity techniques in nonlinear control*. London, UK: Springer, 1996.
- [42] C. A. Desoer and M. Vidyasagar, *Feedback Systems: Input-Output Properties*. New York, NY: Academic Press, 1975.
- [43] K. Lange, *Optimization*. New York, NY: Springer, 2013.
- [44] S. Boyd, L. El Ghaoui, E. Feron, and V. Balakrishnan, *Linear Matrix Inequalities in System and Control Theory*. Philadelphia, PA: Society for Industrial and Applied Mathematics, 1994.
- [45] C. Scherer and S. Weiland, *Linear Matrix Inequalities in Control*. 2015.
- [46] K. Zhou and P. P. Khargonekar, “Robust stabilization of linear systems with norm-bounded time-varying uncertainty,” *Systems & Control Letters*, vol. 10, no. 1, pp. 17–20, 1988.
- [47] A. Zemouch, R. Rajamani, B. Boukroune, H. Rafaralahy, and M. Zasadzinski, “ \mathcal{H}_∞ circle criterion observer design for Lipschitz nonlinear systems with enhanced LMI conditions,” in *American Control Conference*, (Boston, MA), pp. 131–136, 2016.
- [48] D. S. Bernstein, *Matrix Mathematics: Theory, Facts, and Formulas*. Princeton, NJ: Princeton University Press, 2 ed., 2009.
- [49] P. Gahinet and P. Apkarian, “A linear matrix inequality approach to \mathcal{H}_∞ control,” *International Journal of Robust and Nonlinear Control*, vol. 4, no. 4, pp. 421–448, 1994.
- [50] R. E. Skelton, T. Iwasaki, and K. Grigoriadis, *A Unified Algebraic Approach to Linear Control Design*. London, UK: Taylor & Francis, 1997.
- [51] J. B. Hoagg and D. S. Bernstein, “Nonminimum-phase zeros - much to do about nothing - classical control - revisited part II,” *IEEE Control Systems Magazine*, vol. 27, no. 3, pp. 45–57, 2007.

- [52] C. A. Desoer and J. D. Schulman, “Zeros and poles of matrix transfer functions and their dynamical interpretation,” *IEEE Transactions on Circuits and Systems*, vol. 21, no. 1, pp. 3–8, 1974.
- [53] Y. M. Smagina, “System zeros,” *ArXiv Mathematics e-prints*, May 2006.
- [54] A. G. J. MacFarlane and N. Karcanias, “Poles and zeros of linear multivariable systems: A survey of the algebraic, geometric and complex-variable theory,” *International Journal of Control*, vol. 24, no. 1, pp. 33–74, 1976.
- [55] K. G. Arvanitis, “A periodic multirate adaptive pole placer for possibly nonminimum phase plants,” *Journal of Dynamic Systems, Measurement, and Control*, vol. 121, no. 4, pp. 668–677, 1999.
- [56] E. D. Sumer and D. S. Bernstein, “On the role of subspace zeros in retrospective cost adaptive control of non-square plants,” *International Journal of Control*, vol. 88, no. 2, pp. 295–323, 2015.
- [57] E. J. Davison and S. H. Wang, “Properties and calculation of transmission zeros of linear multivariable systems,” *Automatica*, vol. 10, no. 6, pp. 643–658, 1974.
- [58] B. Brogliato, R. Lozano, B. Maschke, and O. Egeland, *Dissipative Systems Analysis and Control: Theory and Applications*. London, UK: Springer-Verlag, 2nd ed., 2007.
- [59] L. J. Bridgeman and J. R. Forbes, “The exterior conic sector lemma,” *International Journal of Control*, vol. 88, no. 11, pp. 2250–2263, 2015.
- [60] Z. Iwai and I. Mizumoto, “Realization of simple adaptive control by using parallel feedforward compensator,” *International Journal of Control*, vol. 59, no. 6, pp. 1543–1565, 1994.
- [61] I. Barkana, “Classical and simple adaptive control for nonminimum phase autopilot design,” *Journal of Guidance, Control, and Dynamics*, vol. 28, no. 4, pp. 631–638, 2005.
- [62] I. Mizumoto, D. Ikeda, T. Hirahata, and Z. Iwai, “Design of discrete-time adaptive PID control systems with parallel feedforward compensator,” *Control Engineering Practice*, vol. 18, no. 2, pp. 168–176, 2010.
- [63] I. Rusnak and I. Barkana, “The duality of parallel feedforward and negative feedback,” in *IEEE 27th Convention of Electrical and Electronics Engineers in Israel*, (Eilat, Israel), pp. 1–4, 2012.
- [64] J. Löftberg, “YALMIP: A toolbox for modeling and optimization in MATLAB,” in *IEEE International Symposium on Computer Aided Control Systems Design*, 2004.

- [65] K. C. Toh, M. J. Todd, and R. H. Tütüncü, “SDPT3 - a MATLAB software package for semidefinite programming,” *Optimization Methods and Software*, vol. 11, no. 1–4, pp. 545–581, 1999.
- [66] D. S. Bernstein and W. M. Haddad, “Robust controller synthesis using Kharitonov’s theorem,” *IEEE Transactions on Automatic Control*, vol. 37, no. 1, 1992.
- [67] V. L. Kharitonov, “Asymptotic stability of an equilibrium position of a family of systems of linear ordinary differential equations,” *Differential Equations*, vol. 14, pp. 1483–1485, 1979.
- [68] G. A. Norris and R. E. Skelton, “Selection of dynamic sensors and actuators in the control of linear systems,” *Journal of Dynamic Systems, Measurement, and Control*, vol. 111, no. 3, pp. 389–397, 1989.
- [69] P. G. Maghami and S. M. Joshi, “Sensor-actuator placement for flexible structures,” *Journal of Guidance, Control, and Dynamics*, vol. 16, no. 2, pp. 301–307, 1993.
- [70] W. Gawronski and K. B. Lim, “Balanced actuator and sensor placement for flexible structures,” *International Journal of Control*, vol. 65, no. 1, pp. 131–145, 1996.
- [71] S. Joshi and S. Boyd, “Sensor selection via convex optimization,” *IEEE Transactions on Signal Processing*, vol. 57, no. 2, pp. 451–462, 2009.
- [72] H. Sane and D. Bernstein, “Asymptotic disturbance rejection for Hammerstein positive real systems,” *IEEE Transactions on Control Systems Technology*, vol. 11, no. 3, pp. 364–374, 2003.
- [73] J. Collado, R. Lozano, and R. Johansson, “Using an observer to transform linear systems into strictly positive real systems,” *IEEE Transactions on Automatic Control*, vol. 52, no. 6, pp. 1082–1088, 2007.
- [74] P. A. Ioannou and J. Sun, *Robust and Adaptive Control*, vol. 1. Upper Saddle River, NJ: Prentice-Hall, 1996.
- [75] I. Barkana, H. Kaufman, and M. Balas, “Model reference adaptive control of large structural systems,” *Journal of Guidance, Control, and Dynamics*, vol. 6, no. 2, pp. 112–118, 1983.
- [76] J. Strum, “Using SeDuMi 1.02, a MATLAB toolbox for optimization over symmetric cones,” *Optimization Methods and Software: Special Issue on Interior Point Methods*, vol. 11, no. 1–4, pp. 625–653, 1999.
- [77] B. Wie and D. S. Bernstein, “Benchmark problems for robust control design,” *Journal of Guidance, Control, and Dynamics*, vol. 15, no. 5, pp. 1057–1059, 1992.

- [78] R. Kelly, V. S. Davila, and A. Loría, *Control of Robot Manipulators in Joint Space*. Advanced Textbooks in Control and Signal Processing, London, UK: Springer-Verlag, 2005.
- [79] M. Green and D. J. N. Limebeer, *Linear Robust Control*. Mineola, NY: Dover, 2012.
- [80] H. H. Rosenbrock, “The stability of multivariable systems,” *IEEE Transactions on Automatic Control*, vol. 17, no. 1, pp. 105–107, 1979.
- [81] C. Desoer and Y.-T. Wang, “On the generalized Nyquist stability criterion,” *IEEE Transactions on Automatic Control*, vol. 25, no. 2, pp. 187–196, 1980.
- [82] S. Zhan, “On the determinantal inequalities,” *Journal of Inequalities in Pure and Applied Mathematics*, vol. 6, no. 4, p. 105, 2005.
- [83] G. Vinnicombe, *Uncertainty and Feedback: \mathcal{H}_∞ Loop-Shaping and the ν -Gap Metric*. London, UK: Imperial College Press, 2001.
- [84] T. Andresen, “Nyquist plot with logarithmic amplitudes,” June 2009.
- [85] D. C. McFarlane and K. Glover, *Robust Controller Design Using Normalized Coprime Factor Plant Description*, vol. 138 of *Lecture Notes in Control and Information Sciences*. Berlin Heidelberg New York: Springer-Verlag, 1990.
- [86] K. Zhou and J. C. Doyle, *Essentials of Robust Control*. Upper Saddle River, NJ: Prentice Hall, 1998.
- [87] R. E. Benton and D. Smith, “A non-iterative LMI-based algorithm for robust static-output-feedback stabilization,” *International Journal of Control*, vol. 72, no. 14, pp. 1322–1330, 1999.
- [88] D. Arzelier, D. Peaucelle, and S. Salhi, “Robust static output feedback stabilization for polytopic uncertain systems: Improving the guaranteed performance bound,” *IFAC Proceedings Volumes: 4th IFAC Symposium on Robust Control Design*, vol. 36, no. 11, pp. 425–430, 2003.
- [89] J. Dong and G.-H. Yang, “Robust static output feedback control synthesis for linear continuous systems with polytopic uncertainties,” *Automatica*, vol. 49, no. 6, pp. 1821–1829, 2013.
- [90] X.-H. Chang, J. H. Park, and J. Zhou, “Robust static output feedback \mathcal{H}_∞ control design for linear systems with polytopic uncertainties,” *Systems & Control Letters*, vol. 85, pp. 23–32, November 2015.
- [91] G. Chesi, “Robust static output feedback controllers via robust stabilizability functions,” *IEEE Transactions on Automatic Control*, vol. 59, no. 6, pp. 1618–1623, 2014.

- [92] D. Zhao and J.-L. Wang, “Robust static output feedback design for polynomial nonlinear systems,” *International Journal of Robust and Nonlinear Control*, vol. 20, no. 14, pp. 1637–1654, 2010.
- [93] G. Zames and A. K. El-Sakkary, “Unstable systems and feedback: The gap metric,” in *Proc. Allerton Conference*, 1980.
- [94] M. Vidyasagar, “The graph metric for unstable plants and robustness estimates for feedback stability,” *IEEE Transactions on Automatic Control*, vol. 5, no. 29, pp. 403–418, 1984.
- [95] L. Qiu and K. Zhou, *Introduction to Feedback Control*. Upper Saddle River, NJ: Prentice Hall, 2009.
- [96] J. C. Doyle, K. Glover, P. P. Khargonekar, and B. A. Francis, “State-space solutions to standard \mathcal{H}_2 and \mathcal{H}_∞ control problems,” *IEEE Transactions on Automatic Control*, vol. 34, no. 8, pp. 831–847, 1989.
- [97] C. Scherer, P. Gahinet, and M. Chilali, “Multiobjective output-feedback control via LMI optimization,” *IEEE Transactions on Automatic Control*, vol. 42, no. 7, pp. 896–911, 1997.
- [98] J. Doyle, “Analysis of feedback systems with structured uncertainties,” *IEE Proceedings D - Control Theory and Applications*, vol. 129, no. 6, pp. 242–250, 1982.
- [99] M. G. Safonov and B. S. Chen, “Multivariable stability-margin optimisation with decoupling and output regulation,” *IEE Proceedings D - Control Theory and Applications*, vol. 129, no. 6, pp. 276–282, 1982.
- [100] A. Packard and J. Doyle, “The complex structured singular value,” *Automatica*, vol. 29, no. 1, pp. 71–109, 1993.
- [101] G. Stein and J. C. Doyle, “Beyond singular values and loop shapes,” *Journal of Guidance, Control, and Dynamics*, vol. 14, no. 1, pp. 5–16, 1991.
- [102] G. J. Balas, J. C. Doyle, K. Glover, A. Packard, and R. Smith, *μ -Analysis and Synthesis Toolbox*. MUSYN Inc. and The MathWorks, Natick, MA, June 2001.
- [103] T. T. Georgiou and M. C. Smith, “w-stability of feedback systems,” *Systems & Control Letters*, vol. 13, no. 4, pp. 271–277, 1989.
- [104] H. Logemann, R. Rebarber, and G. Weiss, “Conditions for robustness and non-robustness of the stability of feedback systems with respect to small delays in the feedback loop,” *SIAM Journal of Control and Optimization*, vol. 34, no. 2, pp. 572–600, 1996.
- [105] J. Doyle, A. Packard, and K. Zhou, “Review of LFTs, LMIs, and μ ,” in *Conference on Decision and Control*, (Brighton, England), pp. 1227–1232, 1991.

- [106] V. H. L. Cheng and C. A. Desoer, “Limitations on the closed-loop transfer function due to right-half plane transmission zeros of the plant,” *IEEE Transactions on Automatic Control*, vol. 25, no. 6, pp. 1218–1220, 1980.
- [107] R. Lind and M. Brenner, “Incorporating flight data into a robust aeroelastic model,” *Journal of Aircraft*, vol. 35, no. 3, pp. 470–477, 1998.
- [108] D. Borglund, “Robust aeroelastic stability analysis considering frequency-domain aerodynamic uncertainty,” *Journal of Aircraft*, vol. 40, no. 1, pp. 189–193, 2003.
- [109] D. S. Bernstein, W. M. Haddad, and D. C. Hyland, “Small gain versus positive real modeling of real parameter uncertainty,” in *Conference on Decision and Control*, (Brighton, England), pp. 539–540, 1991.
- [110] W. M. Haddad and D. S. Bernstein, “Robust stabilization with positive real uncertainty: Beyond the small gain theorem,” *Systems & Control Letters*, vol. 17, no. 3, pp. 191–208, 1991.
- [111] J. Bao, F. Wand, P. L. Lee, and W. Zhou, “New frequency-domain phase-related properties of MIMO LTI passive systems and robust controller synthesis,” *IFAC Proceedings Volumes*, vol. 29, no. 1, pp. 3276–3281, 1996.
- [112] M. G. Safonov, E. A. Jonckheere, M. Verma, and D. J. N. Limebeer, “Synthesis of positive real multivariable feedback systems,” *International Journal of Control*, vol. 45, no. 3, pp. 817–842, 1987.
- [113] E. V. Byrns and A. J. Calise, “Loop transfer recovery approach to \mathcal{H}_∞ design for coupled mass benchmark problem,” *Journal of Guidance, Control, and Dynamics*, vol. 15, no. 5, pp. 1118–1124, 1992.
- [114] Y. J. Wang, L. S. Shieh, and J. W. Sunkel, “Observer-based robust- \mathcal{H}_∞ control laws for uncertain linear systems,” *Journal of Guidance, Control, and Dynamics*, vol. 15, no. 5, pp. 1125–1133, 1992.
- [115] B. Wie, Q. Liu, and K.-W. Byun, “Robust \mathcal{H}_∞ control synthesis method and its application to benchmark problems,” *Journal of Guidance, Control, and Dynamics*, vol. 15, no. 5, pp. 1140–1148, 1992.
- [116] MOSEK ApS, *The MOSEK Optimization Toolbox for MATLAB Manual. Version 8.1 (Revision 37)*.